Programa de Doctorado en Ciencias de la Salud

Departamento de Fisioterapia, Medicina y Ciencias Biomédicas

DOCTORAL THESIS

Validation of a panel of osteoarthritis biomarkers by protein microarrays

María Camacho Encina

A Coruña, 2019

Directores:

Dr. Francisco Javier Blanco García

Dra. Cristina Ruiz Romero

El Dr. Francisco Javier Blanco García, Director Científico del Instituto de Investigación Biomédica de A Coruña (INIBIC), Reumatólogo del Complejo Hospitalario Universitario de A Coruña (CHUAC-XXIAC), Profesor de la UDC, y la Dra. Cristina Ruiz Romero, Investigadora Principal de la Unidad de Proteómica del INIBIC

CERTIFICAN QUE:

La presente memoria de tesis titulada "Validation of a panel of Osteoarthritis biomarkers by protein microarrays" presentada por Doña María Camacho Encina, Licenciada en Biología por la Universidad de Sevilla, ha sido realizada bajo nuestra dirección y reúne todas las condiciones necesarias de originalidad y rigor científico para ser defendida públicamente y optar al Grado de Doctor Internacional en Ciencias de la Salud.

Para que así conste, firman el presente certificado en A Coruña a 5 de Julio de 2019.

Fdo.: Dr. Francisco J. Blanco García

Fdo.: Dra. Cristina Ruiz Romero

Part of the research presented in this thesis project was been carried out under the supervision of the Dr. Joshua LaBaer, Executive Director and Professor of the Biodesign Institute, Center Director of the Biodesign Virginia G. Piper Center for Personalized Diagnostics, and Interim Center Director at the ASU-Banner Neurodegenerative Disease Research Center, during a three-months visiting fellowship in 2017.

"Equipped with his five sense, man explores the universe around him and call the experience Science".

Edwin Powell Hubble

"Nothing in life is to be feared, it is only to be understood. Now is the time to understand more, so that we may fear less".

Marie Curie

A mis padres.

A mi hermana y hermanos.

He estado temiendo este momento desde el día en el que comenzó toda esta locura, y ahora aquí estoy, sentada delante del ordenador con las manos temblorosas y el corazón a mil por hora, temiendo dejar a alguien atrás o no encontrar las palabras adecuadas para expresar lo que estos cuatro años han supuesto para mí. Miro hacia atrás y no puedo parar de preguntarme ¿En qué momento avanzó tan rápido el reloj?¿Cómo es posible que haya pasado todo? Yo nunca he sido buena para cerrar capítulos y siempre me ha costado abrir los nuevos. Si no fuera por vosotros que, cada cual a su manera, habéis puesto vuestro granito de arena durante estos años de locura… creedme… hoy no me encontraría aquí, escribiendo el capítulo final de esta etapa y el preludio de la siguiente.

En primer lugar, me gustaría agradecer a mis directores de tesis el haberme dado la oportunidad y los medios necesarios para que hoy pueda llamarme doctora. Al Dr. Francisco Javier Blanco García, por todos sus consejos y todo el apoyo que me ha brindado a lo largo de mi etapa predoctoral. A la Dra. Cristina Ruiz Romero. Gracias por confiar en mí desde el primer momento en el que entré por las puertas del INIBIC, por el apoyo, y por las palabras de ánimo y consuelo cuando no era capaz de ver más allá.

Gracias también a mis compañeras de grupo, a Patricia, por la paciencia que has tenido intentando que mi cabeza retenga algo de química; a Lucía Lourido, por iniciarme en el maravilloso mundo de los inmunoensayos que tanto he aprendido a amar y odiar a partes iguales… aunque he de decir que el sufrimiento siempre ha terminado mereciendo la pena; A Bea, por ser tan comprensiva, porque siempre tienes las palabras adecuadas en el momento adecuado; a Lucía González, ¡empezamos esto al mismo tiempo y lo hemos logrado!, gracias por ayudarme cuando podías; a Valentina, esta tesis no hubiera salido adelante sin ti. Gracias por confiar en que podía lograrlo, y gracias por ayudarme a conseguirlo; y por último, al terremoto de proteómica, a Rocío Paz. Tienes un corazón tan grande… gracias por tu sonrisa permanente, por estar siempre dispuesta a ayudar.

Gracias a la Unidad de Epidemiología Clínica y Estadística del Complejo Hospitalario Universitario de A Coruña. En especial a Vanesa, porque estos últimos meses apenas he podido dar un paso sin recurrir a ti. Gracias por recibirme cada vez que lo he necesitado, porque aun estando hasta arriba de trabajo y con tus propios agobios, siempre has hecho un hueco para mí.

A todo el personal del INIBIC, gracias por vuestros consejos, apoyo y conocimiento, por ayudarme a aclarar las ideas y ver lo que yo sola no era capaz, por hacer de las comidas experiencias inolvidables, por hacer que los viajes por trabajo se convirtieran en viajes de placer. Espero que me perdonéis que solo ponga algunos nombres… ojalá pudiera nombraros a todos, ¡pero entonces no llegaría a tiempo a depositar! Gracias al Dr. Ignacio Rego, has sido un tutor más para mí. Gracias por recibirme siempre, por responder a mis preguntas, por muy tontas que fueran, y resolver mis múltiples dudas sobre absolutamente todo. Gracias a Noa, Paula, Alex y María. ¡No os imagináis el bien

que me habéis hecho! Gracias por los cafés a primera hora de la mañana con los que jugar a la escondida, por los churros con chocolate, los no cumpleaños, la no amistad, por los cotilleos en cualquier pasillo, por poner vuestra oreja cada vez que necesitaba estallar. Nunca olvidaré todo lo que me habéis ayudado.

Yo solía ser de aquellas personas que pensaban que en el trabajo una no hacía amigos… tenía compañeros, con los que podías llevarte mejor o peor, pero nada más. Ahora lo pienso, y me río de mi misma, porque como siempre y para variar, estaba completamente equivocada. Paula, Juan, Marta, Rocío, Andrés, Adri, Amanda e Irene, hemos compartido tantos momentos juntos… momentos de llantos, de risas, de desesperación, de éxitos. Paula y Juan ¡se os echa tanto de menos! son muchas nuestras historias detrás de un par de cañas. Gracias por todo lo que hicisteis por mí. Marta, tú y yo somos dos personas con muchas diferencias, pero a pesar de todo, has estado a mi lado cuando lo he necesitado, y eso para mí vale más que todos los roces vividos. Rocío, eres la dulzura personificada. Gracias por escucharme y por preocuparte tanto por mí, incluso cuando no lo merecía. Andrés, gracias por tus consejos y por todo el apoyo que siempre he recibido de ti, te admiro muchísimo. Adri… tú sabes que este "chiringuito" no es lo mismo cuando te vas. Gracias por todas las salidas a fumar en las que me dejas quejarme de todo sin rechistar. Y por último, pero no menos importante, estáis vosotras, Amanda e Irene, las peques del grupo. Sois dos personas extraordinarias, gracias por hacerme un huequito en vuestras vidas, por escucharme y por apoyarme tanto.

Gracias a mis informáticos e informáticas. Recuerdo que cuando dejé Sevilla para venir aquí, lloraba como un bebé. Dejaba atrás a mis amigos, a mi familia, y tenía tanto miedo de encontrarme sola… pero desde el primer momento, vosotros me acogisteis como si fuera una más. Gracias por hacerme sentir como en casa. En especial, tengo que darte las gracias a ti, mi Ángel (de la guarda)… después de tanto tiempo sigo sin saber cómo lo haces, pero tienes esa rara capacidad de conseguir que, cuando estoy contigo, todos los problemas a mi alrededor desaparezcan, o parezcan un chiste. Creo que realmente nunca voy a ser capaz de hacerte entender cuanto te quiero.

A Anabel, mi rubia de corazón y a Sally, mi Salitre. Sois dos de las personas más extraordinarias que he conocido nunca y sé a ciencia cierta que vais a conseguir grandes cosas en vuestra vida y que voy a estar ahí para verlo, por muchos kilómetros que nos puedan separar. Gracias por estar a mi lado, por escucharme, por entenderme, por aconsejarme, y por saltar del sofá, sin ni siquiera parar a poneros unos vaqueros, para correr a abrazarme.

Un día, sin comerlo ni beberlo, llegan a tu vida cuatro locos que deciden quedarse. Así, sin más. Y tú claro, lo aceptas, porque tampoco es que te dejen más opción... Si, si… no miréis hacia un lado que sabéis que os hablo a vosotros, mis helados oscuros… Patri, Henar, Mique y José… ¡bendita locura la vuestra!… vosotros hacéis de este mundo un lugar en el que realmente merece la pena quedarse. No sois sólo mis amigos, sois la familia que he escogido. Gracias, porque aunque os viniera con la historia más

inverosímil, nunca dudasteis de mi palabra. Gracias por vuestra amistad incondicional. Gracias por ser mi refugio, porque aunque no entendierais nada de lo que explicaba cuando volvía frustrada de trabajar, me escuchasteis y me consolasteis. Gracias porque nunca me habéis dejado sola y porque aunque sepáis que voy a cometer la mayor de las locuras, estáis ahí para cometerla conmigo. Gracias por esa letra pequeña del contrato de amistad. Gracias y millones de gracias. Os admiro muchísimo, y os quiero aún más.

Me gustaría dar las gracias también a mis tíos, Alfredo y Montse, por abrirme las puertas de su casa, una y otra vez, pasara lo que pasara. Gracias por cuidarme y quererme como si fuera una hija más bajo vuestro techo. No tengo palabras para expresar lo agradecida que estoy con vosotros. Lo que significáis para mí y el enorme respeto que os tengo, aunque a veces no sepa demostrarlo y lo haga todo del revés. Gracias a Jacobo, mi primo y mejor amigo. De nosotros podrían escribir varias novelas. Siempre has estado a mi lado, pasase lo que pasase, queriéndome incluso a veces por encima de tus posibilidades. Gracias por ser un bastón en el que siempre puedo apoyarme.

Y aunque más de uno piense que estoy loca, no tendría la conciencia tranquila si no te nombro también a ti Anxo. Tú te empeñas en pensar que eres tóxico, y sé que pasará el tiempo y aun seguirás sin creerte mis palabras, pero te digo de corazón, que en dos años contigo he aprendido más sobre la vida, la amistad y el amor, que en mis otros 27. Gracias por regalarme los momentos más felices que alcanzo a recordar.

Y por último, y más importante, doy las gracias a mi familia. A mi hermana Celia, eres mi ejemplo a seguir. Ojalá pudiera ser la mitad de valiente y de fuerte de lo que eres tú. Gracias por ser mi mejor amiga, mi confidente, por arroparme, por consolarme, por dejarme dormir contigo en 90 metros de cama cuando tenía pesadillas. A mis hermanos, Jesús, David y Fernando, si soy capaz de levantarme cada día y ver el sol a pesar de la tormenta, es por vosotros. Gracias por ser mis cómplices, por pasar las horas jugando, cantando y riendo. Y por supuesto, gracias a mis padres. Os estoy eternamente agradecida por todo el amor que me habéis dado, por enseñarme a levantarme tras cada tropiezo, a no rendirme nunca y luchar siempre por mis sueños, por no dejarme caer, aun cuando sentía que el mundo se me venían encima. Papá, gracias, porque sé que, aunque a veces eres un poco duro, siempre lo has dado todo por nosotros. Gracias porque a pesar de cualquier disgusto, siempre tienes las palabras adecuadas para solucionarlo todo, por enseñarme a ser fuerte, por inculcarme que hay que esforzarse y trabajar. Mamá, que decirte a ti… tú eres mi roca, mi maestra y mi guardiana, el pilar que me sostiene día tras día. Gracias por el tiempo, el esfuerzo, la dedicación, y el amor que pones en todas y cada una de las cosas que haces. Si al nacer me hubieran dado la opción de fabricar una madre, ten por seguro que sería exactamente igual que tú. Todo, absolutamente todo lo que tengo, y lo que soy, os lo debo a vosotros seis. Siento si alguna vez no he sido la mejor de las hijas o de las hermanas, pero espero que os sintáis tan orgullosos de mí, como lo estoy yo de vosotros.

A todos, no me alcanzarán los días para devolveros tanto amor. Gracias con todo mi corazón.

¡Os amo!

TABLE OF CONTENTS

LIST OF ABBREVIATIONS

2-DE	2-Dimensional Electrophoresis
3D	3-Dimensions
5PL	5-Parameter Logistic
a.u.	Arbitrary Units
AAbs	Autoantibodies
AAOS	American Academy of Orthopaedic Surgeons
ACL	Anterior Cruciate Ligament
ACPAs	Anti-Citrullinated Peptide/Protein Antibodies
ACR	American College of Rheumatology
ADAMT	A Desintegrin And Metalloproteinase with Thrombospondin Motifs
AHSG	Alpha-2-HS-Glycoprotein
APCS	Serum Amyloid P-Component
ASB7	Ankyrin Repeat and SOCS Box Protein 7
ASD	Autism Spectrum Disorder
AUC	Area Under the Curve
BIPED	(B) Burden of disease (I) Investigative (P) Prognostic (E) Efficacy of intervention (D) Diagnostic
BMD	Bone Mineral Density
BMI	Body Mass Index
BML	Bone Marrow Lesion
BS3	Bis(sulfosuccinimidyl)Suberate
BSA	Bovine Serum Albumin

C2C	Collagenase-Mediated Degradation Fragment of Collagen Type II
CA125	Carbohydrate Antigen 125
CCD	Charge-Coupled Device
CDER	Center for Drug Evaluation and Research
cDNA	complementary Deoxyribonucleic Acid
CDRs	Complementary-Determining Regions
CE	Conformational Epitopes
CHECK	Cohort Hip and Cohort Knee
CHI3L1	Chitinase-3-Like Protein 1
CHUAC	*Hospital Universitario de A Coruña* (University Hospital of A Coruna)
CI	Confidence Interval
CILP	Cartilage Intermediate Layer Protein
cm	Centimetres
COMP	Cartilage Oligomeric Matrix Protein
CPD	Centre for Personalized Diagnostics
CRP	C-Reactive Protein
CTXI	C-terminal Telopeptide of Collagen Type I
CTXII	C-terminal Telopeptide of Collagen Type II
CV	Coefficient Variation
CXCL12	C-X-C Motif Chemokine 12
Cy	Cyanine
DAMPs	Damage-Associated Molecular Patterns
DAPA	DNA Array to Protein Array
DBD	Global Burden of Disease

DIGE	Difference Gel Electrophoresis
DMOADs	Disease-Modifying Osteoarthritis Drugs
DNA	Deoxyribonucleic Acid
DV	Dependent Variable
ECM	Extracellular Matrix
EDC	1-Ethyl-3-(3-Dimethylaminopropyl)Carbodiimide
ELISA	Enzyme-Linked Immunosorbent Assay
EMA	European Medicines Agency
Fab	Fragment Antigen Binding
Fc	Fragment Crystallizable
FDA	Food and Drug Administration
fmols	Femtomoles
FOS	Framingham Osteoarthritis Study
GDP	Gross Domestic Product
GIR	*Grupo de Investigación en Reumatología* (Rheumatology Research Group)
GOAL	Genetics of Osteoarthritis and Lifestyle
GST	Glutathione S-transferase
GWAS	Genome-Wide Associated Scan
h	Hours
H-PGDS	Hematopoietic Prostaglandin D2 Synthetase
H0	Null Hypothesis
H1	Alternative Hypothesis
HE4	Human Epididymis Protein 4
HIF1-α	Hypoxia-Inducible Factor 1 alpha

HPP	Human Proteome Project
HR	Hazard Ration
HRP	Horseradish Peroxidase
HSP70	Heat Shock Protein 70
ID	Independent Variable
Ig	Immunoglobulin
IGF	Insulin-like Growth Factors
IL	Interleukin
IR	Incidence Rate
IRB	Institutional Review Board
IUPAC	International Union of Pure and Applied Chemistry
IVTT	In Vitro Transcription and Translation
JSN	Joint Space Narrowing
JSW	Joint Space Width
KDa	KiloDalton
KL	Kellgren and Lawrence
KM	Kaplan-Meier
KOOS	Knee Outcomes in Osteoarthritis Survey
LC	Liquid Chromatography
LE	Lineal Epitopes
LED	Light-Emitting Diode
LLOD	Lower Limit of Detection
LLOQ	Lower Limit of Quantification
ln	Napierian Logarithm

MAT2β	Methionine-Adenosyltransferase II Subunit b
MBDA	Multi-Biomarker Disease Activity
mCP	m-Contact Printing
MES	2-[N-Morpholino]Ethanesulfonic Acid
MFI	Median Fluorescence Intensity
mg	Milligrams
mIgG	mouse Immunoglobulin of class G
min	Minutes
miRNA	micro-Ribonucleic Acid
mL	Millilitre
mM	Millimolar
MMP	Matrix Metalloproteinase
MOST	Multicenter Osteoarthritis Study
MRI	Magnetic Resonance Imaging
MRM	Multiple Reaction Monitoring
mRNA	messenger Ribonucleic Acid
MS	Mass Spectrometry
MVD	Diphosphomevalonate Decarboxylase
NAPPA	Nucleic Acid Programmable Protein Array
NHS	N-Hydroxysuccinimide
NIAMS	National Institute of Arthritis, Musculoskeletal and Skin Disease
NIH	National Institute of Health
nm	Nanometre
NO	Nitric Oxide

NPV	Negative Predictive Value
NSAIDs	Non-Steroidal Anti-Inflammatory Drugs
NTXI	Crosslinked N-terminal Telopeptide of Collagen Type I
OA	Osteoarthritis
OAI	Osteoarthritis Initiative
OARSI	Osteoarthritis Research Society International
OMERACT	Outcome Measures in Rheumatology
OPG	Osteoprotegerin
OPN	Osteopontin
OR	Odd Ratio
ORFs	Open Reading Frames
PBS	Phosphate Buffered Saline
PBST	Phosphate Buffered Saline with Tween20
PCR	Polymerase Chain Reaction
PET	Position Emission Technologies
PG	Prostaglandins
PIIANP	N-terminal Propeptide of Collagen Type IIA
PISA	Protein In Situ Array
pl	Picolitre
pNPII	N-terminal Propeptide of Procolagen Type II
PPV	Positive Predictive Value
PROCOAC	Prospective Cohort of Osteoarthritis A Coruña
PuCa	Puromycin Capture Protein Array
QC	Quality Control

R-PE	R-Phycoerythrin
RA	Rheumatoid Arthritis
RAC3	Ras-Related C3 Botulinum Toxin Substrate 3
RBP4	Retinol Binding Protein 4
RIA	Radioimmunoassay
ROC	Receiver Operating Characteristic
RPA	Reverse-Phase Array
rpm	Revolutions Per Minute
RSF	Random Survival Forests
RT	Room Temperature
SAM	S-Adenosylmethionine
SAPE	Phycoerythrin-Streptavidin
SBA	Suspension Bead Assay
SD	Standard Deviation
SER	*Sociedad Española de Reumatología* (Spanish Society of Rheumatology)
SLE	Systemic Lupus Erythematosus
SOP	Standard Operation Procedure
SPSS	Statistic Package for the Social Sciences
SRM	Selective Reaction Monitoring
SYSADOA	Symptomatic Slow Action Drugs for OA
T2DM	Type II Diabetes Mellitus
TENS	Transcutaneous Electrical Nerve Stimulation
TGF-β	Transforming Growth Factor beta
TICs	Time-Integrated Concentrations

TNF-α	Tumor Necrosis Factor alpha
TPIS	Triosephosphate Isomerase
TPS1	Thrombospondin 1
tRNA	transfer Ribonucleic Acid
UGT1A7	UDP-Glucuronosyltransferase 1-7
VEGF	Vascular Endothelial Growth Factor
VPS4B	Vacuolar Protein Sorting-Associated Protein 4B
WHO	World Health Organization
WOMAC	Western Ontario and McMasters Osteoarthritis Index
MAP	Multi-Analyte Profiling
YKL-39	Chitinase-3-Like Protein 2
µg	Micrograms
µL	Microlitre
µm	Micrometre

LIST OF FIGURES

LIST OF TABLES

ABSTRACT

RESUMEN

Aunque la artrosis (OA) es una patología reumática caracterizada por una larga fase inicial clínicamente silente de deterioro articular, generalmente la enfermedad no se diagnostica hasta etapas muy avanzadas, donde la única solución posible es un reemplazamiento protésico. Esto es mayormente debido a las limitaciones y a la baja sensibilidad que presentan las técnicas de diagnóstico actuales, basadas en la descripción subjetiva de los síntomas del paciente y en pruebas radiológicas. En los últimos años, el uso de técnicas proteómicas ha dado lugar a una larga lista de marcadores solubles asociados con la patología artrósica, que podrían tener cierto potencial para el diagnóstico precoz y/o la predicción de la enfermedad. Sin embargo, ninguno de ellos ha sido suficientemente validado para su uso en la rutina clínica, debido principalmente a la falta de estudios prospectivos en un gran número de muestras procedentes de pacientes que hayan sido seguidos durante largos períodos de tiempo.

En esta tesis se han empleado técnicas proteómicas rápidas y económicas, basadas en microarrays de proteínas en suspensión, para la validación y posterior cualificación como marcadores de predicción de incidencia de OA de un panel de seis proteínas seleccionadas en base a resultados previos de nuestro grupo de investigación.

Así mismo, a pesar de que no se conoce la causa exacta que inicia el proceso artrósico, es bien sabido que el sistema inmune, entre otros, tiene un papel fundamental. La producción de anticuerpos frente a antígenos propios del cuerpo, o *autoanticuerpos* (AAbs) es una de las principales características de la actuación de dicho sistema. Por ello, durante la realización de esta tesis doctoral, se llevó a cabo una fase de descubrimiento de biomarcadores mediante arrays de proteínas en formato plano, con el fin de definir un perfil de inmunoreactividad propio de las etapas clínicamente silentes de la OA que permitiera identificar un panel de AAbs con posible potencial como marcadores de predicción.

Los resultados obtenidos mediante el análisis de un amplio set de muestras de suero a tiempo cero de individuos sin evidencia ni radiográfica ni sintomática de OA de rodilla, procedentes de la cohorte de la Osteoartrhritis Initiative, han demostrado la asociación de distintos biomarcadores protéicos con la futura aparición de la enfermedad. Por otro lado, el uso de pruebas estadísticas multivariantes ha dado lugar a la generación de dos posibles modelos para predecir la incidencia de OA radiográfica de rodilla, formados por la

combinación de marcadores protéicos y clínicos asociados con el desarrollo de la enfermedad. Además, mediante el empleo de análisis de supervivencia, se ha demostrado que los niveles en suero a tiempo cero de estos biomarcadores solubles se asocian con el tiempo de aparición de la misma: a mayores niveles del biomarcador, antes se desarrolla la OA.

RESUMO

Aínda que a artrose (OA) é unha patoloxía reumática caracterizada por unha longa fase inicial clinicamente silente de deterioración articular, xeralmente a enfermidade non se diagnostica ata etapas moi avanzadas, onde a única solución posible é un reemplazamiento protésico. Isto, é maiormente debido ás limitacións e á baixa sensibilidade que presentan as técnicas de diagnóstico actuais, baseadas na descrición subxectiva dos síntomas do paciente e en probas radiolóxicas. Nos últimos anos, o uso de técnicas proteómicas deu lugar a unha longa lista de marcadores solubles asociados coa patoloxía artrósica, que poderían ter certo potencial para o diagnóstico precoz e/ou a predición da enfermidade. Con todo, ningún deles foi suficientemente validado para o seu uso na rutina clínica, debido principalmente á falta de estudos prospectivos nun gran número de mostras procedentes de pacientes que fosen seguidos durante longos períodos de tempo.

Nesta tese empregáronse técnicas proteómicas rápidas e económicas, baseadas en microarrays de proteínas en suspensión, para a validación e posterior cualificación como marcadores de predición de incidencia de OA dun panel de seis proteínas seleccionadas en base a resultados previos do noso grupo de investigación.

Así mesmo, a pesar de que non se coñece a causa exacta que inicia o proceso artrósico, é ben sabido que o sistema inmune, entre outros, ten un papel fundamental. A produción de anticorpos fronte a antíxenos propios do corpo, ou autoanticorpos (AAbs) é unha das principais características da actuación devandito sistema. Por iso, durante a realización desta tese doutoral, levou a cabo unha fase de descubrimento de biomarcadores mediante arrays de proteínas en formato plano, co fin de definir un perfil de inmunoreactividad propio das etapas clinicamente silentes da OA que permitise identificar un panel de AAbs con posible potencial como marcadores de predición.

Os resultados obtidos mediante a análise dun amplo set de mostras de soro a tempo cero de individuos sen evidencia nin radiográfica nin sintomática de OA de xeonllo, procedentes da cohorte da Osteoartrhritis Initiative, demostraron a asociación de distintos biomarcadores protéicos coa futura aparición da enfermidade. Doutra banda, o uso de probas estatísticas multivariantes deu lugar á xeración de dous posibles modelos para predicir a incidencia de OA radiográfica de xeonllo, formados pola combinación de

marcadores protéicos e clínicos asociados co desenvolvemento da enfermidade. Ademais, mediante o emprego de análise de supervivencia, demostrouse que os niveis en soro a tempo cero destes biomarcadores solubles asócianse co tempo de aparición da mesma: A maiores niveis do biomarcador, antes desenvólvese a OA.

ABSTRACT

Although osteoarthritis (OA) is a rheumatic pathology characterized by a long clinically silent early phase of joint degeneration, the disease is generally diagnosed at advanced stages, when the only possible solution is prosthetic replacement. This is mainly due to the limitations and low sensitivity of the actual diagnostic techniques, which are based on the patient's subjective description of the symptoms and radiological tests. In the last years, the use of proteomic technologies have defined a large list of potential OA soluble biomarkers, which may have a putative utility for the early diagnosis and/or prediction of the disease. However, none of them has been sufficiently validated for their use in the daily clinical routine, mostly due to the lack of prospective studies in a large number of individuals who have been followed for long periods of time.

In this thesis project, a high-throughput proteomic technique based on suspension protein arrays has been employed for the validation and subsequent qualification as prognostic markers of incident OA of a panel of six proteins selected based on previous findings from our research group.

Likewise, despite the exactly mechanism involving the onset of the osteoarthritic pathogenesis remains still unknown, the fundamental role of the immune system, among others, is well documented. The production of antibodies against self-antigens, or autoantibodies (AAbs) is one of the main features of the humoral response. Therefore, as part of this thesis, a biomarker discovery phase using planar protein arrays was carried out in order to detect a specific immunoreactivity signature of the very early stage of the disorder, which might determine a panel of OA-associated AAbs with potential use as prognostic biomarkers.

The results obtained by the analysis of a large set of sera at baseline from participants without evident radiological or symptomatic knee OA, belonging to the Osteoarthritis Initiative cohort, have proved the association of different protein biomarkers with the future appearance of radiographic knee OA. On the other hand, the use of multivariable logistic regression analysis has resulted in the generation of two potential prognostic models to predict the incidence of knee OA, which combine protein and clinical markers associated with the development of the disease. In addition, using survival analysis, it has been demonstrated that the baseline serum levels of these biochemical markers are

associated with the time of occurrence of the disease: the higher the levels, the sooner the disease appears.

I. INTRODUCTION

1. OSTEOARTHRITIS

1.1. Definition

Osteoarthritis (OA) is the most prevalent rheumatic disorder in the occidental world and can impact any joint, being the most affected the hands, knees, hips and spine. It is a complex chronic disease originated as a consequence of a dysfunction in a complete organ, which is the joint (Figure 1), leading to the appearance of illness, understanding "disease" as the abnormalities of joint structure and function, and "illness" as the possible clinical manifestations (Kraus et al., 2015). The structures that integrate the joint include periarticular muscles, ligaments, bursae, synovial membrane, cartilage and subchondral bone. In OA, commonly the disease does not coincide with illness, being even possible (and often do) to occur in the absence of symptoms, or in contrast to find definite radiographic features in the joints of a person without symptoms.

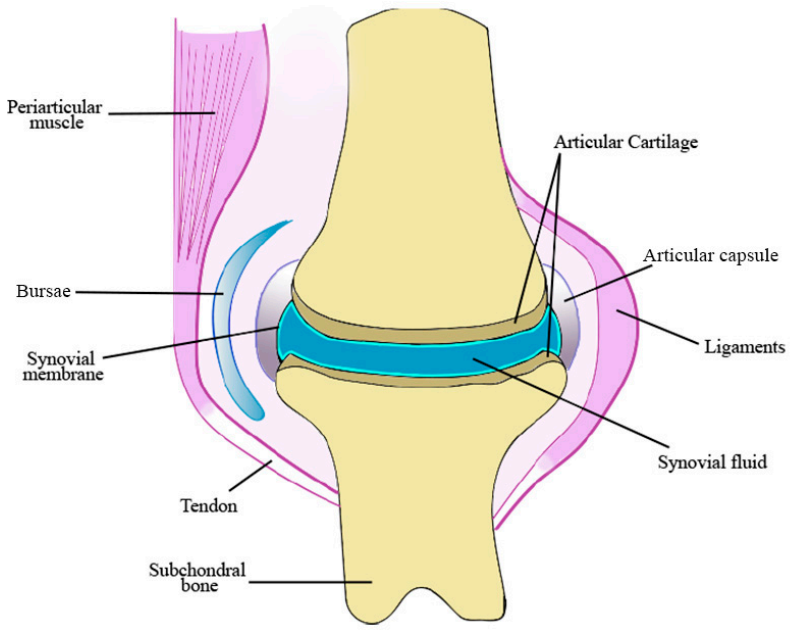

Figure 1. Structure of the human diarthrodial joint.

Recently, the Osteoarthritis Research Society International (OARSI) has endorsed a new definition of OA as a "disorder involving movable joints characterized by cell stress and extracellular matrix degradation initiate by micro- and macro-injury that activates maladaptive repair responses including pro-inflammatory pathways of innate immunity. The disease manifests first as a molecular derangement (abnormal joint tissue

metabolism), followed by anatomic and/or physiologic derangements (characterized by cartilage degradation, bone remodelling, osteophyte formation, joint inflammation and loss of normal joint function), that can culminate in illness" (Kraus et al., 2015). The Figure 2 shows the main alterations occurring in the arthritic process.

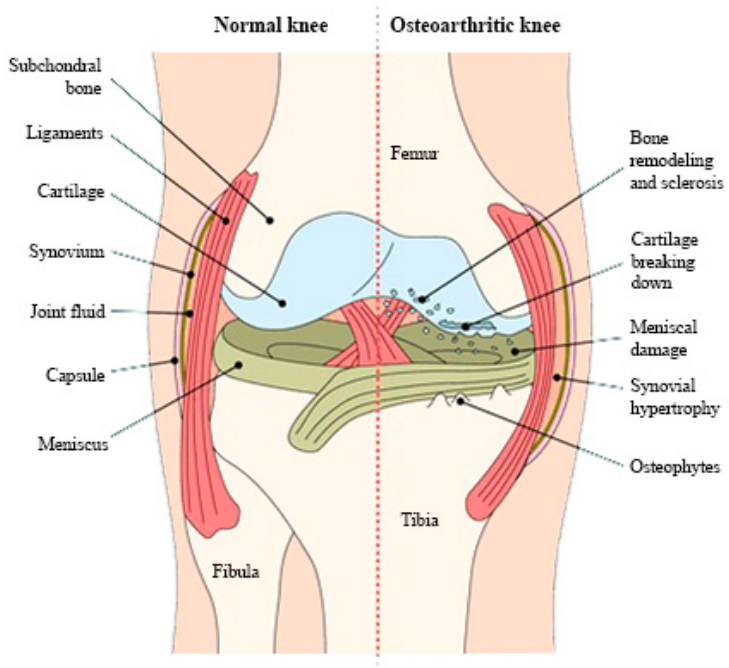

Figure 2. Representation of the main joint structures of the knee and the most important degenerative processes taking place in OA. Image from: Hunter et al. (2006) (Hunter et al., 2006).

OA is very often seen by the rheumatologist at advanced-stages. The disorder is typically develops over decades in a clinically silent phase, offering a wide window of opportunity to potentially alter its course (Migliore et al., 2017). Therefore, an identification of the earlier phases in OA is really important to properly treat patients when there might still be some regenerative ability of the articular cartilage, which is the tissue most characteristically affected in this disease (Madry et al., 2016).

1.1.1. Definition of early knee OA

It is thought that OA may be manifested by a prolonged period of musculoskeletal tissue abnormalities at a molecular and clinically silent level, which can precede the anatomic organ system disease (Kraus et al., 2015). Defining early knee OA is more complicated than established OA, as the signs and symptoms may be limited and sporadic, being manifested only under certain conditions, such as sport activities that

involve long-term loading (Luyten et al., 2012). Thus, a very early OA would be characterized by an asymptomatic disease state.

Classification criteria of early knee OA, although are certainly challenging, are obviously based on the combination of symptoms, signs, and structural changes. Unlike established OA, radiographic criteria defined only by Kellgren and Lawrence (KL) grade will not be enough to identify an early population, and therefore, other methods such as arthroscopy or magnetic resonance imaging (MRI) have been proposed (Luyten et al., 2012).

To be classified as early knee OA, a patient need to fulfill the present criteria:

- Pain in either knee.
- Standard radiographs KL grade 0–1 or 2 (osteophytes only).
- At least one of the following two structural criteria: Arthroscopic findings of cartilage lesions, and/or MRI findings demonstrating damage in the articular cartilage and/or subchondral bone marrow lesions (BMLs).

1.2. Epidemiology and socioeconomical impact

OA can affect to any diarthrodial joint, which are fundamental components for the mobility and autonomy of people. Therefore, any dysfunction on these joints can cause dependence of the individual, and in many cases, permanent disability.

Estimations of OA prevalence are highly variable and depend on the definition of OA, i.e. taking into account the symptoms and/or the radiographic manifestation, the specific joint(s) being evaluated, and other distinctive factors (e.g. age or sex) of the population being studied (Vina et al., 2018). Although all of these reasons lead to a difficult establishment of a global OA prevalence, many data reflect the importance and the socioeconomical impact of this disease. According to the World Health Organization (WHO) Global Burden of Disease (GBD) Study, the global prevalence of radiographically confirmed symptomatic knee and hip OA was estimated at 3.8% (95% confidence interval (CI): 3.6–4.1%) and 0.85% (95% CI: 0.74–1.2%) respectively, ranked both as the 11th highest contributor to global disability in 2010 (Cross et al., 2014). An epidemiological study, called EPISER, carried out by the Spanish Society of Rheumatology (in Spanish, SER) in 2016 showed a prevalence of 7.9%, 5.2%, and 13.9%

for symptomatic hand, hip, and knee OA, respectively, in a population over 65 years old (Seoane-Mato et al., 2018).

The lack of data on the incidence of the disease is a consequence of the difficulty to identify the time at which it begins. However, a recent Spanish study with more than 3 million subjects reported incidence rates (IRs) for knee OA of 6.5/1000 person-years overall, and 8.3 and 4.6/1000 person-years for females and males, respectively. IRs for hip and hand OA were 2.1, and 2.4/1000 person-years overall, 2.4 and 3.5 for females, and 1.7 and 1.3 for males, respectively (Prieto-Alhambra et al., 2014) (Figure 3). This study also showed that knee and hip OA rates increased with age, and females had higher ratios than males, especially over the fifties.

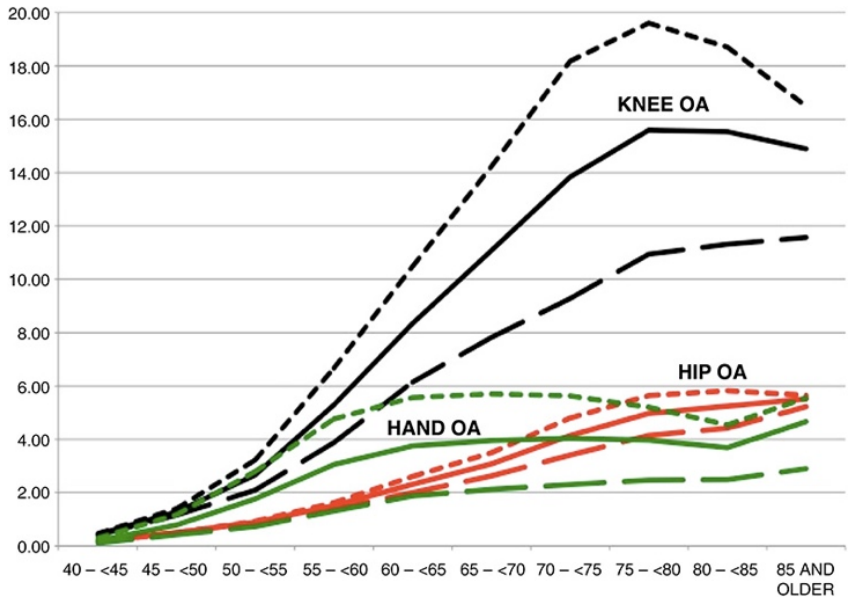

Figure 3. Age and gender-specific IRs (per 1000 person-years) of knee (black color), hip (red color), and hand OA (green color). Solid, short dash, and long dash line refers to all population, women, and men, respectively. Image from: Prieto-Alhambra et al. (2014) (Prieto-Alhambra et al., 2014).

OA, together with cancer, is the second pathology that generates the highest healthcare expenditure, only behind cardiovascular diseases. Its global cost is estimated as the 2% of the gross domestic product (GDP) for the developed countries (Dunlop et al., 2003). According to the ArtRoCad study, the treatments of knee and hip OA involve a direct cost (social cost) and indirect cost (health cost) of almost 5,000 million per year, which means an average cost per patient of 1,500 euros per year (Loza et al., 2009).

As mentioned above, OA is associated with aging. The increase in live expectancy, together with the lack of preventive and therapeutic measurements, anticipate that the prevalence and socioeconomical impact of the disease will increase in the next years.

1.3. Physiopathology

Articular cartilage is a highly specialized visco-elastic tissue that covers the end of the bones of the diarthrodial joints. It acts as a low-friction and load-bearing surface, experiencing different static and dynamic forces, such as shear, compression and tension (Madry et al., 2012). Among its main properties, it should be noted that the articular cartilage is an avascular, alymphatic and aneural tissue, where oxygen and nutrients are principally provided by diffusion from the synovial space (SER, 2010).

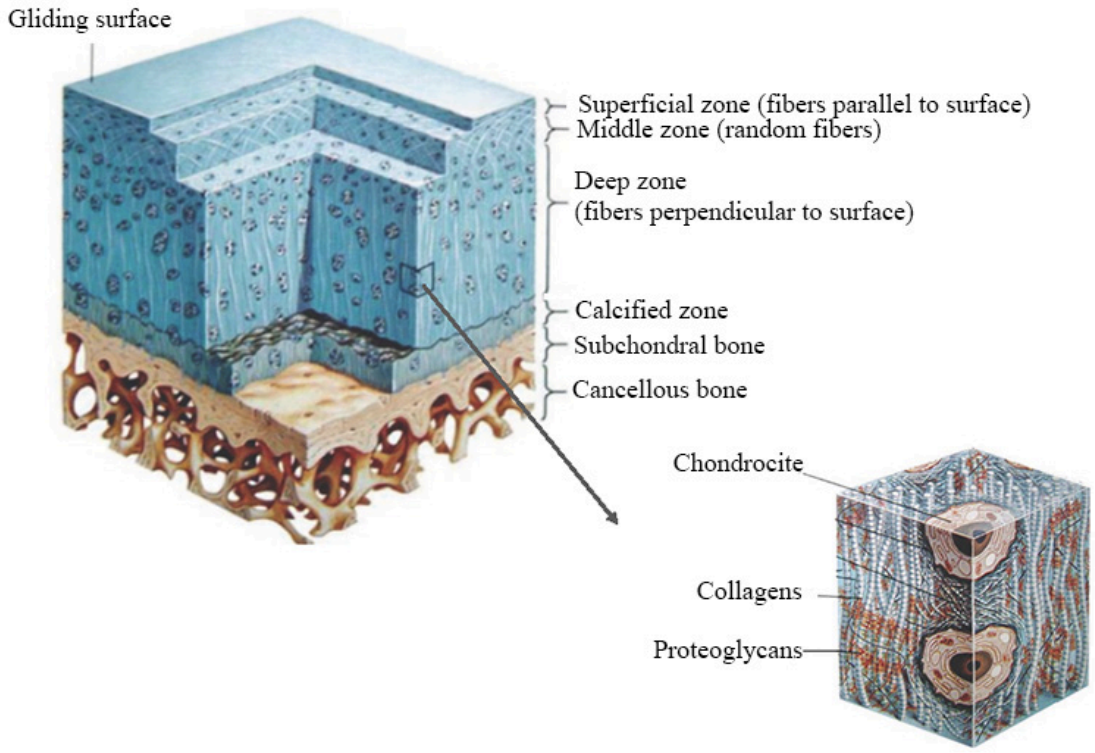

Figure 4. Structure of the hyaline articular cartilage, showing the four structured zones: the superficial zone, the middle zone, the deep zone and the calcified zone. Adapted from: Elsevier.Inc.Netterimagenes.com

Articular cartilage is composed by the extracellular matrix (ECM) and a unique cell type, the chondrocytes, which are responsible of the synthesis and maintenance of the ECM (Figure 4). The biomechanical properties of the articular cartilage are guaranteed

due to the particular organization of the ECM, whose main constituents are collagens (VI, IX, XI, XII and XIV), proteoglycans and hyaluronic acid (Madry et al., 2012).

OA is a multifactorial disease whose pathogenesis includes an overall insufficiency of the entire joint, especially the interaction between the articular cartilage, subchondral bone and synovial membrane (Man et al., 2014). The failure of the repair process of damaged cartilage is the key episode in the pathological process of OA (Bijlsma et al., 2011). It is caused by the contribution of biomechanical and biochemical factors, which alter the tissue homeostasis. In a physiological normal cartilage, chondrocytes are responsible of preserving the ECM homeostasis with a low renewal capacity. However, in a damaged cartilage the repairing attempts fail and determine the predominance of destructive (catabolism) over productive (anabolism) processes (Iannone et al., 2003) (Figure 5). Activation of different pro-catabolic factors, such as tumor necrosis factor alpha (TNF-α) or interleukin-1β (IL1β), lead to an enzymatic degradation of the cartilage matrix by different proteases: collagenases (MMP (matrix metalloproteinase)-1, -13, -8), aggrecanases (MMP3, MMP14, ADAMTS (a desintegrin and metalloproteinase with thrombospondin motifs)-1, -4, -5) or gelatinases (MMP2, MMP9) (Aigner et al., 2007).

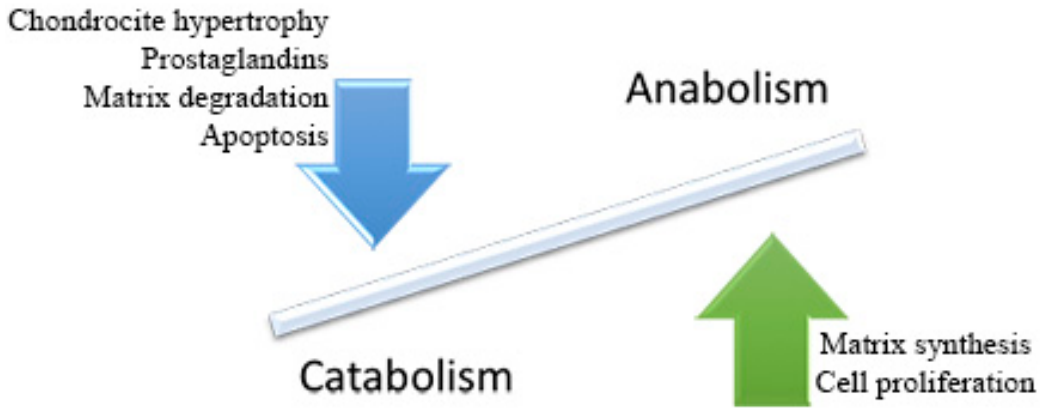

Figure 5. Biological processes involved in the imbalance of the cartilage metabolism in OA.

There are three different theories to explain the imbalance between the catabolism and anabolism in articular cartilage. The simplest theory is based on the *apoptosis or loss of viability of the chondrocytes*. A reduction in the number of these cells limit the tissue capacity to maintain cartilage homeostasis and to repair damage (Aigner et al., 2007).

However, the role of programmed cell death in inducing cartilage damage is a matter for debate, prevailing the idea that apoptosis is a pathway for removing damaged chondrocytes rather than initiating the osteoarthritic process (Iannone et al., 2003). The second theory is referred to *cell senescence*. Here, oxidative stress cause the premature aging of the chondrocytes, limiting their normal capacities to finally give rise to the destruction of the cartilage (Aigner et al., 2007). Finally, the last theory refers to a dysfunction in the cartilage homeostasis is due to a *failure in the ability of the mesenchymal stem cells to differentiate* into chondrocytes. This would disable tissue regeneration processes (Michigami, 2013).

Furthermore, in the pathogenesis of OA there is also an additional and integrated role of the bone. During OA, subchondral bone shows specific anatomical changes characterized by thickening, sclerosis and formation of osteophytes. The sclerosis of the subchondral bone causes a loss of its loads absorption capability. An increase in bone stiffness could be one part of a bigger widespread bone disorder, leading to an enhanced mineralization and/or volume of the affected joint (SER, 2010). In this context, a local increase in growth factors, such as insulin-like growth factors (IGF) 1 and 2 and transforming growth factor beta (TGF-β) (Dequeker et al., 1993), lead to an increment of type I collagen production (Mansell et al., 1998), which stimulates osteoblast metabolism and enhances the synthetic activity of bone tissue.

Finally, another of the key structures involved in the osteoarthritic process is the synovial membrane (Goldring et al., 2011; Hunter et al., 2008; Malemud, 2015; Scanzello, 2017; Sellam et al., 2010). Inflammatory changes of synovium occur in up to 50% of OA patients (Ayral et al., 2005). This affects decisively in the pathogenesis and the degree of clinical manifestations of the disease, including joint pain, swelling and stiffness. On the one hand, the inflamed synovial membrane releases pro-inflammatory cytokines, such as IL1, IL6, Il17, IL18, TNF-α, prostaglandins (PGs) and nitric oxide (NO), which disturb the balance of cartilage matrix degradation and repair (Yuan et al., 2003). Cartilage degradation in turn amplifies synovial inflammation, creating a vicious circle.

On the other hand, although OA is not considered an autoimmune disease, several studies show that cell stress and extracellular matrix degradation may activate maladaptive repair responses, including pro-inflammatory pathways of innate immunity

(Kraus et al., 2015) (Figure 6). In fact, the presence of B and T lymphocytes, macrophages and dendritic cells in the synovial membrane is now considered to be a common finding in OA synovial tissue (Benito et al., 2005; Klein-Wieringa et al., 2016; Li Y. S. et al., 2017; Lopes et al., 2017; Mathiessen et al., 2017). The presence of mediating cells of the immune response in the synovium suggests that different fragments released from the ECM as a consequence of cartilage degradation may act as damage-associated molecular patterns (DAMPS) (Foell et al., 2007). In this sense, DAMPS may activate the complement system of the humoral immunity, acting as autoantigens. This usually involves the production of immunoglobulins against self-proteins or autoantibodies (AAbs), perpetuating the catabolic processes and the inflammation in the joint (Alsalameh et al., 1990).

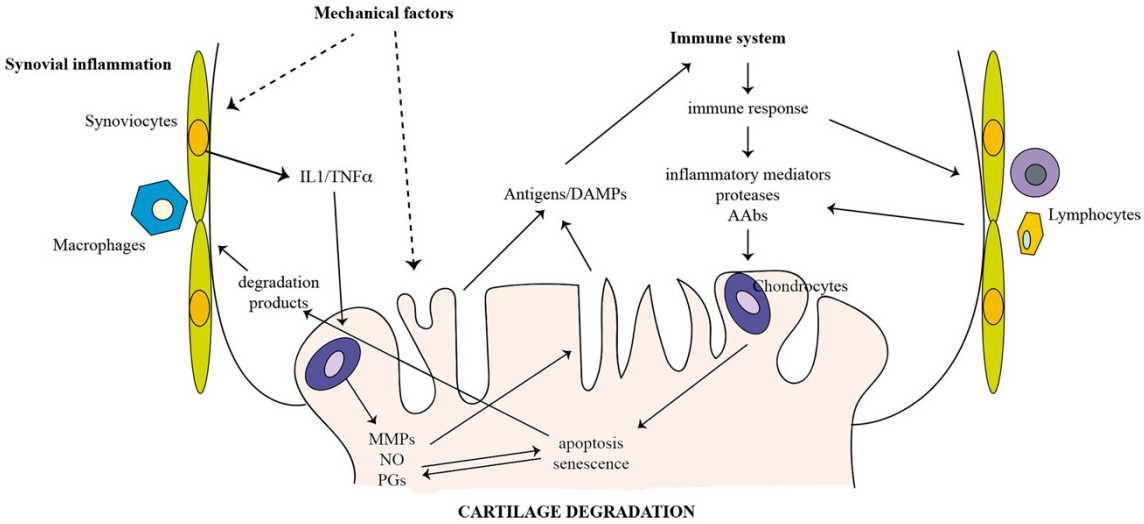

Figure 6. Scheme of the role of the immune system in OA.

Based on this theory, several studies have identified different AAbs against proteins derived from the cartilage, such as cartilage intermediate layer protein (CILP) (Tsuruha et al., 2001), osteopontin (OPN) (Sakata et al., 2001), chitinase-3-like protein 2 (YKL-39) (Tsuruha et al., 2002), fibulin-4 (Xiang et al., 2006) and cyclic citrullinated peptides (Du et al., 2005). Elevated titters of AAbs have been also detected in serum (Austin et al., 1988; Henjes et al., 2014) and synovial fluid (Goldberg et al., 1987) from OA patients. Considering the fact that AAbs can often be detected at the asymptomatic stage, all of these authors suggest that these molecules might have the potential to identify susceptible individuals or populations and facilitate prognosis.

Summarizing all the processes described above, it is clear that OA is a complex and heterogeneous disease. However, in the main pathogenic driver in OA is still a question. It has been traditionally thought that OA is initiated by cartilage degradation. Nevertheless, several of bone changes also take place at the disease onset (Intema et al., 2010), supporting the idea that they occur at least simultaneously or even before than cartilage degradation and thus may be responsible for the initiation of cartilage damage (Nguyen et al., 2017).

1.3.1. Changes in the articular cartilage in early OA.

Early events in OA involve the disruption of the ECM, linked to an abnormal activation of cell surface receptors (Madry et al., 2016). The alteration in the synthesis of lubricin and other superficial proteins lead to an impaired surface lubrication and an increase of friction (Neu et al., 2010; Sakata et al., 2015). The proteoglycan content is also reduced, resulting in the exposition and subsequent erosion of the collagen network. Small collagen fragments are released, activating an inflammatory cascade within the cartilage and triggering the inflammation of the synovial membrane (Scanzello et al., 2012). The increment of catabolic activities causes biochemical changes in the composition of the ECM, leading to a reduced mechanical strength that provokes a higher deformation of the cartilage (Ryd et al., 2015). Early changes also involve a progressive thinning in the subchondral plate (Intema et al., 2010), subarticular subchondral spongiosa thickness (Orth et al., 2014), and synovial inflammation (Ene et al., 2015). In most of the cases, this tissue-related phenomena lead to an established OA.

1.4. Risk factors

The WHO defines risk factor as any attribute, characteristic or exposure of an individual that increases the likelihood of developing a disease or injury (WHO). There are several risk factors described in the literature influencing the prevalence and progression of OA, which can be divided in two different categories: person-level factors and joint-level factors.

1.4.1. Person-level risk factors

1.4.1.1. Sociodemographic

Age. – Although OA is not considered a consequence of aging, older age is probably the best known risk factor for the disease (Allen et al., 2015; Felson et al., 2000; Johnson

et al., 2014; Neogi et al., 2013). The mechanism under the association between age and established OA is poorly understood, but is probably multifactorial (anatomical, structural and biochemical changes) (Litwic et al., 2013).

Gender. – Compared with men, the prevalence of hip, knee and hand OA is higher in women (Palazzo et al., 2016), unlike cervical spine OA (Johnson et al., 2014). Since it is known that incidence rates of knee OA increase in women around menopause (Maleki-Fischbach et al., 2010), several authors have suggested a role of the loss of estrogen levels with the development and severity of OA. However, results are still conflicting (Cirillo et al., 2006; de Klerk et al., 2009; Hanna et al., 2004; Nevitt et al., 2001; Wluka et al., 2001).

Race. – There are known racial and ethnic differences in OA radiographic features (Zhang et al., 2010). Compared with other races, African-American individuals seem to be more likely to develop symptomatic knee and hip OA (Allen et al., 2015; Vina et al., 2018; Zhang et al., 2010).

1.4.1.2. Genetic

The genetic contribution to OA has been strongly supported by many studies, being estimated that around 30-65% of the risk of OA is genetically determined (Allen et al., 2015); Johnson et al.Johnson et al. (146); (Neogi et al., 2013). To date, 21 independent susceptibility loci have been related with OA by genome-wide associated scan (GWAS) studies (Warner et al., 2017).

1.4.1.3. Obesity

Obesity, defined as body mass index (BMI) over 30 kg/m^2, is a well-known risk factor for knee OA (Allen et al., 2015; Johnson et al., 2014; Lane et al., 2017; Neogi et al., 2013; Silverwood et al., 2015). Accordingly, there is a strong relationship between BMI and radiographic and/or symptomatic knee OA: for every 5-unit increase in BMI, the associated increased risk of knee OA is 35% (Jiang et al., 2012). The contribution of BMI for hip OA has been also stablished, but in this case, the association is not as strong as for the knee (Allen et al., 2015; Johnson et al., 2014; Karlson et al., 2003). However, recent studies from Japan (Ohfuji et al., 2016) and Spain (Reyes et al., 2016) found an independent association between weight gain and hip OA diagnosis.

Although it is thought that obesity increases the likelihood of OA appearance because the load over the joint is greater in an obese individual, the role of the fat in OA incidence is still unclear. As the relationship between obesity and hand OA is less evident, there is a tendency to believe that the body fat is affecting the development of the disease in another way (Yusuf et al., 2010), and relate obesity with the inflammation and metabolic effects that occur in the joint (Berenbaum et al., 2013; Sandell, 2009).

1.4.1.4. Diet

A lack of vitamin C, D and K has been suggested to increase OA risk (Felson et al., 2007; McAlindon et al., 2013). However, further studies are needed to improve understanding on the role of the dietary factors in OA development, as there are conflicting results (Arden et al., 2016; Wang X. et al., 2017). In addition to vitamins, research of the role of specific diets has also been published, such as dietary fibre intake using data from different prospective studies (Dai et al., 2017).

1.4.1.5. Bone density and mass

Alteration at the bone level is one of the main features in OA, since they trigger the appearance of both osteophyte formation and bone sclerosis. Because of this, the role of the bone mineral density (BMD) has been deeply studied in the incidence (Neogi et al., 2013) and prevalence (Allen et al., 2015) of the disease. The results suggest that high BMD is a risk factor for OA (Edwards et al., 2017; Gregson et al., 2017; Teichtahl et al., 2017).

1.4.2. Joint-level risk factors

1.4.2.1. Bone shape

Recent evidences describe that patients with acetabular dysplasia (Bouyer et al., 2016) or cam deformity (Saberi Hosnijeh et al., 2017) have doubled the risk of developing hip OA compared with those without deformities. On the other hand, several authors are also exploring the contribution of the changes in the bone area and shape in the development of knee and ankle OA (Hunter et al., 2016; Lu et al., 2017; Nelson et al., 2017).

1.4.2.2. Muscle strength

The association between muscle strength and OA may vary depending of the muscles and joints being studied (Vina et al., 2018).

1.4.2.3. Joint loads

Abnormal loading due to repetitive joint use has been associated with knee, hip and hand OA (Croft et al., 1992; Johnson et al., 2014). In this sense, particular occupations, such as firefighting, construction works, and sports participation have been long associated with greater risk of OA (Cameron et al., 2016; Johnson et al., 2014; Neogi et al., 2013). Specifically regarding sport activities, it is still unclear if the positive association is due to the sport participation itself, or to consequences of injuries that may occur with the practice of the sport (Alentorn-Geli et al., 2017; Driban et al., 2017; Lo et al., 2017). On the other hand, abnormal alignment has been associated with increased structural degradation in the compartment under the greatest compressive stress (Palazzo et al., 2016). Different studies showed that progression of knee OA is associated with varus or valgus alignment (Sharma et al., 2017; Sharma et al., 2001), but not with OA onset (Johnson et al., 2014; Sharma et al., 2017).

1.4.2.4. Injury/surgery

The rupture of the anterior cruciate ligament (ACL) is related with a 13% of cases of early-onset knee OA. Furthermore, the prevalence of knee OA increases between 21–40% when such rupture is associated with cartilage damage, subchondral bone, collateral ligaments or/and menisci (Oiestad et al., 2009; Sanders et al., 2017; Slauterbeck et al., 2009).

Surgery has been postulated to confer risk to develop knee OA (Suter et al., 2017), even if it is just a partial meniscectomy (Han et al., 2016).

1.4.2.5. Pre-radiographic lesions

The predictive value of pre-radiographic lesions may be detected only by MRI. New studies have shown the association between synovitis (Atukorala et al., 2016), BMLs, cartilage damage and menisci extrusion (Sharma et al., 2017; Sharma et al., 2016) with the development of knee OA.

1.5. Clinical features and diagnosis

OA is a heterogeneous disease with a variety of potential pathophysiological drivers. This leads to multiple phenotypes that may represent different mechanisms of the disorder (Dell'Isola et al., 2016). According to the OA phenotype, many of which can overlap in the patients, the specific clinical manifestations of the disease are likely to differ. Thus, each phenotype may be treated and targeted differently, allowing patient stratification and the development of precision medicine strategies for OA (Mobasheri et al., 2017).

Intermittent pain is the first and main symptom that cause patients to visit their family doctor. In early knee OA is suggested that pain should be present at least in two episodes for more than 10 days in the last 12 months (Luyten et al., 2012). During the course of the disease, patients can also describe mild swelling after excessive stress, typically after the practice of sport, light crepitation, inflammatory flames, stiffness, and loss of movement and function (Madry et al., 2016). Taking together, OA symptomatology result in a limitation of the patients' day-to-day activities, causing depression and disturbed sleep, finally diminishing their quality of life (Bijlsma et al., 2011).

Currently, OA diagnosis depends of several items, including clinical history, physical examination of pain and function, structural measures by imaging technologies, and other analysis such as biomarkers –in the form of molecules or molecular fragments released to the biological fluids as a result of joint tissue metabolism– (Bijlsma et al., 2011). There are different diagnosis criteria in the literature, but in all cases the disease is confirmed when OA is stablished and more than 30% of the joint has been destroyed. To date, the most employed criteria to diagnose hand, hip and knee OA have been proposed by the American College of Rheumatology (ACR), and include clinical manifestations, radiological signs and biological parameters (Felson et al., 2011) (Table 1). Although structural abnormalities are part of the diagnosis criteria, imaging techniques are more useful to establish the severity of joint damage and to monitor progression rather than to confirm diagnosis (Bijlsma et al., 2011). Current imaging methodologies include radiography, MRI, position emission technologies (PET), ultrasound or arthroscopy.

Plain radiography is the gold standard in studies involving diagnosis and progression of the OA since is inexpensive, fast, easily available and widely interpretable (Finan et al., 2013; Guermazi et al., 2013; Hayashi et al., 2017). It is accepted by the regulatory agencies as a primary objective to demonstrate the efficacy of the disease-modifying

osteoarthritis drugs (DMOADs) (SER, 2010). However, radiographic measures entail ionic radiation exposure and are less than adequate for assessing diagnosis and progression of the disease for many reasons (Eckstein et al., 2015): (I) they provide an indirect measure of the cartilage thickness, as they only indicate changes in the bone; (II) the measurement of the joint space, performed in a sole plain, is highly variable depending on the position of the joint when performing the radiography; (III) the cartilage changes may be confounded by meniscal cartilage lesions and meniscal extrusion; (IV) soft tissues abnormalities in the synovial tissue or bone marrow are undetected; and (V) plain radiography is usually poorly correlated with joint function. All of this features make this methods not sensible enough either to detect early stages of OA (Raynauld et al., 2004) or in the assessment of changes in the progression of the disease (Guermazi et al., 2013).

Table 1. ACR criteria to diagnose hand, hip, and knee OA.

Hand
Hand pain plus, at least, 3 of the following criteria:
• Thickening of bony structures of more than 2 to 10 interphalangeal joints of both hands. • Thickening of 2 or more distal interphalangeal joints. • Inflammation of 2 or more interphalangeal joints. • Deformation of at least 1 of 10 selected joints of both hands.
Hip
Hip pain plus, at least, 2 of the following criteria:
• Globular sedimentation rate < 20 mm/h. • Presence of osteophytes. • Joint space narrowing (JSN).
Knee
Knee pain plus any of the following criteria:
• Age > 50 years. • Morning stiffness less than 30 min. • Crepitation in the active mobilization of the knee. • Thickening of the bone structures in the clinical exploration. • No increase in the cutaneous temperature of the knee

Assessment of the radiological definition of OA is based on the reduction of the joint space, subchondral sclerosis, presence/absence of osteophytes, cystic geodes, and joint dislocations. Different punctuation scores of radiological assessment have been developed, such as the KL classification (Kellgren et al., 1957) and the Outcome Measures in Rheumatology (OMERACT)-OARSI atlas (Altman et al., 2007). The KL score is considered to date the gold standard for radiographic OA despite it lacks precision, especially for early OA. It considers a sequence of four different items for OA grading: height of the joint line, presence/absence of osteophytes, JSN and bone sclerosis (Kellgren et al., 1957) (Table 2). On the other hand, the OMERACT-OARSI Initiative published an atlas in 1996, which was updated in 2007, where medial and lateral compartment are assessed separately (Altman et al., 2007). In this regard, the atlas pretends to improve the interpretation of radiographs of joint tissues and to assist in grading individual radiographic features of the hand, hip and knee for clinicians and clinical trials.

Table 2. KL grading for knee OA.

KL grade	Description
0 (Healthy)	No radiographic features of OA
1 (Doubtful)	Doubtful JSN and possible osteophytic lipping
2 (Mild)	Definite osteophytes and possible JSN
3 (Moderate)	Multiple osteophytes, definite JSN, sclerosis, possible bony deformity
4 (Severe)	Large osteophytes, marked narrowing of the joint space, severe sclerosis, and definite deformity of bone ends

In the last years, the scientific community has shown a growing interest to search and develop more sensitive indicators of OA, which could be used in conjunction or as a substitute for the traditional plain radiography. In that respect, ultrasound has the advantage of imaging the synovial tissue without contrast agents and allowing the visualization of movements (Hayashi et al., 2017). However, the use of this technology is dependent on the experience and skills of the operator. Arthroscopic procedures is an available imaging technique which allows the visualization of the exterior of the cartilage,

but this procedure is sometimes contraindicated because it involves invasive techniques and there are doubts on the reliability of the assessments (Hutt et al., 2015).

Since 2010, there is a slightly increase in the number of studies using MRI in the OA field (Boesen et al., 2017). This is due to the fact that it might detect subtle changes in the joint, providing objective quantitative assessment of the volume, area, thickness and quality of the articular cartilage. Moreover, advanced MRI techniques (T1ρ, T2, sodium MRI, or gadolinium-enhanced MRI) allow more sensitive analysis and scoring systems to improve assessment of cartilage quality and identify cartilage degeneration at an earlier stage (Guermazi et al., 2015). The advantage of MRI is that it provides information about the cartilage quality with good quantitative analyses. Unfortunately, the cost, analytical time, complexity and time for whole-organ analyses restrict its use in research settings and daily clinical practice.

In most individuals, the earlier stages of the disease are clinically silent, and therefore extensive deterioration of cartilage already exist at the time of diagnosis (Blanco, 2014). Thus, identifying individuals at the early stages of OA is not possible by the existing diagnostic tests. In this sense, there is a tendency to believe that a molecular level of interrogation to detect disease-specific biological markers by omics technologies (genomics, proteomics, metabolomics, etc.) is the only way to facilitate the identification of the disease process before changes in joint structure are evident (Kraus et al., 2015). The research community suggests that this search for one or more biomarkers will be essential in the future to identify OA at its earlier stages, or even predict the disease development, characterize the abnormal joint of a given individual to predict the course of the disease and to assess therapeutic response, which might reduce the cost of treatment for patients.

1.6. Protein biomarkers in OA

The advances that the field of proteomics has undergone in the last decade have opened new perspectives in clinical research, mainly in the search for biomarkers.

1.6.1. Definition and generation process

A biomarker is defined as “a characteristic that is objectively measured and evaluated as an indicator of normal biological processes, pathogenic processes, or pharmacological

responses to a therapeutic intervention" (Glyn-Jones et al., 2015; Kraus et al., 2011), which can be objectively evaluated since a qualitative (presence/absence) or quantitative point of view. Biomarkers might include *soluble analytes* (genetic or biochemical molecules) measured in biological fluids, *imaging parameters* (features), detected by radiography and MRI, or even *physiological and histological measurements*, such as gait analysis or synovitis biopsy, respectively (Kraus et al., 2015).

The generation process of new biomarkers represents a challenge that requires a strong combination of basic and clinical research (Henrotin et al., 2015). In such context, a general pathway for developing disease-related biomarkers has been stablished, and includes four different phases (Kraus, 2018) (Figure 7): discovery, analytical validation, qualification and establishment of clinical utility or implementation.

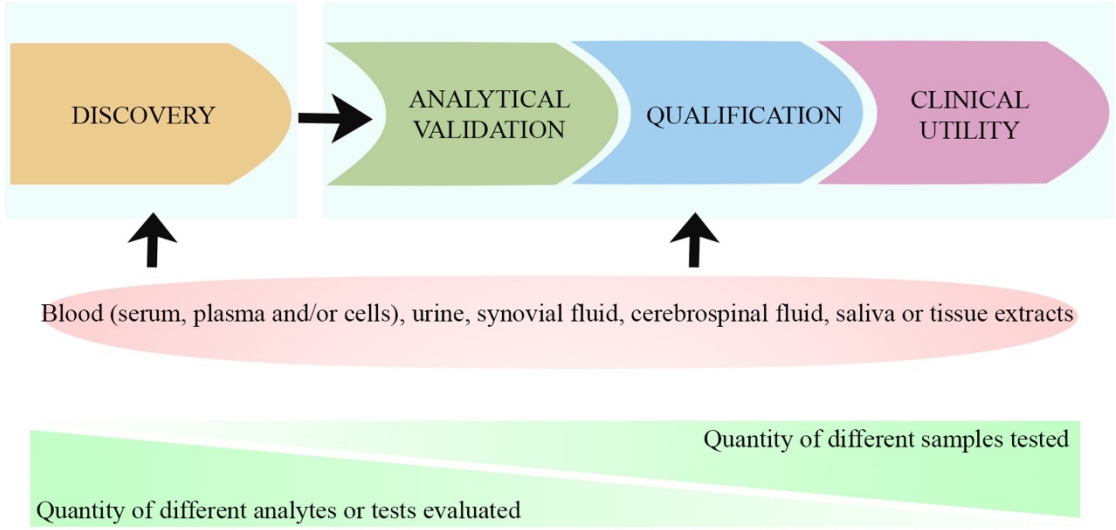

Figure 7. Framework for biomarker development. The generic process of biomarkers generation begins with the analysis of a large number of biomarkers in a small number of sample and culminates with the analysis of a small number of biomarkers in a large number of samples. Samples employed included different biofluids or tissue extracts.

Biomarker *discovery* typically starts with the analysis of a large number of analytes in a small number of samples. This step can rely in the combination of many different technologies, such as imaging, omics technologies and biophysical measurements of organ function. Following discovery, *validation* of a biomarker is the assessment of the assay or measurement performance characteristics to ensure that the biomarker test is reliable, reproducible and of adequate sensitivity and specificity for the proposed use,

which is a necessary component to deliver high-quality research data necessary for its effective use (Wagner, 2002). The clinical relevance of the biomarker in a particular context is confirmed in the *qualification* phase. This qualification phase is necessary to link a biomarker with a *clinical endpoint*, defined as a clinically meaningful measure of how a patient feels, functions, or survives, such that it can be used as a *surrogate endpoint*, defined as a biomarker that is intended to serve as a substitute for a clinical endpoint (Hunter et al., 2010). Finally, the utilization of a biomarker is dependent of their *clinical utility*, which is established by evaluation of biomarker performance in the context of specific procedures, such as disease diagnosis and staging, determination of the need for treatment, selection of a specific treatment, treatment monitoring and dose adjustment.

In 2014, the European Medicines Agency (EMA), in parallel with the Center for Drug Evaluation and Research (CDER) of the US Food and Drug Administration (FDA), published different guidelines for the qualification of biomarkers in the development of new drugs (Bay-Jensen et al., 2016). According with these, biomarkers for drug development are divided in four categories, based on the degree of association with the pathophysiological state or the clinical outcome: exploration (for hypothesis generating research), demonstration (biomarker linked to clinical outcomes), characterization (biomarker reproducibility linked to a clinical outcomes), and surrogacy (biomarker substitution for a clinical end point) (Wagner et al., 2007). However, in OA research, biomarkers can be used not only for drug development, but also for treatment monitoring and as a basis for personalized evidence-based action plans, to facilitate the early diagnosis of OA, evaluate disease progression, and improve disease prognosis (Kraus et al., 2015).

To describe the clinical uses for biomarkers, the Osteoarthritis Biomarker Network, funded by the National Institute of Health (NIH), and the National Institute of Arthritis, Musculoskeletal and Skin Disease (NIAMS) proposed a biomarker classification scheme represented by the acronym BIPEDS to connote six categories of markers: *Burden of Disease* (B, biomarkers associated with the extent or severity of disease among individuals with OA), *Investigative* (I, biomarkers not yet meeting criteria for another category), *Prognostic* (P, predict the future onset or progression of OA), *Efficacy of Intervention* (E, provides information about the efficacy of treatment among those individuals with high risk of developing OA or existing OA), *Diagnostic* (D, classify

individuals as either diseased or non-diseased), and *Safety* (S, indicate presence or extent of toxicity related to an intervention) (Bauer et al., 2006). Based on this classification systems more than one category can describe the current status of a particular biomarker as long as they meet the requirements (van Spil et al., 2010).

1.6.2. Existing biomarkers in the OA disease

In OA, the search for biomarkers has caught the attention of researchers in the last years. This is due to the lack of complete understanding of the disease process, which turns challenging the early diagnosis of the disorder (Ruiz-Romero et al., 2013).

Despite of strong efforts and although interesting biomarker candidates have been identified in OA to date, none of them have been sufficiently validated and qualified to assist diagnosis or prognosis of the disease, nor as clinical outcome in clinical trials or gold standard in the clinical routine. Among these, structural molecules or fragments, such as proteins, linked to a unique type of joint tissue (cartilage, bone or synovium) or common to all of them, are currently the most promising biomarkers in the OA field (Blanco, 2014). They are released into the biological fluids from the ECM turnover and cellular metabolism of the articular cartilage, subchondral bone or synovial tissue (Bijlsma et al., 2011), reflecting the derangements in joint remodelling and therefore, disease progression (Madry et al., 2016).

From this perspective, protein biomarkers can be categorized, according to the OA process that is targeted, as biomarkers of cartilage turnover, bone resorption and formation, synovial inflammation and fibrosis, and inflammatory and metabolic processes (Bay-Jensen et al., 2018). Table 3 lists some of these reported biomarkers that have been associated with diagnosis, prognosis and treatment response. In addition, there are emerging studies on micro-ribonucleic acids (miRNAs) (Nguyen et al., 2017) or AAbs (Henjes et al., 2014) as potential markers of OA.

Table 3. Most studied biomarkers showing association with OA diagnosis, prognosis and treatment response. (SF, synovial fluid; S, sera; P, plasma; U, urine).

Type	Biomarkers	Sample	BIPEDS
Biomarkers of cartilage turnover	Aggrecan fragment	SF	D/B
	Cartilage oligomeric matrix protein (COMP)	SF/S	B/P
	Neoepitope of COMP	SF	B
	Propeptide of type II collagen, isotype A (PIIANP)	S	P
	Collagenase-mediated degradation fragment of type II collagen (C2C)	U	D/P
	C-terminal telopeptide of collagen type-II (CTXII)	S/U	P/E
Biomarkers of bone resorption and formation	Osteoprotegerin (OPG)	S	D/B
	OPN	P	B
	C-terminal telopeptide of collagen type-I (CTXI, CTXIα, CTXIβ)	S/U	P
	Croslinked N-telopeptide of collagen type-I (NTXI)	S	P
Biomarkers of synovial inflammation and fibrosis	Fragment of type-I collagen generate by MMP	S	E
	Fragment of type-III collagen generated by MMP		
	Metabolite of C-reactive protein (CRP) generated by MMP	S	E
		S	D/P
Biomarkers of inflammatory and metabolic process	Adipokines (Adipsin and leptin)	S	B
	CXC chemokine ligand-12 (CXCL12)	P/SF	D/B
	Hipoxia-inducible factor 1α (HIF1α)	SF	D/B
	IL (IL1β, IL21, IL6, IL8)	S/P	D/B/P
	Irisin	S/SF	D/B
	TGF1β	S	D
	TNFα	S	D

1.6.3. Sources for biomarkers

Blood, plasma and/or serum and urine are the main biological sources of biomarkers, due to its easy acquisition. However, molecules released by the articular cartilage may be highly diluted and become undetectable in these biofluids, or even more important, as systemic biomarkers, they may be confounded by other physiological or pathological processes originating from other tissues (Blanco, 2014). Therefore, in OA there is an inclination towards an "inside-out" approach from synovial fluid-based discovery to serum verification (Kraus). In this sense, synovial fluid is more proximal to the disease process, providing an ideal source of direct biomarkers for OA. Nevertheless, the

difficulty to obtain this biological fluid in the clinical practice and the small amounts that can be extracted are important issues that limited its used (Blanco, 2014).

1.7. Treatment

Currently, the American Academy of Orthopaedic Surgeons (AAOS) (Jevsevar, 2013), the OARSI (McAlindon et al., 2014), and the ACR (Hochberg et al., 2012), have developed different guidelines to standardize and recommended the available treatment options. In general terms, the OA treatment is focused in the control of symptoms and the improvement of the functional capacities of the patients (Mora et al., 2018).

There are three main treatment modalities: non-pharmacological, pharmacological, and surgical (Vargas Negrín et al., 2014). In many patients these modalities may be combined or adapted to individual needs (Bijlsma et al., 2011). Patients with OA should receive at least some treatment from the first two categories, reserving surgical management for those who do not improve with the prior modalities SinusasSinusas (269).

1.7.1. Non-pharmacological treatment

Non-pharmacological therapies entail self-management interventions, which should be patient-centred, considering their needs and preferences to promote their active participation in the management of the disease (Bijlsma et al., 2011). They are considered as the first line of treatment, as they constitute the basic pillar of treatment, especially in hip and knee OA, presenting few or no adverse effects.

Non-pharmacological interventions involve patient education to change his/her lifestyle (Gay et al., 2016). Regarding this, exercise has been widely proved to have a positive effect in patients suffering OA, but it is unclear if particular practices are more effective than others and they have to be adapted depending on the specific joint that is affected and the patient's features and capacity. Weight reduction, biomechanical intervention, and other treatment modalities (acupuncture, transcutaneous electrical nerve stimulation (TENS), ultrasound, electrotherapy, insoles or lasers) are also key elements to promote wellbeing and to manage symptoms (Bijlsma et al., 2011; Fibel et al., 2015; Newberry et al., 2017).

1.7.2. Pharmacological treatment

Pharmacotherapy should be used in combination with the non-pharmacological therapy and just in those patients who fail to respond at this first line of treatment to reduce pain and maximize functioning (Majeed et al., 2018). As OA patients are mainly in the elderly and will have multiple comorbidities, special attention should be paid in the adverse effect that systemic medication can cause in this population (Mora et al., 2018).

Betwixt the pharmacological treatment there are three main groups of drugs: traditional analgesics, such as paracetamol, Non-Steroidal Anti-Inflammatory Drugs (NSAIDs), including acetaminophen, duloxetine, capsaicin, and opioids; Symptomatic Slow Action Drugs for OA (SYSADOAs), involving chondroitin, glucosamine, intra-articular steroids, hyaluronic acid, platelet-rich plasma; and biological agents based on genetically engineering proteins that target specific locations of the immune system, in particular monoclonal antibodies against nerve growth or different cytokines (Majeed et al., 2018).

1.7.3. Surgical treatment

Since it is the most invasive and expensive treatment, surgical approaches must be only considered for patients whose symptoms did not responded to conservative treatments or in advanced OA, when there is no other possible procedure (Sinusas, 2012). The surgical treatments are carried out in order to preserve or restored joint surfaces, replace joints with artificial implants, and fuse joints .

The most common surgical procedures are fusion and joint lavage, osteotomy, arthroscopy and arthroplasty .

2. STUDY COHORTS

In the last years, the lack of knowledge about the course of clinical symptoms and radiographic changes in OA have resulted in an increased interest in developing prospective cohort studies with an adequate follow-up time and a well-characterized population, based on the underlying mechanism that is intended to be understood. In this sense, different public and/or private partnerships have launched several study cohorts, including:

The Cohort Hip and Cohort Knee (CHECK) study (Wesseling et al., 2016). – Includes over 1,000 participants followed for 10 years with early symptomatic knee and hip OA to evaluate clinical, radiological and biochemical variables in order to stablish the course, prognosis and underlying mechanisms of early symptomatic OA.

The Multicenter Osteoarthritis Study (MOST) (Thorlund et al., 2016). – Enrolled 3,026 participants with OA disease or at increased risk of developing it followed for 84 months.

The Framingham Osteoarthritis Study (FOS). – Consists of the active (surviving and those not lost during the follow-up) descendants of the original *Framingham Heart Study* cohort, that were invited to participate in a OA study between 1992-1995 (Hunter et al., 2008; Niu et al., 2017). This original study cohort was assembled in 1948 to examine risk factors for heart disease. In the early 1980s, Felson and collaborators found this aging cohort as an ideal target population to study knee OA, and its participants were evaluated for OA of the knee during the 18 biennial examination by history, physical examination and a weight-bearing anteroposterior radiograph of the knee (Felson et al., 1987).

The Prospective Cohort of Osteoarthritis A Coruña (PROCOAC) study. – Contains clinical, radiographic, demographic, anthropometric, analytical and genetic data, as well as biological samples from 1161 participants with diagnosis of hip, knee and/or hand OA who have been followed each 2 years since the beginning of the study in 2006. This prospective cohort is registered in the "Registro Nacional de Biobancos" (Code: NRB C.0000424) as part of the "Colección de Muestras para la Investigación en Enfermedades Reumáticas" created by Dr. Francisco J. Blanco García, from the "Grupo de Investigación en Reumatología" (GIR) at the "Hospital Universitario de A Coruña" (CHUAC).

The Osteoarthritis Initiative (OAI) study cohort. – This cohort will be described in depth in the subsection bellow (4.1.), as it is the cohort of patients that has been employed in this doctoral thesis.

2.1. The OAI study

The OAI is a multi-centre, 10-year longitudinal and observational study cohort designed with the ultimate purpose of improving public health through the prevention or alleviation of pain and disability from primarily knee OA (Rego-Perez et al., 2018). The

OAI consortium includes public funding from the NIH and private funding from several pharmaceutical company partners managed by the Foundation for the National Institutes of Health. It counts with the approval of the Institutional Review Board (IRB) of the OAI Coordinating Center at the University of California, San Francisco and the IRBs of each center.

The OAI developed a research resource available to a broad spectrum of scientists and clinicians for its use in the scientific evaluation of biomarkers in OA. It supports investigation of the natural history of, and risk factors for, knee OA onset and progression using both traditional measures of disease as well as data on novel biomarkers developed from the study. To date, 4,796 men and women with or at risk for knee OA aged 45-79 have been enrolled between February 2004 to May 2006 at four centers across the United States (Halilaj et al., 2018):

- *Ohio State University* (Columbus).
- *University of Maryland School of Medicine and Johns Hopkins University School of Medicine* (Baltimore).
- *University of Pittsburgh School of Medicine* (Pittsburgh).
- *Brown University School of Medicine and Memorial Hospital of Rhode Island* (Pawtucket).

The baseline assessment consisted of an initial eligibility assessment by telephone, a screening clinic visit and an enrolment clinic visit. Participants were followed for changes in the clinical status of the knee, including worsening and onset of symptoms and disabilities, for structural abnormalities, and for the identification of imaging and biochemical markers. Data on the clinical and joint status of all subjects and on risk factors for the development and progression of knee OA were collected at baseline and at the yearly follow-up clinical visits. Clinical assessments were evaluated by questionnaires assessing knee pain, aching and stiffness, and physical disability, which include the Western Ontario and McMasters Osteoarthritis Index (WOMAC), the Knee Outcomes in Osteoarthritis Survey (KOOS) and the Medical Outcomes Study Short Form 12, an examination for knee swelling, tenderness and limited motion, assessment of pain and arthritis in other joints, and questions about use of medications for joint pain and arthritis. The assessed risk factors include examinations and questions evaluating OA in other joints, history of knee injury and surgery, abnormal biomechanics stresses due to

knee alignment abnormality, obesity and heavy physical activities, several nutritional factors and use of certain medications. Materials for the identification of biomarkers include MRI and radiograph images (for imaging biomarkers), and blood and urine (for biochemical and genetic markers), which were collected at baseline and at all follow-up visits. Blood was processed for serum and plasma. An extended overview of cohort study design, together with all collected data over time, is summarized and available in a public archive online (https://data-archive.nimh.nih.gov/oai).

Consistent with the emphasis of the OAI on the onset and progression of knee OA, the study comprises a very well clinically characterized population of individuals divided in two primary subcohorts: (I) those with clinically significant knee OA at baseline (*progression subcohort*) followed for worsening of disease, and (II) those without clinically significant knee OA at baseline, but selected on the basis of having specific characteristics which give them an increased risk of developing incident symptomatic knee OA during the study (*incidence subcohort*). In addition, the study also include a third subcohort or reference control group whose participants did not have either symptomatic knee OA or risk factors at baseline (*non-exposed control group*), with the purpose to provide normal reference data in subjects recruited and evaluated using the same methods as the rest of the OAI participants.

This study design carried out by the OAI positions this cohort as an ideal target population to evaluate relevant biomarkers across the initial onset of symptoms and structural abnormalities, progression of subclinical to clinically overt disease, and worsening of clinically overt disease.

3. PROTEOMIC APPROACHES FOR BIOMARKER PROFILING

3.1. Definition of proteomics

The term “proteomics” was first used in 1996 (Wilkins et al., 1996) by Mark Wilkins referred to the “PROTein complement of a genOME”. Today, proteomics evolve a wide range of methodologies allowing the global-scale characterization of the complete set of proteins in a biological system, including their functionality, structure, modifications, and localization (Hixson et al., 2017). The overall set of proteins expressed by an organism is called *proteome*.

Therefore, proteome is an expression of the organism's genome. However, the proteome of a cell presents some features that make it more complex than the genome: (I) the genome is identical in all cells from a particular pluricellular organism and the proteome is characteristic for each cell type (SEprot, 2014), and (II) unlike the stability presented by the genes, the proteins in an organism (together with their structure, function and localization) are continuously fluctuating from time to time and cell to cell in response to different factors, such as organism's developmental stage, as well as to internal or external signaling events (Nature). The wide dynamic range of the proteome lead to a single individual presenting infinite different proteomes through his entire life.

Due to the complexity of the proteome, challenges in proteomics include not only the identification of all the proteins expressed under health or disease conditions, but also the characterization of protein modifications, interactions and structure (Hixson et al., 2017). With the creation of the Human Proteome Project (HPP), the quantity and complexity of the data derived from the sequencing and mapping of the human proteome has been estimated to be at least three times greater than that involved in the Human Genome Project (HUPO, 2010), which entails that the acquisition, analyses and interpretation of the complete set of data requires well-integrated, high-throughput technologies.

3.2. Applications of proteomics

Advanced proteomics has been a revolution for the systematic analysis of proteins, going from the analysis of a single protein to proteomes, from static to dynamic measures and from the population level to single cells (Breker et al., 2014). According to the main challenges of the proteomic field, there are three main areas of study (Lau et al., 2003): *Descriptive* or *structural proteomic* (identification and characterization of all the proteins in a biological condition), *differential* or *comparative proteomic* (identification of the alterations in protein expression related with a determined biological condition), and *functional proteomic* (study of subcellular localization and distribution of proteins, as well as their interactions).

In the biomarkers field, proteomics is particularly important for early diagnosis, prognosis, and to monitor the disease development (Aslam et al., 2017). Most diseases are manifested at the level of protein activity, since proteins are the essential building

blocks of life (Thul et al., 2018) and the only ones able to reflect the physiological state of cells (Hsu et al., 2009). Among the different types of proteomics, comparative proteomics have a particular interest in biomedicine here since it makes possible to identify and quantify potential protein biomarkers whose abundances will determine the disease onset or progression.

3.3. Proteomic strategies for biomarker detection

In proteomics, biochemical markers include one or more (panels) proteins or peptides. As described above, generation of new biomarkers involves a long and challenging number of steps from discovery to clinical application, and the approaches used in each phase should be carefully selected.

As protein expression by itself is extraordinarily complex (considering post-translational modifications, isoforms and truncations), acquisition of a high number of false data that are technology-dependent is one of the major challenges in the generation process of protein biomarkers. To prevent this, candidate biomarker discovery typically encompasses a set of different high-throughput technologies that allow the analysis of hundreds, or even thousands, of proteins and peptides in the same assay in a small number of samples (Kraus, 2018). These can involve different fraction steps, as well as top-down and bottom-up proteomics strategies, depletion of high abundance proteins, enrichments of low abundance proteins, mass spectrometry technologies and data analysis (Boschetti et al., 2018). Nowadays, the most important analytical approaches for proteomic studies are liquid chromatography coupled to mass spectrometry (LC-MS/MS)-based techniques and affinity arrays. If data converge, the chances of having a potential panel of biomarker candidates become solid, and the study continues on larger cohorts and controls.

For the analysis of the few potential biomarkers reaching the validation phase, western blotting and Enzyme-Linked ImmunoSorbent Assay (ELISA) continues being the gold standard in the vast majority of the laboratories. However, advances in proteomics have created a demand for miniaturized and multiplexed assays displaying higher or at least the same sensitivity, selectivity and specificity. In this sense, diverse mass spectrometry approaches such as Multiple Reaction Monitoring (MRM) (Gillet et al., 2012), or multiplexed protein arrays (Gonzalez-Gonzalez et al., 2012) are becoming the techniques of choice in the validation of biomarker candidates of a disease process.

4. AFFINITY ARRAYS FOR PROTEIN DETECTION

4.1. Definition and history

Historically, the beginnings of affinity arrays for protein detection lie in the development of immunoassays. Shortly, protein arrays can be defined as a miniaturized immunoassay that allows high-throughput studies for the analysis of hundreds to thousands of different proteins presented in small volumes of complex mixtures on a single experiment.

After antibodies were used from 1929 in the serological field to precipitate antigens for subsequent quantification, the analytical immunoassay technology has greatly advanced (MacBeath, 2002). The first immunoassay was born in 1959 from the hands of Rosalyn Sussman Yalow and Solomon Aaron Berson (Yalow et al., 1959), who described the concept of competitive radioactive isotope-labelled antigen detection method, namely radioimmunoassay (RIA), for the detection of insulin in plasma. Despite its great reception by the scientific community, the concerns regarding to the use of radioactive substances led to search for non-radioactive alternatives. Even with the initial scepticism, Eva Engvall and Peter Perlmann (Engvall et al., 1971) developed in 1971 the ELISA immunoassay, demonstrating the feasibility of quantitative measurements of immunoglobulins (Igs) of class G in sera using alkaline phosphatase as the reporter molecule. Then, after the introduction of the hybridoma technology for production of monoclonal antibodies, Uotila and collaborators (Uotila et al., 1981) proposed for the first time the “sandwich ELISA” concept, referred to the use of two monoclonal antibodies with different specificities, one as a capture antibody and another enzyme-labelled one as detection antibody.

The conceptual foundation for producing immunoassays in a “microspot” fashion was first introduced by George Feinberg in 1961 (Feinberg, 1961). But it was not until two decades later when the basic principles of this “microspot-based immunoassays” was moved forward by Roger Eikins through the introduction of the mass action law in his “Ambient Analyte Theory” (Ekins, 1989). Low amounts of certain capture molecules immobilized as microspots on a solid surface can capture a small proportion of analyte, and this fraction would reflect its concentration regardless both the capture molecule concentration and the sample volume. Therefore, this technology would result in maximum fractional occupancy of the capture molecule (Ekins et al., 1992), leading to a

miniaturized assay format that allows the possibility for measuring hundreds or thousands of analytes in parallel, namely multi-analyte or multiplex analysis (Ekins et al., 1994). Indeed, in the latter part of the 1990s the project began to materialize with the introduction of DNA (Deoxyribonucleic Acid) microarrays (Diez et al., 2012).

In the beginning of 2000s, *protein arrays* evolved from this microspots-based multi-analyte immunoassay as the proteomic alternative to the DNA microarrays (Haab et al., 2001; MacBeath et al., 2000). Right now, they are considered as an innovative, versatile and high-throughput strategy, which entails simultaneously and massively the analysis of hundreds to thousands of proteins of different nature –from purified proteins, such as enzymes, peptides, antigens or antibodies, to complex protein mixtures, as e.g. cell lysates and biological fluids– in a small volume of sample. However, several molecular properties of proteins make printing and building protein microarrays more challenging than DNA microarrays (LaBaer et al., 2005). First, there is no similar amplification process like polymerase chain reaction (PCR), capable of simply and rapidly amplifying and generating a large quantities of protein. Second, proteins are notoriously more unstable than DNA, which decreases the half-life of protein microarrays, making their storage and long-term use more difficult. Third, unlike the simple hybridization techniques of nucleic acids, proteins have demonstrate a wide variety of chemistries, affinities and specificities, which greatly complicates the studies of reactivity, functionality and interaction. Lastly, the production, expression and purification systems of recombinant proteins are difficult to automate and are unpredictable in terms of performance, not guaranteeing the functional integrity of the protein.

Due to the need to maintain protein integrity, accessibility to their binding sites, and activity on the surface of the array for its correct functioning, immobilization processes also represent a great challenge in the field. Currently there are two different approaches that are usually employed for capturing protein to the array surface (Ramachandran et al., 2004): random or uniform. For a *random* immobilization of proteins, aldehyde, epoxy, or amine groups, among others, are used. Proteins interact through their amine or carboxyl groups allowing a number of different orientations. On the other hand, proteins can be tagged at the amino- or carboxyl- termini and immobilized to the array by an anti-tag reagent to assure a *uniform* orientation of all the proteins. In contrast with the uniform approach, the random approach ensures that many faces of the protein are exposed for

potential interactions, but it tends to hold proteins close to the array surface. The uniform immobilization not only holds away proteins from the surface, but also tagging provide an added level of selectivity for the binding of the protein of interest.

Proteins arrays take advantages over the conventional techniques for protein analysis, such as ELISA, western blot or mass spectrometry, because of their ability to detect low abundance proteins in complex milieus without requiring any sample fractioning and without losing test sensitivity and specificity. Furthermore, they allow to multiplex protein detection, which entails the reduction in the time of the analysis and reduces the cost associated to the small reagent and sample volume consumption.

4.2. Applications

In a review from 2012, Zhu and Qian referred to protein arrays as a powerful technology platform that will become one of the leading technologies in proteomics and diagnostic fields in the next decades (Zhu et al., 2012).

To date, the number of applications for protein arrays has dramatically increased for basic research (to elucidate the network of protein interactions or identify substrates for enzymes), clinical research (to search for biomarkers which might facilitate the diagnosis, treatment monitoring, etc. of a certain disease) and pharmacological research (to identify different proteins or peptides as drug targets) (SEprot, 2014). Thus, this technology is perfectly suitable to fill in the gap between biomarker discovery to diagnosis, due to the fact that disease signature can be identified, validated, and finally used for routine diagnostics on the same platform (Cretich et al., 2014).

4.3. Formats

In a protein array, the proteins are immobilized on solid surfaces in a planar or bead-based format. The use of one format or another will depend on the requirements of the study. In this thesis, both planar and bead-based formats have been employed.

4.3.1. Planar array

Planar arrays are generated by immobilization of large amounts of proteins in microspots on a planar solid surface, generally at a special density of at least 2,000 proteins/square centimetres (cm^2) (Wingren et al., 2007). Only 50-500 pl (picolitres) of

protein volume are usually spotted, resulting in a spot size of 100-300 μm (micrometres) depending of the solid surface properties and sample viscosity (Espina et al., 2003).

Proteins can be immobilized on the solid support by two different printing strategies: contact printing and non-contact or inkjet printing (Fuentes et al., 2016). Other printing such as μ-contact printing (μCP) and nanobiolithography also exist, but they are of minor commercial importance (Sauer, 2017). Contact spotters use pins that catch the sample by capillarity, which will be subsequently deposited by physical contact with the surface of the solid support (MacBeath et al., 2000; Zhu et al., 2000). This strategy is a relatively simple and flexible system with regards to both substrate type and hydrophobicity, and probe composition and viscosity. On the other hand, non-contact printing devices form droplets onto the support through jetting systems, such as piezoelectric micropumps (which are the most widely used), a continuous stream controlled by valves or thermal inkjet technology (McWilliam et al., 2011). This is a more complex strategy, but offers a higher printing speed and the droplets formation is consistent and reproducible between array batches (Sauer, 2017). However, unlike contact printing strategy, the non-contact devices are limited by the sample viscosity range.

Besides the printing devices, selection of the solid surface and the surface immobilization strategy are the most important parameters to consider for building planar arrays. There are many different solid support options available (Banuls et al., 2016; Kusnezow et al., 2003), such as inorganic materials (silicon and its derivates), oxide of elements (tantalum, indium, and aluminium), metals (gold or silver), carbon and its composite, synthetic polymers and plastics (polycarbonate, polymethylmethacrylate, nylon or polystyrene), or more sophisticated substances such as nanocrystals. The nature of the solid support may determine probe immobilization strategy, bioreceptor properties and detection mode. Regarding to the surface immobilization strategy, it can be categorized as non-covalent or covalent attachment (Jonkheijm et al., 2008). In the non-covalent strategy, proteins are immobilized onto surfaces by absorption through ionic bonds, electrostatic interaction, hydrophobic and polar interactions. Here, the resulting absorbed protein layer is likely to be random orientated, causing a partial or complete lost in the immobilized protein properties. The second strategy is based on the use of functional groups to covalent couple proteins to the surface by a range of different reactions. As no single solid surface or chemistry meets the assay needs for all microarray

users, a considerable amount of time needs to be spent to find the right surface chemistry and optimize the assay protocols according to each individual purpose (Romanov et al., 2014). Here, several aspects need to be considered, such as the optimal buffer composition to block the array surface –e.g. bovine serum albumin (BSA) or milk powder– prior to application of proteins in order to minimize non-specific unions, the buffer composition in which the sample will be resuspended prior to be printed to ensured protein stability, or humidity conditions during the printing process to avoid, as much as possible, sample evaporation (Kusnezow et al., 2003).

To date, the signal generation on planar affinity arrays includes label-based methods, such as fluorescence, chemiluminescence, quantum dots, gold nanoparticles, or surface enhanced Raman scattering, and label-free methods, such as carbon nanotubes, nanowires, and microcantilevers (Chandra et al., 2011; Gonzalez-Gonzalez et al., 2012). Both strategies have their advantages and disadvantages (Ray et al., 2010). Labelling strategies are laborious and lengthy processes which often alter surface characteristics and natural activities of the query protein. However, they are usually the strategy of choice due to simple instrument requirements. Among these label-based methods, fluorescence is the most used, not only because the signal offers high sensitivity and wide dynamic range, but also due to the fact that the laser scanners developed for DNA microarrays compatible with fluorescent dyes, such as cyanine (Cy3 and Cy5), Alexa Fluor or the R-phycoerythrin (R-PE) complex, were directly implemented into the protein array field at its birth.

In the beginning of 2000's, MacBeath and Schreider (MacBeath et al., 2000) demonstrated that planar microarrays were useful for both the screening for protein-protein interactions, and the identification of the substrates for protein kinases and protein targets of small molecules. To date, planar arrays have been widely used in different fields, from basic research to industrial applications. However, there are still some obstacles which need to be overcome to implement this technology in daily clinical practice, such as low reproducibility and sensitivity, long periods of time to obtain the results, heavy and big instruments with low capacity to system integration and high production costs (Sauer, 2017). In addition, planar array platforms theatrically allows to spot a large number of proteins within one slide for a highly multiplex analysis, but this advantage lead at the same time to a low sample throughput capacity. Because all of this,

planar arrays are considered perfect tools for the discovery and identification of a large number of potential biomarker candidates, and they have been widely used for whole proteomes detection (Phizicky et al., 2003; Zhu et al., 2001; Zhu et al., 2000). Results should be then validated on other technological platforms offering higher sample throughput capacity, such as the bead-based arrays that will be discussed next.

4.3.2. Bead-based array

The basic principle of bead-based arrays, sometimes defined as "suspension" or "liquid" array, relies on immobilization of capture reagents on individual and distinguishable microsphere sets as solid support, which are subsequently separated and identify by means of a flow cytometry read-out system.

The concept of utilizing microspheres as a solid support was described 42 years ago by Horan and Wheeless (Horan et al., 1977), in order to immobilize antigens allowing the identification of antigen-specific antibodies in serum. A decade later, the first attempt of multiplexing bead-based arrays was carried out by McHugh and collaborators (McHugh et al., 1988) by immobilizing diverse antigens from Herpes simplex and cytomegalovirus on microsphere sets with different diameters. Towards the end of 1990´s, a group of interdisciplinary scientist created Luminex Corporation with the idea to generate a high-throughput bioassay platform, enabling rapid, cost effective and simultaneous analysis of multiple analytes within a single biological sample. It was the beginning of the multiplex microsphere array technology under the name of xMAP® (MAP = Multi-Analyte Profiling) technology (Kettman et al., 1998).

Today, xMAP® technology is the most prominent stablished bead-based multiplexing platform to develop protein arrays (Hsu et al., 2009). This technology is built on the use of microsphere sets that are internally dyed with different fluorochromes. Although these dyes contain similar excitation properties, they have a unique emission profile, which provides a unique spectral signature for each individual microsphere set and allows each set to be distinguishable from all others in a multiplex analysis (Graham et al., 2019). In this sense, different microsphere sets can be linked to a certain protein and be combined within a single array to measure multiple analytes simultaneously (Lin et al., 2015). At the beginning, the combination of two different fluorophores lead to the production of a 100-member array of spectrally distinct microspheres. Nowadays, the

addition of a third internal dye has allowed to analyze up to 500 analytes in the same sample (FLEXMAP 3D (3-Dimensions) by Luminex) (Jun et al., 2012).

Nowadays there are several types of xMAP microspheres available, and their selection depends on the type of instrumentation used for detection and the particular analyte of interest (Reslova et al., 2017). The basic microspheres (Microplex® microspheres) are 5.6 μm polystyrene beads whose surface is coated with carboxyl groups, which after being activated allow for covalent immobilization of capture molecules via their primary amine groups. Currently, the most widely used xMAP microspheres are the MagPlax® microspheres. These microspheres differ with the previous ones in size (6.5 μm diameter) and structure, through the addition of a magnetic layer, but they are functionalized by the same carboxyl groups covering the surface. These later microspheres allow for an automated plate washing or magnetic bead transfer, which are very important aspects contributing for both recovery and assay reproducibility.

The signal generation in the flow cytometer-like analyzers is in general performed by two lasers (Reslova et al., 2017): a 635 nm (nanometre) laser beam (red classification laser/light-emitting diodes (LED)), which excites the internal fluorescent dyes in each microspheres allowing for the identification of the spectral address; and a 532 nm laser beam (green classification laser/LED), which excites the fluorescent reporter (typically R-PE) bound to the captured analyte (direct assay) or the detection reagent (usually a secondary antibody, in case of sandwich bead-based assays). This enables for read-out in terms of median fluorescence intensity (MFI) across each distinct microsphere sets. The detection can be performed in different instruments, which differ by their mechanism of fluorescence capture and by the maximum number of analytes and samples that can be analyzed (Graham et al., 2019; Reslova et al., 2017).

FlowMetrix was the first Luminex platform consisting in 64 bead sets that were detected on a conventional flow cytometer. Nowadays, the most basic detection reader, namely MAGPIX, utilizes a flow cell and CCD (charge-coupled device)-basic optics only compatible with magnetic microspheres (Figure 8). The principle of microsphere analysis is based on their magnetic immobilization into an imaging chamber where they are hold for optical analysis. The MAGPIX instrument has a low cost and a compact size, providing up to a 50-plex solution in 96-well-plates. On the other hand, the Luminex

100/200 and FLEXMAP 3D are advanced detection instruments based on flow cytometer principles. Here, microspheres are focused into a rapidly flowing fluid stream, passing through an imaging cuvette where each microsphere is individually interrogated. Luminex 100/200 reader operates on 96-well-plate and a maximum of 100 microsphere regions. The capacity of the 3D platform is further increased by the possibility of analyzing up to 500 microspheres on 384-well plates.

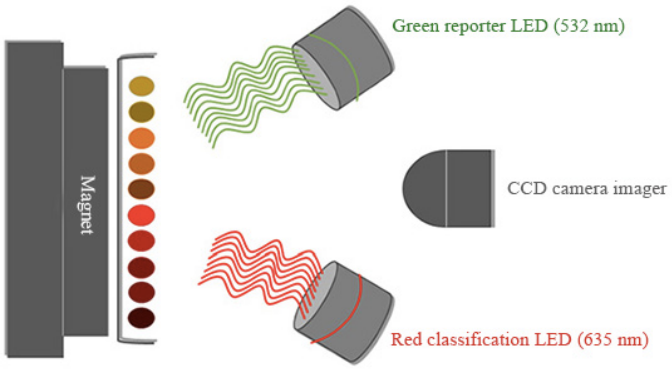

Figure 8. Principle of analysis by the MAGPIX instrument. Image from Reslova et al. (2017) (Reslova et al., 2017).

Although planar arrays allow a greater degree of multiplexing –hundreds to thousands of analytes per cm^2– than that offered by the bead-based platform, their facilities requires scanners, image analysis software and sophisticated printing devices that need for experienced users. A facility based on bead-based arrays are established in less time-frame due to the more user-friendly nature of this array technology. Thus, bead-based arrays have prevailed over the flat surface arrays because of their ease of preparation and use, including no requirement for laborious image analysis and direct collection of data, greater sample throughput, and more flexible and customizable array content.

In order to evaluate the reliability and sensitivity of this strategy, several studies have compared in the last years the bead-based technology with the gold standard assay for biomarker validation, the ELISA technique. In general, these studies reported very high correlations and similar or even better detection sensitivities for bead-based multiplex measurements of cytokines (de Jager et al., 2003; dupont et al., 2005; Elshal et al., 2006) or AAbs (Martins et al., 2004; Martins et al., 2008). Bead-based immunoassays offer less

sample processing time and multiplex capacity than the ELISA technique, leading to less consumption of sample, without compromising analytical sensitivity and accuracy.

4.4. Classification

Protein microarrays may be classified in three main categories (Figure 9): analytical arrays, reverse-phase arrays (RPA), and functional arrays.

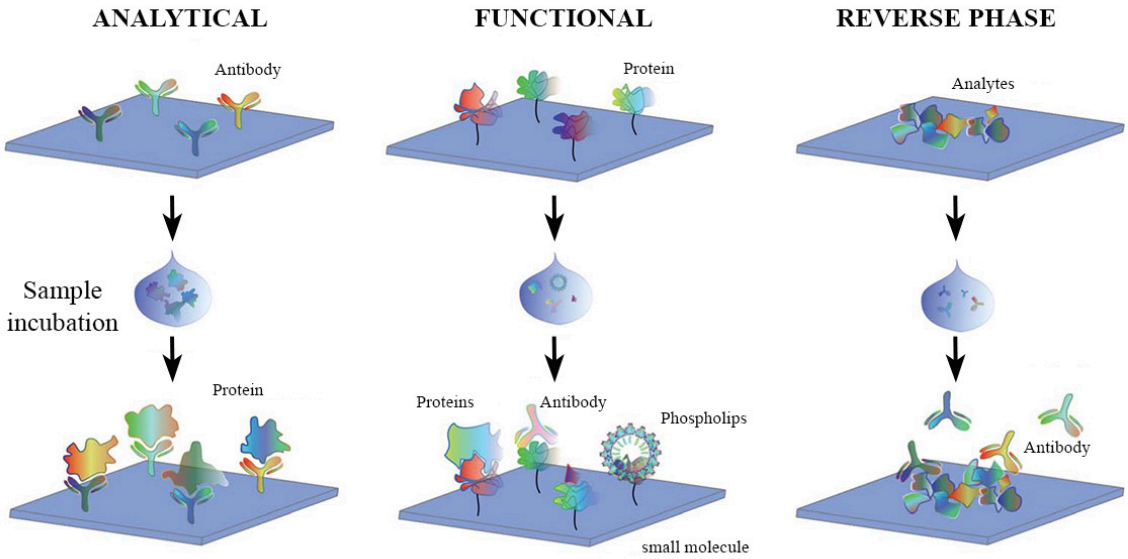

Figure 9. General categories of protein arrays according to their applicability. Adapted from Romanov et al. (2014) (Romanov et al., 2014).

4.4.1. Analytical arrays

Analytical arrays, also called capture, antigen or protein-detecting microarrays, use agents of different nature and affinity properties (e.g.: recombinant protein, aptamers or antibodies), which are immobilized on the solid support of the array (planar or bead-based array) and used as a capture reagent of a certain target protein present in a complex mixture. The captured proteins are subsequently detected and quantified in a relative or absolute fashion. Such approach is typically used for the study of protein expression levels and for measuring parameters such as binding affinity and specificity (Büyükköroğlu et al., 2018; Chandra et al., 2011; Diez et al., 2012), to monitor differential expression profiles, such as protein patterns in response to environmental stress or differences among a healthy tissue respect to a pathological sample, and in clinical

applications (Hall et al., 2007) (e.g.: biomarker discovery and profiling antibody repertories in autoimmunity, cancer, infection or following vaccination).

Antibody-coated analytical arrays represent one of the very early protein array systems, and they are still being one the most used analytical arrays. Their more attractive feature is their capacity of profiling proteins without fractioning biological samples, which allows the detection of a wide concentration range of analytes in a high-throughput and multiplex fashion. The inconveniences of antibody arrays include the possibility of cross-reactivity and the loss of protein activity upon immobilization (Gonzalez-Gonzalez et al., 2012). Antibodies against a specific region may recognized a wrong protein sharing a similar amino acidic sequence or union domain with the target protein, triggering false positive signals and leading to unreliable results and erroneous conclusions. Thus, accuracy and reliability of this type of arrays depends on the affinity and specificity of the selected antibodies.

4.4.1.1. Antibodies: definition and classification

Antibodies, also known as Immunoglobulins (Igs), are roughly Y-shape proteins produced by the B cells of the immune system in response to and counteracting a specific foreign agent, name as antigen. They are large glycoproteins (approximately 1,300 amino acids) consisting of two identical light and two identical heavy polypeptide chains (Figure 10) linked by inter- and intra-chain disulphide bonds.

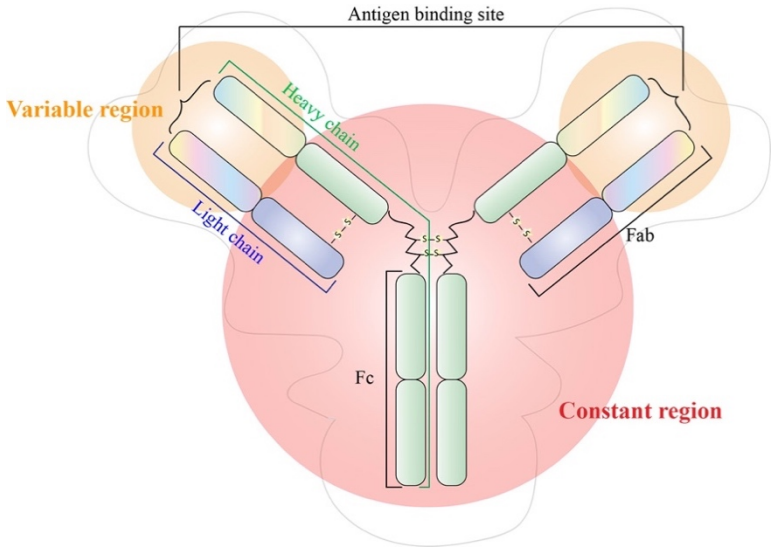

Figure 10. Antibody structure of type IgG, consisting in two identical light and heavy chains.

Both chains, light and heavy, are composed of constant and variable regions (Janeway et al., 2001). The *variable region* of the heavy and light chains contain three regions with extremely variable amino acid sequences, called complementary-determining regions (CDRs), limited to approximately the first 100 amino acids. Together, the variable region of both chains constitute the binding surface of the antigen, so-called paratope, which confers the ability to recognize and bind a specific fragment of the antigen (epitope) and determines the specificity of the antibody. These epitopes can be divided in two classes: *lineal epitopes* (LE), which recognize a consecutive amino acidic sequence, and *conformational epitopes* (CE), which recognize amino acid residues that are separated in sequence, but are spatially near each other in the tertiary structure of the protein (Figure 11). The remaining proportions of the light and heavy chains are called the *constant region*, and make up the C region of the antibody.

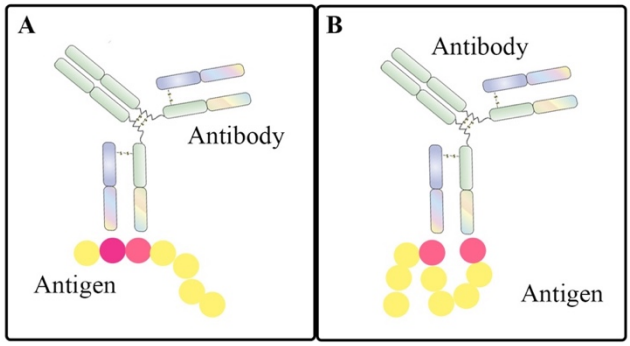

Figure 11. Epitope's types: A. Lineal epitope; B. Conformational epitope. The type of epitope determines whether the protein required (LE) or not (CE) previous denaturalization.

The antibody molecule can also readily be cleaved into two functionally distinct fragments: the Fab fragment (Fab= Fragment Antigen Binding), which contains the antigen-binding activity, and the Fc fragment (Fc = fragment crystallizable), involved in many effector functions, such as binding to proteins of the complement systems or cell surface receptors.

There are two types of light chains, κ and λ, and five types of heavy chains, denoted α, δ, ε, μ and γ. Whereas there are yet not known functional differences between κ and λ-containing antibodies, the five types of heavy chains determine five different classes of immunoglobulins, named as IgA, IgD, IgE, IgM and IgG classes, respectively, which are

closely related but have different structural and functional characteristics. The main functions of the different antibody classes can be briefly summarized as follows: IgA provides localized protection against pathogens in several mucosal surfaces, such as the gut, and the urogenital and respiratory tract; IgD functions as an antigen receptor on B-cells membrane that have not been exposed to antigens yet; IgE is bound to basophiles and mast cells or in low concentration in blood serum and is associated with hypersensitivity and allergic reactions in addition to anti-parasitic activity; IgM is the first immunoglobulin expressed during a primary immune response against an antigen and constitutes 5-10% of the total serum immunoglobulins; and lastly, IgG has the longest half-live in serum (approximately 23 days) and is the predominant antibody in serum during the secondary immune response (80% of the total serum immunoglobulin), namely upon subsequent encounter with the antigen. IgG, as well as IgM, can lead to opsonization of the antigen for destruction and can activate the complement system.

4.4.1.2. Antibody array formats

As shown in the Figure 12, there are two main strategies (Yuan et al., 2017) for antibody microarrays depending on the number of antibodies employed and the labelling and hybridization processes of the samples to be analyzed:

Single-antibody method. – Proteins are captured by an antibody coupled to the solid surface, and its signal is detected by direct or indirect labelling of the sample with different reporter molecules. For direct labelling, proteins are typically labelled with Cy3 or Cy5. The use of intermediate molecules, such as biotin or digoxigenin, indirectly labels proteins within a biological sample, which will be subsequently detected by fluorescent compounds with high affinity for the intermediate reagent. This later strategy lead to the amplification of the target protein's signal. The single-antibody method allows for competitive assays where proteins of two distinct labelled samples are simultaneously incubated and compete to join the antibody. However, it does not allow for absolute quantification of the proteins, and the low label stability might limit signal detection as well as test specificity.

Sandwich-based method. – A pair of antibodies with different specificity against the target protein are used. One of the antibodies is immobilized on the surface of the solid surface to capture the protein from the test sample. Then, the captured protein will be

detected by a labelled secondary antibody, which after recognizing the protein immobilized by the capture antibody will give rise to a fluorescent or chemiluminescent signal, among others, leading to the assessment of the target protein abundance in the sample. The use of two antibodies recognizing different epitopes on the same protein increases test specificity in comparison to direct assays. This increase is also reflected in an increment of the test sensibility by a reduction of the sing-to-noise ratio (Haab, 2005). Moreover, this methodology admit absolute quantification analysis of a certain protein in a sample through the construction of standard calibration curves by serial dilutions of the purified recombinant protein. Challenges developing this strategy include the availability of a functional pair of antibodies and the number of proteins that can be measured within the same assay (Haab, 2005).

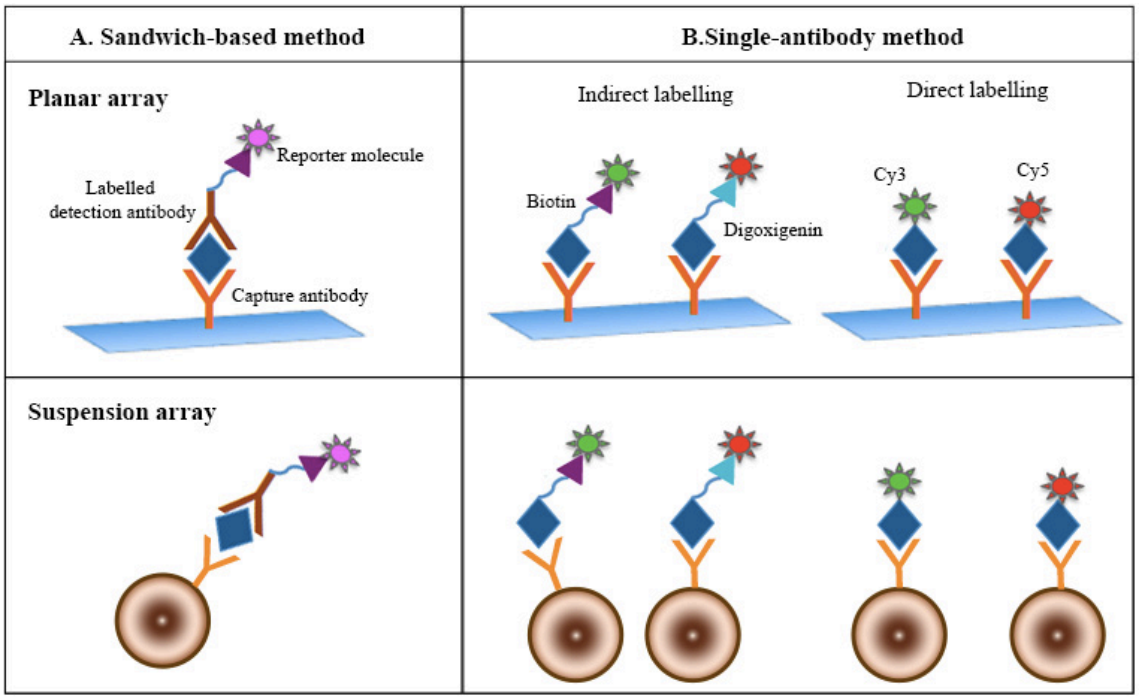

Figure 12. Antibody array formats in planar arrays (above) and suspension-based arrays (below).

4.4.2. Reverse-phase arrays

In case of RPA, cellular and tissue lysates or even serum samples are immobilized, usually onto a nitrocellulose slide, for further detection through an antibody against the target protein. In most of the cases, a fluorochrome-conjugated secondary antibody is used to reveal the antigen-antibody interaction, achieving a higher fluorescence signal

(Ehrlich et al., 2008) and ensuring the signal intensity is directly related with the steric accessibility, the specificity and the binding affinity of the antibody to the target protein (Büyükköroğlu et al., 2018; Diez et al., 2012; Gonzalez-Gonzalez et al., 2012).

RPA were firstly described by Paweletz in 2001 (Paweletz et al., 2001) and today it has become an useful platform in several research fields (Gagaoua et al., 2018; Kuang et al., 2018; Li J. et al., 2017; Macleod et al., 2017; O'Farrell et al., 2019; Zhang et al., 2018).

4.4.3. Functional arrays

Functional protein arrays are composed by arrays containing full-length functional proteins, peptides or protein domains printed onto the array surface in their active state after synthesis and purification using cell-based methods or cell-free expression system (Casado-Vela et al., 2013). Using cell-based strategies, proteins are expressed *in vivo* by cloning the Open Reading Frames (ORFs) –coding region of the protein– in diverse cellular systems, such as bacteria, yeast, plant or mammalian cells (Festa et al., 2013). The expressed proteins are then purified and printed on the surface of the array. The first library, containing almost 6,000 yeast proteins, was developed by Zhu and collaborators in 2001 (Zhu et al., 2001). Nowadays there are several companies that distribute arrays of human recombinant proteins in flat format, such as *ProtoArray™ Human Protein Microarray*, which contains over 9,000 unique human proteins GST (Glutathione S-transferase)-tagged in its latest version (v5.1), or *HuProt™ Human Proteome Microarray* v4.0, which contains the world's largest number of unique human proteins encoded by 17,374 genes, covering approximately 87% of the proteome.

However, despite all these initiatives and commercial platforms, cell-based protocols for protein production, purification, spotting and storage can be laborious, costly, time-consuming, and do not guarantee either the protein integrity on the array, or batch-to-batch reproducibility. To overcome the drawbacks associated to protein arrays generated by cell-based methodologies, an alternative system to express proteins *in situ* –at the time of the assay– was developed (Chandra et al., 2011). Here, proteins are synthesized from their corresponding messenger RNA (mRNA) or complementary DNA (cDNA) templates directly on the surface of the array using *in vitro* cell-free expression systems. Such systems provide the transcriptional and translational machinery necessary for protein synthesis in a cell-independent manner, consisting of RNA polymerases,

ribosomes, transfer RNA (tRNA) and amino acids, enzymatic cofactors, an energy source, and cellular components essential for proper protein folding (Diez et al., 2015). In this sense, different cellular systems have been successfully used to express the proteins of interest, such as *Escherichia coli*, wheat germ, rabbit reticulocytes lysates or human ribosomes from a HeLa cell line (Festa et al., 2013).

Until recently, rabbit reticulocyte lysates were the most used extracts for protein expression, in spite of being the systems with the lowest yield of recombinant protein (Spirin, 2004) and having a significant problem with batch-to-batch variation. This was mainly due to the fact that not only the protein production with this system is very fast and allows to create post-translational modifications in the expressed proteins, but also the rabbit reticulocyte lysate contains chaperones allowing to express the proteins in their three-dimensional conformation (Casado-Vela et al., 2013). Today, however, proteins are typically expressed by human ribosomes and in presence of human chaperones from a HeLa cell line because of its higher efficiency for protein expression and protein levels (more than 10 times higher that rabbit reticulocytes lysate), and a more robust lot-to-lot reproducibility (Festa et al., 2013).

Functional protein arrays provide a flexible platform that allows the development and detection of native proteins, peptides and protein domains, and to study their biochemical characteristics and functions. To date, they have been widely use to examine numerous protein-ligands interactions, including protein-protein, protein-peptide, protein-DNA, protein-RNA, protein-phospholipids, and protein-small molecule interaction, and to identify substrates of various classes of enzymes and post-translational modifications (Zhu et al., 2012). In the clinical research field, functional arrays have been applied for biomarker identification and the analysis of pathogen-host interactions.

Many different functional protein arrays have been developed in the last years, such as Protein In Situ Array (PISA), DNA Array to Protein Array (DAPA), Puromycin Capture Protein Array (PuCa) and Nucleic Acid Programmable Protein Array (NAPPA). Although all of these share their ability to express *in situ* proteins directly on the surface of the array, the processes undergoing in each type of array are different. The processes involved in the NAPPA technology are described next, as it has been the technique of choice in the second study of this thesis project.

4.4.3.1. NAPPA

NAPPA was designed and developed in 2004 by Ramachandran and collaborators (Ramachandran et al., 2004) and has become today one of the most relevant protein arrays in the field (Diez et al., 2012). This technology is based on immobilizing full-length cDNA –not purified proteins– encoding the proteins of interest with a tag, typically GST, in the C termini.

In NAPPA, cDNA templates are shuttled into expression vectors, typically using the Gateway recombinant cloning system that adds a transcriptional promoter, a polypeptide capture tag and an ampicillin resistance vector, and is hosted in bacteria cultures (Diez et al., 2015). The transformed bacteria are grown on a large-scale and selected on the basis of their resistance to ampicillin. Cloning DNA in a specialized expression vector requires a greater time investment than PCR, but presents several advantages: (I) once the clone is generated and storage correctly, it becomes an exhaustible source of plasmid, which can be shared with other laboratories, (II) the clone sequence is stable and valid for long periods of time since it is verified, and (III) the consecutive expression of the polypeptide tag in the vector makes the epitope stable and functional at the time of the expression (Ramachandran et al., 2008).

After lysing the bacteria, the plasmid DNA is purified and printed onto the activated ester surface of the array together with a homo-bifunctional crosslinker (typically bis(sulfosuccinimidyl)suberate (BS^3)), BSA, and the anti-tag antibody. The use of BSA dramatically improves DNA binding efficiency and reduces the unspecific interactions (Ramachandran et al., 2008), while the homo-bifunctional crosslinker helps to the correct orientation of the capture antibody on the array. To express the target proteins, a cell-free coupled *in vitro* transcription and translation (IVTT) system is added to the array, and the nascent protein is immobilized *in situ* through the C termini by the anti-tag antibody printed simultaneously with the expression plasmid, thus assuring the complete translation of the protein. This approach produces an average of about 10 fmols (femtomoles) of protein (LaBaer et al., 2005). The endpoint detection method is based on the use of chemiluminescent molecules or, most frequently, fluorescent dyes (Figure 13).

Advantages of NAPPA platform over the conventional methods include: printing of cDNA instead of proteins, which is more reliable and cheap, avoid the need of expression, purification and storage of proteins, as well as the low half-live of the array since DNA

is a more stable molecule, and guarantees protein integrity by using a mammalian cell-free expression systems and chaperones for its synthesis and folding.

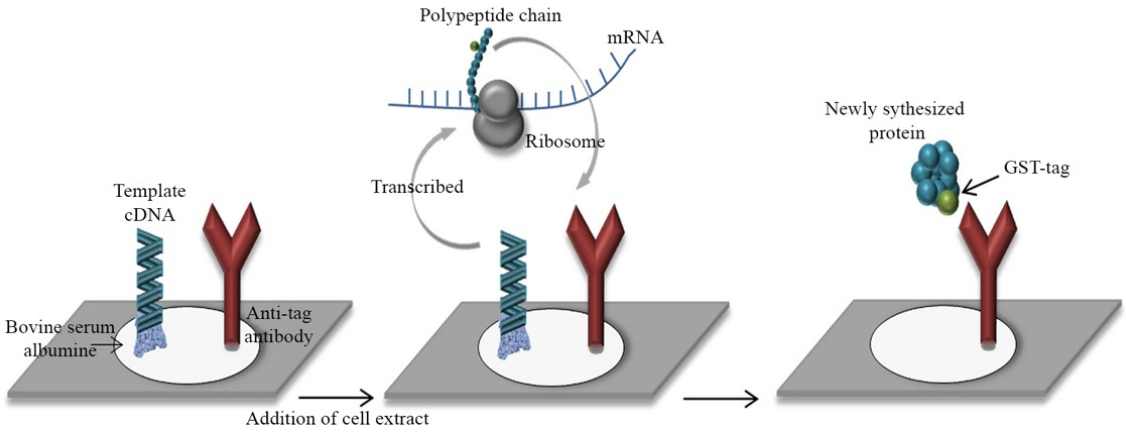

Figure 13. Diagram of NAPPA. Purified template DNAs encoding the proteins of interest with a tag molecule (GST) are printed on the surface of the array together with an antibody that recognizes the specific tag. When the cell extract is added, the transcription and translation are initiated and the expressed protein is captured by the anti-tag antibody. Adapted from Diez et al. (2015) (Diez et al., 2015).

In 2008, Ramachandran and colleagues updated a new version of NAPPA (Ramachandran et al., 2008) with 1,000 human genes, and demonstrated that over 96% of these genes showed a detectable protein signal regardless of protein type –from soluble to membrane proteins–. They also demonstrated that this platform is unbiased in relation to protein size, expressing 98% and 88% of proteins below 50 kilodaltons (KDa) and above 100kDa respectively. To date, more than 16,000 proteins can be displayed on a single slide with reduced inter-feature spacing by ultra-high density NAPPA, avoiding the diffusion of expressed proteins to neighbouring spots (Manzano-Roman et al., 2019).

The NAPPA technology shows an enormous potential in multi-dimensional analysis towards basic and translational research. Up to 2018, almost 1800 papers have been published based on this technology (Manzano-Roman et al., 2019). They describe protein-protein interactions, vaccine development and the evaluation of the autoimmune response (Diez et al., 2015) to search for autoantibodies as a new source of biomarkers in several diseases such as cancer (Katchman et al., 2017), Crohn's disease (Wang H. et al., 2017), type I diabetes (Bian et al., 2017), ankylosing spondylitis (Wright et al., 2012), juvenile arthritis (Gibson et al., 2012), and OA (Henjes et al., 2014).

II. OBJECTIVES

Based on this background, the research was focused on two main objectives, which resulted in four specific objectives.

Main objectives:

A. To validate a panel of proteins previously associated with OA as prognostic markers to predict incident radiographic knee OA.
B. To discover an OA-associated AAbs profile that may be useful as potential prognostic biomarkers of disease incidence.

Specific Objectives:

1. To develop and optimize a custom multiplex sandwich immunoassay with the bead-based xMAP technology to validate and qualify a panel of six potential biomarkers in serum as prognostic biomarkers of incident radiographic knee OA.
2. To discover a profile of AAbs in serum associated with the incidence of radiographic knee OA.
3. To assess whether the inclusion of potential protein biomarkers in a clinical prognostic model improves the predictive capacity of incident radiographic knee OA.
4. To investigate whether the baseline serum levels of the selected biomarkers have any impact in the time of appearance of radiographic knee OA.

III. MATERIAL AND METHODS

1. BIOLOGICAL SAMPLES

All sera analyzed in this thesis were proportioned by the OAI and belong to Caucasian participants from the OAI cohort at the baseline visit. In the case of the validation of a panel of 6 proteins as potential prognostic biomarkers, sera were randomly selected from the incident and progression subcohorts, and the non-exposed control group. For the discovery and validation of AAbs as potential prognostic biomarkers, sera were randomly selected from the incident subcohort and the non-exposed control group.

Patients were not involved during the development of this research, as they were not invited to comment on the study designs and were not consulted to develop patient relevant outcomes or interpret the results.

2. DEFINITION OF INCIDENT RADIOGRAPHIC KNEE OA

The final purpose of this thesis was to validate potential biomarkers that may be used in the clinical routine to predict the incidence of radiographic knee OA. To achieve this purpose 2 main outcomes group, with one study knee per subject, named as target knee, were defined: the incident and the not-incident group. Participants included in both groups were selected on the basis of not having relevant radiographic knee OA (KL grade = 0–1) at the beginning of the OAI study (baseline visit) in the target knee. Incident radiographic knee OA was defined by KL grade ≥ 2 at some point between 12 and 96 months of follow-up.

3. VALIDATION OF PROTEINS AS PROGNOSTIC BIOMARKERS.

3.1. Study design

With the aim of validating the putative ability of the serum concentrations at baseline of different proteins as potential biomarkers to predict the appearance of radiographic knee OA, six proteins were selected from a panel of 20 potential protein biomarkers included in the research project PI16/02124 "*Determinación de índices predictivos de diagnóstico y pronóstico de artrosis de rodilla mediante la validación de biomarcadores protéicos*" funded by the *Fondo de Investigación Sanitaria-ISCIII.* This panel was generated based on thorough mining of experimental evidence in the literature and

previous in-house efforts by proteomic discovery approaches. Proteins included in this study were the retinol binding protein 4 (RBP4), chitinase-3-like protein 1 (CHI3L1), alpha-2-HS-glycoprotein (AHSG), thrombospondin 1 (TPS1), serum amyloid P-component (APCS) and COMP.

The prognostic capacity to predict incident radiographic knee OA of these 6 proteins was blindly validated in 540 individual sera (331 not-incidents and 209 incidents) by sandwich immunoassays using the bead-based xMAP® technology, which were previously generated and optimized. The experimental workflow of the study is represented in the Figure 14.

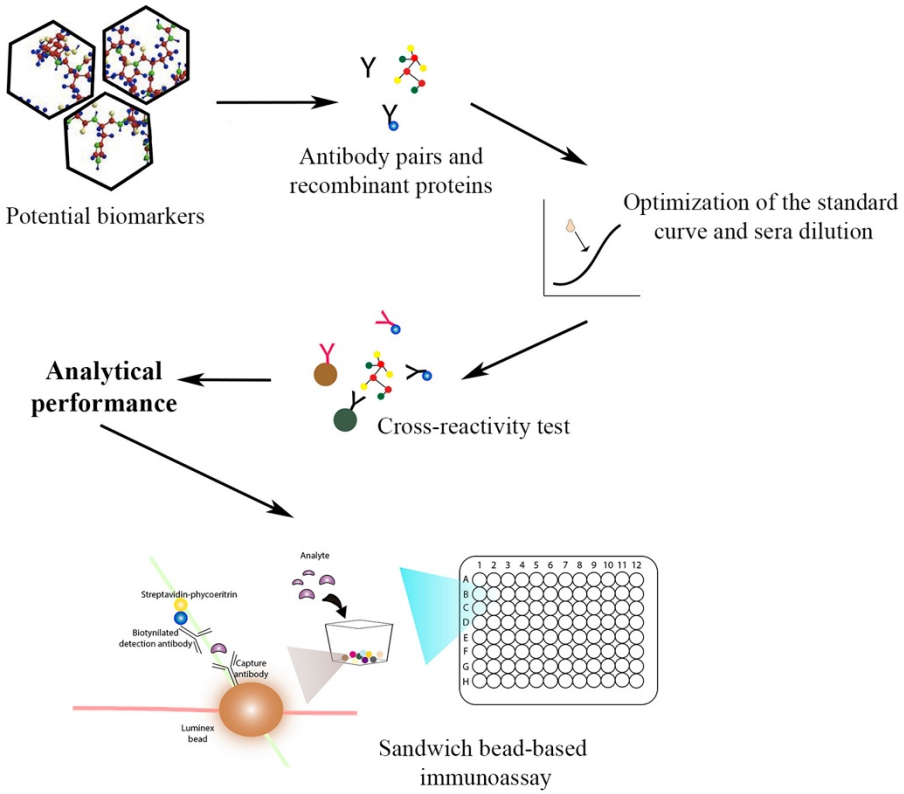

Figure 14. Experimental workflow for biomarker validation. After selection of the potential biomarkers, a capture monoclonal antibody, a detection biotin-labelled polyclonal antibody and a recombinant protein for each analyte were acquired. Assay conditions were optimized for each biomarker in singleplex assays and cross-reactivity of antibodies with the non-target analyte was assessed between those proteins requiring the same sample dilution, in order to generate multiplex sandwich immunoassays. Finally, the analytical characteristics of the tests were evaluated and the custom sandwich immunoassays were used to quantify the selected biomarkers in a large number of sera.

Finally, different clinical variables were combined alone or with the potential biomarkers analyzed in this study to define the best prognostic model of radiographic knee OA prediction by multivariate stepwise logistic regression analysis. The association between the total amounts of these proteins in sera with the relative risk to develop the disorder in time was assessed by survival analysis.

3.2. Antibody pairs and recombinant proteins

The list of all the antibodies and recombinant proteins used in this project is shown below (Table 4), all together with their corresponding catalog numbers as well as the name of the supplier companies.

Table 4. List of antibodies and recombinant proteins.

Reagent	Catalog number	Company
Monoclonal antibody to human AHSG	MAB11841	R&D Systems
Monoclonal antibody to human TPS1	MAB3074	R&D Systems
Biotin-linked polyclonal antibody to human AHSG	BAF1184	R&D Systems
Biotin-linked polyclonal antibody to human TPS1	BAF3074	R&D Systems
Recombinant AHSG human protein	RPA178Hu02	Cloud Clone Corp.
Recombinant TPS1 human protein	3074-TH-050	R&D Systems
Human COMP DuoSet ELISA	DY3134	R&D Systems
Human RBP4 DuoSet ELISA	DY3378	R&D Systems
Human APCS DuoSet ELISA	DY1948-05	R&D Systems
Human CHI3L1 DuoSet ELISA	DY2599	R&D Systems

3.3. Generation of individual antibody suspension bead arrays

Each monoclonal antibody was coupled to an activated bead region to generate the corresponding suspension bead array (SBA) according to the following protocol:

A. Activation of the beads.

The development of each individual SBA with xMAP® microspheres requires the formation of covalent bonds between the primary amines on the monoclonal antibodies and the activated carboxyl groups on the surface of each microsphere. To activate the surface of the beads, the protocol was as follows:

- Eight colour-code magnetic microspheres (MagPlex®, Luminex Corp.) regions were selected; 6 regions to be coupled with each monoclonal antibodies and 2 additional regions to act as negative quality control (QC) beads.
- For each region, a total amount of 500.000 beads was placed on 1.5 mL (millilitre) Protein LoBind Tubes (Eppendorf, catalog number: 0030108116) and washed with 80 µL (microlitre) of phosphate buffer (100mM (millimolar) Monobasic Sodium Phosphate, pH 6.2) on a magnetic stand (Millipore LSKMAGS08).
- Then, 50 µL of the phosphate buffer was added offmagnet to the beads.
- The carboxyl groups on the bead surface were activated by addition of 0.5 mg (milligrams) 1-ethyl-3-(3-dimethylaminopropyl) carbodiimide (EDC, Sigma-Aldrich 3449-1G) and 0.5 mg N-Hydroxysuccinimide (Sulfo-NHS, Life technologies 24510) in a final concentration of 10 mg/mL in 50 µL of the phosphate buffer, followed by 20 minutes (min) incubation at room temperature (RT) in the dark under permanent shaking. To avoid hydrolysis and loss of activity of the activation solution, it was prepared right before use and the procedure was not interrupted until EDC/NHS had been added to the microspheres.
- When the incubation was finished, the activated beads were washed twice with 100 µL 0.1 M MES (2-[N-Morpholino]ethanesulfonic acid, pH 4.5) buffer on the magnet.

B. Coupling of antibodies to the beads.

- Per a half million bead, 1.6 µg (micrograms) of each capture antibody were diluted in 100 µL MES buffer in a 1.5 mL Protein LoBind Tube and saved on ice until use. In addition to the antibodies, two negative QCs were also prepared: 1.6 µg of purified mouse IgG (mIgG, Biorad, catalog number: PMP01X) diluted in 100 µL MES buffer and 100 µL MES buffer without dilution of any antibody (bare beads).
- The 100 µL of each pre-diluted capture antibody and QCs were added to one of the functionalized bead regions and incubated during 2 hours (h) at RT protected from light. The table below (Table 5) reflects the number of the

selected bead regions, their catalogue numbers and the capture molecules coupled to each of them.

- After incubation with the corresponding capture molecule, coupled beads were washed once with 100 µL Phosphate Buffered Saline (PBS) with 0.05% Tween20 (PBST) on magnet.
- Finally, 50 µL storage buffer (Blocking reagent for ELISA (Roche Applied Science 11112589001) supplemented with 0.1% ProClin (Sigma-Aldrich 48912-U) was added to each vial and stored overnight at 4°C to block the antibody-coupled beads from binding further proteins.

Table 5. List of bead regions used in this work and capture molecules coupled to each of them.

Bead region	Catalogue number	Capture molecule
12	MC10012-ID	Anti-human APCS monoclonal antibody
13	MC10013-ID	Anti-human RBP4 monoclonal antibody
18	MC10018-ID	Anti-human AHSG monoclonal antibody
20	MC10020-ID	Purify mIgG
21	MC10021-ID	Bare bead
22	MC10022-ID	Anti-human CHI3L1 monoclonal antibody
26	MC10026-01	Anti-human TPS1 monoclonal antibody
66	MC10066-01	Anti-human COMP monoclonal antibody

3.3.1. Coupling efficiency test

After 24 h, the coupling efficiency for each antibody on the beads was confirmed as follows:

- Two SBA, 50 µL each, were generated by mixing an equal numbers of the corresponding antibody-coupled beads and negative QC-coupled beads in a final dilution 1:50 in storage buffer:
  - *SBA 1*, containing antibody-coupled beads against COMP, RBP4, AHSG, TPS1, APCS plus both QC beads (mIgG and bare beads).
  - *SBA 2*, containing antibody-coupled beads against CHI3L1 and the bare beads control.
- 5 µL SBA –containing a total amount of 1,000 antibody-coated beads per region– was dispensed into 3 wells per each bead-stock on clear-bottom, black 96-well plates (Sigma-Aldrich M5686-40EA).

- 50 µL 1:1000 R-PE-conjugated goat anti-mouse IgG (Abcam ab97024) dilute in 0.05% PBST and 50 µL 1:1000 R-PE-conjugated goat anti-rat IgG (BD PharmigenTM 550767) were incubated with the SBA 1 or SBA 2, respectively, for 20 min at RT in dark.
- Each well was washed 3 times with 100 µL 0.05% PBST on a handheld magnetic separator block for 96-well plates (Millipore, 40-285).
- 100 µL of 0.05% PBST were added to each well and the assay was run on a MAGPIX reader (Luminex Corp.). To obtain accurate results, the bead count should be more than 50 for each region.

To evaluate if the coupling was successful, MFI values were checked. A coupling signal higher than 5,000 MFI was considered as saturated or near to saturation.

3.4. Luminex sandwich immunoassay procedure

The protocol carried out for the absolute quantification of the 6 proteins selected as potential biomarkers was as follows:

- For each immunoassay, equal numbers of the corresponding antibody-coupled beads and the QC beads were properly combined in a bead mixture diluted to 1/50 in storage buffer.
- From the previously prepared suspension bead array, 5 µL were distributed into the wells of clear-bottom, black 96-well plates.
- The SBA was incubated with 25 µL of the diluted standards or sera in 0.05% PBST during 2 h, protected from light while shaking at RT.
- Wells were washed 3 times with 100 µL 0.05% PBST on a magnetic plate separator.
- Then, the specific union of the target protein with the capture antibody was detected by adding 25 µL per well of the proper biotin-label detection antibody (alone or in a mixture when running multiplex sandwich immunoassays) diluted to 1 µg/mL in 0.05% PBST for 1 h covered to avoid the light in constant shaking at RT.
- Wells were washed 3 times with 100 µL 0.05% PBST on a magnetic plate separator.

- To amplify the signal intensity, wells were incubated with 25 µL 1:500 phycoerythrin-streptavidin (SAPE, Invitrogen SA10041) for 20 min while shaking at RT protected from light.
- Wells were washed 3 times with 100 µL 0.05% PBST on a magnetic plate separator.
- Finally, 100 µL 0.05% PBST were added to each well and the MFI signal for each bead population was obtained on a MAGPIX detection reader.

3.4.1. Optimization and generation of multiplex assays

In a first approach, assay conditions related to the standard curve range and sera dilution were assessed for each analyte separately –running singleplex assays– by analysing duplicates of 2 sera randomly selected from the OAI cohorts. The selection of the top standard concentration and sera dilution for each analyte was based on previous results obtained in our group using different antibody pairs and serum samples (Table 6). Twelve -point standard curves were performed by 2-fold serial dilutions. In order to verify that the signal from the serum samples fits within the range of the standard curve, two further dilutions were procured in addition to the dilution selected from the previous test: one double- and one half-concentrated. In the case of RBP4 and AHSG, dilutions to 1:10000 were tested instead of 1:5000, since the signal was lost in these analytes at the latest dilution.

Table 6. 12-point standard curve ranges and dilutions from previous tests.

Analyte	Standard curve range	Sera dilution
CHI3L1	18–0.009	1:40
COMP	20-0.010	1:40
RBP4	40–0.020	1:10000
AHSG	300–0.146	1:100000
TPS1	80–0.040	1:10000
APCS	8–0.004	1:10000

For those biomarkers requiring the same sample dilution, cross-reactivity between the antibody pairs with the non-target analyte was evaluated using a cocktail of its capture antibody-coated beads and a cocktail of its detection antibodies (Figure 15). The highest concentration in the standard curve of each recombinant protein included in the multiplex

assay was individually tested against the proper antibody mixture. Cross-reactivity was determined to be an off-target reactivity ≥ 5% of the MFI observed for the cognate ligand.

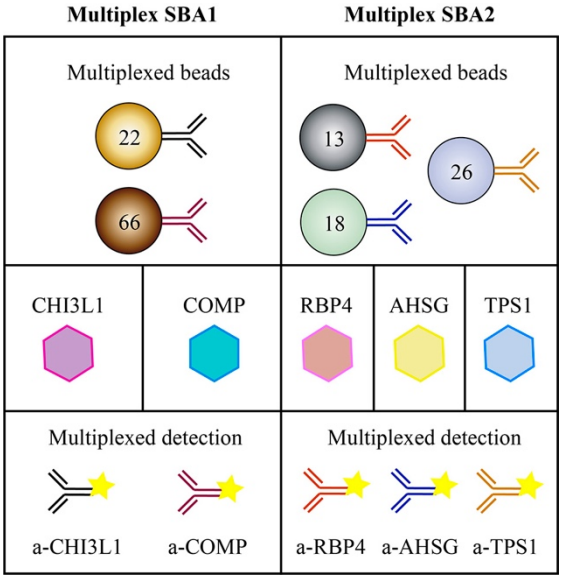

Figure 15. Cross-reactivity test design. Mixed coupled beads sets, individual antigens and multiplexed detection antibodies were used to determine if the antibody pair cross-reacted with non-target analytes.

Finally, in order to confirm that most of the sera fitted within a final 9-point standard curve range at the final serum dilution, 29 serum samples randomly selected from the OAI cohort were analyzed by the developed sandwich immunoassay.

3.4.2. Analytical characteristics of the assay

To assure that all generated sandwich immunoassays were reliable for research use, the analytical performance characteristics and meeting requirements for accuracy, precision, lower limit of detection (LLOD) and lower limit of quantification (LLOQ) were assessed either in the monoplex or multiplex assays.

Accuracy. – It was evaluated following the FDA guidelines for pharmacokinetic immunoassays (Findlay et al., 2000), which describes the closeness of mean test results obtained by the method to the true concentration of the analyte. In this thesis, accuracy was determined by triplicates of 2 known amounts of the analyte. The mean value should be within 70–130% to meet the FDA criteria.

$$Accuracy\ (\%) = \frac{observed\ concentration\ of\ the\ analyte}{expected\ concentration\ of\ the\ analyte} * 100$$

Precision. – Describes the closeness of individual measures of the same analyte in multiple replicates when the procedure is applied repeatedly. It is determinated by the coefficient of variation (CV), which is defined as the standard deviation (SD) of a set of measurements divided by the mean of the set (Urbanowska et al., 2006). As accepted by the FDA, assay precision should be less than 30% (Findlay et al., 2000). Here, precision was determined by the mean %CV of 3 independent measurements of 2 known amounts of the analyte.

$$CV\% = \frac{SD}{mean} * 100$$

LLOD and LLOQ.- LLOD refers to the lowest amount of the analyte that can be detected but not quantified as an exact value. On the other hand, the LLOQ refers to the lowest amount of the analyte that can be quantified with an acceptable level of statistical significance. In this research, LLOD and LLOQ were calculated according to the IUPAC (International Union of Pure and Applied Chemistry) definition (Hsu et al., 2009), as the mean of 8 independent measurements of the zero standard signal plus 3 or 10 times, respectively, the SD obtained on the zero standard signal.

$$LLOD = mean_{zero\ standard} + (3 * SD_{zero\ standard}$$

$$LLOQ = mean_{zero\ standard} + (10 * SD_{zero\ standard})$$

3.4.3. Intra- and inter-assay %CV

In larger studies with many samples to be tested, where it is necessary to run multiple assay plates, intra- and inter-assay %CV should be determined in order to assess the reliability of the results. In this thesis, we decided to run triplicates of a pooled serum sample (control pool) placed in 3 different wells randomly selected for each plate.

Intra-assay %CV. – It was determined by the mean %CV of independent control pool's measurements in a single assay.

Inter-assay %CV. – It was determined by the mean %CV of independent control pool's measurements in independent assays running in 3 consecutive days.

According with the FDA criteria, intra- and inter-assay variation should be less than 10% and 20%, respectively. The control pool was prepared by mixing equal volumes of 3 individual sera from the OAI cohort.

4. DISCOVERY AND VERIFICATION OF AUTOANTIBODIES

4.1. Study design

A two-stage discovery approach was designed to analyze the presence and putative usefulness of OA-associated AAbs to predict the incidence of the disorder in sera, and is illustrated in Figure 16: In a first *screening phase,* reactivity levels of AAbs against 2125 proteins were evaluated in 10 pooled serum samples at baseline per study group (incident and not-incident) using the NAPPA platform. Each pool was prepared by mixing equal volumes of 10 individual sera. In a second stage, a *verification phase* was carried out with one selected AAb candidate among those detected as modulated between the incident and not-incident group by NAPPA-based immunoassay in a total of 327 individual sera at baseline: 181 not-incidents and 146 incidents, which included the same set of samples used at the screening. All assays were run blinded to the clinical information.

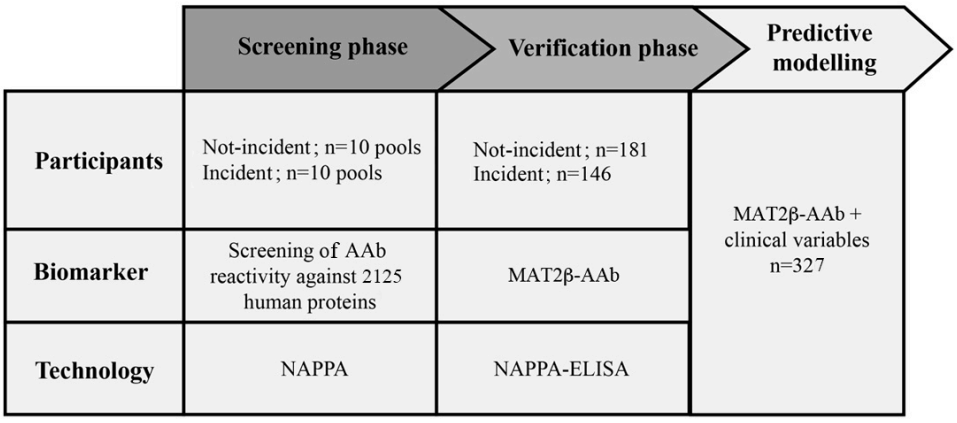

Figure 16. Design of the two-stage discovery approach to analyze the presence and putative utility of AAbs to predict radiographic knee OA.

Finally, a suitable prognostic model to predict OA development in the clinical routine was defined combining different clinical variables alone or with the potential biomarker by multivariate stepwise logistic regression analysis. The levels of reactivity of the selected AAb were associated with the relative risk to develop the disorder in time by the Cox proportional hazards model.

4.2. NAPPA profiling of serum autoantibodies

The NAPPA core CPD (Centre for Personalized Diagnostics) at the Biodesign Institute (Arizona State University, USA) had printed and stored all human genes available at the DNASU (www.dnasu.org) on 6 different array sets; HC1 to HC6. The HC5 set was selected for the screening, on the basis of having the greatest number of genes that could be related with OA pathogenesis according existing bibliography (Annex 1).

4.2.1. Array quality assessment

Prior to the functional experiments, QC assays were performed to ensure the reproducibility of protein display on a set of HC5 slides stored since January 2015 (QC experiments). The protocol followed to verify that protein display was universal through the whole array was the Standard Operation Procedure (SOP) from the Biodesign Institute:

- Three HC5 slides were blocked in 30 mL Pierce™ SuperBlock™ blocking buffer (Thermo Fisher Scientific, catalogue number: 37535) at RT for 1 h on rocking shaker.
- Slides were rinsed 6 times with Milli-Q water and dried by filtered compressed air.
- HybriWell (Grace Bio-Labs, catalogue number: HBW2160-1LA) gaskets were applied to each slide to the side that has the array printed on it, placing the end of the HybriWell that has more negative space towards the bottom of the array.
- The proteins on the array were expressed *in situ* by injecting into the HybriWell 150 µL human HeLa cell lysate-based IVTT expression system, which was previously prepared using the 1-Step Human Coupled IVT kit (Thermo Fisher Scientific, catalogue number: 88881) at 60% lysate. Briefly,

all provided reagents were thawed on ice immediately before its use. Once defrosted, 45 µL HeLa lysate, 15 µL accessory proteins and 30 µL reaction mix per slide were mixed in 60 µL nuclease-free water in the order listed by gently mixing and saved on ice until use. Enough volume for one extra slide was prepared. The mix was added slowly from the non-label end and each HybriWell was gently massaged to spread out the IVTT mix and cover all the area of the array.

- After removing as many bubbles as possible using a wooden stick to push out the air from the holes, port seals were applied to both ports on HybriWell.
- Slides were then placed on a bioassay dish covered with Milli-Q water to preserve humidity and incubated at 30°C for 1.5 h for protein expression followed by 30 min at 15°C for protein capture.
- After removing the HybriWell, slides were rinsed twice with 0.02% PBST and immersed in 5% milk 0.02% PBST to be washed 3 times, 5 min each.
- To avoid unspecific binding, slides were blocked with 5% milk 0.02% PBST on rocking shaker at RT for 30 min. Then, the excess of blocking buffer was removed by gently tapping the edge of the slide onto a paper tower.
- To apply the primary antibody, the slides were placed in a Corning Hybridization Chamber and incubated with 2 mL of anti-GST monoclonal antibody (Cell Signaling technology, catalogue number: 2624) diluted to 1:300 in 5% milk 0.02% PBST for 1 h at RT on a rotator.
- Before the incubation with the secondary antibody, slides were placed out on a bioassay dish and washed with 5% milk 0.02% PBST 3 times on a rocking shaker, 5 min each.
- Specific unions of the primary antibody with the expressed proteins were detected by incubating the slides in the Corning chamber with 2 mL of diluted Direct Labelled Alexa Fluor 647 goat anti-mouse IgG antibody (Life TechnologiesTM, catalogue number: A21235) diluted to 1:500 in 5% milk 0.02% PBST for 1 h at RT on a rotator.
- Finally, slides were washed 3 times with 0.02% PBST, 5 min each, rinsed thoroughly with deionized water and dried with compressed air.

- The image of the array was obtained by scanning each slide using a Tecan PowerscannerTM (Tecan Group LTD) with the following scan settings: Resolution 10, Channel 2/647 nm, Gain 50%, and Intensity 50%.

4.2.2. Serum autoantibody profiling

To detect the presence of autoantibodies in sera, proteins were first expressed on the array, following the same protocol described above. Serum autoantibodies were profiled on the HS 4800 Pro hybridization station (Tecan) following the SOP from the Biodesign Institute:

- The machine was turned on and the "NAPPA Manual expression 16 Hr" protocol was opened on the HSPro software.
- Before starting, nitrogen was tuning on, buffers were loaded into the corresponding containers and the proper channel tube was inserted in each of them (0.02% PBST in channel 1 and 5% milk 0.02% PBST in channel 2).
- The expressed slides were placed into the HSPro hybridization chambers without any label or barcode, with the array facing up. Once all the slides were loaded, the module was slowly closed and the machine was primed with each buffer, priming last 0.02% PBST.
- Then, the run was started with 1 h of blocking with 5% milk 0.02% PBST.
- When the machine was ready for the primary injection, the injection cap of the first chamber was unscrewed and 150 μL 1:20 diluted serum in 5% milk 0.02% PBST were slowly injected with the pipette and tips that are specifically designed for the HSPro machine. An extra slide with no serum injection (150 μL 5% milk 0.02% PBST) was also run as negative control. The incubation was programmed 16 h at 4°C, to ensure that the run was going to cover all night. To set up the optimal serum dilution, 1:20 and 1:50 serum were previously tested using one pool randomly selected. Serum dilution was determined by the optimal sensitivity with minimum diffusion, through visual analysis of one experimented researcher.
- 150 μL of Direct Labelled Alexa Fluor 647 goat anti-human IgG (Life Technologies, catalog number: A21445) diluted to 1:500 in 5% milk 0.02% PBST were injected into each hybridization chamber, repeating the same steps

as injection of the sera and incubating with the slides for 1 h at RT covered with black shields to keep the light out.

- When the run was finished, modules were carefully opened and the slides were rinsed 3 times with deionized water, dried by centrifugation at 1,200 revolutions per minute (rpm) for 3 min, and scanned by Tecan PowerscannerTM, maintaining the scan settings as the QC experiments.

4.3. NAPPA-ELISA assay

ELISA-based NAPPA immunoassays were performed following the SOP from the *Centro de Investigación del Cáncer-IBMCC de Salamanca*:

A. Coating and blocking of 96-well plates.

- 40 mL of 4 μg/mL polyclonal anti-GST antibody (GE Healthcare, catalogue number: 27-4577-01) were diluted in carbonate/bicarbonate buffer pH 9.6.
- Four 96-well plates (Costar, catalogue number: 3915) were coated with 100 μL of the diluted antibody at 4°C overnight.
- The excess of the antibody solution was eliminated by turning the plate over a paper tower, and blocked with 200 μL 5% milk 0.02% PBST for 4 h at RT.

B. Expression of the recombinant protein.

For all the assays, eight 1-Step Human Coupled IVT kits (Thermo Fisher Scientific, catalog number: 88882) were used, each containing sufficient reagents to perform 40 reactions. A total of 320 reactions from the HeLa cell lysate-based protein expression system were prepared following the manufacturer's instructions:

- The components of the kit (HeLa Lysate, accessory proteins and reaction mix) and plasmid cDNA encoding human full-length methionine-adenosyltransferase II subunit β (MAT2β) fused to GST recombinant protein were thawed on ice immediately before use.
- All reagents were gently mixed in nuclease-free water in a 1.5 mL vial at RT. Among all the reactions required to carry out the assays, 312 reactions (divided in 8 vials: 7 of 40 reactions and 1 of 32 reactions) were mixed with 20

μg/mL of plasmid cDNA (Target Protein reaction mix). The remaining 8 reactions were free of the plasmid cDNA and acted as negative controls of the assay (no cDNA control reaction mix). The order in which the reagents should be mixed and the required volumes for one reaction mix are listed below in Table 7.The reaction mix was incubated for 3 h at 30°C and straight away put on ice to stop the reaction.

Table 7. Components of the IVT for one reaction mix.

Components	**Target Protein (μL)**	**No cDNA control (μL)**
HeLa Lysate	500	100
Accesory Proteins	100	20
Reaction Mix	200	40
Clone DNA	87	-
Nuclease-free water	143	40
TOTAL volume per reaction (vial)	1030	200

C. Coating 96-well plates with the expressed recombinant protein.

- Blocking solution was retired and wells were washed 5 times with 200 μL PBS 1X by turning the plate over and removing the excess on a paper tower.
- Each well was incubated with 20 μL of the expressed recombinant human protein overnight at 4°C on a rocking shaker. Two wells per plate were incubated with 20 μL of the no-cDNA control mix.
- Wells were washed 5 times, repeating the same steps as before with 200 μL PBS 1X.

D. Incubation with sera.

- Each well was incubated with 100 μL of the corresponding sera diluted to 1:20 in 5% milk 0.02% PBST at 4°C overnight on a rocking shaker. Control wells without cDNA were incubated with 100 μL of anti-GST monoclonal antibody (Cell Signaling technology, catalogue number: 2624) diluted to 1:1000 in 5% milk 0.02% PBST.
- Wells were washed 3 times with 200 μL 5% milk 0.02% PBST as previously described.

E. Revelation of the 96-well plates.

- The presence of specific autoantibodies against human MAT2β protein in sera was detected by incubation with 100 µL HRP (horseradish peroxidase)-linked anti-Human IgG (Jackson ImmunoResearch Laboratories, catalogue number: 109-035-098) diluted 1:1000 in 5% milk 0.02% PBST, for 1 h at RT on a rocking shaker. The negative control wells were incubated with 100 µL 1:1000 diluted HRP-linked anti-mouse IgG (Amersham, catalogue number: NA931).
- Wells were washed 3 times with 200 µL PBS 1X by turning the plate over and removing the excess on a drying paper.
- 100 µL 1-StepTM Ultra Tetramethyl-benzidine (TMB)-ELISA substrate solution (Thermo Fisher Scientific, catalogue number: 34028) were added to each well and incubated on a rocking shaker preserving from light until the reaction turned to blue colour.
- The reaction was then stopped by adding 50 µL of sulfuric acid per well, and the absorbance signals at 450 nm were read on the Synergy 4 plate reader (BioTek).

5. STATISTICAL TREATMENT OF THE DATA

5.1. Validation of proteins as potential biomarkers

A 9-point standard curve was run by duplicate for each analyte present on the sandwich immunoassay in all the plates analyzed. For all the analytes, an asymmetrical (five-parameter (5PL)) logistic standard curve was generated from each plate using GraphPad Prims in its 6.0 version for Mac. The MFI signal of the analyte in each individual sera analyzed within the same plate was extrapolated to its corresponding standard curve in order to obtain the total amount of the analyte at baseline in the sample.

For the incident and not-incident groups the mean, SD, median and range of the serum concentrations for each protein, expressed ng/mL or µg/mL, were obtained, and the presence of statistical differences between the two outcome groups were assessed by non-parametric Mann-Whitney U test. Participants whose concentration of the proteins in serum was below the LLOQ were eliminated from the analysis. The Kolmogorov-

Smirnov normality test was previously applied to examine if they were normally distributed. A value of $p < 0.05$ was used to determine significance of the test. In addition, a putative correlation between the different biomarkers was evaluated by the Spearman's coefficient (Rho).

To look for atypical data, an extreme outlier was defined as a value above 5 times the interquartile range. The mean with or without outliers was calculated using the "outlierKD script" created by Klodian Dhana in RStudio, which is available online in the DataScience^{+} website (https://datascienceplus.com/).

Furthermore, to determine whether the baseline serum concentration of each analyte, alone or in combination with others included in the same multiplex assay, may be associated with the incidence of radiographic knee OA, the odds ratio (OR) was assessed by univariate logistic regression. Here, the OR represents the odds for knee OA development associated with a one-unit increase in the concentration of the analyzed biomarker (Szumilas, 2010). To estimate the precision of the OR, the 95%CI was used. The effectiveness of each biomarker-only model for the prediction of knee OA development was assessed by the receiver operating characteristic (ROC) curve and the predictive capacity was quantified using the c-statistic (area under the curve (AUC)). The diagnostic performance of each biomarkers-only model in terms of sensitivity, specificity and predictive values (positive predictive value (PPV) and negative predictive value (NPV)) were also estimated by the Youden Index (*J*), which defines the maximum potential effectiveness of a biomarker (Youden, 1950). *Sensitivity* is the percentage of subjects with the clinical outcome who have a positive test result. Alternatively, *specificity* is the percentage of individuals without the clinical outcome who have a negative test result. The *predictive values* refer to the proportion of individuals with a positive (PPV) or negative (NPV) test result who truly have the case status or who do not have it, respectively (Parikh et al., 2008).

Biomarker assessment was performed using the IBM SPSS (Statistic Package for the Social Sciences, IBM Corporation) software package in its version 25.0 for Mac (Copyright© IBM Corporation 1989, 2017). All metrics related to the sensitivity, specificity, PPV, NPV and AUC were calculated using the pROC package in RStudio statistical software for Mac in its version 1.1.456 (Copyright© RStudio Inc, 2009-2018).

5.2. Discovery and verification of autoantibodies as potential biomarkers

Spot intensities in the scanned slides were measured using the ArrayPro Analyzer (MediaCybernetics) software in its 6.3 version. Raw intensity values expressed in arbitrary units (a.u.) of absorbance were normalized at the statistical department of the Biodesign Institute by subtracting the background signal of the slide, which was estimated by the first quartile of signal intensity in spots with no printed DNA, and divided by the median of background-subtracted intensity from non-control spots.

$$Normalized\ value = \frac{Raw\ Intensity - background\ Intensity}{Median\ of\ NonControl\ spots - backgroud\ Intensity}$$

For the incident and not-incident groups the mean value and SD of the baseline immunoreactivity levels were obtained for all the proteins expressed in the array. To quantitatively determine the positive AAb response, a cut-off level was calculated by the median intensity absolute deviation rule from all the spots through all the pooled sera. In addition, AAb candidates were qualitatively examined by one experimented researcher to capture diffused signals that cannot be quantified by the image analysis software, in order to identify and confirm positive responses. The researcher examined all the slides by adjusting an identical black and full colour threshold scale. The antigens that did not exhibit intensities over the cut-off were eliminated, and a differential spot analysis was performed with the remaining antigens by Wilcoxon Rank-Sum test. Significance was determined by $p<0.05$.

Among the final panel of candidate AAbs, one of them was selected to enter the verification phase based on its relationship with the OA pathology in the existing literature. The biological context network of the selected candidate was analyzed with the STRING (https://string-db.org/) bioinformatics webtool, using the K-means clustering method. For the baseline levels of the analyzed AAb the mean, SD, median and range, expressed in a.u. of absorbance, were obtained for the incident and not-incident groups, and the Kolmogorov-Smirnov normality test was applied to examine if they were normally distributed. To assess if the levels of the AAb were equal (H0; null hypothesis) or different (H1; alternative hypothesis) between the two outcome groups, the non-parametric Mann-Whitney U test was carried out. A level of significance of $p < 0.05$ was determined. All analyses were performed using the IBM SPSS 25.0.

The association of the baseline levels of AAb with the incidence of radiographic knee OA and its predictive ability in a biomarker-only model were assessed by the OR and the proper AUC, respectively. In the same way as described above, sensibility, specificity and positive and negative predictive values (PPV and NPV) were also estimated to determine the validity and security of the models using the pROC package.

5.3. Generation of clinical prognostic models

In the statistical analysis carried out to generate a suitable prognostic model of knee OA prediction, incident radiographic knee OA at 96 months of follow-up was defined as the *dependent* or *responding variable* (DV).

5.3.1. Univariate regression analysis

Clinical data at the baseline visit related to the participants included in this thesis were obtained from the OAI database (https://data-archive.nimh.nih.gov/oai). Among all of them, no-radiographic clinical variables were defined as *independent variables* (ID) to determine a clinical prognostic model of OA that avoids exposing patients to radiation. These variables, named as *covariates* throughout this manuscript, are listed in the Annexed 2. They were selected from the specific OAI eligibility risk factor criteria for the incident subcohort (e.g. age, gender, BMI, history of knee injury, etc.) as well as from both the WOMAC and KOOS pain questionnaires. For all variables concerning the joint, knee-value predictors were recoded to indicate they were for the target knee. When neither or both knees have incident knee OA, one of them was randomly selected and used in the analysis. The variable referring to the frequency of pain was recoded to indicate presence (whether it was frequent or infrequent) or absence of pain.

Categorical variables data were determined as percentages and continuous variables were determined by the mean and the SD of the mean value. In order to assess association with the incidence of radiographic knee OA, each covariate was individually analyzed by univariate logistic regression analysis. To avoid redundancies in the logistic regression model, the different subscales from the WOMAC and KOOS questionnaires were evaluated by Spearman's correlation. All the analysis were performed using IMB SPSS 25.0.

5.3.2. Multivariate regression analysis

Using those covariates showing significant association with the development of the disorder in the target knee, prognostic covariates-only models to predict incident radiographic knee OA were defined by stepwise logistic regression analysis. In this method, the choice of predictive variables is carried out by a combination of the *forward* and *backward* automatic procedures, where in each step a variable is considered for addition to or subtraction from, respectively, the set of predictive variables based on some pre-specified criteria. Sometimes, both the forward and backward methods define a single model, and sometimes they do not. In these cases in which more than one model is defined, the most parsimonious should be selected, i.e., the model that generates a precise and valid prediction of the evaluated response with the lower number of possible covariates. All the regression analyses were performed using SPSS version 25.

To evaluate the utility of the biomarkers (alone or in combination when they are included in the same sandwich immunoassay) as putative prognostic markers to predict incident radiographic knee OA in the clinical routine, different prognostic models were generated by combining the biomarkers-only model with the covariates-only model. For all the models generated (covariates-only model and biomarkers plus covariates models) the predictive accuracy was evaluated based on the ROC curve, the AUC and performance characteristics (sensitivity, specificity and predictive values). The superiority of one model over another was estimated by comparing the AUC for each model and the DeLong test was applied to determine the significance of the differences in the AUC of the covariates-only model after the inclusion of one or more biomarkers. Significance was defined as $p < 0.05$. All metrics were calculated using the pROC package in R.

5.4. Association of the proposed biomarkers with the time of incidence

With the aim of knowing whether the baseline levels of biomarkers could be associated with the time in which the disorder will develop, survival analyses were performed. A survival analysis is defined as a set of methods for analysing data where the outcome variable is the time until the occurrence of an event of interest, named as *time to even*t or *survival time*. In our case, the survival time is given by the time to radiographic knee OA development.

To perform the survival analysis, a cut-off value (tertiles) for each biomarker was assessed to categorise the participants into high-, intermediate- and low-level groups. Subjects were followed during 96 months, focusing on the time at which the disorder appeared. For those participants whose information about their time to OA development was incomplete, the survival time was considered as the time of their last visit. For those subjects who did not experience the event during the follow-up period, the survival time was considered to be as long as the duration of the study. Kaplan-Meier (KM) curves were used to estimate and visualize survival probabilities, which determine the probability to develop the disorder in a specific period of time, depending on whether the participants presented high, medium or low levels of the biomarker. Statistical differences between the outcome groups were assessed by the Long Rank test and the level of significance was determined by a $p < 0.05$. In addition, the Cox proportional hazards regression model was performed to evaluate the impact of the biomarker's levels in the relative risk (*hazard ratio* (HR)) for the development radiographic knee OA in time, adjusting for the covariates present in the proposed prognostic model from the logistic regression analysis. All calculations were performed using IBM SPSS 25.

IV. RESULTS

1. PROTEINS AS POTENTIAL PROGNOSTIC MARKERS OF KNEE OA

1.1. Generation of suspension bead arrays

1.1.1. All capture antibodies were efficiently coupled to the beads

Before starting to generate the sandwich assays, we verified that all capture antibodies acquired have been efficiently coupled to the magnetic microspheres. For that, beads coupled to antibodies generated in mouse, together with the mIgG-bead were mixed in the same array (SBA1). Coupling efficiency of monoclonal anti-human CHI3L1 was evaluated in a different SBA (SBA2) since it was generated in rat. The bare bead was included in both SBA as negative control of the coupling efficiency. In Figure 17 it can be observed a MFI signal higher than 5000 for all the capture molecules.

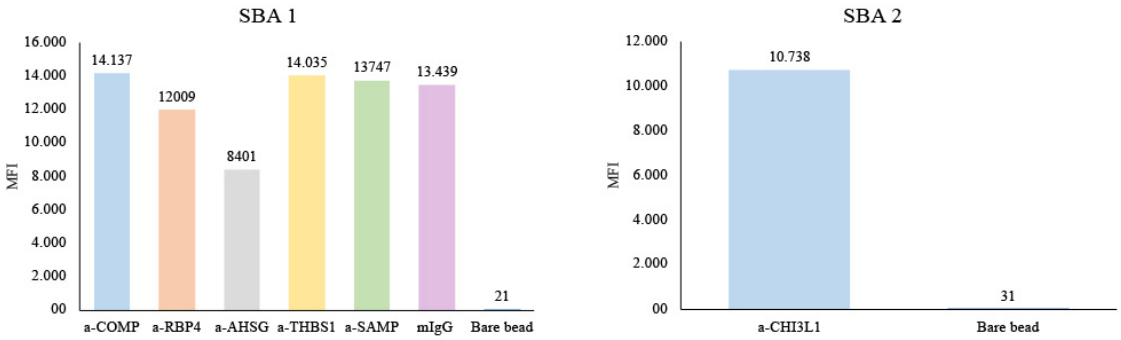

Figure 17. MFI showing the coupling efficiency of the captured antibodies to the beads surface.

1.1.2. Running singleplex assays to set up the standard curve range and serum dilution

The top standard concentration to generate a 12-point standard curve for each analyte was selected based on previous experiments of the research group using different antibody pairs and recombinant proteins and the adjustment to an 5PL-asymmetrical logistic standard curve were evaluated running singleplex assays (Figure 18). Standard curves for COMP, RBP4, AHSG and CHI3L1 recombinant proteins were still in the exponential phase at the top standard concentration. In the curves for APCS and TPS1 recombinant proteins, the typical S-shape of the sigmoidal response curves in which the X-axis is the logarithm of the concentration, could be intuited.

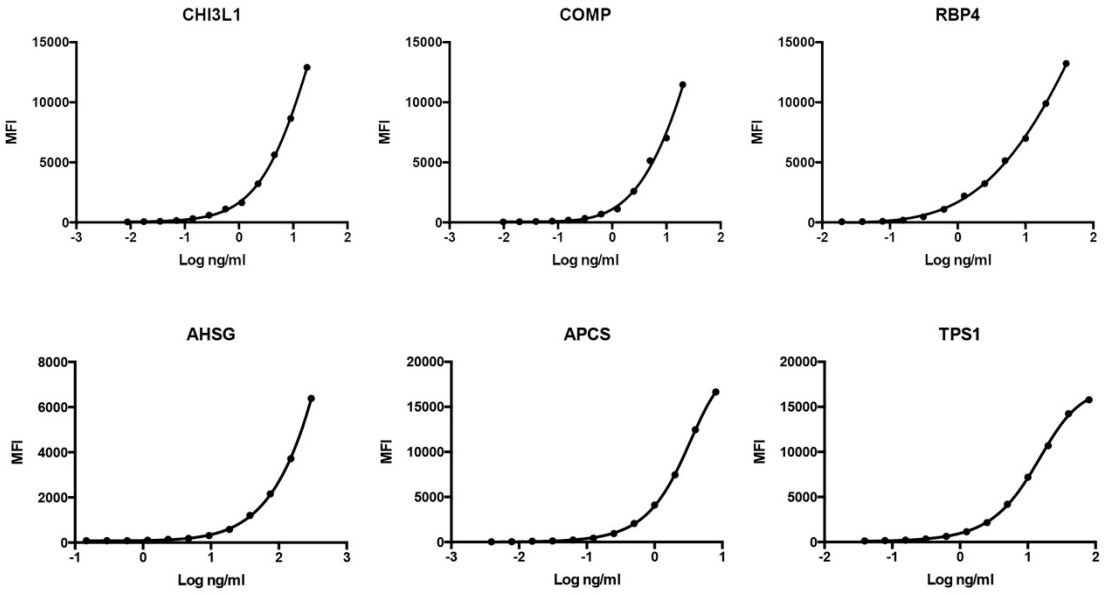

Figure 18. 12-point 5PL-standard curves for each biomarker running in singleplex assays.

With respect to the dilutions evaluated (Figure 19):

CHI3L1.- all sera diluted to 1:20 fitted in the linear range of the standard curve. The MFI for the serum sample 1 diluted to 1:40 was also situated at the linear range, but not for the serum sample 2. None of the analyzed sera obtained a MFI that would fit in the linear range of the curve when a 1:80 dilution was used.

COMP.- all dilutions analyzed in both sera showed an average fluorescence intensity that was between points eight and eleven of the standard curve, coinciding with the linear range of the curve.

RBP4.- only when the sera were diluted to 1:10000 the MFI could fitted in the linear range of the standard curve. Higher dilutions to 1:100000 and 1:200000 showed MFI signals too low to trust that the quantification will be reliable.

AHSG.- both sera diluted to 1:10000 showed a MFI inside the linear range of the standard curve, while dilutions of 1:100000 and 1:200000 were below the linear range.

APCS.- the MFI obtained for the most concentrated dilutions, 1:5000 and 1:10000 were, in both sera, above the MFI signal given by the top standard concentration. In case of 1:20000 dilution, only one of the sera was slightly above this signal.

TPS1.- sera dilute to 1:5000 and 1:10000 showed a MFI signal which fitted in the linear range of the standard curve, although the signals at the latest dilution were situated

in the lower limit of the linear range in both analyzed sera. Samples at the highest dilution showed a MFI outside the linear range of the curve.

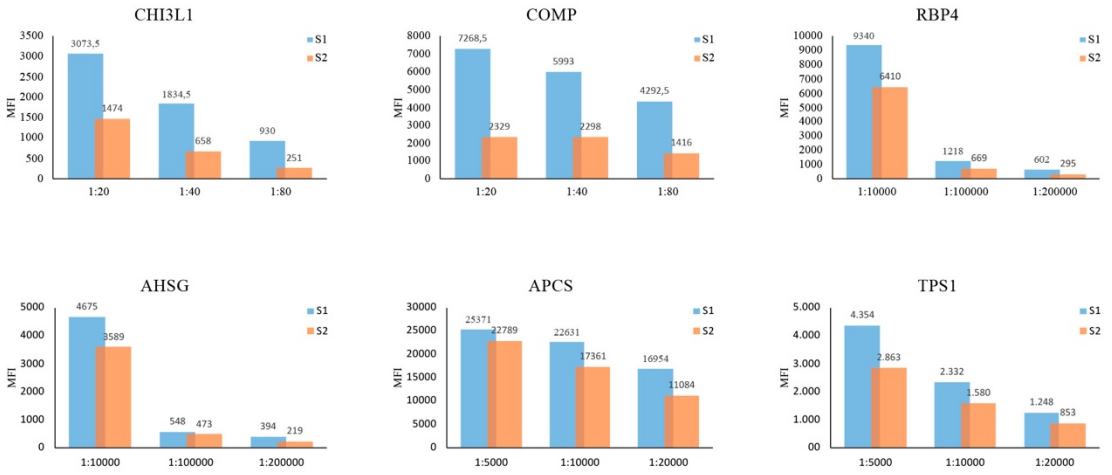

Figure 19. Serum MFI for each biomarker in the different tested dilutions. S1, serum sample 1; S2, serum sample 2.

1.1.3. Cross-reactivity test on multiplex assays

Based on the required serum dilution, we develop 2 custom multiplex sandwich immunoassays: a duplex sandwich immunoassays including COMP and CHI3L1 proteins at 1:20 dilution, and a triplex sandwich immunoassays including RBP4, AHSG and TPS1 protein at 1:10000 dilution. To determine the optimal procedure for the multiplex assay cross-reactivity of the antibody pairs was evaluated.

A

%	a-CHI3L1	a-COMP
RP CHI3L1	0.15	
RP COMP		0.24

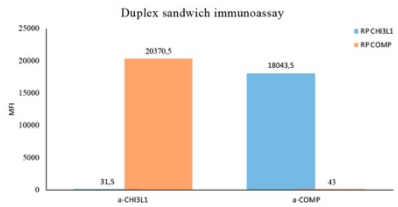

B

%	a-RBP4	a-AHSG	a-TPS1
RP RBP4		0.55	0.49
RP AHSG	0.62		2.03
RP TPS1	0.40	1.08	

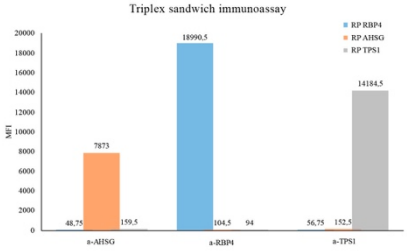

Figure 20. Cross-reactivity test in the duplex (A) and triplex (B) sandwich immunoassay. Values in the tables refers the percentage of the off-target MFI divided by the MFI observed for the cognate ligand. RP, recombinant protein.

None of the cases showed an off-target MFI was ≥5% of the cognate ligand (Figure 20), which confirm the specificity of the antibodies to recognized it target antigen.

1.1.4. A final standard curve range and serum dilution was evaluated

Finally, based on the result showed above, a final 9-point standard curve range and a serum dilution was determine (Table 8). The validity to quantify the baseline concentration of each analyte was verified in 29 sera randomly selected from the OAI cohorts.

Table 8. Final standard curve range and serum dilution for each biomarker.

Assay	Biomarkers	Standard curve range (ng/mL)	Serum dilution	Nº of samples below the lower standard MFI
Duplex	CHI3L1	18–0.070	1:10	0
	COMP	20–0.078	1:10	0
Triplex	RBP4	40–0.156	1:10000	2
	AHSG	300–1.172	1:10000	2
	TPS1	40–0.156	1:10000	3
Monoplex	APCS	8–0.031	1:20000	0

A graphic representation of the 5PL-standard curve obtained for the analytes in the multi- or mono-plex sandwich immunoassay could be observed in the Figure 21. Only one of the sera analyzed showed a positive MFI signal for TPS1 below the obtained MFI for the lower standard concentration (MFI 530 vs 607, respectively). The remaining sera that could not be quantified was due to the fact that they showed a negative MFI for these analytes, which was very close to QC beads signals (MFI ≈ 80).

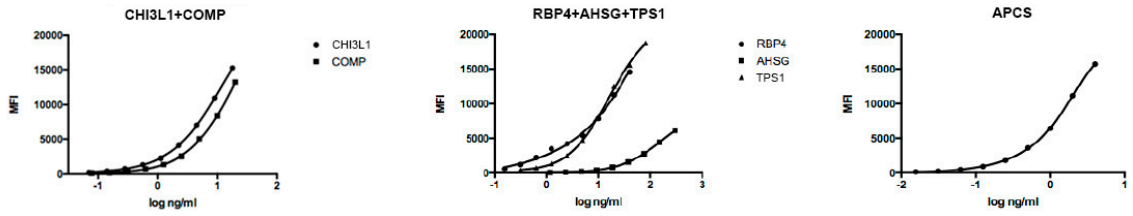

Figure 21. Standard curve for the multiplex and monoplex sandwich immunoassays.

1.1.5. Analytical performance of the assays

Finally, for each sandwich immunoassay, the analytical characteristics in terms of accuracy, precision and LLOD and LLOQ were evaluated and they are summarized in the Table 9.

LLOD and LLOQ of the assay for each analyte were evaluated as the mean value of 8 independent measures of the zero standard plus 3 or 10 times, respectively, the SD obtained on the zero standard signal. On the other hand, precision and accuracy were determined by the mean %CV or the mean %closeness of 3 independent measures of 2 known amounts of the analyte, respectively. All analytes met with the established criterion by the FDA for accuracy (70–130%) and precision (CV < 10%).

Table 9. Analytical performance of the developed immunoassay.

Assay	Biomarkers	LLOD (ng/ml)	LLOQ (ng/ml)	Precision (%CV)	Accuracy (%)
Duplex	CHI3L1	0.016	0.019	5.1	103.7
	COMP	0.058	0.058	2.9	110.9
Triplex	RBP4	0.060	0.062	4.6	109.0
	AHSG	3.422	3.923	2.4	101.4
	TPS1	0.153	0.176	2.6	111.8
Monoplex	APCS	0.002	0.004	1.7	91.4

1.2. Validation of six proteins as potential prognosis marker of OA incidence

All of the proteins selected in this project had been previously associated with the OA disease in different proteomic discovery approaches throughout the existing bibliography as well as in house efforts.

With the aim of validate this association and evaluate the putative ability of these potential biomarkers to predict the incidence of radiographic knee OA, 749 individual sera at baseline from the OAI cohorts that were followed for 96-months were blindly analyzed. Among these 749, only 540 meet the KL radiographic knee OA criterion. From the 540 participants, 209 develop knee OA in the target knee during the study and were classified as incident patients, whereas 331 did not develop the disease in the target knee and were classified as not-incident. Baseline serum concentrations of the biomarkers were quantified by sandwich immunoassays on bead-based arrays.

In a first step, before to evaluate if exist significant differences in the baseline serum concentration of the six potential selected proteins between the study groups, the incident and the not-incident group, intra- and inter- assay %CV and the number of extreme outliers were assessed. As it is shown in Table 10, both, the intra- and inter-assay %CV was bellow 10% for the six analytes assessed, complying with the acceptance criterion established by the FDA and confirming the reliability of the results.

On the other hand, the number of extreme outliers was relatively low for all the analytes, being CHI3L1 protein the one showing the highest percentage (1.31%). In addition, the differences between the mean of the baseline serum concentration with or without outliers for all the analyzed proteins were of minor importance.

Table 10. Inter- and intra-assay %CV.

Biomarker	intra-CV (%)	inter-CV (%)	Number of extreme outliers (%)	mean with vs without outliers
CHI3L1	4.2	8.4	7 (1.3)	14.50 vs 13.66
COMP	6.9	9.9	0 (0.0)	47.11
RBP4	4.0	6.3	1 (0.2)	40.24 vs 39.50
AHSG	4.5	6.2	1 (0.2)	532.39 vs 529.54
TPS1	2.8	5.1	3 (0.6)	7.62 vs 6.33
APCS	3.7	6.0	0 (0.0)	46.13

The biomarkers characteristics related with the mean, SD, median and range were obtained for each biomarker for the incident and the not-incident group and they are summarized in Table 11. As none of the analytes were normally distributed ($p < 0.05$), the Mann-Whitney U test was applied to contrast the H0: baseline serum concentration of the target analyte was equal between the outcomes group. For all the potential biomarkers, serum concentration at baseline was significant higher in those patients who will develop knee OA in the follow-up period (Figure 22).

Although none of the biomarkers showed Rho > 0.7, correlation level between RBP4 and TPS1 was close (Rho= 0.6) and highly significant (p= 5.464E-65). (Annexed 3**)**.

Table 11. Concentrations of the panel of soluble biomarkers analyzed in the study.

Biomarkers (unit)	Incident Baseline mean (SD) Median (range) (n=209)	Not-incident Baseline mean (SD) Median (range) (n=331)	Number of samples bellow LLOQ
CHI3L1 (ng/ml)	19.49 (20.29) 12.19 (0.45–107.94)	11.38 (14.18) 7.26 (0.45–116.54)	5
COMP (ng/ml)	59.15 (34.79) 52.55 (6.63–175.17)	39.56 (20.37) 36.14 (0.34–165.50)	3
RBP4 (µg/ml)	50.28 (33.48) 39.30 (4.69–233.44)	33.93 (31.27) 28.68 (3.42–437.79)	4
AHSG (µg/ml)	597.04 (213.82) 570.11 (137.55–1543.89)	491.71 (245.86) 434.72 (82.12–2054.08)	4
TPS1 (µg/ml)	8.50 (15.65) 6.94 (1.32–226.85)	7.06 (24.77) 5.21 (0.98–451.03)	8
APCS (µg/ml)	56.56 (26.48) 53.18 (5.16–155.28)	39.56 (23.16) 34.28 (4.49–174.97)	2

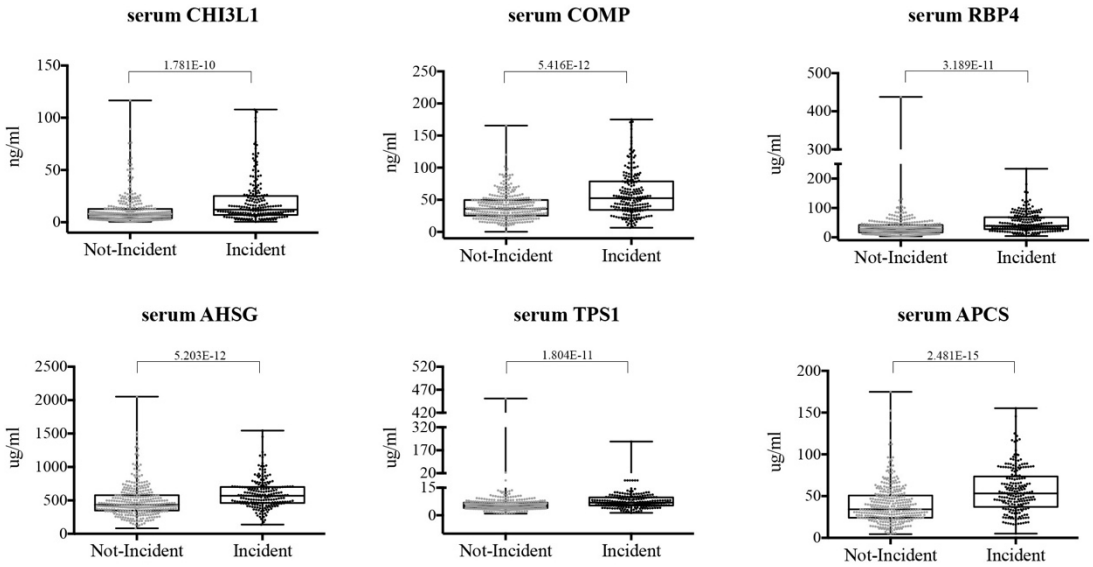

Figure 22. Box-plots comparing baseline serum concentration of the 6 potential biomarkers between the incident and not-incident group (p values over the brackets). For each sample group, the box- plot represent concentration values within the interquartile range (box), the median (horizontal line within box), lowest and highest concentration values in the data (horizontal line outside the box).

Finally, the OR of each biomarker was evaluated in order to know its association with the risk of knee OA development (Table 12). TPS1 was the only biomarker that did not show a significant association when it was evaluated alone (OR= 1.00 (95%CI: 1.00–1.00), p= 4.820E-01). When the individual predictive capacity of the potential biomarkers was individually analyzed, the lowest AUC was reached by CHI3L1, yielding 0.66 (95%CI: 0.62–0.71) and the highest AUC was reached by APCS , yielding 0.70 (95%CI: 0.66–0.75), however, this difference was not significant (p= 0.247).

Table 12. Biomarker assessment in the validation phase.

	CHI3L1	COMP	RBP4	AHSG	TPS1	APCS
OR (95%CI, p value)	1.03 (1.02–1.04, 1.000E-06)	1.03 (1.02–1.04, 1.773E-12)	1.02 (1.01–1.03, 5.225E-08)	1.00 (1.00–1.00, 2.000E-06)	1.00 (1.00–1.00, 4.829E-01)	1.03 (1.02–1.04, 4.311E-12)
AUC (95%CI)	0.66 (0.62–0.71)	0.68 (0.63–0.72)	0.67 (0.62–0.72)	0.68 (0.63–0.72)	0.67 (0.63–0.72)	0.70 (0.66–0.75)
Specificity (95%CI)	0.63 (0.57-0.68)	0.78 (0.74-0.83)	0.60 (0.55–0.65)	0.53 (0.48–0.58)	0.67 (0.62–0.72)	0.65 (0.60–0.70)
Sensitivity (95%CI)	0.66 (0.59-0.72)	0.53 (0.46-0.60)	0.65 (0.58–0.71)	0.79 (0.73–0.84)	0.61 (0.55–0.68)	0.69 (0.62–0.75)
PPV (95%CI)	0.53 (0.48-0.57)	0.61 (0.55-0.67)	0.51 (0.47–0.55)	0.51 (0.48–0.55)	0.54 (0.49–0.59)	0.55 (0.51–0.60)
NPV (95%CI)	0.74 (0.71-0.78)	0.73 (0.70-0.76)	0.73 (0.69–0.77)	0.80 (0.75–0.85)	0.73 (0.70–0.77)	0.77 (0.73–0.81)

In order to try to improve the diagnostic accuracy of the biomarkers, all possible combinations between the analytes quantify in the same multiplex sandwich immunoassay were assessed. The AUC obtained with the combination between CHI3L1 and COMP yielded an AUC 0.70 (95%CI: 0.65–0.75), which was not a significant increment compared with the AUC obtained by the biomarkers, individually (p= 0.278 to CHI3L1, and p= 0.483 to COMP). A similar case was found after assessing all possible combinations between the biomarkers analyzed in the triplex sandwich immunoassay, where the highest AUC was obtained in the combination of RBP4 with AHSG (AUC 0.69 (95%CI: 0.65–0.74)), which was close to the one obtained for AHSG alone. Differences between the AUCs of all of the combinations in these multiplex sandwich immunoassay were not significant, excepting the comparison between AHSG+TPS1 with the combination of the three analytes in the array (AUC 0.66 (95%CI: 0.62–0.71) vs 0.68 (95%CI: 0.64–0.73), p= 4.500E-02). Results from the regression analysis and all metrics related with sensitivity, specificity, PPV and NPV for the combinations of the biomarkers,

together with the DeLong test p values from the comparison between their AUC are summarized in the Annexed 4.

1.3. A combination of clinical variables and proteins improve the prediction of OA development

To generate the best covariates-only model a serie of clinical variables related with the risk of OA development was selected and evaluated in all the participants included in this study (Annexed 2). The mean and SD for quantitative characteristics, and the number and percentages for qualitative characteristics at baseline of the participants included could be observed in the Table 13 bellow. In general, both outcome groups included middle-aged women with baseline BMI levels above the overweight level, which carry out daily activities that required frequent bending of the knees and who complain of pain in either knee.

Table 13. Baseline characteristics of the participants included in the study.

Covariates	Incident (n=209)	Not-incident (n=331)
Age, mean years (SD)	60.77 (8.65)	57.60 (8.68)
Sex, n (%) female	131 (62.7)	156 (47.1)
BMI, mean kg/m2 (SD)	29.22 (4.62)	26.64 (4.04)
Family history of knee replacement, n (%) yes	36 (17.2)	49 (14.8)
Frequent knee bending activity, n (%) yes	151 (72.2)	207 (62.5)
History of knee injury, n (%) yes	47 (22.5)	52 (15.7)
History of knee surgery, n (%) yes	42 (20.1)	54 (16.3)
Pain in either knee, n (%)	187 (89.5)	226 (68.3)
WOMAC index:		
WOMAC Total score	10.41 (12.44)	5.07 (8.84)
WOMAC Disability score	7.06 (9.05)	3.31 (6.32)
WOMAC Stiffness score	1.40 (1.43)	0.79 (1.20)
WOMAC pain score	1.97 (2.70)	0.96 (1.93)
KOOS index:		
KOOS Symptoms score	88.98 (11.60)	93.50 (8.98)
KOOS pain score	86.41 (14.99)	92.59 (11.31)

Significant association was found in all the variables (Table 14), excepting for family history of knee OA (OR 1.22 (95%CI: 0.76–1.95), p= 4.162E-01) and history of knee

surgery (OR 1.28 (95%CI: 0.82–2.00), p= 2.776E-01). Referring to the face validity of these associations, both scores from the KOOS questionnaires were inversely associated with knee OA incidence. The rest of the clinical variables were all positively associated with knee OA incidence. The highest OR was found in the variable related with the presence of pain in either of the knees, yielding 3.95 (95%CI: 2.40–6.50), followed by the fact of being a female, with an OR 1.88 (95%CI: 1.32–2.68).

Table 14. Univariate analysis of the selected clinical variables.

Covariates	p value	OR	95% CI
Age, year	5.600E-05	1.04	1.02–1.06
Sex, female	4.490E-04	1.88	1.32–2.68
BMI, kg/m2	2.787E-10	1.15	1.10–1.20
Family history of knee replacement, yes	4.162E-01	1.22	0.76–1.95
Frequent knee bending activity, yes	2.132E-02	1.56	1.07–2.29
History of knee injury, yes	4.609E-02	1.57	1.01–2.43
History of knee surgery, yes	2.776E-01	1.28	0.82–2.00
Pain in either knee, yes	6.752E-08	3.95	2.40–6.50
WOMAC Total score (range= 0–62)	1.310E-07	1.05	1.03–1.07
WOMAC Disability score (range= 0–47)	2.585E-07	1.07	1.04–1.09
WOMAC Stiffness score (range= 0–6)	5.232E-07	1.41	1.23–1.62
WOMAC pain score (range= 0–13)	3.000E-06	1.22	1.12–1.32
KOOS Symptoms score (range= 43–100)	2.000E-06	0.96	0.94–0.98
KOOS pain score (range= 28–100)	4.765E-07	0.96	0.95–0.98

Excepting the WOMAC total and WOMAC disability scores, which were eliminated because of their high level of correlation with all the WOMAC subscales (Rho > 0.8, p < 0.001) (Annexed 3), the remaining significant variables were used in a stepwise logistic regression analysis to define the best covariates-only model to predict radiographic knee OA development. The WOMAC stiffness and pain scores also showed a correlation above 0.7 with the KOOS symptoms (Rho= -0.825, p= 3.135E-135) and KOOS pain scores (Rho= -0.896, p= 1.9363E-191), respectively. However, all of them were introduced in the analysis because they belong to different questionnaires. For the set of participants included in this study, the regression analysis defined 2 different covariates-only models (Table 15): *model 1*, including the age, gender, BMI, frequent bending activity, presence of pain in either knee and the KOOS symptoms score; and *model 2* including these same variables plus the history of knee injury. As there was not statistical

differences between their predictive capacity in terms of AUC (0.77 (95%CI: 0.73–0.81) vs 0.77 (95%CI: 0.73–0.81), p= 9.000E-01) we selected the covariates-only model 1 since it was the most parsimonious.

Table 15. Covariates-only models defined by stepwise regression analysis.

	Covariates-only model 1		**Covariates-only model 2**	
	OR (95%CI)	p value	OR (95%CI)	p value
Age	1.05 (1.03–1.08)	6.000E-06	1.06 (1.03–1.08)	2.000E-06
Gender, female	2.36 (1.58–3.54)	3.100E-05	2.39 (1.58–3.61)	3.400E-05
BMI	1.16 (1.10–1.22)	3.046E-09	1.16 (1.11–1.22)	2.613E-09
Frequent bending activity	1.72 (1.12–2.65)	1.304E-02	1.61 (1.04–2.50)	3.114E-02
History of knee injury			1.57 (0.95–2.59)	7.983E-02
Pain in either knee	2.47 (1.40–4.33)	1.686E-03	2.57 (1.43–4.61)	1.611E-03
KOOS symptoms score	0.97 (0.95–0.99)	7.431E-03	0.98 (0.96–1.00)	2.324E-02
AUC (95%CI)	0.77 (0.73–0.81)		0.77 (0.73–0.81)	
Specificity (95%CI)	0.79 (0.75–0.83)		0.77 (0.72–0.81)	
Sensitivity (95%CI)	0.66 (0.59–0.72)		0.68 (0.61–0.74)	
PPV (95%CI)	0.67 (0.62–0.72)		0.65 (0.60–0.70)	
NPV (95%CI)	0.78 (0.75–0.82)		0.79 (0.76–0.83)	

We evaluated if the combination of any of the biomarkers-only model to the covariates-only model 1 lead to a significant improvement of the capacity to predict the incidence of radiographic knee OA. The highest AUC were obtained with the inclusion of COMP (AUC 0.82 (95%CI: 0.78–0.85)) or CHI3L1+COMP (AUC 0.82 (95%CI: 0.79–0.86)) to the covariate-only model. However, only the CHI3L1+COMP plus covariates model showed significant higher AUC than the covariates-only model (p= 4.400E-02). In the Figure 23 could be observed the results from the multivariate logistic regression analysis, all together with the metrics and ROC curves comparing both, the covariates-only model with the CHI3L1+COMP plus covariates model. For the remaining biomarkers plus covariates model, metrics and ROC curves are summarized in the Annexed 4.

A

	Covariates-only model 1		CHI3L1+COMP + covariates model 1	
	OR (95%CI)	p value	OR (95%CI)	p value
Age	1.05 (1.03–1.08)	6.000E-06	1.04 (1.01–1.06)	8.167E-03
Gender, female	2.36 (1.58–3.54)	3.100E-05	2.55 (1.64–3.96)	3.000E-05
BMI	1.16 (1.10–1.22)	3.046E-09	1.17 (1.11–1.24)	3.399E-09
Frequent bending activity	1.72 (1.12–2.65)	1.304E-02	1.79 (1.12–2.84)	1.440E-02
Pain in either knee	2.47 (1.40–4.33)	1.686E-03	3.23 (1.71–6.10)	3.110E-04
KOOS symptoms score	0.97 (0.95–0.99)	7.431E-03	0.97 (0.95–0.99)	7.185E-03
serum CHI3L1			1.01 (1.00–1.03)	3.530E-02
serum COMP			1.03 (1.02–1.04)	1.208E-10
AUC (95%CI)	0.78 (0.73–0.81)		0.82 (0.79–0.86)	
Specificity (95%CI)	0.79 (0.75–0.83)		0.65 (0.60–0.70)	
Sensitivity (95%CI)	0.66 (0.59–0.72)		0.86 (0.81–0.91)	
PPV (95%CI)	0.67 (0.62–0.72)		0.61 (0.57–0.65)	
NPV (95%CI)	0.78 (0.75–0.82)		0.88 (0.85–0.92)	

B

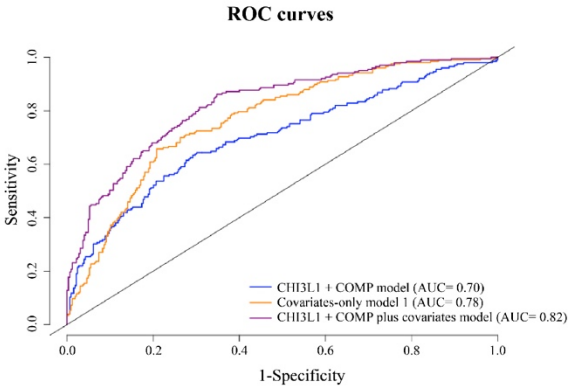

Figure 23. Prognostic model for incident radiographic knee OA. A) Metrics for the model comparing the covariates-only model 1 with the CHI3L1+COMP plus covariates model. B) ROC curves for the biomarker-only model (blue line), covariates-only model 1 (orange line), and CHI3L1+COMP plus covariates model (purple line).

Our definition of radiographic knee OA is being made on the basis of having at least one knee with a KL grade 0–1 (target knee) at baseline, which was followed during a period of 96 months regardless the diagnostic of the other knee. Among all the patients involved in this study, the 50.7% from the incident group and the 24.8% from the not-incident group had already develop at baseline radiographic knee OA in the off-target knee (KL > 2), which was highly associated with the fact of develop radiographic knee OA in the followed knee, yielding an OR 3.22 (95%CI: 2.22–4.66, p = 5.949E-10). However, the addition of the presence of contralateral OA to the proposed CHI3L1+COMP plus covariates prognostic model did not improve the predictive capacity (p= 0.597). The Figure 24 reflects the ROC curves of the biomarkers plus covariates model with and without adjusting by contralaterality.

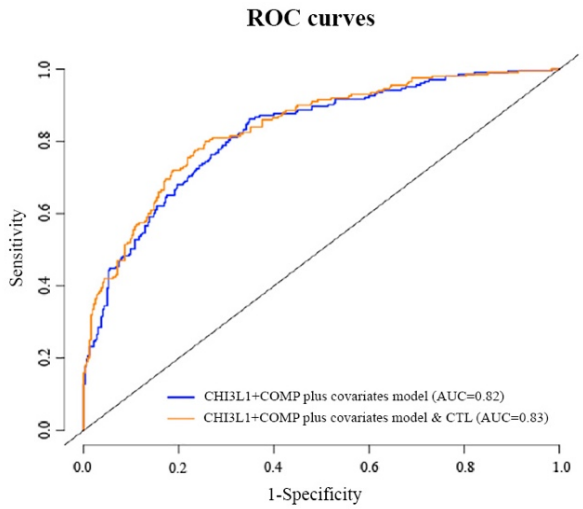

Figure 24. ROC curves for the prognostic model combining both, biochemical and clinical markers with or without the addition of having contralateral knee OA at the baseline visit.

1.4. High levels of CHI3L1 and COMP are associated with the earlier appearance of the disease

In order to assess if different baseline concentrations in sera of CHI3L1 and COMP grouped by tertile were significant associated with the probability to knee OA development sooner in time KM survival analysis were performed (Figure 25). The mean time to incident OA was 57.63 ± 2.79 (95%CI: 52.16–63.10), 71.84 ± 2.63 (95%CI: 66.69–76.99), and 79.80 ± 2.31 (95%CI: 75.28–84.32) months for the high-, medium- and low-levels group, respectively.

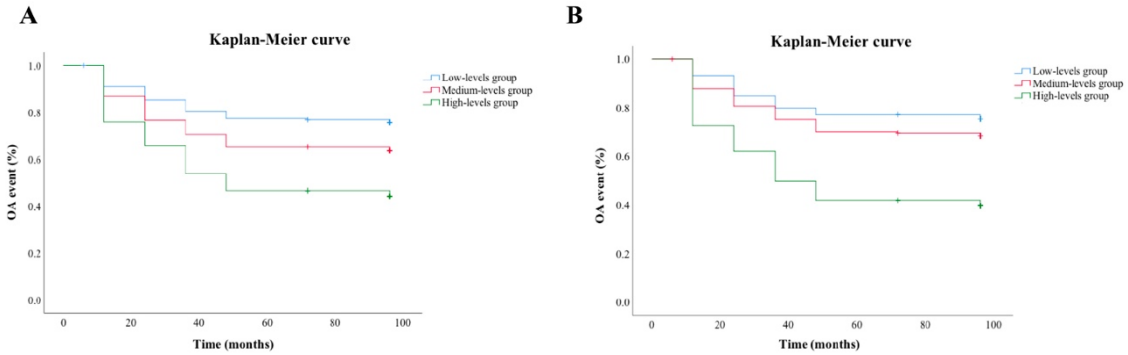

Figure 25. KM curve for CHI3L1 (A) and COMP (B) in the OAI participants included in this study. X-axis refers the times at which the appearance of the event (to have radiographic knee OA) was evaluated. Y-axis refers the percentage of individuals who did not have radiographic knee OA at the end of a specific period of time.

When applying the Log Rank test, significant differences were found for CHI3L1 between the high-levels group (range= 13.15–277.22 a.u.) with either, the medium-levels (range= 5.75–13.07 a.u., p= 1.350E-04) or the low-levels group (range= 0.88–5.70 a.u., p= 9.229E-10), as well as between the medium-levels group with the low-levels group (p= 0.019).

In case of COMP, the mean to incident knee OA was 54.24 ± 2.77 (95%CI: 48.81–59.66), 75.18 ± 2.52 (95%CI: 70.23–80.13), and 79.79 ± 2.30 (95%CI: 75.30–84.29) months for the high-, medium-, and low-levels group, respectively. Differences between the high-levels group (range= 51.21–164.80 a.u.) were found significant when it was compared with both, the medium-levels (range= 32.23–50.98 a.u., p= 2.198E-08) or the low-levels group (range= 5.61–32.01 a.u., p= 4.600E-12). However, in the comparison between the medium-levels group with the low-levels group, the differences found were not statistically significant (p= 0.183).

Defining low-levels group as the group of reference, the impact of the serum concentration of CHI3L1 and COMP biomarkers was assessed adjusting by all the covariates included in the logistic regression model defined to predict radiographic knee OA in this study. As it can be observed in Table 16, the hazard of incident radiographic knee OA was only significant increased with higher baseline serum CHI3L1 (1.74 (95%CI: 1.19–2.55), p= 4.345E-03) and COMP (HR 2.76 (95%CI: 1.91–3.99), p= 6.916E-08) levels when compared with the corresponding low-levels group.

Table 16. Cox proportional hazards regression model.

Covariates	HR (95%CI)	p value
Age	1.02 (1.00–1.04)	2.085E-02
Gender, female	1.69 (1.26–2.28)	5.450E-04
BMI	1.08 (1.05–1.11)	4.608E-07
Frequent bending activity	1.53 (1.12–2.09)	8.260E-03
Pain in either knee	2.35 (1.45–3.82)	5.360E-04
KOOS symptoms score	0.98 (0.97–0.99)	2.382E-03
Levels of CHI3L1		1.713E-02
Medium- vs low-levels	1.45 (0.97–2.16)	6.976E-02
High- vs low-levels	1.74 (1.19–2.55)	4.345E-03
Levels of COMP		2.440E-08
Medium- vs low-levels	1.36 (0.90–2.04)	1.443E-01
High- vs low-levels	2.76 (1.91–3.99)	6.916E-08

2. AABS AS POTENTIAL PROGNOSTIC MARKERS OF KNEE OA

2.1. Determination of serum dilution

Because the arrays used in this project had been stored for two years at the NAPPA core at CPD, we decided to run a first assay analysing three replicates of one pooled serum sample randomly selected from the incident group, to test the standardized dilution at 1:50 and a more concentrated dilution at 1:20. Through visual analysis of one experimented researcher, 1:20 dilution showed the optimal sensitivity with minimum diffusion (Figure 26).

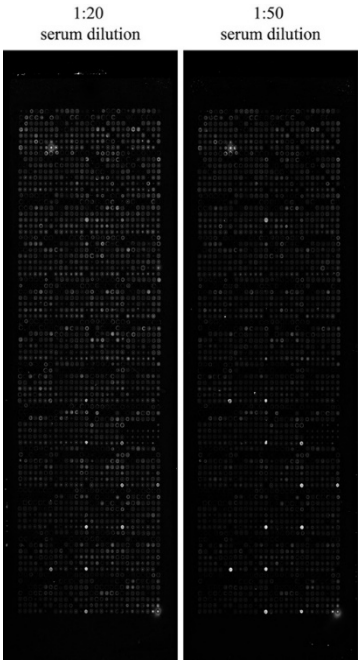

Figure 26. Visual comparison of the serum AAb profile in a representative array image diluted at 1:20 and 1:50.

2.2. Identification of autoantibodies associated with the incidence of knee OA

To search for AAbs in the serum that could be associated with a future development of knee OA, a comprehensive AAb profiling against 2125 full-length proteins fused with GST was performed by the NAPPA technique at the Biodesign Institute. It was carried out comparing pools of serum samples at baseline from two outcomes groups: the incident group (n= 100, 10 pools), which contains participants belonging to the incidence subcohort from the OAI study who did develop radiographic knee OA during the 96 months follow-up, and the not-incident group (n= 100, 10 pools), which contains participants from the non-exposed subcohort.

For each outcomes group, the mean values and SD of the immunoreactivity levels of all the proteins expressed in the array are summarized in the Annexed 1. The analysis of the normalized data using the median intensity absolute deviation rule from all the spots through all the pooled serum determined a signal cut-off > 1.1 to assure a sufficient margin between positive and negative AAbs reactivities. From the 2215 proteins screened in the array, immunoreactivity levels over the cut-off was detected against 1031 proteins (Annexed 1). Among these, a panel of 6 AAbs (Table 17) was found significant modulated between the outcome groups by the Wilcoxon Rank-Sum test ($p < 0.05$).

Table 17. Candidate autoantibodies identified in the screening phase of this study.

Protein name	Incident Mean (SD) (n= 10 pools)	Not-incident Mean (SD) (n= 10 pools)	AUC
Ankyrin repeat and SOCS box protein 7 (ASB7)	1.37 (0.23)	1.06 (0.16)	0.002
Methionine adenosyltransferase 2 subunit beta (MAT2β)	2.82 (0.47)	2.24 (0.35)	0.005
Diphosphomevalonate decarboxylase (MVD)	1.85 (0.27)	1.38 (0.62)	0.002
Ras-related C3 botulinum toxin substrate 3 (RAC3)	1.02 (0.16)	1.28 (0.13)	0.003
UDP-glucuronosyltransferase 1-7 (UGT1A7)	2.19 (0.32)	1.86 (0.24)	0.015
Vacuolar protein sorting-associated protein 4B (VPS4B)	1.78 (0.30)	1.42 (0.15)	0.005

In addition, AAbs showing reactivity over the cut-off were qualitatively analyzed by an experimented researcher (Figure 27). The visually discernible differences for the antigens MAT2β, UGT7A1, RAC3, MVD, and ASB7, demonstrated that the normalization criteria employed did neither create signal differences that do not exist, nor destroy true signal differences.

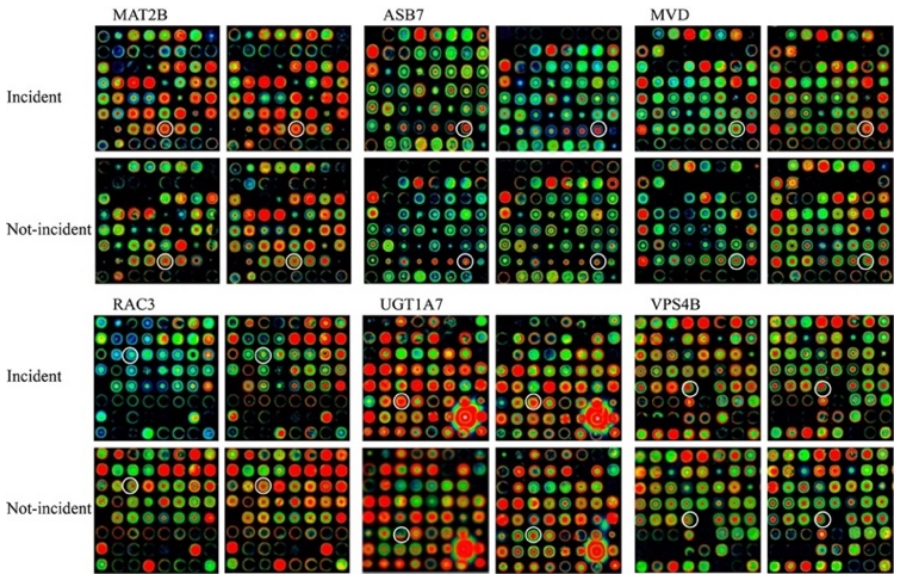

Figure 27. Visual comparison of immunoreactivity between the incident and not-incident group of the panel of 6 AAbs identified by statistical analysis in a representative array image. Intensity scale = red > orange > yellow > green.

2.3. MAT2β-AAb levels as potential prognosis marker of OA incidence

In order to confirm the putative ability of any of these AAbs to predict the incidence of OA, MAT2β protein was selected to enter the verification phase. This selection was based on its role in the formation of S-adenosylmethionine (SAM) as the regulatory subunit of the enzyme in charge of the catalysis, S-adenosylmethionine synthetase 2. In addition, the biological context network (Figure 28) suggests a bottleneck role of this protein in metabolic pathways that are known to be related with OA pathogenesis.

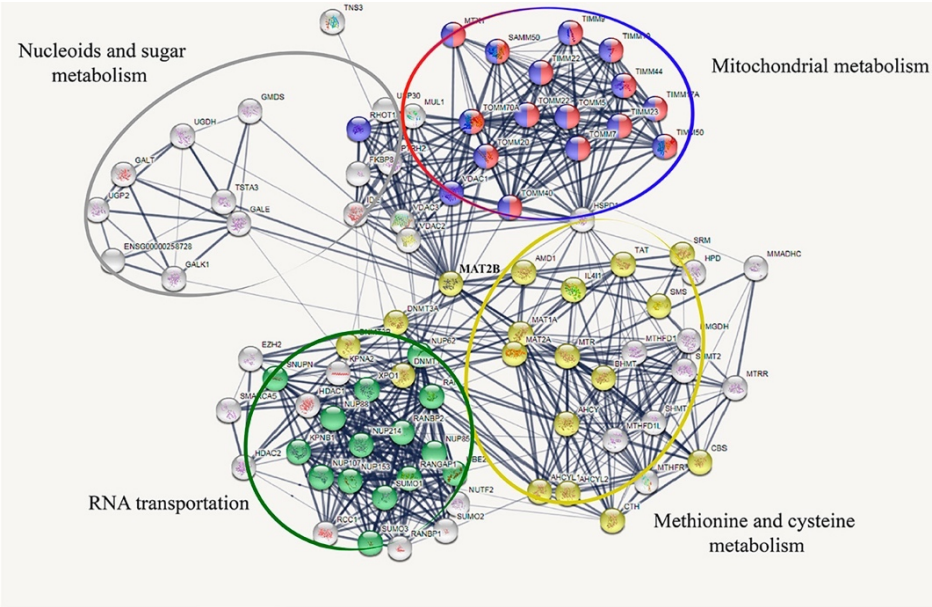

Figure 28. Biological context network of MAT2β protein by STRING clustering K-means.

The results of the baseline levels of AAbs against MAT2β protein in those patients who will develop knee OA during the follow up was verified by analysing 354 individual sera from the incident subcohorts and non-exposed control group of the OAI study. From these 354, 327 did not have relevant radiographic knee OA (KL= 0–1) at the beginning of the study in at least one knee and they were include in the statistical analysis; 146 classified as incident patients (KL > 2) and 181 classified as not-incident patients (KL= 0–1). Levels of AAb reactivity against MAT2β protein were quantify using the NAPPA-ELISA technique.

Mean, SD, median and range for both outcome groups were obtained and they are summarized in the Figure 29. As the baseline levels of MAT2β-AAbs were not normally

distribute ($p < 0.05$), the Mann-Whitney U test was used to contrast if there were significant differences between the two outcomes groups. The differences in the baseline levels of this AAb were statistically significant (p= 3.140E-04) being the incident group the one who presented the highest reactivities (0.58 ± 0.22 vs 0.49 ± 0.23 a.u.).

A

Biomarkers (unit)	Incident Baseline mean (SD) Median (range) (n=146)	Not-incident Baseline mean (SD) Median (range) (n=181)
MAT2B-AAb (a.u)	0.58 (0.22) 0.56 (0.17–1.58)	0.49 (0.23) 0.47 (2.00E-2–1.09)

B

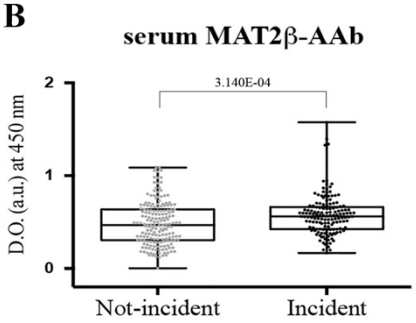

Figure 29. Immunoreactivity levels (a.u.) against MAT2β protein in serum at baseline in the incident and not-incident group (A), and box-plot (B) showing the median (horizontal line within the box), interquartile range (box), and minimum and maximum value (horizontal line outside the box) for each groups (p value over the bracket).

Although the baseline levels of MAT2β-AAb showed a strong association with the risk of incident radiographic knee OA (Table 18), yielding an OR 5.99 (95%CI: 2.16–16.63), this proposed biomarker had a modest capacity to predict the development of knee OA by its own, yielding an AUC 0.62 (95%CI: 0.56–0.68).

Table 18. Biomarker assessment in the verification phase.

	Estimate value	95% CI	
OR (p value)	5.99 (1.000E-03)	2.16	16.63
AUC	0.62	0.56	0.68
Specificity	0.39	0.31	0.46
Sensitivity	0.86	0.81	0.92
PPV	0.53	0.50	0.57
NPV	0.78	0.70	0.85

2.4. A MAT2β-AAb plus covariates model to predict incidence of knee OA

To generate a prognostic covariates-only model we evaluated the same clinical variables included in the previous study (Annexed 2). As we can see in the Table 19 below, participants were also mostly females on its middle age (exceeding the sixties)

with overweight (BMI > 25 kg/m^2), whose daily routine include frequent knee bending activities. In this study, the proportions of individuals who complain of pain in either knees reach almost the double in the incident to the not-incident group.

Table 19. Baseline characteristics of the participants included in this study.

Covariates	Incident (n=146)	No incident (n=181)
Age, mean years (SD)	60.65 (8.51)	56.61 (8.57)
Sex, n (%) female	98 (67.1)	102 (56.4)
BMI, mean kg/m2 (SD)	28.93 (4.59)	25.88 (4.14)
Family history of knee replacement, n (%) yes	21 (14.4)	17 (9.4)
Frequent knee bending activity, n (%) yes	110 (75.3)	106 (58.6)
History of knee injury, n (%) yes	39 (26.7)	23 (12.7)
History of knee surgery, n (%) yes	22 (15.1)	15 (8.3)
Pain in either knee, n (%)	124 (84.9)	86 (47.5)
WOMAC index:		
WOMAC Total score	9.04 (10.96)	2.94 (6.96)
WOMAC Disability score	6.06 (7.92)	1.77 (4.93)
WOMAC Stiffness score	1.38 (1.48)	0.56 (1.10)
WOMAC pain score	1.63 (2.36)	0.61 (1.63)
KOOS index:		
KOOS Symptoms score	89.58 (11.17)	95.11 (8.22)
KOOS pain score	82.13 (13.51)	95.24 (9.28)

Excepting the family history of knee OA and the history of knee surgery, all covariates showed significant association with the incidence of radiographic knee OA (Table 20), being the KOOS questionnaires inversely associated with the incidence of knee OA, whereas the others were positively associated. The presence of pain in either knee showed the highest OR, yielding 6.16 (95%CI: 3.59–10.57), which present a large distance with the second OR 2.57 (95%CI: 1.45–4.55) for history of knee injury. These significant variables were used to define a covariates-only model by stepwise regression analysis. Because the WOMAC total and WOMAC disability subscales showed a Rho value > 0.8 ($p < 0.05$) between them and with the other WOMAC subscales (Annexed 3), we decided not to take them into account for the selection of the model. The WOMAC stiffness and pain scores also showed a high correlation with the KOOS symptoms (Rho= -0.812, p=4.931E-78) and KOOS pain scores (Rho= -0.876, p= 1.057E-104),

respectively. However, the four of them were introduced in the regression analysis since they are different questionnaires.

Table 20. Univariate analysis of the selected clinical variables

Covariates	p value	OR	95% CI
Age, years	4.700E-05	1.06	1.03–1.08
Sex, female	4.757E-02	1.58	1.01–2.49
BMI, kg/m2	1.439E-08	1.17	1.11–1.24
Family history of knee replacement, yes	1.414E-01	1.67	0.84–3.30
Frequent knee bending activity, yes	1.543E-03	2.20	1.35–3.58
History of knee injury, yes	1.235E-03	2.57	1.45–4.55
History of knee surgery, yes	5.985E-02	1.95	0.97–3.92
Pain in either knee, yes	2.972E-11	6.23	3.63–10.68
WOMAC Total score (range= 0–62)	1.771E-07	1.10	1.06–1.13
WOMAC Disability score (range= 0–47)	3.749E-07	1.13	1.08–1.19
WOMAC Stiffness score (range= 0–6)	2.230E-07	1.64	1.36–1.98
WOMAC pain score (range= 0–13)	4.200E-05	1.35	1.17–1.56
KOOS Symptoms score (range= 43–100)	4.000E-06	0.94	0.92–0.97
KOOS pain score (range= 23–100)	7.819E-07	0.94	0.92–0.96

The final covariates-only model included the age, gender, BMI, frequent bending activity, history of knee injury, presence of pain in either knee and the WOMAC stiffness score as predictive variables, which yielded an AUC 0.83 (95%CI: 0.79–0.87). When we evaluated if the inclusion of the levels of MAT2β-AAb to this clinical model improved its predictive capacity, we found that the AUC for the MAT2β-AAb plus covariates model yielded 0.86 (95%CI: 0.81–0.90), which showed significant differences when it was compared with the covariates-only model (p= 1.321E-02). In the Figure 30 could be observed the results from the multivariate logistic analysis, together with the metrics and ROC curve comparing the covariates-only model with the biomarker plus covariates model.

Although in a lower percentage than in the case of the first study presented in this thesis, patients included in the incident group for the verification of the reactivity levels of MAT2β-AAb, also presented contralateral OA (42.5%). However, the number of participants with contralateral OA in the not-incident group was almost inexistent (1.7%),

leading to a 44.86 (95%CI: 13.68-147.14) times greater risk of radiographic knee incidence in the target knee for those patients with contralateral OA.

A

	Covariates-only model		MAT2β-AAb plus covariates model	
	OR (95%CI)	p value	OR (95%CI)	p value
Age	1.08 (1.04–1.12)	6.000E-06	1.08 (1.04–1.11)	2.300E-05
Gender, female	2.19 (1.23–3.89)	7.745E-03	2.52 (1.37–4.63)	2.886E-03
BMI	1.18 (1.10–1.26)	2.000E-06	1.20 (1.12–1.29)	4.686E-07
Frequent bending activity	2.58 (1.40–4.75)	2.340E-03	2.71 (1.44–5.12)	2.078E-03
History of knee injury	2.65 (1.31–5.36)	6.801E-03	2.64 (1.28–5.47)	8.927E-03
Pain in either knee	3.07 (1.58–5.96)	9.510E-04	3.89 (1.93–7.86)	1.530E-04
WOMAC stiffness score	1.32 (1.06–1.65)	1.338E-02	1.28 (1.01–1.60)	3.760E-02
MAT2β-AAb (a.u.)			18.37 (4.62–73.03)	3.600E-05
AUC (95%CI)	0.83 (0.79–0.87)		0.86 (0.81–0.90)	
Specificity (95%CI)	0.75 (0.69–0.82)		0.82 (0.77–0.88)	
Sensitivity (95%CI)	0.79 (0.72–0.86)		0.80 (0.74–0.86)	
PPV (95%CI)	0.72 (0.66–0.78)		0.78 (0.73–0.84)	
NPV (95%CI)	0.82 (0.77–0.87)		0.84 (0.79–0.88)	

B

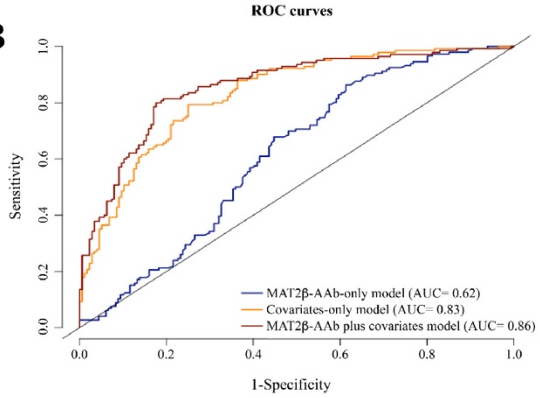

Figure 30. Prognostic model for incident radiographic knee OA in the verification phase. A) metrics for the model comparing the covariate-only model with the MAT2β-AAb plus covariates model. B) ROC curve for MAT2β-AAb-only model (blue line), covariates-only model (orange line), and MAT2β-AAb plus covariates model (purple line).

Despite this strong association with the future appearance of the disease in the followed knee, the AUC yielded after the addition of this variable was 0.90 (95%CI: 0.87–0.94), which had no significant impact in the predictive capacity in comparison with the proposed prognostic model, which combined the reactivity levels of MAT2β-AAb with the clinical variables (p = 0.093). The ROC curves of each model is represented in the Figure 31.

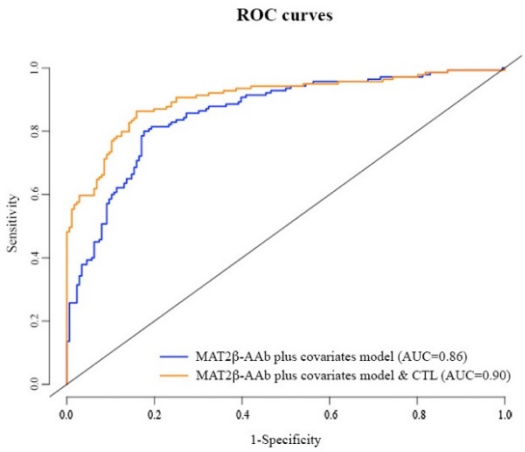

Figure 31. ROC curves for the prognostic model combining both, biochemical and clinical markers with or without the addition of having contralateral knee OA at the baseline visit.

2.5. Levels of MAT2β-AAb are associated with the time to OA incidence.

Finally, the association between the baseline levels of MAT2β-AAb in sera and the survival probability to OA incidence in a certain period of time was inferred by survival analysis. The mean time to OA incidence was 55.93 ± 3.61 (95%CI: 48.85–63.01), 62.30 ± 3.40 (95%CI: 55.62–68.97), and 79.01 ± 3.18 (95%CI: 72.78–85.24) months for the high-, medium-, and low-levels group.

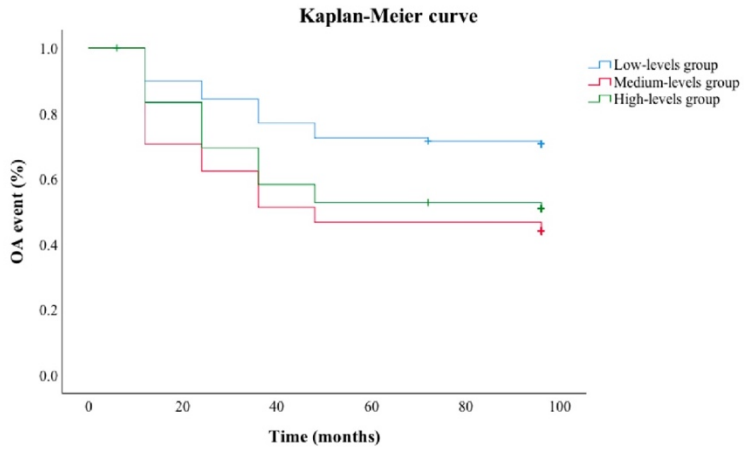

Figure 31. Association of the MAT2β-AAb levels at baseline with the time for radiographic knee OA incidence by KM curves in the OAI participants included in the study.

As represented in Figure 32 above, individuals with low levels (range= 2.00E-3–0.39 a.u.) had a significantly lower risk to develop knee OA sooner in time than those with high (range= 0.60–1.58 a.u., p= 5.000E-06) or medium (range= 0.39–0.60 a.u., p= 2.510E-04) levels of MAT2β-AAb. In contrast, there was not significant differences in the time to OA incidence when the high- and medium-level group were compared (p= 0.263).

In addition, this significant impact of the high (p= 2.680E-04) and medium (p= 7.440E-04) reactivity levels in sera of this AAb in the time to incident knee OA was maintained when compared to the low-levels group, adjusting for all the covariates included in the proposed prognostic model. As it can be observed in Table 21, the relative risk to develop the disorder sooner in time of those participants with high or medium levels of MAT2β-AAb was 2.53 (95%CI: 1.56–4.10) or 2.37 (95%CI: 1.46–3.84) times higher than the participants with low levels of the AAb. In this regression model, where

the time was taken into account, the gender does not have a significant impact in the appearance of radiographic knee OA (HR 1.32 (95%CI: 0.91–1.91), p= 1.422E-01).

Table 21. Cox proportional hazards regression model.

Covariates	Hazard ratio (95%CI)	p value
Age	1.04 (1.012–1.06)	2.600E-04
Gender, female	1.32 (0.91–1.91)	1.422E-01
BMI	1.08 (1.04–1.12)	2.400E-05
Frequent bending activity	1.64 (1.10–2.45)	1.583E-02
History of knee injury	2.74 (1.64–4.57)	1.250E-04
Pain in either knee	1.51 (1.03–2.22)	3.593E-02
WOMAC stiffness score	1.15 (1.02–1.30)	2.250E-02
Levels of MAT2□-AAb		3.700E-04
Medium- vs low levels	2.37 (1.46–3.84)	4.690E-04
High- vs low levels	2.53 (1.56–4.10)	1.650E-04

V. DISCUSSION

OA is the one of the most common form of arthritides and one of the major cause of chronic pain, stiffness and disability in the elderly. However, due to the current diagnosis methods, OA is usually diagnosed when destruction of joint tissue is irreversible. Although today there are no drug available which reverse the damage in the cartilage, large efforts are ongoing to develop such agents for targeted interventions in pre-radiological OA. This reinforce the need to improve the existing diagnostic methods, which allow a prompt earlier treatment or even detect who is in a risk for OA development before the onset of the disease to develop preventive strategies. In this sense, the measurement of biochemical markers in blood, urine or synovial fluid samples have been shown a great value to detect the asymptomatic molecular phase (pre-radiographic or early knee OA) of the disease (Lotz et al., 2014).

Over the years, proteomics has demonstrated its ability to identify proteins with potential marker of disease, allowing for the identification of an extensive list of potential biochemical biomarkers which may provide an early warning of the initiation of structural alterations occurring in the joint allowing an earlier treatment to prevent the joint destruction that leads to disability (Kraus et al., 2011). Despite the active research in the field, none of this biomarkers stands out as the gold standard or is sufficiently well validated and recognized for systematic use in the clinical routine to allow the prediction of patients who are at risk of knee OA (Bay-Jensen et al., 2016; Hosnijeh et al., 2015). This is mainly due to the lack of validation and qualification studies in large and long prospective cohorts, which makes the findings questionable to be considered as robust biomarkers for OA (Hunter et al., 2010).

Thus, the first study of this thesis project has focused on the validation of potential OA biomarkers by proteomic techniques based on protein arrays in a large number of sera from the OAI cohorts. In addition, sera from the OAI cohorts were also used to carried out a discovery phase using protein arrays in order to assess the putative utility of AAbs as prognostic biomarkers of knee OA. The results from the screening were verified in one selected candidate by ELISA-based NAPPA immunoassay.

Protein arrays in the generation process of protein biomarkers

Contemporary quantitative ELISA immunoassays have long been the primary tool for the detection of analytes of interest in biological samples for both, life science research

and clinical diagnostics since they are be able to accurate diagnose diseases whereby characterization of a single analyte is sufficient (Tighe et al., 2015). However, it is increasingly known that the measurement of a single biomarker may not be sufficiently specific and sensitive to provide accurate information in complex diseases, where multiple biological networks become perturbated, such as OA (Guo et al., 2018).

Therefore, in the last years there is a tendency to identify and develop panels of specific-biomarkers showing higher sensitivity and specificity than current diagnostic methods, especially using body fluid samples as a non-invasive and convenient test, which for the case of OA may supplant e.g. the radiological diagnostic techniques, avoiding the patient's exposure to radiation. In fact, the FDA have approved different multiplexed proteomics test which are actually integrated in the clinical practice to complement clinical assessment of different cancer types: the OVA1 test for assessing ovarian cancer risk in women previously diagnosed with a pelvic mass by analyzing the serum levels of five proteomic biomarkers (Nolen et al., 2013), and the Xpresys® Lung and PreTRM® test for evaluating the cancer risk of lung nodules using selective reaction monitoring (SRM)-MS (Kearney et al., 2018).

In the field of rheumatic diseases a multi-biomarker disease activity (MBDA) test was develop as a novel index based on 12 serum proteins to complement currently available disease activity measures and improve patient care and outcomes in rheumatoid arthritis (RA) (Centola et al., 2013), although it clinical usefulness is still being evaluated. In addition, Garcia-Moreno and collaborators have published, in the middle of the present year, a multiplex assay based on chimeric citrullinated peptides as proof of concept for diagnosis of RA (Garcia-Moreno et al., 2019). Here, they prove the suitability to detect anti-citrullinated peptide/protein antibodies (ACPAs) –the most specific serological biomarkers for RA– in serum samples using a multiplex protein array platform composed of eight chimeric citrullinated peptides derived from human proteins which is known that abound in the rheumatoid synovial.

Customization of multiplex sandwich immunoassays for xMAP technology

Recently, bead-based xMAP technology has become, in the protein biomarkers field, the most widely adopted multiplexing platform for translating biomarker candidates discovered into multiplex protein-based assays for clinical use (Boja et al., 2011). To

date, there are a vast selection of proteomic assays for the analysis of cytokines and other protein commercially available (Graham et al., 2019). One of the most attractive characteristic that contribute to the success of this technology is that it offers a high-throughput, flexible and open platform allowing users to construct their own custom immunoassays to simultaneous detection and quantification of different secreted proteins, with equal or higher reproducibility, accuracy and sensitivity than ELISA immunoassays, thereby minimizing assay costs, time and sample volume (Tighe et al., 2015). Since in 1999, Carson and Vignali (Carson et al., 1999) developed one of the earliest multiplex capture sandwich immunoassay for the simultaneous quantitation of 15 cytokines on the FlowMetrix systems (Luminex Corp.), numerous multiplex sandwich immunoassays have been successfully developed to simultaneously detected multiple analytes using different Luminex instruments (Hsu et al., 2008; Huang et al., 2019; Urbanowska et al., 2006; Wu et al., 2018; Xiao et al., 2019).

The first study presented in this thesis focused on the development of a sixplex sandwich immunoassay to blinded validate the serum concentrations at baseline of 6 proteins, previously associated with the osteoarthritic process, as prognostic markers to predict the future development of radiographic knee OA among a large number of subject included at the OAI cohorts.

From a panel of 20 proteins, integrated in a research project financed by the *Fondo de Investigación Sanitaria-ISCIII,* we selected 6 proteins for validation: CHI3L1 (Mateos et al., 2012), which belongs to glycohydrolase family 18 and has been suggested as a surrogate marker of synovial inflammation and joint destruction in OA (Huang et al., 2009); COMP (Fernandez-Puente et al., 2011; Mateos et al., 2012), which plays a role in cartilage degradation and it has been highly correlated with different OA processes (Tseng et al., 2009); AHSG (Fernández-Costa et al., 2012), which has been related with the negative regulation of bone mineralization; RBP4 (Fernandez-Puente et al., 2011), a member of the lipocalin family which has recently proven to be produced within OA joints (Scotece et al., 2018); TPS1 (Calamia et al., 2014; Calamia et al., 2011), a trimeric glycoprotein involved in cell-matrix interactions of various tissues, particularly in cartilage (Pfander et al., 2000); and APCS (Fernandez-Puente et al., 2017; Lourido et al., 2014), which is a member of the pentraxin family of proteins involved classical complement pathway of the innate immunity, a key component in the pathogenesis of the

disease (Wang et al., 2011). These proteins were selected based on the availability of commercial monoclonal and biotin-labeled polyclonal antibodies as well as recombinant proteins.

In previous in-house efforts, different monoclonal, biotin-label polyclonal antibodies against the target analytes and human recombinant proteins (standard) for each of the potential biomarkers were purchased from different sources and tested in singleplex assays to work in the xMAP technology. However, the results obtained were not satisfactory: for the most of the cases the antibody pairs detected the recombinant protein but not the native analyte in the sera or vice versa, neither denaturing the sample nor without denaturing. For those cases in which the antibody pairs detected both, the standard and the native protein, the obtained MFI signals were lower than desirable and it was not reproducible between different test running in distinct days. The difficulty of finding suitable antibody pairs and recombinant proteins is a challenge with which we knew we were going to face. It is highly known by the Luminex users that the main limitation when customizing their own sandwich immunoassay is to find the right combination of commercial available antibodies or recombinant proteins, since the method of antibody generation and purification can have serious impact on the assay (Marx, 2013).

Harold and collaborators demonstrated how a typical capture ELISA immunoassay could be converted to the xMAP platform for multiplexing assays using the Human TNF-α DuoSet ELISA kit and three other antibody pairs from different sources (Baker et al., 2012). The results of their study indicated that the antibody pair from the DuoSet kit performed best with a resulting response of more than 6000 MFI units. Based on it, we decided to purchase R&D system DuoSet ELISA kits containing the antibody pairs and the recombinant proteins when they were available for the analytes of interest. For those cases in which no DuoSet ELISA kits were developed, a monoclonal antibody, biotin-label polyclonal antibody and recombinant protein previously tested to work as capture antibody, detection antibody and standard, respectively, in ELISA immunoassays were purchased.

In a first approach, we generate 12-points standard curves and assessed different sera dilution for each analyte separately. The top standard concentration used was the one in which we obtained the best response in the test prior to the acquisition of the new reagents.

Then, two-fold serial dilutions were performed from this top standard concentration up to generate a 12-point standard curve for each analyte. In addition, we analyzed in the same run duplicates of 2 sera randomly selected from the OAI cohorts to test three different dilutions of the sample. To choice the dilutions, we decided first to selected for each analyte a dilution in which it had previously seen that the obtained MFI signal for the sera was below the MFI for the top standard concentration, and then we performed a double concentrated and a double diluted sample dilution. In the case of RBP4 and AHSG, downward dilution of the sample was done by diluting up to 1:10000 instead 1:5000 since in the previous studies it had shown that at this dilution the protein was so concentrated in the sample that the signal was lost. The serum dilution for each analyte was determined by the best fits the linear range of the curve. Based on this results, we limited each standard curve range to 9-point. Although CHI3L1, COMP, RBP4 and AHSG standard curves were still found in the exponential phase, we decided to continue with the same top standard concentration and not to increase the range because at least one of the tested dilution of the sera fit the linear range for all the analytes, which was: 1:10 for CHI3L1 and COMP, 1:10000 for RBP4, AHSG and TPS1, and 1:20000 for APCS. At this point, it is necessary to point out that the dilution of the sera determined for the quantification of TPS1 was not the best fitting the linear range of the curve, which would have been the 1:5000 dilution. Many of the MFI signals obtained for the sera diluted at 1:10000 were found in the lowest part of the linear range, corresponding with the area of the curve where the MFI began to be exponentially linear. However, the decision to measure this analyte at a dilution not entirely appropriated was based on minimizing as much as possible the number of different sandwich immunoassay.

One of the advantages of the bead-based assays over ELISA is the multiplex capacity, which reduce the time of the assay and the sample consume by analysing large number of analytes in a unique assay. The aim of this study was to develop a sixplex to validate simultaneously all the potential biomarkers. However, the differences between the required sample dilution for each analyte was too large to include all of them in the same multiplex sandwich assay. In that respect, we included CHI3L1 and COMP in a duplex sandwich assay, and RBP4, AHSG and TPS1 in a triplex sandwich assay. APCS was assessed alone in a singleplex assay. One of the most important requirements in a multiplex assay is to address interferences of analytes within the panel (Jani et al., 2016). Thus, the specificity of the capture antibodies for its cognate ligand has to be evaluated

using mixed coupled beads, individual antigens and mixed detectable antibodies (V., 2014-2014). Here, we showed that the MFI signals of the cross-reactivity test in each multiplex sandwich immunoassay was below 5%. Hence, no significant unspecific binding of the off-target analyte to the antibody-coupled beads was observed, supporting the great specificity of the capture antibody to recognize the cognate ligand.

Before to start running the immunoassays it should be taken into account that the variability in the serum concentration of the proteins between patients may be very wide. Thus, we decided to analyze a set of 29 sera randomly selected from the OAI cohorts in order to confirm that the selected 9-point curve range was adequate to quantify all the analytes at the determined sample dilution in all or the most of the samples. In our case, we did not need to make any readjustment in the curve ranges, since for the most of the cases, the analyte signal in the sample could be perfectly extrapolated. We only found one patient in whom the concentration of RBP4 in serum could not be quantified, because it showed a MFI signal outside the curve range. The rest of the patients who were excluded was because they showed a negative signal, very close to the background (QC beads).

Finally, when evaluating a quantitative assay it is important to assess the LLOD and LLOQ and the analytical performance characteristics described in terms of reproducibility or precision and accuracy (FDA, 2018). A multiplex assay requires that all analytes meet the analytical-performance criteria. In this context, our results showed a precision below 10 % and an accuracy between the 70–130 % for all the analytes, which meet the acceptance criteria established by the FDA for the validation of immunoassays (Findlay et al., 2000).

NAPPA strategy for the serum autoantibody profiling

Planar protein arrays have also showed an enormous potential in both, basic and translational research for the study of protein interactions, immune profiling, vaccine development, clinical diagnostics, and the one in which the second study of this thesis was focused, biomarker discovery (Casado-Vela et al., 2014; Diez et al., 2015; Lee et al., 2013; von der Heyde et al., 2016; Wang D. et al., 2017; Yang et al., 2016; Yu et al., 2016; Zhang et al., 2015). For example, Anderson et al. used planar proteins arrays for the discovery of a 28-autoantibody biomarker signature of early stage breast cancer

(Anderson et al., 2011), which were later used in combination with several protein biomarkers to develop Videssa® Breast, the first protein-based blood test for early breast cancer detection (Henderson et al., 2016).

Among the different types of planar arrays, the NAPPA technology offers a high-throughput miniaturized small-volume detection platform in which cDNA molecules encoding the desired protein fused with a GST tag are directly printed onto the array instead printing proteins (Miersch et al., 2011). This allow proteins to be transcribed and translated by a cell-free system directly on-chip and capture in situ by an anti-tag antibody just-in-time for assay, avoiding the delicate task and concerns associated with the expression of recombinant proteins in heterologous systems, including protein purification and stability during storage (Qiu et al., 2011). In fact, in the last years the number of studies which have been published based on NAPPA strategy yield almost 1800 papers (Manzano-Roman et al., 2019).

Among all the applications of the NAPPA technology, one of the most interesting is the identification of disease immunosignatures (Sibani et al., 2011), where it has been successfully proven in cancer (Anderson et al., 2015; Ewaisha et al., 2016; Fortner et al., 2017; Katchman et al., 2017), type I diabetes (Bian et al., 2017; Miersch et al., 2013), or crohn's disease (Wang H. et al., 2017). Thus, the second study presented in this thesis was focused in the screening of pooled serum samples at baseline from the incident subcohorts and the non-exposed control group of the OAI to identify antibody immune responses that could be associated with an early stage of the disease using the NAPPA strategy. This study was carried out during a three months-visiting fellowship at the Virginia G. Piper Center for Personalized Diagnostics (Biodesign Institute), under the supervision of Dr. Joshua LaBaer, one of the fathers of the NAPPA technology (Ramachandran et al., 2004). Here, the NAPPA protein array core had stored a series of each set of arrays (HC1 to HC6) for two years. To select one of the sets to carried out the sera screening, we analyzed the list of genes printed on each slide, which was provided by the NAPPA core facility. Among all of them, the HC5 was chosen because it was the array showing a greater number of encoding protein genes previously related with OA (Annexed 1).

Although the printing of cDNA instead of proteins provides a more stable array (Da Silva-Baptista et al., 2006), it was the first time in that an array that had been printed and

stored for such a long period of time was used. Because of this, we decided to test first whether reactivity obtained at 1:50 serum dilution (determined in the SOP from the Biodesign Institute) was enough to be detected. Despite the arrays showed a low protein display, we were be able to overwhelm this limitation using a more concentrating dilution of the sera (1:20). Among the 2,125 proteins captured on the surface of the array, we found 6 autoantibodies which showed significant differences in the levels of reactivity against their target proteins between the incident and the non-exposed control pooled sera. At this point, a characteristic of this approach should be taken into consideration when interpreting the findings presented herein: The low sera dilutions employed in this work lead to the primary detection of IgM, which, in contrast to IgGs, have no immune memory. However, IgMs are not subjected to immunoregulation (Díaz-Zaragoza et al., 2015) and are formed early in the immune response. Therefore, specific antibodies of the IgM class might be important in the diagnosis of chronic diseases (Burrell et al., 2017).

Biochemical markers to predict pre-radiological knee OA by proteomics techniques

Protein as potential prognostic markers

Despite a large number of proteins have been proposed as potential biomarkers of OA, none of them are already being used in the clinical routine to predict the future occurrence of the disease, which allow preventive treatment. This is mainly because OA is a very complex disease whose pathogenic course can last during decades in a molecular silent level. Therefore, the generation process of prognosis biomarkers to predict knee OA incidence requires its validation and qualification in large and long prospective trial to ensure biomarker test are reliable, reproducible and adequately specific and sensitive, as well as to make possible a robust evaluation of its association with the incidence of the disease (Kraus, 2018).

To date, the relationship between protein biomarker levels and incident radiographic knee OA has been poorly investigated (Henrotin, 2012). Among the most studies biomarkers, only the urine CTX-II and serum COMP have been studied in sufficient number of studies to draw robust conclusions. In this sense, Dahaghin and collaborators (Dahaghin et al., 2005) while studying the risk of hip or knee OA in subjects with hand OA from the Rotterdam Study founded that the presence of high levels of CTX-II in urine at baseline was independently associated with the risk of the future development of the

disease (OR 2.7 (95%CI: 1.5–4.9) for future knee OA and OR 1.8 (95%CI: 0.9–3.6) for future hip OA). On the other hand, high serum concentrations of COMP at baseline were also associated with incident knee OA (relative risk (RR) 2.87 (95%CI: 1.20–6.89)) in a subset of Causasian females from the Chingford cohort (Blumenfeld et al., 2013) and in a large cohort from African American and Caucasian men and women (HR 1.39 (95%CI: 0.90–2.13)) (Golightly et al., 2011). In addition, in a recent study including individuals from four different cohorts (Chingford study, TwinsUK, GARP study and Rotterdam study), elevate levels of both, CTX-II (log_{10} OR 2.29 (95%CI: 1.55–5.07)) and COMP (log_{10} OR 9.92 (95%CI: 3.12–89.70)), have also been significant associated incident radiographic knee OA even after adjustment for age, gender and BMI (Valdes et al., 2014).

To carried out this doctoral thesis, we have been fortunate to be able to access sera at baseline from participants belonging to the OAI cohorts. This is a very detailed and comprehensive longitudinal study were clinical analysis, imaging and biospecimens collection have been conducted over a 96-months period, leading to new ways to detect and validate relevant biomarker characteristics for assessment the risk for OA (Poole, 2016). By blindly analysis of 540 sera at baseline from the OAI cohorts that meet with the determine incidence criterion, we found significant higher concentrations of COMP, CHI3L1, RBP4, AHSG, TPS1 and APCS in those participants classified as incident patients, validating the previous results obtained in the discovery phases where these analytes were found related with the osteoarthritic disease.

Based in univariable models, five biomarkers were significant associated with case status reflecting radiographic knee OA consisting in the increment of a KL grade 0–1 to 2 or more, in some point of the follow-up period in at least one knee (target knee); these included serum COMP, CHI3L1, RBP4, AHSG and APCS. Underscoring the face validity of these associations, all of them were positively associated with OA incidence. In this study, CHI3L1, COMP and APCS yielded the highest OR for predicting incident radiographic knee OA: OR 1.03 for being a case compared with the not-incident group, followed by RBP4 (OR 1.02) and AHSG (OR 1.00). These ORs indicate that for every 1 unit increase in the biomarkers, the odds of incidence in the target knee increased 3%, 2% and 0%, respectively. These results suggest that the differences on the order of 1 unit do not appear clinically meaningful for these biomarkers. However, on the order of 10 units,

the odds of knee OA incidence rise up to ≈ 30% for COMP, CHI3L1 and APCS, and 20% for RBP4, and it reached more than 70% and 40%, respectively, per 20-unit increase. For AHSG, the odds in the order of neither, 10 nor 20 units still appear clinically unmeaningful, and even per 100-unit increase, this biomarkers showed an odds of have incident knee OA of only 21%.

In addition, the biomarkers were further evaluated for their ability to predict incident knee OA development. Based in the analysis of the AUC, all of this five analytes were individually able to predict the future occurrence of the disease in the target knee, although none of them reached a clinical usefulness (AUC < 0.7) (Wians, 2009). The highest predictive capacity was found in serum APCS, yielding an AUC 0.70, followed by COMP and AHSG (AUC 0.68), RBP4 (AUC 0.67) and finally, CHI3L1 (AUC 0.66). As far as we know, this is the first study that report a ROC analysis to characterize individual biomarker performance in the prediction of incident knee OA. In the literature exist different studies that assess the capacity of specific biomarkers to predict incidence in several diseases, in which it can be observed higher values of the AUC than we have obtained here, reaching levels of 0.85 in case of the protein carbonyl for detecting type II diabetes mellitus (T2DM) with associated vascular complications (Goycheva et al., 2019), and 0.83 for the heat shock protein 70 (HSP70) to predict autism spectrum disorder (ASD) (Hamed et al., 2019). However, this findings are hindered by the somewhat small sample size (72 and 187, respectively), and should be, therefore, carefully interpreted.

In the OA field, the modest predictive capacity found in the analyzed biomarkers in this project is in agreement with the obtained predictive capacity of different biomarkers evaluated to predict relevant OA progression. For example, Eckstein and collaborators examined the relationship of 15 molecular markers with structural progression based on femorotibial cartilage loss assessed by subregional MRI was evaluated in 152 women from the A9001140 study (Eckstein et al., 2011). The relatively strongest predictors of longitudinal thinning were serum sCTX-I and plasma N-terminal propeptide of type II procollagen (pNPII), yielding an AUC 0.65 and 0.64, respectively. The remaining biomarkers, including serum concentrations of COMP, showed an AUC < 0.60. In the meta-scale published by Valdes and collaborators (Valdes et al., 2014), urine CTX-II also showed a poor predictive capacity (AUC ≤ 0.63) for the 4 cohorts focused on progression of knee OA. Recently, Kraus and collaborators have investigated a target set of 18

biochemical markers (baseline and time-integrated concentrations (TICs) over 12 and 24 months) as predictors of symptomatic and radiographic knee OA progression (Kraus et al., 2017). Among all of them, the best single biomarkers was the 24 M TIC CTX-II measured in urine, yielding an AUC 0.58.

In terms of sensitivity and specificity, the potential biomarkers analyzed in the study published by Kraus et al. (Kraus et al., 2017) were found to be ≈ 60%. Only COMP showed a specificity close to 80%, but also a sensitivity of 53%, i.e. although the number of false positives is low, there are many false negatives. In the other way, AHSG showed the less number of false negatives, with a specificity of 79%, but the number of false positives was high, showing a sensitivity of 53%. This findings were similar to those published by Goycheva et al. (Goycheva et al., 2019), where sensitivity and specificity of the analyzed proteins ranged from 60% to 70%. Also Hamed et al. (Hamed et al., 2019) found specificities around the 60% for HSP70 and H-PGDS (hematopoietic prostaglandin D2 synthetase) and 45% for TGFβ-2. However, the sensitivity for all of them exceed the 80%.

Several studies have shown that the combination of two biomarkers were more effective for predicting disease progression than a single biomarkers in hip OA (Garnero et al., 2006; Mazieres et al., 2006), but also in knee OA (Cahue et al., 2007; Dam et al., 2009; Sharif et al., 2007). For example, Bedkowska and collaborators have published one study this year in which they determined the diagnostic power of non-invasive ovarian cancer tumor markers by analysing 140 postmenopausal ovarian cancer patients and 140 participants including both, benign ovarian cancer and healthy controls (Bedkowska et al., 2019). Among all the studied biomarkers, they found that the combination of CA125 (carbohydrate antigen 125) plus HE4 (human epididymis protein 4) with MMP7, MMP9 or VEGF (vascular endothelial growth factor) resulted in the best diagnostic capacity with the highest AUC value, up to 0.92. In this sense, we also analyzed the predictive capacity of the combination of those biomarkers that were quantified in a unique multiplex sandwich immunoassay. However, in our case, the combination of 2 or 3 biomarkers did not results in a significant increase of the predictive accuracy obtained by a single biomarker. Here, the highest AUC was found in the combination of COMP with CHI3L1, yielding 0.70, which entail an insignificant difference with the AUC of the independent biomarkers.

Autoantibodies as a new source of potential biomarkers

Although OA is not considered an autoimmune disorder, the immune system has been related with early disease (Ene et al., 2015). One of the main feature of many diseases involving the humoral immune response is the production of AAbs (Gibson et al., 2012), which can often be detected at asymptomatic stages (Leslie et al., 2001), having the potential to identify susceptible individuals or populations and facilitating prognosis. In fact, this idea that AAbs can be used to predict a disease state has been extensively studied in different disorders, such as cancer (Chen et al., 2017; Kunizaki et al., 2018; Qi et al., 2015; Tan et al., 2009) or type 1 diabetes (Bonifacio et al., 1995; Fabris et al., 2015), and also in the field of rheumatic diseases, where AAbs have a fundamental value in the diagnosis of those with an autoimmune pathogenesis, such as systemic lupus erythematosus (SLE) (Putterman et al., 2016) and RA (Aletaha et al., 2010). However, existing literature related to the presence of AAbs in OA patients is limited (Du et al., 2005; Henjes et al., 2014; Jasin, 1985; Ruthard et al., 2018) . Indeed, we present in this thesis the largest screening of AAbs as a new source of potential biomarkers performed to date in the OA field, and the first study that evaluates the usefulness of OA to stratify patients who are at risk of radiographic knee OA development.

Among the panel of 6 AAbs as potential prognostic biomarkers, we selected MAT2β-AAb to be verified on individual samples at baseline from the OAI cohort, which provides a robust evaluation of its ability to classify patients at baseline as incident or not-incident during a 96-months period. MAT2β is the regulatory subunit responsible of enhancing or inhibiting the synthesis of SAM. This latter compound plays a vital role in methylation, transsulfuration and aminopropylation pathways Hosea BlewettHosea Blewett (127), and it has been employed as dietary supplement for OA management (adomet) (Hosea Blewett, 2008; Kim et al., 2009; Najm et al., 2004; Soeken et al., 2002). Although there is no evidence of the direct involvement of MAT2β in OA, its fundamental role in key biological processes for the pathogenesis of this disease (Figure 28) turns it into a potential marker of interest.

The measurement of the reactivity levels at baseline of MAT2β-AAb in 327 sera revealed the presence of significant higher levels in the incident group, compared with the not-incident group (0.58 ± 0.22 a.u. vs 0.49 ± 0.23 a.u., p= 3.140E-04). This finding

goes in concordance with the results obtained from the discovery phase, were the reactivity levels of MAT2β-AAb were also significant higher in the pooled samples from the incident subcohorts at baseline of the OAI (p= 0.005). In addition, this study also demonstrates that the presence of AAbs against MAT2β was significant associated with the incidence of radiographic knee OA development, which confers an odd 5.99 higher to incise per one-unit increase. The predictive capacity of this proposed biomarker was lowest than the one founded in the previous study, yielding an AUC 0.62, with 39% specificity and 86% sensitivity. In a study analysing 149 patients with esophageal squamous cell carcinoma (Chen et al., 2017), the diagnostic accuracy of the levels of AAbs against Fascin were as modest as the one showed by MAT2β-AAb, yielding an AUC 0.63 with 99% and 24.8% specificity and sensitivity, respectively. Also low AUC were found in a meta-analysis for the diagnostic capacity of a panel of 6 tumor-associated AAbs (AUC 0.52), although it raised up to 0.90 in a different panel of 7 AAbs (Tang et al., 2017). However, it should be take into account that among the 327 samples analyzed by NAPPA-ELISA, 200 were already used as pools in the discovery phase of the study. Thus, since the clinical utility of prognostic models hinges on their ability to make predictions on new data, a further validation of these results in a different cohort of OA incidence would be very valuable to confirm these results.

OA prediction models by combining clinical variable and biochemical biomarkers

It has been postulated that combining biochemical markers with other markers, such as imaging, genetic and clinical markers, may facilitate the prognostic of who is in a high risk for developing OA (Saberi Hosnijeh et al., 2019). Because of this, for both studies presented in this thesis, different clinical factors related with risk of incident OA have been analyzed by univariate logistic regression analysis to look for significant predictors of radiographic knee OA development which can define a clinical prognostic model of OA prediction. The putative utility of biochemical markers to predict knee OA appearance was evaluated by comparing the AUC from the covariates-only model with the biomarker plus covariate model. It is important to specify that this study is based on a Caucasian US population, which may not comprise all the factors that enhance predisposition to OA.

As shown herein, using stepwise logistic regression with significant predictors resulted in 2 different prognostic models of OA incidence in the first study, yielding AUC 0.77, and a single prognostic model in the second one, yielding AUC 0.83. The difference between the covariates including in the models from the first study lies in the absence (model 1) or presence (model 2) of the history of knee injury in the target knee, which do not cause a significant effect in the predictive accuracy of the model. Therefore, the covariates-only model 1 was selected as the best clinical prognostic model for the population of study because it matched the same predictive capacity as model 2 with a smaller number of variables. The clinical prognostic model defined in the second study, also count with the age, gender, BMI, frequent bending activity, history of knee injury, pain in either knee as covariates, however, instead the KOOS symptoms score, this model included the WOMAC stiffness score. The generation of the models was carried out by an forward and backward automatic procedures of the statistic package SPSS, which using an algorithm based in prespecified criteria select the variables in function of its impact in the population of the study and the prevalence of the clinical outcome.

There are several studies in which different clinical variables are combined to generate an OA incidence model in large prospective cohorts. For example, using data from individuals in the Rotterdam Study-I, different prediction models using clinical factors, questionnaires variables and genetic factors were defined. The model including only age, gender and BMI resulted in an AUC of 0.66, and the inclusion of the others variables did not improve the model (AUC 0.67) (Kerkhof et al., 2014). In another study, Zhang and collaborators defined a model of incidence of radiographic knee OA using data from the Nottingham cohort, the OAI cohort and the Genetics of Osteoarthritis and Lifestyle (GOAL) study (Zhang et al., 2011). This model, including variables such as age, gender, BMI, occupational risk, family history and knee injury yielded the greatest AUC in the GOAL population (AUC 0.74), compared to the OAI (AUC 0.60) and the Nottingham population (AUC 0.69). Also an AUC of 0.74 was obtained in a prognostic model to predict radiographic knee OA analysing individuals from the CHECK cohort, which include different demographic and clinical characteristics as well as radiographic features (Kinds et al., 2012). In our case, the remarkably high ability to predict the appearance of radiographic knee OA using the covariates-only model defined in the second study (AUC 0.83) could be due to the high prevalence of the disease in our target

population (45% of incident participants). Indeed, the application of this model into the whole OAI database yielded a lower AUC (AUC 0.69).

Finally, the putative utility of this biomarkers in a prognostic model of knee OA prediction was evaluated. Using the DeLong test we could observe that, despite the modest predictive capacity of the biomarkers, the inclusion of CHI3L1 together with COMP, and MAT2β-AAb to their corresponding covariates-only models led in both cases to an increase in their discriminative ability, yielding AUCs of 0.82 for the CHI33L1+COMP plus covariates-model, and 0.86 for the MAT2β-AAb plus covariates model. Remarkably, the addition of this biomarkers to the corresponding clinical model provides a statistically significant increase in the AUC for both models ($p= 0.045$ and $p= 0.013$, respectively). In a similar study, where the incidence of OA was defined as a KL score < 2 at baseline and a KL ≥ 2 at follow-up, addition of urine CTX-II levels in a clinical prediction model for knee OA led to an improvement in the AUC of the model, but in this case, it was not significant (Kerkhof et al., 2014).

In this latest study, the authors only included individuals with unilateral knee OA. However, we found that among the 540 individuals included in the first study, the 35% of them showed contralateral OA, as well as the 20% from the 327 participants included in the second study. Thus, the presence of contralateral knee OA was included in both, the MAT2β-AAb plus covariates model and the CHI3L1+COMP plus covariates model in order to evaluate whether the inclusion of this information was really necessary to improve the predictive capacity of the models. In both cases it was seen that introducing this variable to the model did not improve the predictive capacity of the previous model, supporting the idea that it is not necessary to know the patient's radiographic information in order to accurately predict the risk of OA incidence and strengthens the utility of these biomarkers to predict incidence of knee OA at the very early stage.

However, the use of patient which already developed radiographic knee OA to generate a prognostic model to predict radiographic knee OA development is a huge limitation from a clinical point of view and it has to be taken into account. For this reason, we also evaluate whether the prognostic ability of these biomarkers were maintained after removing all subjects with contralateral OA at baseline. For both cases, the CHIL31+COMP-only model and MAT2β-AAb-only model, the prognostic ability

remaining the same (AUC 0.71 and AUC 0.61, respectively). Nevertheless, although a similar increment of the AUC was observed when CHI3L1+COMP were introduced to the proper clinical model 1, the difference was not significant (AUC 0.83 vs 0.79, p= 0.329). Following the same line, no significant increase was found after the inclusion of MAT2β-AAb to the clinical model (AUC 0.84 vs 0.83, p= 0.217).

In order to discern whether the loss of significant differences between the clinical models, with or without the biomarkers, is due to the elimination of more that 20% of the patients in the analysis (the most of them belonged to the incident group) rather than the fact to these high serum concentrations of the analytes are linked to the presence of knee OA in the off-target knee, a more exhaustive analysis should be done by in a large number of subjects with unilateral knee OA.

Survival analysis

Nowadays, KM curves and estimates of survival data have become a familiar way of dealing with differing times-to-event, especially when not all the subjects continue in the study. To understood KM analysis, it is necessary to know that the lengths of the horizontal lines along the X-axis of serial times represent the time until the occurrence of the event of interest (death, occurrence of a disease, divorce, etc.) for that interval. On the other hand, the vertical distance between horizontals illustrated the change in cumulative probability of not having the event as the curve advance (Rich et al., 2010). Horizontal lines and attendant probabilities are only constructed based in participants who reached the event of interest (known time-to-event). Subjects for who the required data are not available (e.g. they drops out) or who not present the event at the end of the study, are not appropriated to consider as indicators of the time-to-event and they are indicated in the curve as tick marks.

This statistical approach has been widely used in cancer biomarkers (Aguirre-Gamboa et al., 2013; Albertus et al., 2008; Rinaldetti et al., 2018). For example, Aguirre and collaborator have developed a cancer-wide gene expression database, named SurvExpress, with clinical outcomes and a web-based tool that provides survival analysis and risk assessment of cancer dataset, and they had proved its utility in two biomarkers applications (predict recurrence or survival) for breast and lung cancer (Aguirre-Gamboa et al., 2013). Recently, the use of KM curve has been also introduced in the rheumatology

field to predict mortality in RA by developing a multivariate predictive model using the machine learning method Random Survival Forests (RSF) (Lezcano-Valverde et al., 2017), and to describe the functional outcome of surviving high tibial osteotomy10–20 years after surgery (van Wulfften Palthe et al., 2018).

Here, we applied KM curves in order to investigate the impact of CHI3L1 and COMP serum concentrations, and MAT2β-AAb reactivity levels on the time to OA incidence. Our findings show that, using the Log Rank test, CHI3L1 was able to significant separate 3 different risk groups characterized by their serum concentrations of the biomarker. However, both COMP was only able to significant differentiate the risk to develop sooner the disease depending on whether they present high or either, medium and low serum concentrations. In a similar way, MAT2β-AAb reactivity levels was able to significant differentiate between either, the high- or medium-levels group versus the low-levels group.

Another method of comparing KM curves is using the HR, which gives a relative event rate in the groups at the time that allows adjusting for several variables. The hazard, per 1-unit increase, of sooner incidence knee radiographic OA outcome was significant elevated in those patients with high, but not medium, baseline CHI3L1 (HR 1.72, p= 5.189E-03) and COMP (HR 2.81, p=3.600E-08) concentrations after adjustment by all the covariates including in the proper covariates-only model, which are: age, gender, BMI, frequent of knee bending, pain in either knee and the KOOS symptoms score. The HR of incident knee OA based on KL grade between serum levels of COMP and incidence of radiographic knee OA in a large cohort has been evaluated before (Golightly et al., 2011). In this sense, Golightly et al. investigated the HR of incident radiographic knee OA based in the KL grade (n= 542), osteophyte formation (n= 353) and JSN (n= 446). In concordance with our findings, they also found that the hazard of incident knee OA also increased with higher baseline COMP levels, expressed in Napierian logarithm (ln), although these associations were only significant in both knee osteophyte and JSN outcomes.

With regards to MAT2β-AAbs, we found that both, high (HR 2.34, p= 2.680E-04) and medium (HR 2.17, p= 7.440E-04) reactivity levels at baseline in sera of this AAb was significant associated with the time when the disorder was manifested after the

adjustment for all the variables included in the corresponding clinical model (age, gender, BMI, frequent bending activity, history of knee injury, pain in either knee and the WOMAC stiffness score), supporting our hypothesis “the higher the levels, the sooner the disease appears”.

VI. CONCLUSIONS

Conclusions related to specific objective 1: *To develop and optimize a custom multiplex sandwich immunoassay for the bead-based xMAP technology to validate and qualify a panel of six potential biomarkers in sera as prognostic biomarkers of incident radiographic knee OA.*

1.1. Individual sandwich ELISA immunoassays against COMP, CHI3L1, RBP4, AHSG, TPS1 and APCS were successfully converted to the Luminex xMAP platform, leading to the development of three different sandwich immunoassays: a duplex sandwich immunoassays including CHI3L1 and COMP, a triplex sandwich immunoassays including RBP4, AHSG, and TPSI, and a singleplex sandwich immunoassays for APCS.

1.2. Increased baseline serum concentration of CHI3L1, COMP, RBP4, AHSG, and APCS were significant associated with the future occurrence of radiographic knee OA, which showed a moderate predictive capacity, both individually and combined with others in the case of multiplexed immunoassays.

Conclusions related to the specific objective 2: *To discover a serum AAbs profile associated with the incidence of radiographic knee OA.*

2.1. Serum AAb profiling using the NAPPA technology allowed for the identification of a panel of 6 AAbs with significant different baseline reactivity levels between incident and not-incident subjects.

2.2. In the verification phase, baseline reactivity levels of MAT2β-AAb showed a moderate predictive capacity as prognostic biomarker of incident radiographic knee OA.

Conclusions related to the specific objective 3: *To assess whether the inclusion of potential protein biomarkers in a clinical prognostic model improve the prediction capacity of incident radiographic knee OA.*

3.1. In the first study, the inclusion of CHI3L1 together with COMP caused a significant increase in the predictive capacity of the corresponding clinical prognostic model to predict incident radiographic knee OA.

3.2. In the second study, the inclusion of MAT2β-AAb in the corresponding clinical prognostic model resulted in a significant increase of the predictive capacity of incident radiographic knee OA.

Conclusions related with the specific objective 4: *To investigate whether the baseline serum levels of the selected biomarkers have any impact in the time at radiographic knee OA appear.*

4.1. Both, baseline serum concentrations of two proteins, CHI3L1 and COMP, and baseline reactivity levels of MAT2β-AAb showed a significant association with the time of radiographic knee OA development, even after the adjustment for all variables included in the corresponding clinical prognostic model: the higher the levels of the biomarker, the sooner the disease appeared.

VII. REFERENCES

A

Aguirre-Gamboa R, Gomez-Rueda H et al. SurvExpress: an online biomarker validation tool and database for cancer gene expression data using survival analysis. PLoS One. 2013;8(9):e74250.

Aigner T, Soder S et al. Mechanisms of disease: role of chondrocytes in the pathogenesis of osteoarthritis--structure, chaos and senescence. Nat Clin Pract Rheumatol. 2007;3(7):391-9.

Albertus DL, Seder CW et al. AZGP1 autoantibody predicts survival and histone deacetylase inhibitors increase expression in lung adenocarcinoma. J Thorac Oncol. 2008;3(11):1236-44.

Alentorn-Geli E, Samuelsson K et al. The Association of Recreational and Competitive Running With Hip and Knee Osteoarthritis: A Systematic Review and Meta-analysis. J Orthop Sports Phys Ther. 2017;47(6):373-90.

Aletaha D, Neogi T et al. 2010 Rheumatoid arthritis classification criteria: an American College of Rheumatology/European League Against Rheumatism collaborative initiative. Arthritis Rheum. 2010;62(9):2569-81.

Allen KD, Golightly YM. State of the evidence. Curr Opin Rheumatol. 2015;27(3):276-83.

Alsalameh S, Mollenhauer J et al. Cellular immune response toward human articular chondrocytes. T cell reactivities against chondrocyte and fibroblast membranes in destructive joint diseases. Arthritis Rheum. 1990;33(10):1477-86.

Altman RD, Gold GE. Atlas of individual radiographic features in osteoarthritis, revised. Osteoarthritis Cartilage. 2007;15 Suppl A:A1-56.

Anderson KS, Cramer DW et al. Autoantibody signature for the serologic detection of ovarian cancer. J Proteome Res. 2015;14(1):578-86.

Anderson KS, Sibani S et al. Protein microarray signature of autoantibody biomarkers for the early detection of breast cancer. J Proteome Res. 2011;10(1):85-96.

Arden NK, Cro S et al. The effect of vitamin D supplementation on knee osteoarthritis, the VIDEO study: a randomised controlled trial. Osteoarthritis Cartilage. 2016;24(11):1858-66.

Aslam B, Basit M et al. Proteomics: Technologies and Their Applications. J Chromatogr Sci. 2017;55(2):182-96.

Atukorala I, Kwoh CK et al. Synovitis in knee osteoarthritis: a precursor of disease? Ann Rheum Dis. 2016;75(2):390-5.

Austin AK, Hobbs RN et al. Humoral immunity to link protein in patients with inflammatory joint disease, osteoarthritis, and in non-arthritic controls. Ann Rheum Dis. 1988;47(11):886-92.

Ayral X, Pickering EH et al. Synovitis: a potential predictive factor of structural progression of medial tibiofemoral knee osteoarthritis -- results of a 1 year longitudinal arthroscopic study in 422 patients. Osteoarthritis Cartilage. 2005;13(5):361-7.

B

Baker HN, Murphy R et al. Conversion of a capture ELISA to a Luminex xMAP assay using a multiplex antibody screening method. J Vis Exp. 2012(65).

Banuls MJ, Morais SB et al. Microarray Developed on Plastic Substrates. Methods Mol Biol. 2016;1368:37-51.

Bauer DC, Hunter DJ et al. Classification of osteoarthritis biomarkers: a proposed approach. Osteoarthritis Cartilage. 2006;14(8):723-7.

Bay-Jensen AC, Reker D et al. Osteoarthritis year in review 2015: soluble biomarkers and the BIPED criteria. Osteoarthritis Cartilage. 2016;24(1):9-20.

Bay-Jensen AC, Thudium CS et al. Development and use of biochemical markers in osteoarthritis: current update. Curr Opin Rheumatol. 2018;30(1):121-8.

Bedkowska GE, Piskor B et al. Diagnostic Power of Selected Cytokines, MMPs and TIMPs in Ovarian Cancer Patients - ROC Analysis. Anticancer Res. 2019;39(5):2575-82.

Benito MJ, Veale DJ et al. Synovial tissue inflammation in early and late osteoarthritis. Ann Rheum Dis. 2005;64(9):1263-7.

Berenbaum F, Eymard F et al. Osteoarthritis, inflammation and obesity. Curr Opin Rheumatol. 2013;25(1):114-8.

Bian X, Wasserfall C et al. Tracking the Antibody Immunome in Type 1 Diabetes Using Protein Arrays. J Proteome Res. 2017;16(1):195-203.

Bijlsma JWJ, Berenbaum F et al. Osteoarthritis: an update with relevance for clinical practice. The Lancet. 2011;377(9783):2115-26.

Blanco FJ. Osteoarthritis year in review 2014: we need more biochemical biomarkers in qualification phase. Osteoarthritis Cartilage. 2014;22(12):2025-32.

Blumenfeld O, Williams FM et al. Association between cartilage and bone biomarkers and incidence of radiographic knee osteoarthritis (RKOA) in UK females: a prospective study. Osteoarthritis Cartilage. 2013;21(7):923-9.

Boesen M, Ellegaard K et al. Osteoarthritis year in review 2016: imaging. Osteoarthritis Cartilage. 2017;25(2):216-26.

Boja ES, Jortani SA et al. The journey to regulation of protein-based multiplex quantitative assays. Clin Chem. 2011;57(4):560-7.

Bonifacio E, Genovese S et al. Islet autoantibody markers in IDDM: risk assessment strategies yielding high sensitivity. Diabetologia. 1995;38(5):816-22.

Boschetti E, D'Amato A et al. Protein biomarkers for early detection of diseases: The decisive contribution of combinatorial peptide ligand libraries. J Proteomics. 2018;188:1-14.

Bouyer B, Mazieres B et al. Association between hip morphology and prevalence, clinical severity and progression of hip osteoarthritis over 3 years: The knee and hip osteoarthritis long-term assessment cohort results. Joint Bone Spine. 2016;83(4):432-8.

Breker M, Schuldiner M. The emergence of proteome-wide technologies: systematic analysis of proteins comes of age. Nat Rev Mol Cell Biol. 2014;15(7):453-64.

Burrell CJ, Howard CR et al. Adaptive Immune Responses to Infection. Fenner and White's Medical Virology2017. p. 65-76.

Büyükköroğlu G, Dora DD et al. Techniques for Protein Analysis. Omics Technologies and Bio-Engineering2018. p. 317-51.

C

Cahue S, Sharma L et al. The ratio of type II collagen breakdown to synthesis and its relationship with the progression of knee osteoarthritis. Osteoarthritis Cartilage. 2007;15(7):819-23.

Calamia V, Mateos J et al. A pharmacoproteomic study confirms the synergistic effect of chondroitin sulfate and glucosamine. Sci Rep. 2014;4:5069.

Calamia V, Rocha B et al. Metabolic labeling of chondrocytes for the quantitative analysis of the interleukin-1-beta-mediated modulation of their intracellular and extracellular proteomes. J Proteome Res. 2011;10(8):3701-11.

Cameron KL, Driban JB et al. Osteoarthritis and the Tactical Athlete: A Systematic Review. J Athl Train. 2016;51(11):952-61.

Carson RT, Vignali DA. Simultaneous quantitation of 15 cytokines using a multiplexed flow cytometric assay. J Immunol Methods. 1999;227(1-2):41-52.

Casado-Vela J, Fuentes M et al. Screening of protein-protein and protein-DNA interactions using microarrays: applications in biomedicine. Adv Protein Chem Struct Biol. 2014;95:231-81.

Casado-Vela J, González-González M et al. Protein Arrays: Recent Achievements and their Application to Study the Human Proteome. Curr Proteomics. 2013;10(2):83-97.

Centola M, Cavet G et al. Development of a multi-biomarker disease activity test for rheumatoid arthritis. PLoS One. 2013;8(4):e60635.

Chandra H, Reddy PJ et al. Protein microarrays and novel detection platforms. Expert Rev Proteomics. 2011;8(1):61-79.

Chen WX, Hong XB et al. Tumor-associated autoantibodies against Fascin as a novel diagnostic biomarker for esophageal squamous cell carcinoma. Clin Res Hepatol Gastroenterol. 2017;41(3):327-32.

Cirillo DJ, Wallace RB et al. Effect of hormone therapy on risk of hip and knee joint replacement in the Women's Health Initiative. Arthritis Rheum. 2006;54(10):3194-204.

Cretich M, Damin F et al. Protein microarray technology: how far off is routine diagnostics? Analyst. 2014;139(3):528-42.

Croft P, Coggon D et al. Osteoarthritis of the hip: an occupational disease in farmers. BMJ. 1992;304(6837):1269-72.

Cross M, Smith E et al. The global burden of hip and knee osteoarthritis: estimates from the global burden of disease 2010 study. Ann Rheum Dis. 2014;73(7):1323-30.

D

Da Silva-Baptista C, Munroe DJ. Protein Microarrays. In: D. VT, R. YJ, editors. Proteomics for Biological Discovery: John Wiley & Sons, Inc; 2006.

Dahaghin S, Bierma-Zeinstra SM et al. Does hand osteoarthritis predict future hip or knee osteoarthritis? Arthritis Rheum. 2005;52(11):3520-7.

Dai Z, Lu N et al. Dietary Fiber Intake in Relation to Knee Pain Trajectory. Arthritis Care Res (Hoboken). 2017;69(9):1331-9.

Dam EB, Loog M et al. Identification of progressors in osteoarthritis by combining biochemical and MRI-based markers. Arthritis Res Ther. 2009;11(4):R115.

de Jager W, te Velthuis H et al. Simultaneous detection of 15 human cytokines in a single sample of stimulated peripheral blood mononuclear cells. Clin Diagn Lab Immunol. 2003;10(1):133-9.

de Klerk BM, Schiphof D et al. No clear association between female hormonal aspects and osteoarthritis of the hand, hip and knee: a systematic review. Rheumatology (Oxford). 2009;48(9):1160-5.

Dell'Isola A, Allan R et al. Identification of clinical phenotypes in knee osteoarthritis: a systematic review of the literature. BMC Musculoskelet Disord. 2016;17(1):425.

Dequeker MD, Mohan S et al. Generalized osteoarthritis associated with increased insulin-like growth factor types i and ii and transforming growth factor β in cortical bone from the iliac crest. possible mechanism of increased bone density and protection against osteoporosis. Arthritis and Rheumatology. 1993;36(12):1702-8.

Díaz-Zaragoza M, Hernández-Ávila R et al. Natural and adaptive IgM antibodies in the recognition of tumor-associated antigens of breast cancer (Review). Oncol Rep. 2015;34(3):1106-14.

Diez P, Dasilva N et al. Data Analysis Strategies for Protein Microarrays. Microarrays (Basel). 2012;1(2):64-83.

Diez P, Gonzalez-Gonzalez M et al. NAPPA as a Real New Method for Protein Microarray Generation. Microarrays (Basel). 2015;4(2):214-27.

Driban JB, Hootman JM et al. Is Participation in Certain Sports Associated With Knee Osteoarthritis? A Systematic Review. J Athl Train. 2017;52(6):497-506.

Du H, Masuko-Hongo K et al. The prevalence of autoantibodies against cartilage intermediate layer protein, YKL-39, osteopontin, and cyclic citrullinated peptide in patients with early-stage knee osteoarthritis: evidence of a variety of autoimmune processes. Rheumatol Int. 2005;26(1):35-41.

Dunlop DD, Manheim LM et al. The costs of arthritis. Arthritis Rheum. 2003;49(1):101-13.

dupont NC, Wang K et al. Validation and comparison of luminex multiplex cytokine analysis kits with ELISA: determinations of a panel of nine cytokines in clinical sample culture supernatants. J Reprod Immunol. 2005;66(2):175-91.

E

Eckstein F, Le Graverand MP. Plain radiography or magnetic resonance imaging (MRI): Which is better in assessing outcome in clinical trials of disease-modifying osteoarthritis drugs? Summary of a debate held at the World Congress of Osteoarthritis 2014. Semin Arthritis Rheum. 2015;45(3):251-6.

Eckstein F, Le Graverand MP et al. Clinical, radiographic, molecular and MRI-based predictors of cartilage loss in knee osteoarthritis. Ann Rheum Dis. 2011;70(7):1223-30.

Edwards MH, Paccou J et al. The relationship of bone properties using high resolution peripheral quantitative computed tomography to radiographic components of hip osteoarthritis. Osteoarthritis Cartilage. 2017;25(9):1478-83.

Ehrlich JR, Tang L et al. The "reverse capture" autoantibody microarray : an innovative approach to profiling the autoantibody response to tissue-derived native antigens. Methods Mol Biol. 2008;441:175-92.

Ekins RP. Multi-analyte immunoassay. J Pharm Biomed Anal. 1989;7(2):155-68.

Ekins RP, Chu F. Multianalyte microspot immunoassay. The microanalytical 'compact disk' of the future. Ann Biol Clin. 1992;50(5):337-53.

Ekins RP, Chu F. Developing multianalyte assays. Trends Biotechnol. 1994;12(3):89-94.

Elshal MF, McCoy JP. Multiplex bead array assays: performance evaluation and comparison of sensitivity to ELISA. Methods. 2006;38(4):317-23.

Ene R, Sinescu RD et al. Synovial inflammation in patients with different stages of knee osteoarthritis. Rom J Morphol Embryol. 2015;56(1):169-73.

Engvall E, Perlmann P. Enzyme-linked immunosorbent assay (ELISA). Quantitative assay of immunoglobulin G. Immunochemistry. 1971;8(9):871-4.

Espina V, Mehta AI et al. Protein microarrays: molecular profiling technologies for clinical specimens. Proteomics. 2003;3(11):2091-100.

Ewaisha R, Meshay I et al. Programmable protein arrays for immunoprofiling HPV-associated cancers. Proteomics. 2016;16(8):1215-24.

F

Fabris M, Zago S et al. Anti-zinc transporter protein 8 autoantibodies significantly improve the diagnostic approach to type 1 diabetes: an Italian multicentre study on paediatric patients. Auto Immun Highlights. 2015;6(1-2):17-22.

FDA. Guidance for Industry. Bioanalytical Method Valiidation. 2018.

Feinberg JG. A 'microspot' test for antigens and antibodies. Nature. 1961;9(192):985-6.

Felson D, Lawrence RC et al. Osteoarthritis: new insights. Part 1: the disease and its risk factors. Ann Intern Med. 2000;133(8):635-46.

Felson D, Naimark A et al. The prevalence of knee osteoarthritis in the elderly. The Framingham Osteoarthritis Study. Arthritis Rheum. 1987;30(8):914-8.

Felson DT, Niu J et al. Low levels of vitamin D and worsening of knee osteoarthritis: results of two longitudinal studies. Arthritis Rheum. 2007;56(1):129-36.

Felson DT, Niu J et al. Defining radiographic incidence and progression of knee osteoarthritis: suggested modifications of the Kellgren and Lawrence scale. Ann Rheum Dis. 2011;70(11):1884-6.

Fernández-Costa C, Calamia V et al. Sequential depletion of human serum for the search of osteoarthritis biomarkers. Proteome Sci. 2012;10(1).

Fernandez-Puente P, Calamia V et al. Multiplexed mass spectrometry monitoring of biomarker candidates for osteoarthritis. J Proteomics. 2017;152:216-25.

Fernandez-Puente P, Mateos J et al. Identification of a panel of novel serum osteoarthritis biomarkers. J Proteome Res. 2011;10(11):5095-101.

Festa F, Rollins SM et al. Robust microarray production of freshly expressed proteins in a human milieu. Proteomics Clin Appl. 2013;7(5-6):372-7.

Fibel KH, Hillstrom HJ et al. State-of-the-Art management of knee osteoarthritis. World J Clin Cases. 2015;3(2):89-101.

Finan PH, Buenaver LF et al. Discordance between pain and radiographic severity in knee osteoarthritis: findings from quantitative sensory testing of central sensitization. Arthritis Rheum. 2013;65(2):363-72.

Findlay JW, Smith WC et al. Validation of immunoassays for bioanalysis: a pharmaceutical industry perspective. J Pharm Biomed Anal. 2000;21(6):1249-73.

Foell D, Wittkowski H et al. Mechanisms of disease: a 'DAMP' view of inflammatory arthritis. Nat Clin Pract Rheumatol. 2007;3(7):382-90.

Fortner RT, Damms-Machado A et al. Systematic review: Tumor-associated antigen autoantibodies and ovarian cancer early detection. Gynecol Oncol. 2017;147(2):465-80.

Fuentes M, Diez P et al. Nanotechnology in the Fabrication of Protein Microarrays. Methods Mol Biol. 2016;1368:197-208.

G

Gagaoua M, Bonnet M et al. Reverse Phase Protein array for the quantification and validation of protein biomarkers of beef qualities: The case of meat color from Charolais breed. Meat Sci. 2018;145:308-19.

Garcia-Moreno C, Gomara MJ et al. Development of a multiplex assay based on chimeric citrullinated peptides as proof of concept for diagnosis of rheumatoid arthritis. PLoS One. 2019;14(5):e0215927.

Garnero P, Charni N et al. Increased urinary type II collagen helical and C telopeptide levels are independently associated with a rapidly destructive hip osteoarthritis. Ann Rheum Dis. 2006;65(12):1639-44.

Gay C, Chabaud A et al. Educating patients about the benefits of physical activity and exercise for their hip and knee osteoarthritis. Systematic literature review. Ann Phys Rehabil Med. 2016;59(3):174-83.

Gibson DS, Qiu J et al. Circulating and synovial antibody profiling of juvenile arthritis patients by nucleic acid programmable protein arrays. Arthritis Res Ther. 2012;14(2):R77.

Gillet LC, Navarro P et al. Targeted data extraction of the MS/MS spectra generated by data-independent acquisition: a new concept for consistent and accurate proteome analysis. Mol Cell Proteomics. 2012;11(6):O111 016717.

Glyn-Jones S, Palmer AJR et al. Osteoarthritis. The Lancet. 2015;386(9991):376-87.

Goldberg VM, Kresina TF. Immunology of articular cartilage. J Rheumatol. 1987;14(73):6.

Goldring MB, Otero M. Inflammation in osteoarthritis. Curr Opin Rheumatol. 2011;23(5):471-8.

Golightly YM, Marshall SW et al. Biomarkers of incident radiographic knee osteoarthritis: do they vary by chronic knee symptoms? Arthritis Rheum. 2011;63(8):2276-83.

Gonzalez-Gonzalez M, Jara-Acevedo R et al. Nanotechniques in proteomics: protein microarrays and novel detection platforms. Eur J Pharm Sci. 2012;45(4):499-506.

Goycheva P, Nikolova G et al. Predictive value of some pro-oxidants in type 2 diabetes mellitus with vascular complications. Biosci Trends. 2019;13(2):168-75.

Graham H, Chandler DJ et al. The genesis and evolution of bead-based multiplexing. Methods. 2019;158:2-11.

Gregson CL, Hardcastle SA et al. High Bone Mass is associated with bone-forming features of osteoarthritis in non-weight bearing joints independent of body mass index. Bone. 2017;97:306-13.

Guermazi A, Alizai H et al. Compositional MRI techniques for evaluation of cartilage degeneration in osteoarthritis. Osteoarthritis Cartilage. 2015;23(10):1639-53.

Guermazi A, Hayashi D et al. Osteoarthritis: a review of strengths and weaknesses of different imaging options. Rheum Dis Clin North Am. 2013;39(3):567-91.

Guo J, Yang J et al. A Panel of Biomarkers for Diagnosis of Prostate Cancer Using Urine Samples. Anticancer Res. 2018;38(3):1471-7.

H

Haab BB. Antibody arrays in cancer research. Mol Cell Proteomics. 2005;4(4):377-83.

Haab BB, Dunham MJ et al. Protein microarrays for highly parallel detection and quantitation of specific proteins and antibodies in complex solutions. Genome Biol. 2001;2(2).

Halilaj E, Le Y et al. Modeling and predicting osteoarthritis progression: data from the osteoarthritis initiative. Osteoarthritis Cartilage. 2018;26(12):1643-50.

Hall D, Ptacek J et al. Protein microarray technology. Mech Ageing Dev. 2007;128(1):161-7.

Hamed NO, Laila Al A et al. Determination of neuroinflammatory biomarkers in autistic and neurotypical Saudi children. Metab Brain Dis. 2019.

Han W, Aitken D et al. Signal intensity alteration in the infrapatellar fat pad at baseline for the prediction of knee symptoms and structure in older adults: a cohort study. Ann Rheum Dis. 2016;75(10):1783-8.

Hanna FS, Wluka AE et al. Osteoarthritis and the postmenopausal woman: Epidemiological, magnetic resonance imaging, and radiological findings. Seminars in Arthritis and Rheumatism. 2004;34(3):631-6.

Hayashi D, Roemer FW et al. Imaging in Osteoarthritis. Radiol Clin North Am. 2017;55(5):1085-102.

Henderson MC, Hollingsworth AB et al. Integration of Serum Protein Biomarker and Tumor Associated Autoantibody Expression Data Increases the Ability of a Blood-Based Proteomic Assay to Identify Breast Cancer. PLoS One. 2016;11(8):e0157692.

Henjes F, Lourido L et al. Analysis of autoantibody profiles in osteoarthritis using comprehensive protein array concepts. J Proteome Res. 2014;13(11):5218-29.

Henrotin Y. Osteoarthritis year 2011 in review: biochemical markers of osteoarthritis: an overview of research and initiatives. Osteoarthritis Cartilage. 2012;20(3):215-7.

Henrotin Y, Sanchez C et al. Soluble biomarkers development in osteoarthritis: from discovery to personalized medicine. Biomarkers. 2015;20(8):540-6.

Hixson KK, Lopez-Ferrer D et al. Proteomics. Encyclopedia of Spectroscopy and Spectrometry2017. p. 766-73.

Hochberg MC, Altman RD et al. American College of Rheumatology 2012 recommendations for the use of nonpharmacologic and pharmacologic therapies in osteoarthritis of the hand, hip, and knee. Arthritis Care & Research. 2012;64(4):465-74.

Horan PK, Wheeless LLJ. Quantitative single cell analysis and sorting. Science. 1977;198(4313):149-57.

Hosea Blewett HJ. Exploring the mechanisms behind S-adenosylmethionine (SAMe) in the treatment of osteoarthritis. Crit Rev Food Sci Nutr. 2008;48(5):458-63.

Hosnijeh FS, Runhaar J et al. Biomarkers for osteoarthritis: Can they be used for risk assessment? A systematic review. Maturitas. 2015;82(1):36-49.

Hsu HY, Joos TO et al. Multiplex microsphere-based flow cytometric platforms for protein analysis and their application in clinical proteomics - from assays to results. Electrophoresis. 2009;30(23):4008-19.

Hsu HY, Wittemann S et al. Suspension microarrays for the identification of the response patterns in hyperinflammatory diseases. Med Eng Phys. 2008;30(8):976-83.

Huang K, Wu LD. YKL-40: a Potential Biomarker for Osteoarthritis. J Int Med Res. 2009;37(1):18-24.

Huang ZL, Meng PP et al. Establishment of a bead-based duplex assay for the simultaneous quantitative detection of Neuropilin-1 and Neuropilin-2 using xMAP technology and its clinical application. J Clin Lab Anal. 2019;33(4):e22850.

Hunter D, Felson D. Osteoarthritis. BMJ. 2006;332(7542):639-42.

Hunter D, Nevitt M et al. Longitudinal validation of periarticular bone area and 3D shape as biomarkers for knee OA progression? Data from the FNIH OA Biomarkers Consortium. Ann Rheum Dis. 2016;75(9):1607-14.

Hunter DJ, Losina E et al. A Pathway and Approach to Biomarker Validation and Qualification for Osteoarthritis Clinical Trials. Curr Drug Targets. 2010;11(5):536-45.

Hunter DJ, Niu JB et al. Premorbid knee osteoarthritis is not characterised by diffuse thinness: the Framingham Osteoarthritis Study. Ann Rheum Dis. 2008;67(11):1545-9.

HUPO. A Gene-centric Human Proteome Project. Mol Cell Proteomics. 2010;9(2):427-9.

Hutt JR, Craik J et al. Arthroscopy for mechanical symptoms in osteoarthritis: a cost-effective procedure. Knee Surg Sports Traumatol Arthrosc. 2015;23(12):3545-9.

I

Iannone F, Lapadula G. The pathophysiology of osteoarthritis. Aging Clin Exp Res. 2003;15(5):364-72.

Intema F, Hazewinkel HA et al. In early OA, thinning of the subchondral plate is directly related to cartilage damage: results from a canine ACLT-meniscectomy model. Osteoarthritis Cartilage. 2010;18(5):691-8.

J

Janeway CA, Travers P et al. Immunobiology : the immune system in health and disease. 5th ed. New York: Garland Publishing; 2001.

Jani D, Allinson J et al. Recommendations for Use and Fit-for-Purpose Validation of Biomarker Multiplex Ligand Binding Assays in Drug Development. AAPS J. 2016;18(1):1-14.

Jasin HE. Autoantibody specificities of immune complexes sequestered in articular cartilage of patients with rheumatoid arthritis and osteoarthritis. Arthritis Rheum. 1985;28(3):241-8.

Jevsevar DS. Treatment of osteoarthritis of the knee: evidence-based guideline, 2nd edition. J Am Acad Orthop Surg. 2013;21(9):571-6.

Jiang L, Tian W et al. Body mass index and susceptibility to knee osteoarthritis: a systematic review and meta-analysis. Joint Bone Spine. 2012;79(3):291-7.

Johnson VL, Hunter DJ. The epidemiology of osteoarthritis. Best Pract Res Clin Rheumatol. 2014;28(1):5-15.

Jonkheijm P, Weinrich D et al. Chemical strategies for generating protein biochips. Angew Chem Int Ed Engl. 2008;47(50):9618-47.

Jun BH, Kang H et al. Fluorescence-based multiplex protein detection using optically encoded microbeads. Molecules. 2012;17(3):2474-90.

K

Karlson EW, Mandl LA et al. Total hip replacement due to osteoarthritis: the importance of age, obesity, and other modifiable risk factors. Am J Med. 2003;114(2):93-8.

Katchman BA, Chowell D et al. Autoantibody biomarkers for the detection of serous ovarian cancer. Gynecol Oncol. 2017;146(1):129-36.

Kearney P, Boniface JJ et al. The building blocks of successful translation of proteomics to the clinic. Curr Opin Biotechnol. 2018;51:123-9.

Kellgren JH, Lawrence JS. Radiological assessment of osteo-arthrosis. Ann Rheum Dis. 1957;16(4):494-502.

Kerkhof HJ, Bierma-Zeinstra SM et al. Prediction model for knee osteoarthritis incidence, including clinical, genetic and biochemical risk factors. Ann Rheum Dis. 2014;73(12):2116-21.

Kettman JR, Davies T et al. Classification and properties of 64 multiplexed microsphere sets. Cytometry. 1998;33(2):234-43.

Kim J, Lee EY et al. Comparative clinical trial of S-adenosylmethionine versus nabumetone for the treatment of knee osteoarthritis: an 8-week, multicenter, randomized, double-blind, double-dummy, Phase IV study in Korean patients. Clin Ther. 2009;31(12):2860-72.

Kinds MB, Marijnissen AC et al. Evaluation of separate quantitative radiographic features adds to the prediction of incident radiographic osteoarthritis in individuals with recent onset of knee pain: 5-year follow-up in the CHECK cohort. Osteoarthritis Cartilage. 2012;20(6):548-56.

Klein-Wieringa IR, de Lange-Brokaar BJ et al. Inflammatory Cells in Patients with Endstage Knee Osteoarthritis: A Comparison between the Synovium and the Infrapatellar Fat Pad. J Rheumatol. 2016;43(4):771-8.

Kraus VB. Biomarkers as drug development tools: discovery, validation, qualification and use. Nat Rev Rheumatol. 2018;14(6):354-62.

Kraus VB, Blanco FJ et al. OARSI Clinical Trials Recommendations: Soluble biomarker assessments in clinical trials in osteoarthritis. Osteoarthritis Cartilage. 2015;23(5):686-97.

Kraus VB, Blanco FJ et al. Call for standardized definitions of osteoarthritis and risk stratification for clinical trials and clinical use. Osteoarthritis Cartilage. 2015;23(8):1233-41.

Kraus VB, Burnett B et al. Application of biomarkers in the development of drugs intended for the treatment of osteoarthritis. Osteoarthritis Cartilage. 2011;19(5):515-42.

Kraus VB, Collins JE et al. Predictive validity of biochemical biomarkers in knee osteoarthritis: data from the FNIH OA Biomarkers Consortium. Ann Rheum Dis. 2017;76(1):186-95.

Kuang Z, Huang R et al. Quantitative screening of serum protein biomarkers by reverse phase protein arrays. Oncotarget. 2018;9(66):32624-41.

Kunizaki M, Hamasaki K et al. Clinical Value of Serum p53 Antibody in the Diagnosis and Prognosis of Esophageal Squamous Cell Carcinoma. Anticancer Res. 2018;38(3):1807-13.

Kusnezow W, Hoheisel JD. Solid supports for microarray immunoassays. J Mol Recognit. 2003;16(4):165-76.

Kusnezow W, Jacob A et al. Antibody microarrays: An evaluation of production parameters. Proteomics. 2003;3(3):254-64.

L

LaBaer J, Ramachandran N. Protein microarrays as tools for functional proteomics. Curr Opin Chem Biol. 2005;9(1):14-9.

Lane NE, Shidara K et al. Osteoarthritis year in review 2016: clinical. Osteoarthritis Cartilage. 2017;25(2):209-15.

Lau AT, He QY et al. Proteomic technology and its biomedical applications. Sheng Wu Hua Xue Yu Sheng Wu Wu Li Xue Bao (Shanghai). 2003;35(11):965-75.

Lee JR, Magee DM et al. Emerging protein array technologies for proteomics. Expert Rev Proteomics. 2013;10(1):65-75.

Leslie D, Lipsky P et al. Autoantibodies as predictors of disease. Journal of Clinical Investigation. 2001;108(10):1417-22.

Lezcano-Valverde JM, Salazar F et al. Development and validation of a multivariate predictive model for rheumatoid arthritis mortality using a machine learning approach. Sci Rep. 2017;7(1):10189.

Li J, Zhao W et al. Characterization of Human Cancer Cell Lines by Reverse-phase Protein Arrays. Cancer Cell. 2017;31(2):225-39.

Li YS, Luo W et al. T Cells in Osteoarthritis: Alterations and Beyond. Front Immunol. 2017;8:356.

Lin A, Salvador A et al. Multiplexed Microsphere Suspension Array-Based Immunoassays. Methods Mol Biol. 2015;1318:107-18.

Litwic A, Edwards MH et al. Epidemiology and burden of osteoarthritis. Br Med Bull. 2013;105:185-99.

Lo GH, Driban JB et al. Is There an Association Between a History of Running and Symptomatic Knee Osteoarthritis? A Cross-Sectional Study From the Osteoarthritis Initiative. Arthritis Care Res (Hoboken). 2017;69(2):183-91.

Lopes EBP, Filiberti A et al. Immune Contributions to Osteoarthritis. Curr Osteoporos Rep. 2017;15(6):593-600.

Lotz M, Martel-Pelletier J et al. Republished: Value of biomarkers in osteoarthritis: current status and perspectives. Postgrad Med J. 2014;90(1061):171-8.

Lourido L, Calamia V et al. Quantitative proteomic profiling of human articular cartilage degradation in osteoarthritis. J Proteome Res. 2014;13(12):6096-106.

Loza E, Lopez-Gomez JM et al. Economic burden of knee and hip osteoarthritis in Spain. Arthritis Rheum. 2009;61(2):158-65.

Lu M, Han W et al. Associations between proximal tibiofibular joint (PTFJ) types and knee osteoarthritic changes in older adults. Osteoarthritis Cartilage. 2017;25(9):1452-8.

Luyten FP, Denti M et al. Definition and classification of early osteoarthritis of the knee. Knee Surg Sports Traumatol Arthrosc. 2012;20(3):401-6.

M

MacBeath G. Protein microarrays and proteomics. Nat Genet. 2002;32 Suppl:526-32.

MacBeath G, Schreiber SL. Printing proteins as microarrays for high-throughput function determination. Science. 2000;298(5485):1760-3.

Macleod KG, Serrels B et al. Reverse Phase Protein Arrays and Drug Discovery. Methods Mol Biol. 2017;1647:153-69.

Madry H, Kon E et al. Early osteoarthritis of the knee. Knee Surg Sports Traumatol Arthrosc. 2016;24(6):1753-62.

Madry H, Luyten FP et al. Biological aspects of early osteoarthritis. Knee Surg Sports Traumatol Arthrosc. 2012;20(3):407-22.

Majeed MH, Sherazi SAA et al. Pharmacological Treatment of Pain in Osteoarthritis: A Descriptive Review. Curr Rheumatol Rep. 2018;20(12):88.

Maleki-Fischbach M, Jordan JM. New developments in osteoarthritis. Sex differences in magnetic resonance imaging-based biomarkers and in those of joint metabolism. Arthritis Research & Therapy. 2010;12(4).

Malemud CJ. Biologic basis of osteoarthritis: state of the evidence. Curr Opin Rheumatol. 2015;27(3):289-94.

Man GS, Mologhianu G. Osteoarthritis pathogenesis – a complex process that involves the entire joint. Journal of Medicine and Life. 2014;7(1):37-41.

Mansell JP, Bailey AJ. Abnormal cancellous bone collagen metabolism in osteoarthritis. J Clin Invest. 1998;101(8):1596-603.

Manzano-Roman R, Fuentes M. A decade of Nucleic Acid Programmable Protein Arrays (NAPPA) availability: News, actors, progress, prospects and access. J Proteomics. 2019;198:27-35.

Martins TB, Burlingame R et al. Evaluation of multiplexed fluorescent microsphere immunoassay for detection of autoantibodies to nuclear antigens. Clin Diagn Lab Immunol. 2004;11(6):1054-9.

Martins TB, Litwin CM et al. Evaluation of a multiplex fluorescent microsphere immunoassay for the determination of epstein-barr virus serologic status. Am J Clin Pathol. 2008;129(1):34-41.

Marx V. Finding the right antibody for the job. Nat Methods. 2013;10(8):703-7.

Mateos J, Lourido L et al. Differential protein profiling of synovial fluid from rheumatoid arthritis and osteoarthritis patients using LC-MALDI TOF/TOF. J Proteomics. 2012;75(10):2869-78.

Mathiessen A, Conaghan PG. Synovitis in osteoarthritis: current understanding with therapeutic implications. Arthritis Res Ther. 2017;19(1):18.

Mazieres B, Garnero P et al. Molecular markers of cartilage breakdown and synovitis at baseline as predictors of structural progression of hip osteoarthritis. The ECHODIAH Cohort. Ann Rheum Dis. 2006;65(3):354-9.

McAlindon T, LaValley M et al. Effect of vitamin D supplementation on progression of knee pain and cartilage volume loss in patients with symptomatic osteoarthritis: a randomized controlled trial. JAMA. 2013;309(2):155-62.

McAlindon TE, Bannuru RR et al. OARSI guidelines for the non-surgical management of knee osteoarthritis. Osteoarthritis Cartilage. 2014;22(3):363-88.

McHugh TM, Miner RC et al. Simultaneous detection of antibodies to cytomegalovirus and herpes simplex virus by using flow cytometry and a microsphere-based fluorescence immunoassay. J Clin Microbiol. 1988;26(10):1957-61.

McWilliam I, Chong Kwan M et al. Inkjet printing for the production of protein microarrays. Methods Mol Biol. 2011;785:345-61.

Michigami T. Regulatory mechanisms for the development of growth plate cartilage. Cell Mol Life Sci. 2013;70(22):4213-21.

Miersch S, Bian X et al. Serological autoantibody profiling of type 1 diabetes by protein arrays. J Proteomics. 2013;94:486-96.

Miersch S, LaBaer J. Nucleic Acid programmable protein arrays: versatile tools for array-based functional protein studies. Curr Protoc Protein Sci. 2011;Chapter 27:Unit27 2.

Migliore A, Scire CA et al. The challenge of the definition of early symptomatic knee osteoarthritis: a proposal of criteria and red flags from an international initiative promoted by the Italian Society for Rheumatology. Rheumatol Int. 2017;37(8):1227-36.

Mobasheri A, Bay-Jensen AC et al. Osteoarthritis Year in Review 2016: biomarkers (biochemical markers). Osteoarthritis Cartilage. 2017;25(2):199-208.

Mora JC, Przkora R et al. Knee osteoarthritis: pathophysiology and current treatment modalities. J Pain Res. 2018;11:2189-96.

N

Najm WI, Reinsch S et al. S-adenosyl methionine (SAMe) versus celecoxib for the treatment of osteoarthritis symptoms: a double-blind cross-over trial. BMC Musculoskelet Disord. 2004;26:5-6.

Nature. [Available from: https://www.nature.com/scitable/definition/proteome-297.

Nelson AE, Golightly YM et al. Cross-sectional associations between variations in ankle shape by statistical shape modeling, injury history, and race: the Johnston County Osteoarthritis Project. J Foot Ankle Res. 2017;10:34.

Neogi T, Zhang Y. Epidemiology of osteoarthritis. Rheum Dis Clin North Am. 2013;39(1):1-19.

Neu CP, Reddi AH et al. Increased friction coefficient and superficial zone protein expression in patients with advanced osteoarthritis. Arthritis Rheum. 2010;62(9):2680-7.

Nevitt M, Felson D et al. The effect of estrogen plus progestin on knee symptoms and related disability in postmenopausal women: The Heart and Estrogen/Progestin Replacement Study, a randomized, double-blind, placebo-controlled trial. Arthritis Rheum. 2001;44(4):811-8.

Newberry JS, FitzGerald J et al. Treatment of Osteoarthritis of the Knee: An Update Review. Comparative Effectiveness Reviews. 2017;190.

Nguyen LT, Sharma AR et al. Review of Prospects of Biological Fluid Biomarkers in Osteoarthritis. Int J Mol Sci. 2017;18(3).

Niu J, Clancy M et al. Metabolic Syndrome, Its Components, and Knee Osteoarthritis: The Framingham Osteoarthritis Study. Arthritis Rheumatol. 2017;69(6):1194-203.

Nolen BM, Lokshin AE. Biomarker testing for ovarian cancer: clinical utility of multiplex assays. Mol Diagn Ther. 2013;17(3):139-46.

O

O'Farrell AC, Miller IS et al. Implementing Reverse Phase Protein Array Profiling as a Sensitive Method for the Early Pre-Clinical Detection of Off-Target Toxicities Associated with Sunitinib Malate. Proteomics Clin Appl. 2019:e1800159.

Ohfuji S, Jingushi S et al. Factors associated with diagnostic stage of hip osteoarthritis due to acetabular dysplasia among Japanese female patients: a cross-sectional study. BMC Musculoskelet Disord. 2016;17:320.

Oiestad BE, Engebretsen L et al. Knee osteoarthritis after anterior cruciate ligament injury: a systematic review. Am J Sports Med. 2009;37(7):1434-43.

Orth P, Cucchiarini M et al. PTH [1-34]-induced alterations of the subchondral bone provoke early osteoarthritis. Osteoarthritis Cartilage. 2014;22(6):813-21.

P

Palazzo C, Nguyen C et al. Risk factors and burden of osteoarthritis. Ann Phys Rehabil Med. 2016;59(3):134-8.

Parikh R, Mathai A et al. Understanding and using sensitivity, specificity and predictive values. Indian J Ophthalmol. 2008;56(1):45-50.

Paweletz CP, Charboneau L et al. Reverse phase protein microarrays which capture disease progression show activation of pro-survival pathways at the cancer invasion front. Oncogene. 2001;20(16):1981-9.

Pfander D, Cramer T et al. Expression of thrombospondin-1 and its receptor CD36 in human osteoarthritic cartilage. Ann Rheum Dis. 2000;59(6):448-54.

Phizicky E, Bastiaens PI et al. Protein analysis on a proteomic scale. Nature. 2003;422(6928):208-15.

Poole AR. Current opinion: where are we in our understanding and treatment of osteoarthritis? Swiss Med Wkly. 2016;146:w14340.

Prieto-Alhambra D, Judge A et al. Incidence and risk factors for clinically diagnosed knee, hip and hand osteoarthritis: influences of age, gender and osteoarthritis affecting other joints. Ann Rheum Dis. 2014;73(9):1659-64.

Putterman C, Wu A et al. SLE-key((R)) rule-out serologic test for excluding the diagnosis of systemic lupus erythematosus: Developing the ImmunArray iCHIP((R)). J Immunol Methods. 2016;429:1-6.

Q

Qi S, Huang M et al. Autoantibodies to chromogranin A are potential diagnostic biomarkers for non-small cell lung cancer. Tumour Biol. 2015;36(12):9979-85.

Qiu J, LaBaer J. Nucleic acid programmable protein array a just-in-time multiplexed protein expression and purification platform. Methods Enzymol. 2011;500:151-63.

R

Ramachandran N, Hainsworth E et al. Self-assembling protein microarrays. Science. 2004;305(5680):86-90.

Ramachandran N, Srivastava S et al. Applications of protein microarrays for biomarker discovery. Proteomics Clin Appl. 2008;2(10-11):1444-59.

Ray S, Mehta G et al. Label-free detection techniques for protein microarrays: prospects, merits and challenges. Proteomics. 2010;10(4):731-48.

Raynauld JP, Martel-Pelletier J et al. Quantitative magnetic resonance imaging evaluation of knee osteoarthritis progression over two years and correlation with clinical symptoms and radiologic changes. Arthritis Rheum. 2004;50(2):476-87.

Rego-Perez I, Blanco FJ et al. Mitochondrial DNA haplogroups associated with MRI-detected structural damage in early knee osteoarthritis. Osteoarthritis Cartilage. 2018;26(11):1562-9.

Reslova N, Michna V et al. xMAP Technology: Applications in Detection of Pathogens. Front Microbiol. 2017;8:55.

Reyes C, Leyland KM et al. Association Between Overweight and Obesity and Risk of Clinically Diagnosed Knee, Hip, and Hand Osteoarthritis: A Population-Based Cohort Study. Arthritis Rheumatol. 2016;68(8):1869-75.

Rich JT, Neely JG et al. A practical guide to understanding Kaplan-Meier curves. Otolaryngol Head Neck Surg. 2010;143(3):331-6.

Rinaldetti S, Wirtz R et al. FOXM1 predicts disease progression in non-muscle invasive bladder cancer. J Cancer Res Clin Oncol. 2018;144(9):1701-9.

Romanov V, Davidoff SN et al. A critical comparison of protein microarray fabrication technologies. Analyst. 2014;139(6):1303-26.

Ruiz-Romero C, Blanco FJ. Use of biomarkers for the purposes of diagnosis and drug discovery programs: where do we stand? Addressing Unmet Needs in Osteoarthritis2013. p. 54-68.

Ruthard J, Hermes G et al. Identification of antibodies against extracellular matrix proteins in human osteoarthritis. Biochem Biophys Res Commun. 2018;503(3):1273-7.

Ryd L, Brittberg M et al. Pre-Osteoarthritis: Definition and Diagnosis of an Elusive Clinical Entity. Cartilage. 2015;6(3):156-65.

S

Saberi Hosnijeh F, Bierma-Zeinstra SM et al. Osteoarthritis year in review 2018: biomarkers (biochemical markers). Osteoarthritis Cartilage. 2019;27(3):412-23.

Saberi Hosnijeh F, Zuiderwijk ME et al. Cam Deformity and Acetabular Dysplasia as Risk Factors for Hip Osteoarthritis. Arthritis Rheumatol. 2017;69(1):86-93.

Sakata M, Tsuruha J et al. Autoantibodies to osteopontin in patients with osteoarthritis and rheumatoid arthritis. J Rheumatol. 2001;28(7):1492-5.

Sakata R, McNary SM et al. Stimulation of the superficial zone protein and lubrication in the articular cartilage by human platelet-rich plasma. Am J Sports Med. 2015;43(6):1467-73.

Sandell LJ. Obesity and osteoarthritis: is leptin the link? Arthritis Rheum. 2009;60(10):2858-60.

Sanders TL, Pareek A et al. Long-term follow-up of isolated ACL tears treated without ligament reconstruction. Knee Surg Sports Traumatol Arthrosc. 2017;25(2):493-500.

Sauer U. Analytical Protein Microarrays: Advancements Towards Clinical Applications. Sensors (Basel). 2017;17(2).

Scanzello CR. Role of low-grade inflammation in osteoarthritis. Curr Opin Rheumatol. 2017;29(1):79-85.

Scanzello CR, Goldring SR. The role of synovitis in osteoarthritis pathogenesis. Bone. 2012;51(2):249-57.

Scotece M, Koskinen-Kolasa A et al. Novel adipokine associated with osteoarthritis: retinol binding protein 4 is produced by cartilage and correlates withmatrix metalloproteinasesin osteoarthritis patients. Osteoarthritis and Cartilage. 2018;26:S126-S7.

Sellam J, Berenbaum F. The role of synovitis in pathophysiology and clinical symptoms of osteoarthritis. Nat Rev Rheumatol. 2010;6(11):625-35.

Seoane-Mato D, Sánchez-Piedra C et al. Prevalence of rheumatic diseases in adul population in Spain. EPISER 2016 Study. EULAR 20182018. p. 535-6.

SEprot. Manual de Proteómica: Ilustraciones Científicas S.L.; 2014.

SER. Artrosis. Fisiopatología, diagnóstico y tratamiento. Madrid: Editorial Médica Panamericana; 2010.

Sharif M, Kirwan J et al. A 5-yr longitudinal study of type IIA collagen synthesis and total type II collagen degradation in patients with knee osteoarthritis--association with disease progression. Rheumatology (Oxford). 2007;46(6):938-43.

Sharma L, Chang AH et al. Varus Thrust and Incident and Progressive Knee Osteoarthritis. Arthritis Rheumatol. 2017;69(11):2136-43.

Sharma L, Hochberg M et al. Knee tissue lesions and prediction of incident knee osteoarthritis over 7 years in a cohort of persons at higher risk. Osteoarthritis Cartilage. 2017;25(7):1068-75.

Sharma L, Nevitt M et al. Clinical significance of worsening versus stable preradiographic MRI lesions in a cohort study of persons at higher risk for knee osteoarthritis. Ann Rheum Dis. 2016;75(9):1630-6.

Sharma L, Song J et al. The role of knee alignment in disease progression and functional decline in knee osteoarthritis. JAMA. 2001;286(2):188-95.

Sibani S, LaBaer J. Immunoprofiling using NAPPA protein microarrays. Methods Mol Biol. 2011;723:149-61.

Silverwood V, Blagojevic-Bucknall M et al. Current evidence on risk factors for knee osteoarthritis in older adults: a systematic review and meta-analysis. Osteoarthritis Cartilage. 2015;23(4):507-15.

Sinusas K. Osteoarthritis: diagnosis and treatment. Am Fam Physician. 2012;85(1):49-56.

Slauterbeck JR, Kousa P et al. Geographic mapping of meniscus and cartilage lesions associated with anterior cruciate ligament injuries. J Bone Joint Surg Am. 2009;91(9):2094-103.

Soeken KL, Lee WL et al. Safety and efficacy of S-adenosylmethionine (SAMe) for osteoarthritis. J Fam Pract. 2002;51(5):425-30.

Spirin AS. High-throughput cell-free systems for synthesis of functionally active proteins. Trends Biotechnol. 2004;22(10):538-45.

Suter LG, Smith SR et al. Projecting Lifetime Risk of Symptomatic Knee Osteoarthritis and Total Knee Replacement in Individuals Sustaining a Complete Anterior Cruciate Ligament Tear in Early Adulthood. Arthritis Care Res (Hoboken). 2017;69(2):201-8.

Szumilas M. Explaining Odds Ratios. J Can Acad Child Adolesc Psychiatry 2010;19(3):227-9.

T

Tan HT, Low J et al. Serum autoantibodies as biomarkers for early cancer detection. FEBS J. 2009;276(23):6880-904.

Tang ZM, Ling ZG et al. Serum tumor-associated autoantibodies as diagnostic biomarkers for lung cancer: A systematic review and meta-analysis. PLoS One. 2017;12(7):e0182117.

Teichtahl AJ, Wang Y et al. Associations between systemic bone mineral density and early knee cartilage changes in middle-aged adults without clinical knee disease: a prospective cohort study. Arthritis Res Ther. 2017;19(1):98.

Thorlund JB, Felson DT et al. Effect of Knee Extensor Strength on Incident Radiographic and Symptomatic Knee Osteoarthritis in Individuals With Meniscal Pathology: Data From the Multicenter Osteoarthritis Study. Arthritis Care Res (Hoboken). 2016;68(11):1640-6.

Thul PJ, Lindskog C. The human protein atlas: A spatial map of the human proteome. Protein Sci. 2018;27(1):233-44.

Tighe PJ, Ryder RR et al. ELISA in the multiplex era: potentials and pitfalls. Proteomics Clin Appl. 2015;9(3-4):406-22.

Tseng S, Hari-Reddi A et al. Cartilage Oligomeric Matrix Protein (COMP): A Biomarker of Arthritis. Biomark Insights. 2009;4:33-44.

Tsuruha J, Masuko-Hongo K et al. Implication of cartilage intermediate layer protein in cartilage destruction in subsets of patients with osteoarthritis and rheumatoid arthritis. Arthritis Rheum. 2001;44(4):838-45.

Tsuruha J, Masuko-Hongo K et al. Autoimmunity against YKL-39, a human cartilage derived protein, in patients with osteoarthritis. J Rheumatol. 2002;29(7):1459-66.

U

Uotila M, Ruoslahti E et al. Two-site sandwich enzyme immunoassay with monoclonal antibodies to human alpha-fetoprotein. J Immunol Methods. 1981;42(1):11-5.

Urbanowska T, Mangialaio S et al. Protein microarray platform for the multiplex analysis of biomarkers in human sera. J Immunol Methods. 2006;316(1-2):1-7.

V

Valdes AM, Meulenbelt I et al. Large scale meta-analysis of urinary C-terminal telopeptide, serum cartilage oligomeric protein and matrix metalloprotease degraded type II collagen and their role in prevalence, incidence and progression of osteoarthritis. Osteoarthritis Cartilage. 2014;22(5):683-9.

van Spil WE, DeGroot J et al. Serum and urinary biochemical markers for knee and hip-osteoarthritis: a systematic review applying the consensus BIPED criteria. Osteoarthritis Cartilage. 2010;18(5):605-12.

van Wulfften Palthe AFY, Clement ND et al. Survival and functional outcome of high tibial osteotomy for medial knee osteoarthritis: a 10-20-year cohort study. Eur J Orthop Surg Traumatol. 2018;28(7):1381-9.

Vargas Negrín F, Medina Abellán MD et al. Tratamiento del paciente con artrosis. Atención Primaria. 2014;46:39-61.

Vina ER, Kwoh CK. Epidemiology of osteoarthritis: literature update. Curr Opin Rheumatol. 2018;30(2):160-7.

Vina ER, Ran D et al. Race, sex, and risk factors in radiographic worsening of knee osteoarthritis. Semin Arthritis Rheum. 2018;47(4):464-71.

von der Heyde S, Sonntag J et al. Reconstruction of Protein Networks Using Reverse-Phase Protein Array Data. Methods Mol Biol. 2016;1362:227-46.

W

Wagner JA. Overview of biomarkers and surrogate endpoints in drug development. Dis Markers. 2002;18(2):41-6.

Wagner JA, Williams SA et al. Biomarkers and surrogate end points for fit-for-purpose development and regulatory evaluation of new drugs. Clin Pharmacol Ther. 2007;81(1):104-7.

Wang D, Yang L et al. AAgAtlas 1.0: a human autoantigen database. Nucleic Acids Res. 2017;45(D1):D769-D76.

Wang H, Demirkan G et al. Identification of Antibody Against SNRPB, Small Nuclear Ribonucleoprotein-Associated Proteins B and B', as an Autoantibody Marker in Crohn's Disease using an Immunoproteomics Approach. J Crohns Colitis. 2017;11(7):848-56.

Wang Q, Rozelle AL et al. Identification of a central role for complement in osteoarthritis. Nat Med. 2011;17(12):1674-9.

Wang X, Cicuttini F et al. Knee effusion-synovitis volume measurement and effects of vitamin D supplementation in patients with knee osteoarthritis. Osteoarthritis Cartilage. 2017;25(8):1304-12.

Warner SC, Valdes AM. Genetic association studies in osteoarthritis: is it fairytale? Curr Opin Rheumatol. 2017;29(1):103-9.

Wesseling J, Boers M et al. Cohort Profile: Cohort Hip and Cohort Knee (CHECK) study. Int J Epidemiol. 2016;45(1):36-44.

WHO. [Available from: https://www.who.int/topics/risk_factors/en/.

Wians FH. Clinical Laboratory Tests: Which, Why, and What Do The Results Mean? Laboratory Medicine. 2009;40(2):105-13.

Wilkins MR, Sanchez J-C et al. Progress with Proteome Projects: Why all Proteins Expressed by a Genome Should be Identified and How To Do It. Biotechnology and Genetic Engineering Reviews. 1996;13(1):19-50.

Wingren C, Borrebaeck CA. Progress in miniaturization of protein arrays--a step closer to high-density nanoarrays. Drug Discov Today. 2007;12(19-20):813-9.

Wluka A, S. D et al. Users of oestrogen replacement therapy have more knee cartilage than non-users. Ann Rheum Dis. 2001;60(4):332-6.

Wright C, Sibani S et al. Detection of multiple autoantibodies in patients with ankylosing spondylitis using nucleic acid programmable protein arrays. Mol Cell Proteomics. 2012;11(2).

Wu Y, Ma J et al. Development of an alpha-fetoprotein and Golgi protein 73 multiplex detection assay using xMAP technology. Clin Chim Acta. 2018;482:209-14.

X

Xiang Y, Sekine T et al. Fibulin-4 is a target of autoimmunity predominantly in patients with osteoarthritis. J Immunol. 2006;176(5):3196-204.

Xiao J, Long F et al. Development and potential application of a simultaneous multiplex assay of Golgi protein 73 and alpha-fetoprotein for hepatocellular carcinoma diagnosis. Eur Rev Med Pharmacol Sci. 2019;23(8):3302-10.

xMAP Cookbook. A collection of methods and protocols for developing multiplex assays with xMAP Technology. 2nd ed2014-2014.

Y

Yalow RS, Berson SA. Assay of Plasma Insulin in Human Subjects by Immunological Methods. Nature. 1959;184(4699):1648-9.

Yang L, Wang J et al. Identification of Serum Biomarkers for Gastric Cancer Diagnosis Using a Human Proteome Microarray. Mol Cell Proteomics. 2016;15(2):614-23.

Youden WJ. Index for rating diagnostic tests. Cancer. 1950;3(1):32-5.

Yu X, Petritis B et al. Advancing translational research with next-generation protein microarrays. Proteomics. 2016;16(8):1238-50.

Yuan GH, Masuko-Hongo K et al. Immunologic intervention in the pathogenesis of osteoarthritis. Arthritis Rheum. 2003;48(3):602-11.

Yuan Y, Lin ZT et al. Protein Arrays I: Antibody Arrays. Methods Mol Biol. 2017;1654:261-9.

Yusuf E, Nelissen RG et al. Association between weight or body mass index and hand osteoarthritis: a systematic review. Ann Rheum Dis. 2010;69(4):761-5.

Z

Zhang HN, Yang L et al. Systematic identification of arsenic-binding proteins reveals that hexokinase-2 is inhibited by arsenic. Proc Natl Acad Sci U S A. 2015;112(49):15084-9.

Zhang W, McWilliams DF et al. Nottingham knee osteoarthritis risk prediction models. Ann Rheum Dis. 2011;70(9):1599-604.

Zhang Y, Jordan JM. Epidemiology of osteoarthritis. Clin Geriatr Med. 2010;26(3):355-69.

Zhang Y, Zhao C et al. High-Throughput Phosphorylation Screening and Validation through Ti(IV)-Nanopolymer Functionalized Reverse Phase Phosphoprotein Array. Anal Chem. 2018;90(17):10263-70.

Zhu H, Bilgin M et al. Global analysis of protein activities using proteome chips. Science. 2001;293(5537):2101-5.

Zhu H, Klemic JF et al. Analysis of yeast protein kinases using protein chips. Nat Genet. 2000;26(3):283-9.

Zhu H, Qian J. Applications of functional protein microarrays in basic and clinical research. Adv Genet. 2012;79:123-55.

VIII. ANNEXES

ANNEXED 1

Table 1. List of genes printed in the HC5 microarray employed in the screening phase of the second study in this research (file included in the attached CD).

Table 2. Mean and SD (expressed in arbitrary units (a.u.) of fluorescence) of the immunoreactivity levels against all the proteins expressed in the array for the incident and not-incident group (file included in the attached CD).

Table 3. Median intensity absolute deviation rule for each protein through all the pooled serum (file included in the attached CD).

Table 1. Selected clinical variables as predictors of incident knee OA.

Variable name	Description	Recoded to target knee
V00AGE	Age (calc, used for study eligibility)	NO
P02SEX	Gender, male or female	NO
P01BMI	Body mass index (calc)	NO
P02FAMHXKR	Mother, father, sister, or brother (blood relative) had knee replacement surgery where all/part of knee replaced (used for study eligibility)	NO
P02ACTRISK	Engage in at least one frequent knee bending activity (calc, used for study eligibility initially)	NO
P01INJR	Right knee, ever injured badly enough to limit ability to walk for at least two days	YES
P01INJL	Left knee, ever injured badly enough to limit ability to walk for at least two days	YES
P02KSURG	Either knee, history of knee surgery (incl. arthroscopy, ligament repair, meniscectomy; used for study elig.)	NO
P02IKPRISK	Either knee symptom status at IEI (calc, used for study eligibility)	NO
V00WOMKPR	Right knee: WOMAC Pain Score (calc)	YES
V00KOOSKPR	Right knee: KOOS Pain Score (calc)	YES
V00WOMSTFR	Right knee: WOMAC Stiffness Score (calc)	YES
V00KOOSYMR	Right knee: KOOS Symptoms Score (calc)	YES
V00WOMADLR	Right knee: WOMAC Disability Score (calc)	YES
V00WOMTSR	Right knee: WOMAC Total Score (calc)	YES
V00WOMKPL	Left knee: WOMAC Pain Score (calc)	YES
V00KOOSKPL	Left knee: KOOS Pain Score (calc)	YES
V00WOMSTFL	Left knee: WOMAC Stiffness Score (calc)	YES
V00KOOSYML	Left knee: KOOS Symptoms Score (calc)	YES
V00WOMADLL	Left knee: WOMAC Disability Score (calc)	YES
V00WOMTSL	Left knee: WOMAC Total Score (calc)	YES

WOMAC, Western Ontario and McMaster Universities Osteoarthritis Index; KOOS, Knee injury and Osteoarthritis Outcome Score.

Table 1. Spearman's correlation between the baseline concentration of the six potential biomarkers selected in the first study of this thesis.

		CHI3L1	COMP	RBP4	AHSG	TPS1	APCS
CHI3L1	Rho	1	0.239**	0.325**	0.309**	0.210**	0.362**
	p value	.	2.326E-08	1.452E-14	2.955E-13	1.000E-06	5.749E-18
COMP	Rho		1	0.234**	0.058	0.276**	0.181**
	p value		.	4.615E-08	1.817E-01	1.006E-10	2.500E-05
RBP4	Rho			1	0.549**	0.649**	0.625**
	p value			.	1.636E-43	5.464E-65	1.593E-59
AHSG	Rho				1	0.419**	0.594**
	p value				.	4.915E-24	2.074E-52
TPS1	Rho					1	0.516**
	p value					.	1.60E-37
APCS	Rho						1
	p value						.

** Correlation is significant at the 0.01 level.

Table 2. Spearman's correlation between the baseline WOMAC and KOOS subscales for the participants included in the first study of this thesis.

		WOMAC total score	WOMAC disability score	WOMAC stiffness score	WOMAC knee pain	KOOS symptoms score	KOOS knee pain score
WOMAC total score	Rho	1	0.952**	0.832**	0.855**	–0.783**	–0.877**
	p value	.	5.643E-277	1.578E-139	3.254E-155	8.946E-113	8.067E-173
WOMAC disability score	Rho		1	0.731**	0.785**	–0.701**	–0.816**
	p value		.	6.067E-91	1.742E-113	1.417E-80	1.080E-129
WOMAC stiffness score	Rho			1	0.631**	–0.825**	–0.679**
	p value			.	2.220E-61	3.135E-135	2.266E-74
WOMAC knee pain	Rho				1	–0.630**	–0.896**
	p value				.	5.060E-61	1.936E-191
KOOS symptoms score	Rho					1	0.699**
	p value					.	2.673E-80
KOOS knee pain	Rho						1
	p value						.

** Correlation is significant at the 0.01 level.

Table 3. Spearman's correlation between the baseline WOMAC and KOOS subscales for the participants included in the second study of this thesis.

		WOMAC total score	WOMAC disability score	WOMAC stiffness score	WOMAC knee pain	KOOS symptoms score	KOOS knee pain score
WOMAC total score	Rho	1	0.944**	0.835**	0.843**	–0.782**	–0.849**
	p value	.	3.213E-158	4.647E-86	1.845E-89	1.627E-68	6.384E-92
WOMAC disability score	Rho		1	0.722**	0.790**	–0.683**	–0.802**
	p value		.	7.544E-54	1.088E-70	4.512E-46	1.827E-74
WOMAC stiffness score	Rho			1	0.618**	–0.812**	–0.658**
	p value			.	8.969E-36	4.931E-78	6.587E-42
WOMAC knee pain	Rho				1	–0.612**	–0.876**
	p value				.	5.656E-35	1.057E-104
KOOS symptoms score	Rho					1	0.679**
	p value					.	1.643E-45
KOOS knee pain	Rho						1
	p value						.

** Correlation is significant at the 0.01 level.

Table 1. Regression analysis and metrics for the models generated by combining those biomarkers analyzed at the baseline visit in the duplex or triplex sandwich immunoassay.

	CHI3L1 + COMP		**RBP4 + AHSG**		**RBP4 + TPS1**		**AHSG + TPS1**		**RBP4 + AHSG + TPS1**	
	OR (95%CI)	**p value**	**OR (95%CI)**	**p value**	**OR (95%CI)**	**p value**	**OR (95%CI)**	**p value**	**OR (95%CI)**	**p value**
CHI3L1	1.02 (1.01–1.04)	2.020E-04	1.02 (1.01–1.02)	5.600E-05						
COMP	1.03 (1.02–1.03)	4.368E-10	1.00 (1.00–1.00)	9.534E-03						
RBP4					1.03 (1.02–1.03)	5.251E-10			1.02 (1.01–1.03)	9.031E-07
AHSG							1.00 (1.00–1.00)	1.000E-06	1.00 (1.00–1.00)	5.733E-03
TPS1					0.98 (0.97–0.99)	1.360E-04	1.00 (0.99–1.00)	2.984E-01	0.98 (0.97–0.99)	9.500E-05
AUC (95%CI)	0.70 (0.65–0.75)		0.69 (0.65–0.74)		0.66 (0.62–0.71)		0.68 (0.63–0.72)		0.68 (0.64–0.73)	
Specificity (95%CI)	0.70 (0.65-0.75)		0.69 (0.62–0.72)		0.59 (0.54–0.65)		0.51 (0.45–0.56)		0.64 (0.59–0.69)	
Sensitivity (95%CI)	0.64 (0.58-0.71)		0.63 (0.56–0.69)		0.64 (0.57–0.70)		0.82 (0.77–0.87)		0.63 (0.57–0.70)	
PPV (95%CI)	0.57 (0.52-0.62)		0.54 (0.50–0.59)		0.50 (0.45–0.54)		0.51 (0.48–0.54)		0.53 (0.48–0.69)	
NPV (95%CI)	0.76 (0.72-0.79)		0.74 (0.70–0.78)		0.72 (0.68–0.77)		0.82 (0.77–0.86)		0.74 (0.70–0.78)	

Table 2. Regression analysis and predictive accuracy for the models generated by the combination of baseline serum concentrations of CHI3L1 or COMP with the covariates-only model 1.

	CHI3L1 + covariates model 1		**COMP + covariates model 1**	
	OR (95%CI)	p value	OR (95%CI)	p value
Age	1.05 (1.02–1.07)	2.630E-04	1.04 (1.01–1.07)	2.147E-03
Gender, female	2.39 (1.59–3.62)	3.300E-05	2.56 (1.65–3.96)	2.500E-05
BMI	1.15 (1.10–1.21)	2.716E-08	1.18 (1.12–1.24)	9.056E-10
Frequent bending activity	1.60 (1.03–2.47)	3.527E-02	1.86 (1.17–2.94)	8.717E-03
Pain in either knee	2.48 (1.39–4.43)	2.125E-03	3.25 (1.74–6.08)	2.240E-04
KOOS symptoms score	0.97 (0.95–0.99)	6.245E-03	0.97 (0.95–0.99)	8.619E-03
CHI3L1	1.02 (1.01–1.03)	9.330E-04		
COMP			1.03 (1.02–1.04)	3.229E-12
AUC (95%CI)	0.79 (0.75–0.83)		0.82 (0.78–0.85)	
Specificity (95%CI)	0.68 (0.63–0.73)		0.67 (0.62–0.72)	
Sensitivity (95%CI)	0.78 (0.73–0.84)		0.84 (0.79–0.89)	
PPV (95%CI)	0.61 (0.57–0.65)		0.61 (0.58–0.65)	
NPV (95%CI)	0.83 (0.80–0.87)		0.87 (0.83–0.91)	

Table 3. Regression analysis and predictive accuracy for the models generated by the combination of baseline serum concentrations of RBP4, AHSG or TPS1 (alone or combined) with the covariates-only model 1.

	RBP4 + covariates model 1		**AHSG + covariates model 1**		**TPS1 + covariates model 1**		**RBP4+AHSG + covariates model 1**		**AHSG+TPS1 + covariates model 1**		**RBP4+AHSG+TPS1 + covariates model 1**	
	OR (95%CI)	p value	OR (95%CI)	p value	OR (95%CI)	p value	OR (95%CI)	p value	OR (95%CI)	p value	OR (95%CI)	p value
Age	1.05 (1.02–1.07)	7.200E-05	1.05 (1.03–1.08)	1.000E-05	1.05 (1.03–1.08)	1.500E-05	1.05 (1.03–1.08)	6.000E-05	1.05 (1.03–1.08)	1.600E-05	1.05 (1.02–1.07)	1.230E-04
Gender, female	2.35 (1.55–3.55)	5.300E-05	2.39 (1.59–3.61)	3.100E-05	2.30 (1.53–3.45)	5.700E-05	2.37 (1.57–3.59)	4.500E-05	2.39 (1.58–3.60)	3.400E-05	2.44 (1.60–3.72)	3.300E-05
BMI	1.15 (1.10–1.21)	1.310E-08	1.15 (1.09–1.20)	6.375E-08	1.16 (1.10–1.22)	5.327E-09	1.15 (1.09–1.21)	4.789E-08	1.14 (1.09–1.20)	1.109E-07	1.15 (1.09–1.21)	8.869E-08
Frequent bending activity	1.61 (1.04–2.49)	3.454E-02	1.64 (1.07–2.54)	2.460E-02	1.70 (1.11–2.62)	1.553E-02	1.60 (1.03–2.48)	3.773E-02	1.65 (1.07–2.55)	2.379E-02	1.60 (1.03–2.50)	3.880E-02
Pain in either knee	2.23 (1.25–3.96)	6.482E-03	2.16 (1.22–3.82)	8.539E-03	2.38 (1.36–4.19)	2.575E-03	2.14 (1.20–3.83)	1.026E-02	2.12 (1.20–3.77)	9.992E-03	2.12 (1.18–3.82)	1.208E-02
KOOS symptoms score	0.97 (0.95–0.99)	6.175E-03	0.97 (0.95–0.99)	6.333E-03	0.97 (0.95–0.99)	6.610E-03	0.97 (0.95–0.99)	6.178E-03	0.97 (0.95–0.99)	7.359E-03	0.97 (0.95–0.99)	1.033E-02
RBP4	1.02 (1.01–1.02)	5.000E-05					1.01 (1.01–1.02)	1.057E-03			1.02 (1.01–1.03)	2.400E-05
AHSG			1.00 (1.00–1.00)	2.245E-03			1.00 (1.00–1.00)	2.206E-01	1.00 (1.00–1.00)	2.046E-03	1.00 (1.00–1.00)	1.850E-01
TPS1					1.00 (0.99–1.01)	6.245E-01			1.00 (0.99–1.01)	4.931E-01	0.98 (0.97–0.99)	1.103E-03
AUC (95%CI)	0.79 (0.75–0.83)		0.78 (0.74–0.82)		0.76 (0.72–0.80)		0.80 (0.76–0.83)		0.78 (0.74–0.82)		0.79 (0.75–0.83)	
Specificity (95%CI)	0.64 (0.59–0.69)		0.76 (0.71–0.80)		0.61 (0.55–0.66)		0.74 (0.69–0.79)		0.76 (0.71–0.80)		0.62 (0.57–0.68)	
Sensitivity (95%CI)	0.83 (0.77–0.88)		0.70 (0.64–0.76)		0.82 (0.76–0.87)		0.74 (0.68–0.80)		0.70 (0.63–0.76)		0.84 (0.79–0.89)	
PPV (95%CI)	0.59 (0.56–0.63)		0.64 (0.60–0.69)		0.57 (0.53–0.61)		0.64 (0.59–0.69)		0.64 (0.59–0.69)		0.58 (0.55–0.62)	
NPV (95%CI)	0.86 (0.82–0.89)		0.80 (0.77–0.84)		0.84 (0.80–0.89)		0.82 (0.78–0.85)		0.80 (0.77–0.83)		0.87 (0.83–0.90)	

Table 4. p values from the comparison between the biomarkers plus covariates model 1 with the covariates-only model 1.

	Covariates-only model 1
CHI3L1 + covariates model	4.797E-01
COMP + covariates model	7.426E-02
CHI3L1+COMP + covariates model	4.476E-02
RBP4 + covariates model	3.614E-01
AHSG + covariates model	7.059E-01
TPS1 + covariates model	8.946E-01
RBP4+AHSG + covariates model	3.213E-01
AHSG+TPS1 + covariates model	7.419E-01
RBP4+AHSG+TSP1 + covariates model	3.654E-01
APCS + covariates model	3.540E-01

Figure 1. (A) ROC curves for CHI3L1 (orange line) or COMP (purple line) plus covariates model 1; (B) Biomarkers plus covariates model 1 generated from the triplex sandwich immunoassay. RBP4 (orange line), AHSG (purple line), TPS1 (green line), RBP4+AHSG (yellow line), AHSG+TPS1 (pink line) or RBP4+AHSG+TPS1 (grey line) plus covariates model 1; (C) APCS plus covariates model 1 (orange line). In all the graphics, the blue line represents the ROC curve for the covariates-only model 1.

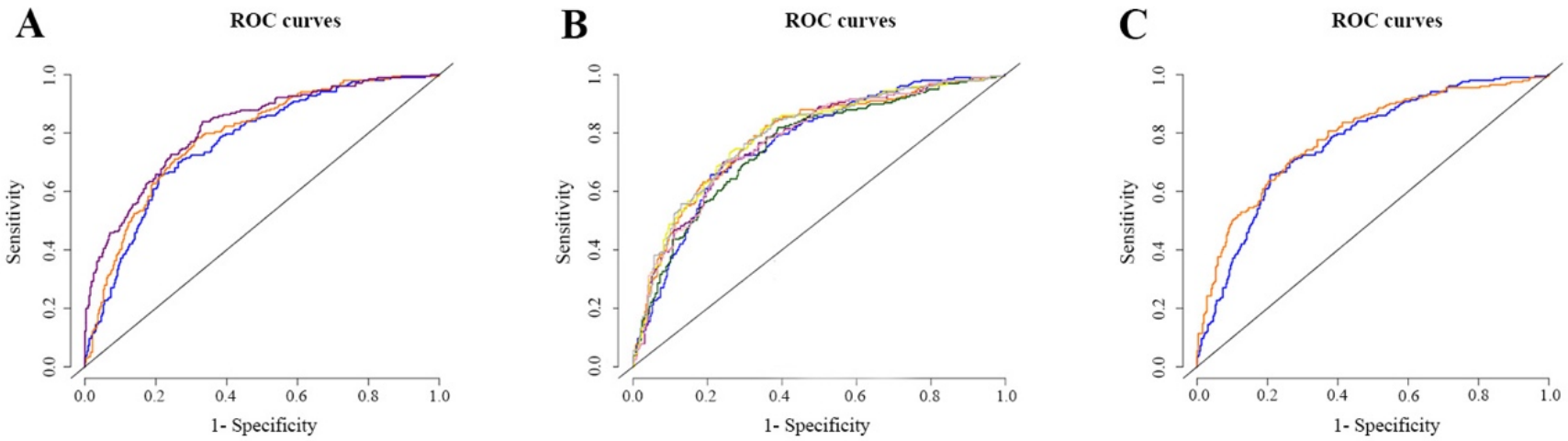

RESUMEN

Las articulaciones diartroidales son las más numerosas y perfeccionadas del cuerpo humano, tanto desde el punto de vista fisiológico como anatómico, y poseen gran movilidad, permitiendo el movimiento y autonomía de las personas. Están formadas por diversas estructuras: los huesos, los músculos y tendones (encargados del mantenimiento de la estabilidad articular), la bursa o bolsa sinovial (encargada de disminuir la fricción del hueso con los músculos, tendones y la piel que envuelven la articulación), la capsula articular y el cartílago hialino. La cápsula articular cierra la cavidad articular mediante dos capas: una capa externa que es fibrosa y una interna sinovial, la cual se encarga de la secreción del líquido sinovial que lubrica la articulación y nutre el cartílago, un tejido altamente especializado que recubre las superficies de los huesos en la articulación, facilitando el movimiento del esqueleto sin la aparición del dolor. En esencia, el cartílago hialino es un tejido alinfático, aneural y avascular que está compuesto por una abundante matriz extracelular (MEC) y única población celular altamente escasa (1–2% del volumen total), los condrocitos, encargados de sintetizar y mantener los distintos componentes de la MEC, entre los que se encuentran principalmente, el colágeno tipo II, los proteoglicanos y los glucosaminoglucanos.

Una de las enfermedades que afectan a las articulaciones diartroidales es la artrosis (OA), la cual se define como una enfermedad que afecta a toda la articulación y se caracteriza por estrés celular y degradación de la MEC iniciada por micro y macro lesiones que activan respuestas de reparación maladaptativas, incluyendo rutas pro-inflamatorias de la inmunidad innata. La enfermedad se manifiesta primero como alteraciones a nivel molecular debidas al metabolismo anormal de la articulación (predominancia de los procesos catabólicos destructivos sobre los procesos anabólicos productivos), a las que siguen alteraciones anatómicas y fisiológicas caracterizadas por la degradación del cartílago articular, remodelamiento óseo, formación de osteofitos, inflamación sinovial y pérdida de la función normal de la articulación, dando finalmente lugar a la aparición de la sintomatología típica de dolor crónico y pérdida de movilidad de la OA.

La OA es la enfermedad musculoesquelética más prevalente a nivel mundial, siendo la principal causa de discapacidad entre la tercera edad. Se estima que aproximadamente un 10% de la población adulta occidental (mayores de 60 años) presenta algún tipo de grado de OA, siendo mayor la prevalencia entre la población femenina. A pesar de la gran

importancia de la enfermedad, la elevada complejidad de la OA, que incluye diversos subtipos y fenotipos donde los síntomas pueden aparecer sin signos radiográficos o viceversa, hacen que sea muy difícil conocer la etiología exacta de la enfermedad.

En la actualidad, el diagnóstico de la OA se lleva a cabo mediante exploración física del paciente, y si es necesario con radiografía convencional (RC), resonancia magnética (RM) nuclear o artroscopia. Sin embargo, estos métodos de diagnóstico no son lo suficientemente sensibles como para detectar la enfermedad en las etapas iniciales, que son asintomáticas y pueden tener lugar durante décadas, y como consecuencia, el diagnóstico se produce en etapas muy avanzadas. Además, la OA no tiene cura. A pesar de los esfuerzos en desarrollar fármacos modificadores de la enfermedad (FAME), los tratamientos farmacológicos accesibles en la actualidad son sintomáticos, limitándose a controlar el dolor sin ser capaces de frenar la evolución de la misma, siendo el reemplazo de la articulación por prótesis la única solución en los estados avanzados. Todo esto, resalta la importancia de contar con métodos de diagnóstico molecular de la OA en su fase más temprana y asintomática, que permitan establecer lo antes posible estrategias preventivas.

En este sentido, la irrupción de la proteómica en la última década ha permitido grandes avances en la búsqueda de marcadores bioquímicos, secretados por el cartílago, hueso o compartimento sinovial, que reflejen los cambios en el metabolismo o degradación de la articulación. Empleando muestras de fluidos corporales como suero, plasma u orina, de pacientes con OA y controles, varios estudios proteómicos han conducido a la identificación de una larga lista de proteínas diferenciales que pueden tener potencial utilidad biomarcadora para el diagnóstico precoz, pronóstico y desarrollo de fármacos para el tratamiento de la OA. Sin embargo, ninguno de estos candidatos han sido validados en la clínica, principalmente debido a la ausencia de estudios de validación que incluyan grandes números de muestras de pacientes que cuenten con un extenso seguimiento tanto clínico, como de imagen, permitiendo estratificar a los pacientes y definir de manera precisa el valor del biomarcador encontrado en la OA. Por lo tanto, no es de extrañar la aparición, en los últimos años de distintos estudios de cohortes, como es el caso de la cohorte de la *Osteoarthritis Initiative* (OAI), un estudio multicéntrico, observacional longitudinal y prospectivo que posee datos clínicos de evaluación, imágenes y un repositorio de muestras biológicas de un elevado número de pacientes,

reclutados entre 2004 y 2006, y cuyo seguimiento continúa en la actualidad. Este estudio divide a los pacientes en tres subcohortes: de progresión, donde los participantes presentan OA desde el inicio del estudio; de incidencia, con participantes que no tienen OA sintomática ni radiográfica desde el inicio pero escogidos en base a la presencia de ciertos factores de riesgo de la enfermedad; y no expuestos, un grupo control. Este diseño de estudio hace de la OAI una población ideal para estudios de incidencia y progresión de la enfermedad. En nuestro grupo de investigación contamos con muestras de suero de las tres subcohortes.

Actualmente, existe una tendencia a creer que en enfermedades tan complejas y heterogéneas como la OA, la identificación de un único biomarcador es insuficiente para obtener información fiable sobre la enfermedad. Es por eso que hoy en día, el interés se centra en la realización de ensayos múltiplex para validar paneles de proteínas en amplias cohortes de pacientes, con el fin de avanzar en el flujo de desarrollo de nuevos biomarcadores y cualificar su uso en función de la clasificación BIPEDS, desarrollada como marco para el uso de estas moléculas en la rutina clínica: de alcance de la enfermedad (*Burden of disease*), de investigación (*Investigative*), de pronóstico (*Prognosis*), de eficacia de la intervención (*Efficacy of intervention*), de diagnóstico (*Diagnosis*) o de seguridad (*Safety*). Para ello, tienen gran valor las tecnologías de proteómica dirigida, tales como la tecnología de esferas de Luminex, no solo debido a su capacidad para analizar simultáneamente múltiples analitos, sino también por su aplicabilidad en estudios de altos rendimientos, tales como los ensayos clínicos.

La Unidad de Proteómica del Grupo de Investigación de Reumatología (GIR) ha trabajado en el campo de los biomarcadores de OA aplicando dos pilares esenciales del proyecto proteoma humano (HPP) para la identificación y análisis de estos candidatos: la espectrometría de masas, mediante ensayos de monitorización de reacción múltiple (MRM) y la proteómica de afinidad o microarrays de proteínas. El resultado global de estos análisis ha sido una lista de 20 proteínas candidatas con potencial biomarcador para la OA. Una vez identificadas estas proteínas, el siguiente paso lógico es su validación y cualificación en un gran número de muestras, que permita finalmente materializar este conocimiento en un producto de utilidad clínica. Este salto de la investigación básica a la posible aplicación clínica es el foco principal de esta tesis doctoral.

El objetivo de la primera parte de este proyecto se focaliza en la validación de seis de las proteínas incluidas en el panel anteriormente mencionado, mediante su cuantificación absoluta a través de técnicas de immunoensayos múltiples basadas en tecnología de esferas de Luminex, para su uso como marcadores de pronóstico de OA que permitan predecir la aparición futura de la enfermedad entre personas que no la padecen. Las seis proteínas seleccionadas fueron: COMP (*cartilage oligomeric matrix protein*), CHI3L1 (*chitinase-3-like protein 1*), RBP4 (*retinol binding protein 4*), AHSG (*alpha-2-HS-glycoprotein*), TPS1 (*thrombospondin 1*), y APCS (*serum amyloid P-component*). El análisis se realizó directamente en muestras de suero procedentes de pacientes de la cohorte de la OAI, facilitando así su aplicabilidad en la práctica clínica mediante una intervención que permita: (1) evitar métodos actuales más invasivos (p.ej. biopsias) o perjudiciales para la salud (p.ej. radiografías) y (2) que minimice el coste del test.

Para el desarrollo de los immunoensayos cuantitativos se adquirieron kits preparados para ensayos tipo ELISA (acrónimo del inglés *Enzyme-Linked ImmunoSorbent Assay*), que incluían un anticuerpo monoclonal de captura, un anticuerpo policlonal de detección marcado con biotina y una proteína recombinante para usar como estándar, frente a las proteínas COMP, CHI3L1, RBP4 y APCS . Como no existían estos kits frente TPS1 y AHSG, se adquirieron por separado una pareja de anticuerpos y una proteína estándar que hubieran sido previamente testadas para su uso en ensayos ELISA.

En un principio, la optimización de la curva estándar y dilución necesaria de la muestra se llevó a cabo en ensayos individuales. Así, se generó para cada analito una curva estándar asimétrica de nueve puntos, en la que el eje “X” representaba el logaritmo de la concentración, y el eje “Y” la intensidad media de fluorescencia (IMF). La dilución optima de suero que se seleccionó para la cuantificación del analito en la muestra fue aquella cuya IMF se encontrara en el rango lineal de la curva. Una vez optimizados estos parámetros, se agruparon en un mismo array en suspensión aquellas proteínas que coincidían en la dilución necesaria de la muestra, quedando por un lado, un array dúplex que incluía a COMP y CHI3L1 (dilución de suero 1:10), un array tríplex que incluía RBP4, AHSG y TPS1 (dilución de suero 1:10000), y un array individual para APSC (dilución de suero 1:20000). Analizando de manera individual la concentración más alta de estándar utilizada en la curva, frente al mix de anticuerpos de captura y al mix de los anticuerpos detección, encontramos que las señales de fluorescencia para los analitos no

diana estaban, tanto para el caso del ensayo dúplex como el tríplex, por debajo del 5% de la señal obtenida para el analito diana, demostrando la especificidad de la pareja de anticuerpos frente a su ligando connato y permitiendo el análisis simultáneo de dichas proteínas.

Por otro lado, hay que tener en cuenta que uno de los inconvenientes inherentes en el campo de los biomarcadores es la gran variabilidad que puede haber entre los pacientes. En nuestro caso, el análisis de 29 muestras de suero escogidas al azar de la cohorte de la OAI demostró que las condiciones seleccionadas para cada una de las proteínas permitían cuantificar la concentración de las mismas en todas, o la mayor parte de las muestras. Además, tras analizar las características analíticas de los tres immunoensayos generados se comprobó que dicha cuantificación se llevaba a cabo con una precisión por debajo del 10% y una exactitud que oscilaba entre el 90% y el 112%, cumpliendo con los criterios que establece la Administración de Alimentos y Medicamentos o FDA (acrónimo del inglés *Food and Drug Administration*).

Una vez generados los ensayos y comprobado su aplicabilidad, se analizaron a ciegas 749 muestras de suero a tiempo cero procedentes de pacientes de la cohorte de la OAI. De estos 749, solo 540 cumplían el criterio establecido de incidencia de OA radiográfica de rodilla, el cual se basaba en la no presencia de OA radiográfica evidente (grado 0–1) en al menos, una rodilla, que sería establecida como rodilla diana y seguida durante 96 meses para evaluar el desarrollo de la enfermedad (aumento a grado 2 o más en algún punto del seguimiento). Una vez clasificados los individuos como incidentes o no incidentes, se llevó a cabo el análisis de los datos mediante el uso de técnicas estadísticas no paramétricas, las cuales revelaron la existencia de concentraciones basales significativamente mayores ($p < 0.05$) en aquellas personas que habían incidido durante el seguimiento para los seis candidatos analizados. Además, de estos seis candidatos, COMP, CHI3L1, RBP4, AHSG y APCS demostraron una asociación significativa con la futura aparición de la enfermedad, donde el aumento de 10 unidades de concentración de dichas proteínas confería un riesgo de incidir del 30% más en el caso de COMP, CHI3L1 y APCS, del 20% en el caso en el caso de RBP4, y del 3% en el caso de AHSG. Sin embargo, la capacidad individual que mostraron estos marcadores para predecir el desarrollo de OA de rodilla fue modesta (entre 0,66–0,68), siendo APCS la única proteína que alcanzó un área bajo la curva (AUC) de 0,70. Con la finalidad de intentar mejorar

dicha capacidad de predicción se combinaron en un mismo modelo los marcadores que fueron simultáneamente analizados, pero ninguna de las combinaciones dio lugar una mejora significativa.

Aun así, y a pesar de la modesta capacidad predictiva que mostraron todos los potenciales marcadores, incluso cuando se combinaban entre sí, quisimos evaluar si incluirlos, individualmente o combinados, en un modelo pronóstico para predecir la incidencia de OA de rodilla, formado por variables clínicas, producía un aporte significativo en el AUC. Tras seleccionar distintas variables relacionadas con el riesgo de desarrollar OA, se realizó un análisis de regresión logístico por pasos para definir el mejor modelo pronóstico clínico para el conjunto de pacientes que se habían incluido en el análisis. Este modelo quedó finalmente formado por la edad, el sexo, el índice de masa corporal (IMC), participar en alguna actividad que conlleve flexiones frecuentes de las rodillas, presencia de dolor en al menos una rodilla, y la subescala "*symptoms*" del cuestionario KOOS (acrónimo del inglés *Knee injury and Osteoarthritis Outcome Score*) referida a la rodilla diana. De todos los modelos generados al incluir los biomarcadores solubles, solo aquel que contaba con la combinación de COMP y CHI3L1 mostró una capacidad de predicción que superaba de manera significativa a la obtenida en el modelo con solo las variables clínicas (AUC 0,82 vs 0,77, p= 0,044).

Como el panel formado por CHI3L1 y COMP parece tener cierta utilidad en la rutina clínica, decidimos investigar si los niveles basales en suero de estos marcadores, al dividirlos en terciles, tenían alguna relación con el tiempo en el que aparecía la OA utilizando las curvas de Kaplan-Meier (KM). El análisis reveló que niveles altos de ambos analitos se asociaban significativamente con un desarrollo más temprano de la OA de rodilla. Además realizando un análisis de regresión de Cox, que permite el ajuste por las variables clínicas anteriormente mencionadas, se pudo observar que el riesgo de desarrollar la enfermedad con anterioridad en el tiempo, cuando se presentan niveles basales altos de estos marcadores, es de 1,74 veces mayor por cada unidad de concentración incrementada en CHI3L1, y 2,76 veces mayor por cada unidad de concentración incrementada en COMP.

Tal y como se ha mencionado al inicio de este resumen, la OA es una enfermedad que afecta a toda la articulación y que está caracterizada, generalmente, por el deterioro del cartílago articular. Sin embargo, y aunque se conocen muchos de los procesos implicados

en el desarrollo de la patología, las causas exactas por las cuales se inicia permanecen aún desconocidas. Una de las teorías que en los últimos años está tomando gran importancia, a pesar de que la artrosis no es considerada como una enfermedad autoinmune, es la que implica a la sistema inmune como uno de los componentes principales que desencadenan todo el proceso patológico. Entre las principales características de la respuesta humoral innata, se encuentra la producción de anticuerpos patogénicos que reconocen antígenos propios del cuerpo o autoanticuerpos (AAbs). En un trabajo llevado a cabo por nuestro grupo de investigación, se demostró la presencia de AAbs en suero de pacientes con OA. En base a esto, y a que, como ya se ha demostrado en otras patologías, los AAbs pueden ser detectados en los estadios asintomáticos de la enfermedad, confiriéndoles cierto potencial para identificar individuos susceptibles, decidimos evaluar la presencia de un perfil de AAbs asociado la incidencia de OA de rodilla.

Para cumplir con este objetivo se diseñó un estudio de descubrimiento de biomarcadores en dos fases, una fase de *screening* y una fase de verificación. En la primera fase se evaluó un perfil de AAbs frente a 2125 proteínas humanas distintas mediante la tecnología NAPPA (del inglés *Nucleic Acid Programmable Protein Array*) utilizando pooles de muestras de suero a tiempo cero de la cohorte de la OAI pertenecientes a pacientes que desarrollarían (incidentes, n=10) o no (no incidentes, n=10) OA radiográfica de rodilla durante los 96 meses de seguimiento. Cada pool de muestras se construyó mezclando volúmenes idénticos de 10 sueros individuales. Este análisis llevó a definir un panel de seis AAbs que estaban diferencialmente modulados frente a seis de las proteínas expresadas en el array entre los individuos incidentes y no incidentes, entre las cuales escogimos la proteína MAT2β (del inglés, *methionine adenosyltransferase II subunit betha*) para llevar a cabo la fase de verificación analizando individualmente 354 muestras de la cohorte OAI, 200 de las cuales ya se habían utilizado en la fase anterior. De los 354 participantes seleccionados, el análisis mediante pruebas estadísticas no paramétricas de los 327 individuos que cumplían con el criterio de OA radiográfica definido arriba verificó que aquellos que desarrollaron la enfermedad durante el tiempo de seguimiento mostraban niveles basales significativamente elevados de AAbs frente a MAT2β frente a los que no incidieron.

La capacidad predictiva de estos AAbs fue también moderada (AUC 0,62), a pesar de que su asociación con la aparición de OA de rodilla reveló que el riego de incidir era 5,99

veces mayor por cada incremento en una unidad, expresada en unidades arbitrarias (u.a.) de fluorescencia. Sin embargo, al introducir este AAb en un modelo clínico definido mediante un análisis de regresión por pasos, compuesto por edad, sexo, IMC, participar en alguna actividad que conlleve flexiones frecuentes de las rodillas, historia previa de lesión en la rodilla diana, presencia de dolor en al menos una rodilla, y la subescala "*stiffness*" del cuestionario WOMAC (acrónimo del inglés *Western Ontario and McMaster Universities Osteoarthritis Index*) referida a la rodilla diana, la capacidad predictiva del modelo se vio significativamente aumentada, reforzando la hipótesis de que los niveles de AAb frente a la proteína MAT2β tienen cierto potencial biomarcador en la rutina clínica para identificar aquellos pacientes susceptibles de desarrollar OA de rodilla.

Por otro lado, y visto el potencial de este marcador, también se llevaron a cabo análisis de supervivencia con la finalidad de conocer si los niveles basales de este AAb se asociaban con el tiempo de aparición de la enfermedad. Del mismo modo que en el caso de CHI3L1 y COMP, a medida que los niveles basales de AAb frente a MAT2β aumentaban, también lo hacía el riesgo de desarrollar OA de rodilla, siendo éste 2,53 veces mayor cuando los niveles eran altos (tercer tercil) y 2,37 veces cuando los niveles eran medios (segundo tercil).

Con este trabajo hemos podido demostrar que medir los niveles basales en suero de las proteínas COMP y CHI3L1, así como de AAbs frente a MAT2β aumentan de manera significativa la capacidad predictiva de un modelo clínico para la identificación de pacientes con riesgo de incidir en OA radiográfica de rodilla. Sin embargo, hay una limitación bastante importante de este estudio que debe ser tomada en cuenta, y es que un alto porcentaje de los participantes que se incluyeron en los estudios aquí presentados tenían un grado radiográfico de 2 o más en la rodilla no diana. Nosotros aquí hemos demostrado que incluir una variable que tenga en cuenta si el individuo tiene OA contralateral no proporciona información adicional al modelo formado por las variables clínicas y los biomarcadores solubles, siendo la capacidad de predicción de estos estadísticamente similar. Aun así, y aunque desde un punto de vista epidemiológico este diseño sería adecuado, pues la rodilla que se analiza es sana, desde el punto de vista clínico, los individuos que ya desde el inicio ya tiene una rodilla con OA, no serían sujetos adecuados para incluir en un estudio que analiza la incidencia de la enfermedad. Es por

eso que decidimos replicar el análisis eliminando los participantes con OA contralateral. Cuando incluimos los marcadores en el modelo de predicción clínica pudimos observar que a pesar de producirse un aumento el AUC, este ya no era significativo. Este hecho no tiene porqué significar que los niveles aumentados de estos biomarcadores se deban a la presencia de OA en la rodilla no diana, ya que puede deberse a la pérdida de información al reducir el número de individuos en el estudio. Para poder discernir la causa y cualificar correctamente estos marcadores sería necesario replicar el análisis en un número mayor de individuos completamente sanos, en los que no haya signos radiográficos de OA en ninguna de las dos rodillas. Además, con respecto a los niveles de AAb frente a MAT2β, la fase de verificación se llevó a cabo en un set de muestras que en su mayor parte ya habían sido analizadas en el *screening*, lo que hace que su potencial como marcador de incidencia deba ser validado en un conjunto de pacientes distinto.

Journal of Proteomics 152 (2017) 216–225

Contents lists available at ScienceDirect

Journal of Proteomics

journal homepage: www.elsevier.com/locate/jprot

Multiplexed mass spectrometry monitoring of biomarker candidates for osteoarthritis

Patricia Fernández-Puente [a], Valentina Calamia [a], Lucía González-Rodríguez [a], Lucía Lourido [a], María Camacho-Encina [a], Natividad Oreiro [a], Cristina Ruiz-Romero [a,b,*], Francisco J Blanco [a,c,*]

[a] Proteomics Group-PBR2-ProteoRed/ISCIII, Rheumatology Division, Instituto de Investigación Biomédica de A Coruña (INIBIC), Complexo Hospitalario Universitario de A Coruña (CHUAC), Sergas, Universidade da Coruña (UDC), As Xubias, 84, 15006 A Coruña, Spain
[b] CIBER-BBN Instituto de Salud Carlos III, INIBIC-CHUAC, As Xubias 84, 15006 A Coruña, Spain
[c] RIER-RED de Inflamación y Enfermedades Reumáticas, INIBIC-CHUAC, As Xubias 84, 15006 A Coruña, Spain

ARTICLE INFO

Article history:
Received 1 August 2016
Received in revised form 10 November 2016
Accepted 14 November 2016
Available online 16 November 2016

Keywords:
Osteoarthritis
Biomarkers
SRM/MRM
Cartilage
Chondrocytes
Synovial fluid
Serum

ABSTRACT

The methods currently available for the diagnosis and monitoring of osteoarthritis (OA) are very limited and lack sensitivity. Being the most prevalent rheumatic disease, one of the most disabling pathologies worldwide and currently untreatable, there is a considerable interest pointed in the verification of specific biological markers for improving its diagnosis and disease progression studies. Considering the remarkable development of targeted proteomics methodologies in the frame of the Human Proteome Project, the aim of this work was to develop and apply a MRM-based method for the multiplexed analysis of a panel of 6 biomarker candidates for OA encoded by the Chromosome 16, and another 8 proteins identified in previous shotgun studies as related with this pathology, in specimens derived from the human joint and serum. The method, targeting 35 different peptides, was applied to samples from human articular chondrocytes, healthy and osteoarthritic cartilage, synovial fluid and serum. Subsequently, a verification analysis of the biomarker value of these proteins was performed by single point measurements on a set of 116 serum samples, leading to the identification of increased amounts of Haptoglobin and von Willebrand Factor in OA patients. Altogether, the present work provides a tool for the multiplexed monitoring of 14 biomarker candidates for OA, and verifies for the first time the increased amount of two of these circulating markers in patients diagnosed with this disease.

Significance: We have developed an MRM method for the identification and relative quantification of a panel of 14 protein biomarker candidates for osteoarthritis. This method has been applied to analyze human articular chondrocytes, articular cartilage, synovial fluid, and finally a collection of 116 serum samples from healthy controls and patients suffering different degrees of osteoarthritis, in order to verify the biomarker usefulness of the candidates. HPT and VWF were validated as increased in OA patients.

1. Introduction

The Spanish Chromosome 16 Consortium is integrated in the global initiative Human Proteome Project, which aims to develop an entire map of the proteins encoded following a gene-centric strategy (C-HPP) [1]. Framed in this consortium, our group aims to specifically analyze proteins encoded in Chr 16 that might be associated with the pathogenesis of rheumatic diseases [2]. Among these, osteoarthritis (OA) is the one causing the highest socioeconomic impact worldwide. This is due to its high prevalence, the important disabling consequences that its incidence and progression causes in the patients, and the lack of effective therapeutic treatments, which are currently limited to relieve pain but are unable to slow or reverse the pathogenic process.

OA is a common slowly progressive condition associated with aging, which may affect the structure of all joint tissues, although is primarily characterized by articular cartilage degradation. There is a complexity of processes underlying its pathogenesis [3] leading to a high diversity in its clinical presentation, rate of disease progression, pattern of joint involvement, and joint tissue affected [4]. A definition for OA has been recently described taking into account all these facts by the OARSI (Osteoarthritis Research Society International) [5]. Currently, its diagnosis is based on radiographic criteria (such as joint space narrowing or width) and clinical symptoms, which are insensitive to detect small changes and do not allow the visualization of articular cartilage. The limited knowledge about OA etiopathogenesis and the absence of specific and sensitive biomarkers impedes its early diagnosis, the performance of prognosis studies and also the development of new efficient disease-modifying osteoarthritis drugs (DMOADs). The discovery and

* Corresponding authors at: INIBIC-Complejo Hospitalario Universitario A Coruña, As Xubias, 84, 15006, A Coruña, Spain.
E-mail addresses: cristina.ruiz.romero@sergas.es (C. Ruiz-Romero), francisco.blanco.garcia@sergas.es (F.J. Blanco).

http://dx.doi.org/10.1016/j.jprot.2016.11.012
1874-3919/

application of novel, noninvasive, specific biochemical markers of OA remain to be achieved. These biomarkers would allow carrying out screenings for early diagnosis, thus enabling the beforehand settlement of procedures directed to slow disease progression [6]. To solve this problem, there is an essential need of novel technological tools for easing the existing bottleneck in moving novel marker candidates from discovery phases into clinical applications.

In this field and after two decades of basic research, a number of biochemical markers for OA have been evaluated essentially by performing ELISA on blood-derived samples, urine or synovial fluid. Unfortunately, none of the markers that have been described to date is sufficiently well validated, qualified and accepted for systematic use in diagnostic or monitoring tests for this disease [7]. Proteomics technologies, enabling the multiplexed analysis of several molecules in a high throughput fashion have now matured to the point that their use in clinic appears practical and helpful [8]. Targeted proteomics strategies either based on MS – such as selected/multiple reaction monitoring assays [9] – or antibodies – such as multiplex bead array assays [10] are increasingly being applied for biomarker verification also in the field of OA. Therefore, in the present work we aimed to apply the MRM technology to detect a panel of OA protein biomarker candidates in different specimens from the human joint, and then verify their putative marker value in a set of serum samples from OA patients and healthy controls. These proteins were selected either because they were found altered in sera from OA patients by a shotgun proteomic analysis [11], or because they are encoded by Chromosome 16 and have a reported relationship with this pathology.

2. Materials and methods

2.1. Chondrocytes, cartilage, synovial fluid and serum samples

An immortalized chondrocyte cell line (Tc28A2) was employed in this study. This cell line was obtained by transfection of primary rib chondrocytes with SV40 [12]. The cell line was cultured in DMEM supplemented with 100 U/mL penicillin, 100 mg/mL streptomycin and 10% FBS, and were incubated at 37 °C in a humidified gas mixture containing 5% CO_2 balanced with air. For protein extraction, 1×10^6 cells were recovered and washed twice with PBS.

Human knee articular cartilage samples were obtained from adult donors undergoing joint surgery, after informed consent and Institutional Ethics Committee approval. All tissue samples were provided by the Tissue Bank and the Autopsy Service at Hospital Universitario de A Coruña. Full thickness cartilage or cartilage slices were snap frozen in liquid nitrogen and stored at −80 °C. For protein extraction, the samples were pulverized in a freezer mill and the powder was transferred to Eppendorf tubes and dissolved in 6 M Urea and 2% SDS. Then, samples were vortexed and sonicated three times for ~1 s, and agitated at 4 °C overnight. Extracted material was centrifuged at 4 °C for 20 min at 14,000 rpm. Supernatants containing cartilage proteins were transferred to fresh tubes and the samples were precipitated with ice cold acetone overnight at −20 °C. Protein was collected by centrifugation and the protein pellet was washed once with ice cold acetone and air-dried. Finally, the pellets were dissolved in 25 mM ammonium bicarbonate (AB).

Synovial fluid (SF) samples were collected after informed consent from osteoarthritic knee joints by arthrocentesis in the Rheumatology Department at Hospital Universitario de A Coruña, following our institutional regulations and procedures for sample collection. The study was approved by the local Ethics Committee (Galicia, Spain). The SF samples were visually inspected for blood contamination and stored in liquid nitrogen. A 1 mL aliquot from each pool was treated with 4 mg/mL of hyaluronidase (Sigma-Aldrich, St. Louis, (MO), USA) at 37 °C for 1 h to reduce viscosity and then centrifuged for 5 min at 1000 × *g*.

The sera used for this study were obtained from OA patients and controls with no history of joint disease, after written informed consent. The study was approved by the local Ethics Committee (Galicia, Spain). All experiments were carried out in accordance with the approved guidelines. The patients were diagnosed with OA according to the American College of Rheumatology (ACR) criteria [13]. Knee radiographs from all individuals were classified from grade I to grade IV according to the Kellgren and Lawrence (K/L) scoring system, which assesses the severity of the disease by the radiographic evaluation of joint space narrowing, presence of osteophytes, sclerosis and bone deformity [14].

2.2. Protein digestion and peptide clean-up

The protein concentrations of the Tc28A2 cells and cartilage were determined by the Bradford assay [15]. The SF and serum samples were quantified using the nanoDrop instrument at 580 nm [16]. For in-solution digestion, 10 μg of proteins from chondrocytes, cartilage, synovial fluid and serum samples were dissolved in denaturing and reducing buffer (6 M Urea/2 M Thiourea, 25 mM ammonium bicarbonate, 10 mM Dithiothreitol (DTT)) for 1 h at 37 °C, and cysteins were alkylated with 50 mM iodoacetamide (IA) for 45 min in the dark. Samples were diluted with 25 mM ammonium bicarbonate to a final concentration of 1 M Urea and Promega Grade Trypsin (Promega) was added at a 1:25 ratio (enzyme:protein) for 16 h at 37 °C. Samples were acidified with TFA and a fixed amount of a mixture of stable isotope–labeled peptides was added before the digested peptides were desalted using in-house made stage tips (3M Empore SPE-C18 disk, 47 mm, Sigma Aldrich) and finally samples were dried under speed-vacuum (Thermo, USA).

2.3. Labeled peptides

Heavy stable synthetic isotope-labeled peptides (SIS peptides, crude purity) with a C-terminal ^{15}N- and ^{13}C-labeled arginine or lysine residue and matched light versions were purchased from JPT (Germany). Heavy peptides incorporated a fully atom labeled ^{13}C and ^{15}N isotope at the C-terminal lysine, ($^{13}C_6$,$^{15}N_2$-Lys) (K) or arginine ($^{13}C_6$,$^{15}N_4$-Arg) (R) position of each (tryptic) peptide, resulting in a mass shift of +8 or +10 Da, respectively.

2.4. Design of multiple reaction monitoring (MRM) methods

To generate an empirical data set for selecting target analytes for MRM assay development, two strategies were followed. First, a label-free analysis doing Enhanced Mass and Enhanced Resolution (EM ER) was performed in unfractionated and digested serum samples using a nanoLC-5500 QTRAP to detect the peptides from any of the target proteins. Each MS/MS fragmentation from the 5500 QTRAP was used to search for protein candidates using ProteinPilot software (AB Sciex, version 4.0). Due to the lack of accurate fragments generated in the QTRAP system, the search was conducted with low confidence settings. Second, for those proteins that were not identified in the EM ER, a more detailed strategy was followed using the Skyline software v1.3 (MacCoss Lab Software, Seattle, WA, USA) [17] to build and optimize the best peptides for the target proteins with several filters. Proteotypic peptides with the highest spectral counts, only fully tryptic peptides, with no missed cleavages, with a length between 8 and 30 amino acids and devoid of methionine and cysteine residues, if possible, were chosen for MRM assays development. In addition, sequences that may cause incomplete digestion, such as continuous sequences of arginine (R) or lysine (K) and a proline (P) at the C-terminal side of R or K, were also excluded since partial tryptic hydrolysis at the peptide bond is often observed in MS/MS. The top transitions were selected for method development on the basis of the presence of abundant *y* ions at *m/z* greater than that of the precursor. In the absence of high-*m/z y* ions, the most abundant fragment *b* ions were selected. The initial transitions selected for each peptide included both the MS/MS spectra observed in the LC-MS/MS

Table 1
Proteins and peptides analyzed in the MRM method developed in this work.

Gene name	Protein	UniProt		Peptide sequence	Ref.
ALDOA	Fructose-bisphosphate aldolase A	P04075	#1	GILAADESTGSIAK	[20]
			#2	FSHEEIAMATVTALR	
ALS	Insulin-like growth factor-binding protein complex acid labile subunit	P35858	#1	LAYLQPALFSGLAELR	
			#2	VAGLLEDTFPGLLGLR	
C1S	Complement C1s subcomponent	P09871	#1	TNFDNDIALVR	[11]
CFAD	Complement factor D	P00746	#1	ATLGPAVRPLPWQR	[11]
			#2	RPDSLQHVLLPVLDR	
CLC3A	C-type lectin domain family 3 member A	O75596	#1	EIQALQTVCLR	[21]
			#2	LWTEVNALK	
			#3	GGILVIPR	
			#4	HFHEANEDC[*CAM*]ISK	
CO6	Complement component C6	P13671	#1	DLHLSDVFLK	[11]
			#2	ALNHLPLEYNSALYSR	
CO9	Complement component C9	P02748	#1	TSNFNAAISLK	[11]
			#2	TEHYEEQIEAFK	
			#3	LSPIYNLVPVK	
HPT	Haptoglobin	P00738	#1	TEGDGVYTLNNEK	[23]
			#2	VTSIQDWVQK	
LUM	Lumican	P51884	#1	SLEYLDLSFNQIAR	[11]
			#2	ISNIPDEYFK	
			#3	FNALQYLR	
MMP2	72 kDa type IV collagenase	P08253	#1	FPFLFNGK	[21,24]
			#2	QDIVFDGIAQIR	
			#3	VDAAFNWSK	
PEDF	Pigment epithelium-derived factor	P36955	#1	TVQAVLTVPK	[11]
			#2	LQSLFDSPDFSK	
			#3	KTSLEDFYLDEER	
SAMP	Serum amyloid P-component	P02743	#1	VGEYSLYIGR	[11]
			#2	IVLGQEQDSYGGK	
VASN	Vasorin	Q6EMK4	#1	NLHDLDVSDNQLER	[24]
			#2	SLTLGIEPVSPTSLR	
			#3	YLQGSSVQLR	
VWF	Von Willebrand Factor	P04275	#1	YTLFQIFSK	[11]
			#2	AHLLSLVDVMQR	
			#3	LLDLVFLLDGSSR	

[CAM]: cysteine carbamidomethylation.

analysis of serum samples, predictions derived from the sequences, and data available from databases. The Global Proteome Machine database [18] was used to select peptides from target proteins that were frequently detected (multiple experiments). Then, a Consensus spectral library constructed from the 177 public data sets in Human Plasma PeptideAtlas (Human) from the ion trap instrument (NIST_human_IT_2012-05-30_7AAs) was downloaded to the Skyline program. Several peptide precursors and fragment ion masses were selected per each protein and assayed for MRM analysis. MRM results from the approaches described above were pooled, and a set of optimized MRM methods covering a total of 14 proteins was assembled. It was divided into two methods of acquisition: one including the six Chromosome-16 encoded proteins, which targeted 16 peptides (118 transitions), and the other for the 8 other OA-related biomarker candidates, targeting 19 peptides (148 transitions). Table 1 shows the list of peptides screened in this work, whereas Supplementary Table S1 lists all transitions and settings for their analysis.

2.5. Liquid chromatography-multiple reaction monitoring mass spectrometry analysis

An enhanced MS and enhanced resolution (EM ER) with a linear gradient of 120 min and MRM with a linear gradient of 70 min were performed injecting 1 μg of digested samples onto the nanoLC-5500 QTRAP. Protein digests with and without added labeled peptides were analyzed by LC-MS/MS using a nanoLC system (TEMPO) coupled to a 5500-QTRAP instrument (AB Sciex). After precolumn desalting using a C18 column (5 μm, 300A, 100 μm∗2 cm, Acclaim PepMap, Thermo Scientific, USA) at a flow of 3 μL/min during 10 min, tryptic digests were separated on C18 nanocolumns (75 μm id, 15 cm, Acclaim PepMap 100, Thermo Scientific, USA) at a flow rate of 300 nL/min. The gradient for the EM ER method start with 5% buffer B (0.1% Formic acid in 95% acetonitrile) for 3 min, from 3 until 90 min 30% of buffer B, from 10 min until 40% of buffer B, 1 min at 95% buffer B, hold for 10 min, and finally, equilibration of the column for 15 min with 5% of buffer B. The gradient for the MRM method start with 5% buffer B (0.1% Formic acid in 95% acetonitrile) for 3 min, from 3 until 45 min 35% of buffer B, 1 min at 95% buffer B, hold for 10 min, and finally, equilibration of the column for 15 min with 5% of buffer B. The mass spectrometer was interfaced with a nanospray source equipped with an uncoated fused silica emitter tip (20 μm inner diameter, 10 μm tip, NewObjective, Woburn, MA) and was operated in the positive ion mode. MS Source parameters were as follows: ion spray voltage (IS) 2600 V, interface heater temperature (IHT) 150 °C, ion source gas 2 (GS2) was 0, curtain gas (CUR) was 20 and ion source gas 1 (GS1) was 25 psi, and collision gas (CAD) high. MS compound parameters were set to 10 for the entrance potential (EP) and to 15 for the Collision cell exit potential (CXP). Skyline was used to predict and optimize collision energies for each peptide, both analyte and IS [17]. Q1 and Q3 were set to unit/unit resolution (0.7 Da) and the pause between mass ranges was set to 3 ms. In order to confirm the identity of the peptides, a MRM Information Dependent Acquisition (IDA) experiment was performed for each peptide. The mass spectrometer was instructed to switch from MRM to enhanced product ion (EPI) scanning mode when an individual MRM signal exceeded 1000 counts. Each precursor was fragmented a maximum of twice before being excluded for 10 s and the mass were scanned from 250 to 1000 Da. MRM analysis was conducted with up to 118 transitions per run (dwell time, 15 ms; cycle time or 2.5 s). The rolling collision energy (CE) option was employed to automatically ramp up the CE value in the collision cell as the *m/z* value increased. The best transitions were pooled in one scheduled SRM method with a 45-min gradient, using retention times extracted during the assay refinement. A target scan time of 3 s and a MRM detection window of 480 s (time window of ±4 min) were used.

2.6. Data analysis

The MS/MS data generated were analyzed with the ProteinPilot software. The Paragon algorithm in ProteinPilot software served as the default search program for protein identification, with trypsin as the digestion agent and iodoacetamide as a fixed modification of cysteine. Biological modifications were programmed in the algorithm. The searches for peptide mass fingerprints and tandem MS spectra were performed using the SwissProt knowledge base (2015_05 release version), by searching in the UniProtKB/Swiss-Prot (http://www.expasy.ch/sprot) database, containing 547,599 sequences and 195,014,757 residues, with taxonomy restriction (*Homo sapiens*).

Data analysis of the best peptides for the target proteins was performed using Skyline for method refinement, optimization and peak integration. Raw files were imported to Skyline and integration was manually inspected to ensure correct peak detection, absence of interferences, and accurate integration. MRM signal was defined as the detection of all the transitions from the endogenous peptide exactly coeluting with all the transitions from the stable isotope–labeled peptide. Reports of peak area ratios between the light and heavy peptide of each peptide in the serum samples were exported by Skyline to MS Excel. All subsequent data analyses were performed in MS Excel to generate the mean, the standard deviations, and % coefficient of variation (% CV) of the mean peak ratio area and retention time (RT) for all sample replicates, and also the relative quantitation comparing samples with different grades of OA to controls. An interference screening was carries out based on the fragment-ion ratios of the transitions and using the exported responses from the heavy and light peptides. With this aim,

the SIS mixture standard was first analyzed to confirm that there was no signal due to contamination from the heavy peptide synthesis at the *m/z* transitions for the light peptides. Then, the pool of serum sample used as a background was analyzed without spiked light or heavy peptide standards, to prove that there was not signal at the *m/z* transitions for the heavy peptide.

Quantitation was conducted by single point measurements. The molecular weight of the protein was used to calculate protein concentrations (ng/mL), as previously described [19]. Kruskal–Wallis and Mann–Whitney *U* test and the box plot graphs were performed using GraphPad Prism 5.01 software (La Jolla, CA, USA). The clustering analysis and heatmap graphic were made with the Multiple Experiment Viewer MeV 4.9 (GitHub, San Francisco, CA, USA).

2.7. Suspension bead array analysis

A quantitative protein analysis by magnetic suspension bead array technology was performed according manufacturer's recommendation (MILLIPLEX; HCVD3MAG-67 K) for the detection of von Willebrand Factor. The study was carried out on an independent set of 38 serum samples (12 OA GIV, 13 OA GII, and 13 non-OA individuals). A lyophilized standard of the recombinant protein tested, included in the kit, was reconstituted and diluted at seven serial concentrations (standard curve). All serum samples were diluted 1:4000 in assay buffer, and 25 μL of each diluted sample was bound for overnight incubation at 4 °C in a 96-well plate with shaking. Then, the wells were washed three times with wash buffer and incubated with 50 μL of detection secondary antibodies mix for 1 h at room temperature (RT). 50 μL of streptavidin-phycoerythrin were subsequently added to each well and incubated 30 min at RT to label the target analyte in the samples. Finally, wells were washed again three times and 100 μL of Sheath Fluid was added per well. The MAGPIX System (Luminex Europe, Oosterhout, The Netherlands) was used to detect the fluorescence signal. Concentration of VWF was obtained by interpolating fluorescence intensities to the standard curve, and calculated by the MILLIPLEX Analyst 5.1Software (Millipore).

3. Results and discussion

3.1. Selection of proteins related with OA

In the last years, shotgun proteomics analyses in the field of osteoarthritis have led to panels of proteins whose abundance is altered in OA compared to healthy controls or other rheumatic diseases. In this area, our group performed these differential studies on human articular chondrocytes (the only cell type resident in mature cartilage) [20], cartilage [21], synovial fluid [22] and serum [11]. Therefore, we aimed in the present work to develop targeted assays to verify the putative biomarker value for OA of some of these candidates, with a special focus on those encoded by Chromosome 16. Based on the previous knowledge from our group, referenced above, and also after bibliographic revision of all Chr. 16 proteins with known function, a panel of six Chr. 16 proteins was selected for verification (Table 1): Haptoglobin (HPT) [23], Fructose-bisphosphate aldolase A (ALDOA) [20], Insulin-like growth factor-binding protein complex acid labile subunit (ALS) (Mateos J. et al., unpublished work 2016), C-type lectin domain family 3 member A (CLC3A), matrix metallopeptidase 2 (gelatinase A, 72 kDa type IV collagenase, or MMP2) [21,24] and vasorin (VASN) [24]. We added to the panel another 8 proteins previously identified by our group as putative circulating markers for OA [11]: von Willebrand Factor (VWF), Pigment epithelium-derived factor (PEDF), Lumican (LUM), Complement Factor D (CFAD), Complement C1s subcomponent (C1S), Complement component C9 (CO9), Complement component C6 (CO6) and Serum amyloid P-component (SAMP). It has been suggested that complement components play an important role in OA, since dysregulation of complement in synovial joints has shown to be key in the pathogenesis of this disease [25]. Therefore, in the present work we aimed to explore the putative marker value of complement components for OA.

3.2. Selection of the best peptides and development of MRM methods

An enhanced MS and enhanced resolution (EM ER) analysis was performed in the samples using a nanoLC-5500 QTRAP workflow. The MSMS spectra generated was launched against a uniprot_sprot_human.fasta using the Protein Pilot software, leading to a list of 104 proteins in which several of the targets were included such as Haptoglobin, von Willebrand Factor, most of the complement components and Serum Amyloid P. For the proteins that are at minor concentrations in the serum samples and were not identified with the EM ER screening, transitions were selected based on data available from databases on ion trap MS/MS spectra with further optimization, although it has been reported the intensity order of transitions is well correlated between ion trap CID and SRM [26]. In the present approach, each target peptide was quantified by measuring at least three different SRM/MRM transitions. Stable isotope-labeled internal standards were employed to provide the highest level of detection confidence and measurement precision in the experiments, increasing the selectivity for the target peptides by monitoring the chromatographic co-elution of six or eight transitions of the target and internal standard peptides, thereby ensuring the reliable identification of signal peaks.

Another issue taken into account was the effect of the ion suppression in the biological samples employed in this work (fluids, tissues and cells), since other matrix component different from the target proteins (lipids and other small molecules, salts, etc.) co-elute and compete for ionization, resulting in a decrease in the ion current detected for the same amount of protein analyzed in different samples [27]. According to this, we found that the same amount of spiked internal standard gave different signal depending on the matrix sample. In our case the same amount of heavy peptide was spiked to the different digested samples (chondrocytes, cartilage, synovial fluid and serum) before the cleaning step, and the signal was quite different. Ideally, the internal standard has the same structure as the analyte and coelutes with it, thereby experiencing the same matrix-induced suppressive effects [28]. Furthermore, sensitivity correction using SIS peptides is important for the accurate quantification of target proteins [29]. The precursor/product ion pairs used were selected and prioritized by ion intensity and lack of interferences. Importantly, the selected transitions were tested in the presence of digested, undepleted serum to account for interferences from the sample matrix or from the standards themselves. Supplementary Table S1 shows the retention times and peak areas obtained for all the transitions analyzed in the different matrices that were employed in this work by triplicate. The final results of this interference screening, based on the fragment-ion ratios of the transitions, are summarized in Supplementary Table S2. According to previously established requirements [30,31], peptides were considered interference-free when the extracted ion chromatogram (XIC) traces of the candidate SIS and NAT peptides co-elute in retention time, exhibit similar peak symmetry and width, and had a coefficient of variation (CV) below 25% of the peak area ratios calculated on a per-transition basis in the SIS and/or NAT peptide MRM channels [32]. All transitions not accomplishing these requirements (marked in red in Supplementary Table S2) were removed from further data analysis. An example is presented in Fig. 1, which shows the XICs corresponding to three peptides that were monitored from VWF. The co-elution of the transitions from all endogenous and heavy peptides was analyzed in crude serum without the spiked heavy internal standard (upper row), and serum spiked with the internal light and heavy standards (bottom row). As shown in the Figure, a very high signal at the *m/z* heavy transitions (Q1/Q3) was detected for the peptide LLDLVFLLDGSSR without the addition of any SIS, and this peptide was thus removed from the panel. The peptide ATLGPAVRPLPWQR from CFAD was also removed, since the order of co-elution of the transitions

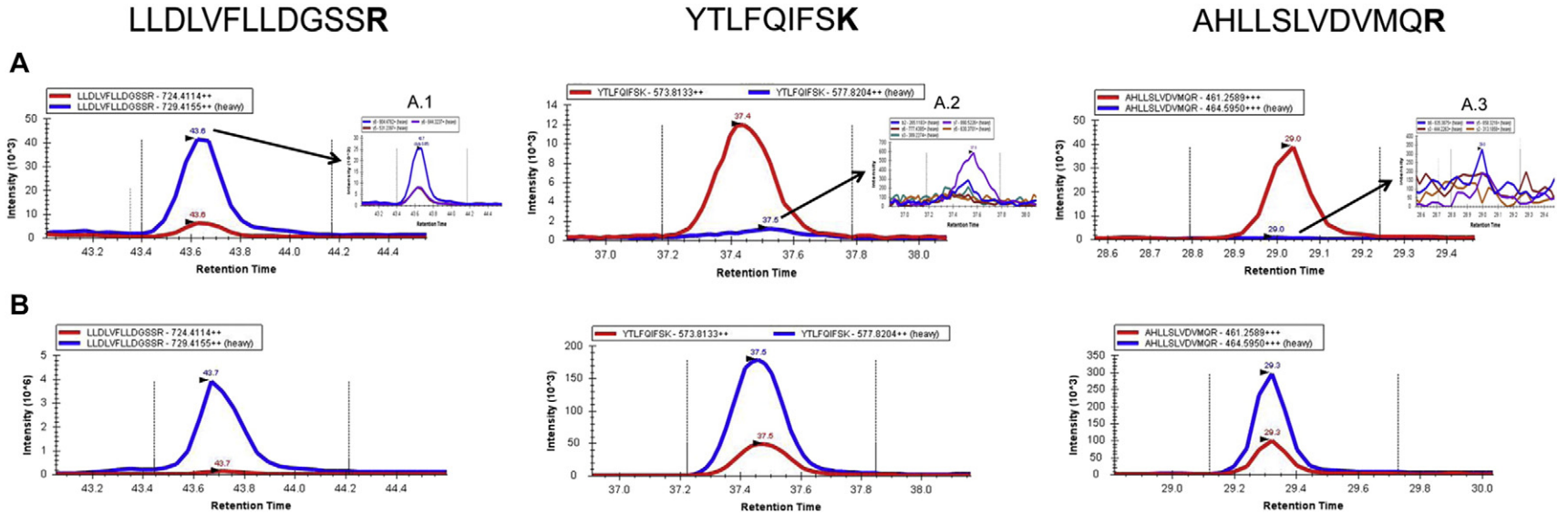

Fig. 1. Representative extracted ion chromatograms (XICs) of 3 peptides from the protein VWF. The endogenous proteotypic peptides LLDLVFLLDGSSR, YTLFQIFSK, and AHLLSLVDVMQR were screened in A) crude serum (upper row) and B) crude serum with the addition of heavy peptides (bottom row). The endogenous peptides (light) are displayed in red, whereas the SIS (heavy peptides) are displayed in blue. The amount of SIS spiked into each sample was kept constant. As shown in the top left graphic, a high interference was found for the peptide LLDLVFLLDGSSR.

from the endogenous peptide (NAT) was different from the SIS standards in all the matrices analyzed.

The use of at least six transitions per peptide made possible the accurate determination of chromatographic retention time. Retention times on the LC platform were observed using serum samples and a mixture of the SIS peptides in a non-scheduled fashion (IDA experiments), and employed for scheduling to reduce the number of concurrent transitions enabling a shorter cycle time and thus a sufficient number of points per peak for proper peak integration [33]. Altogether, the 14 different proteins were quantified by single point measurements targeting 35 peptides and 244 transitions. The final transitions and settings for their analysis are listed in Supplementary Table S3.

3.3. Application of the SRM methods to different specimens from the human joint

In order to evaluate the performance of these methods for the targeted analysis of the 14-protein panel in samples derived from the human joint, we analyzed digested extracts from a cell line of articular chondrocytes, human healthy and osteoarthritic articular cartilage, synovial fluid obtained by knee arthrocentesis and serum as reference. Three replicates were performed for each type of sample. Supplementary Table S4 lists the mean retention times, mean peak area ratios and % CVs obtained in this analysis for each peptide in each of the samples analyzed. The concentration of the peptides (ng/mL) was calculated using single point measurement-derived quantitation values. Fig. 2 shows representative examples of proteins encoded by Chromosome 16: ALDOA was identified with two peptides (GILAADESTGSIAK and FSHEEIAMATVTALR) but displaying the best signal in chondrocytes, as expected being a cytoplasmic protein. Interestingly, in all sample types the signal was better for the GILAADESTGSIAK peptide, whereas FSHEEIAMATVTALR was only detected in chondrocytes. In contrast, the secreted protein C-type lectin domain family 3 member A (CLC3A), which has been reported to be restricted to cartilage and breast [34], was identified only in cartilage (Fig. 2). From the several peptides screened for this protein, the best signal was found for EIQALQTVCLR and LWTEVNALK. From the other proteins from the panel, LUM, HPT and VASN were detected in all samples, whereas ALS, PEDF, CO6, CO9, C1S, CFAD and SAMP failed to be detected in chondrocytes, VWF was only identified in serum, and MMP2 only in cartilage. The heatmap shown in Fig. 3 summarizes the result of this analysis, and Supplementary Fig. S1 illustrates representative XICs obtained for each target peptide in the different samples. In all

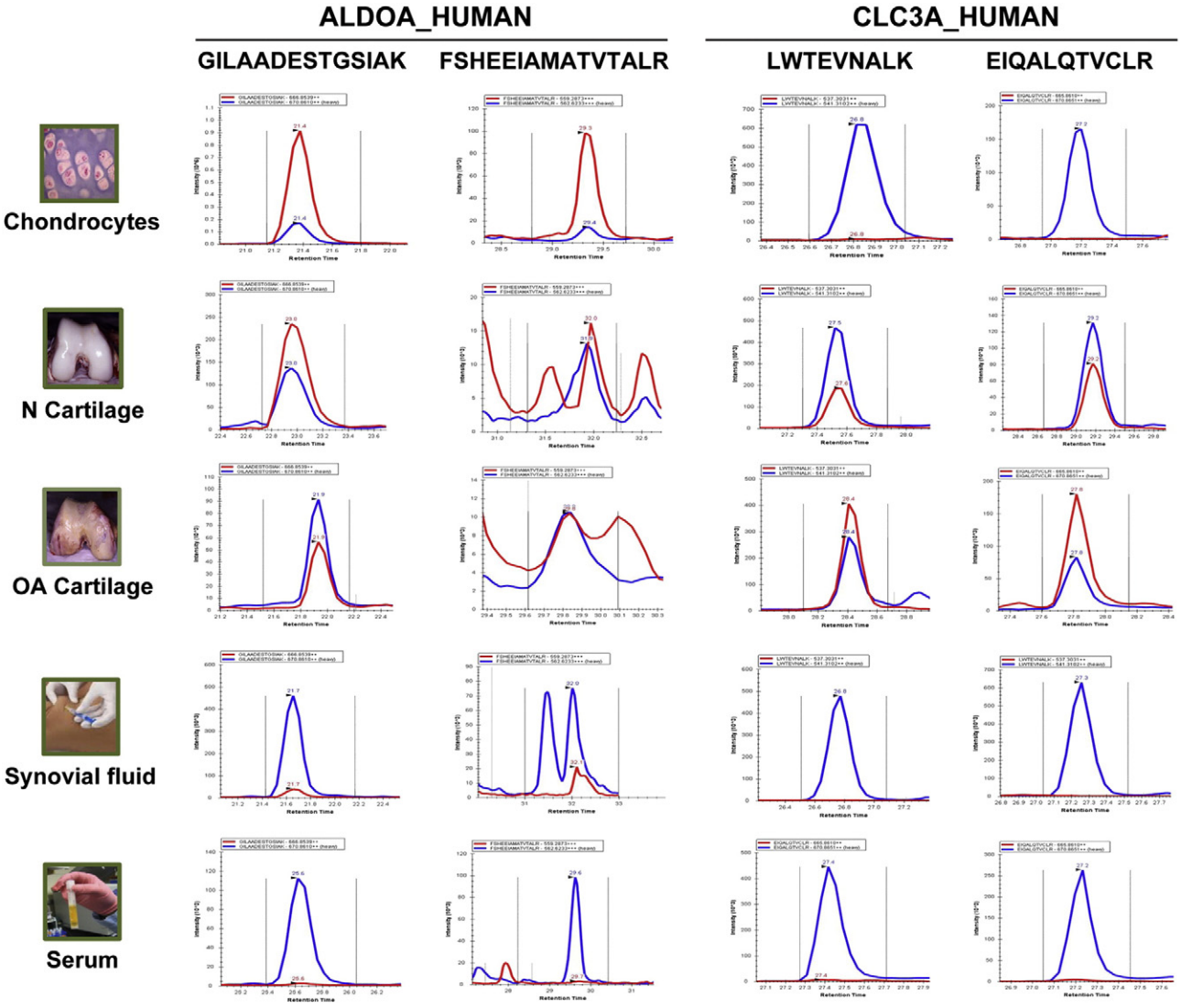

Fig. 2. Representative XICs of peptides belonging to the Chromosome 16-encoded proteins ALDOA and CLC3A in different human samples. Fructose-bisphosphate aldolase A (ALDOA) and C-type lectin domain family 3 member A (CLC3) were searched in five different types of samples: chondrocytes, normal (N) and osteoarthritic (OA) knee cartilage, synovial liquid and undepleted serum. The natural peptides (light) are displayed in red, whereas the heavy peptides (SIS) are displayed in blue. The amount of SIS spiked into each sample was kept constant. Representative XICs of all peptides analyzed on these samples are shown in Supplementary Fig. S1.

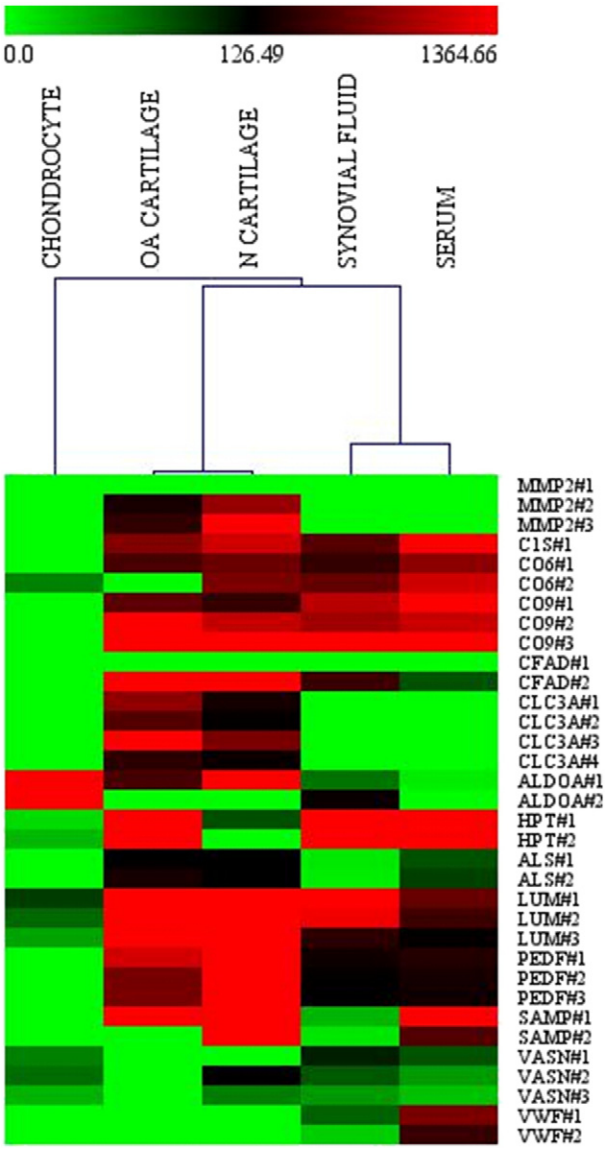

Fig. 3. Heatmap showing the quantification of the panel of peptides in the different matrices analyzed in this work. Peptide names and numbers are shown according to Table 1. The mean area ratios obtained in the MRM analysis were used to calculate the protein concentrations in ng/mL for each peptide, using one point calibration curves with an equimolar mixture of internal standards (SIS, 20 fmol/μL).

cases, some peptides showed lower signals or interferences than others in a specific type of samples, highlighting the importance of the matrix background for achieving a good identification/quantification of the target proteins. Retention times were very reproducible for all peptides (% CV < 5) in this analysis, while the reproducibility of the peak area ratios was highly dependent on the target peptide, being their % CV < 15 in most cases if the peptide was well identified. Regarding the differences in peptide measurements for the same target protein, we observed some proteins showing a high agreement in the peptide concentrations (such as PEDF, with fold changes approaching unity between the three peptides analyzed), whereas in other cases the ratio comparing the peptide with the highest signal to the lowest increases up to around 3 (CO9, LUM, VASN). This discrepancy has been commonly observed before in serum samples [32,35], as well as in other biofluids and cells [31,36]. The most widely accepted hypothesis for the larger fold changes observed for specific proteins are likely due to the variability in denaturation or digestion efficiency, steric hindrance of modified residues, or post-translational modifications [37,38].

3.4. MRM-based verification of biomarker candidates related with OA in serum samples

The MRM method was then applied to verify the putative biomarker value of this panel of 14 proteins in serum samples from OA patients and controls without history of joint disease. The demographic characteristics of the samples included in this study (n = 116) are detailed in Table 2. Three technical replicates were measured, leading to peak area ratios between the endogenous and heavy peptide (SIS) with good coefficients of variation (% CVs < 20) and area counts >5000 for most peptides. Kamiie and collaborators [39] have validated that protein expression levels that yield % CV of <20 when determined from three peaks with area counts >5000 and are detected at the same retention time (±0.10 min) as an IS peptide are defined as positive. As shown in Supplementary Table S2, peptides from HPT, ALS, VWF, PEDF, LUM, C1S, CO9, CO6, SAMP and VASN showed a good reproducibility between replicates (% CV < 20). Two proteins, CLC3A and MMP2, and the peptide FSHEEIAMATVTALR from ALDOA were removed from the data analysis of the serum samples as the detectability of the NAT peptide was hampered by the inherently low protein concentrations present in this sample matrix.

Results from the relative quantitation of the proteins between the early and late OA and control serum samples are presented as average values of the peak areas out of all transitions and peptides per protein, after an intensity normalization step with their corresponding heavy isotope–labeled standard references. Quantification data (in ng/mL) was then obtained by single point calibration measurements with an equimolar mixture of SIS peptides (20 fmol/μL). All the results obtained per sample and target protein are summarized in Supplementary Table S5, and their scatter plot representation is illustrated in Supplementary Fig. S2. Two proteins were found increased in OA compared to control samples with a significant p-value ($p < 0.05$): Haptoglobin [23] and von Willebrand Factor [11] (Fig. 4A). Interestingly, when the two different grades of OA (K/L II and K/L IV) were analyzed independently, both proteins show statistically significant differences in early OA (K/L II) compared to controls (Fig. 4B) suggesting a putative utility in diagnostic and prognostic strategies. Although the relationship of Haptoglobin polymorphisms with diseases such as cancer or rheumatoid arthritis has been largely studied due to the antioxidant [40], anti-inflammatory [41] and immunomodulatory properties [42] of this protein that is encoded in Chromosome 16, the first time an alteration of the HPT protein pattern was reported in OA corresponds to a DIGE-based proteomic study in which the alpha and beta chains of HPT displayed different alterations in abundance [23] in pooled serum samples from OA patients compared to controls. In this work, we could confirm by MRM on individual samples the increased amount of the HPT beta chain, two of whose peptides were included in the method. Further analyses are currently ongoing to establish the role of the different HPT chains in OA (Fernández-Costa, unpublished results).

Apart from VWF and HPT, from the 14-protein panel only Serum Amyloid P (SAMP) was found altered with significant p-value ($p = 0.0496$) in this verification screening, in this case showing a decrease in advanced stages of the disease (K/L GIV) compared to GII (Supplementary Fig. S2) and has therefore putative marker value, although only for disease severity. We did not find any statistically significant differences in OA serum samples vs healthy controls on the other proteins

Table 2
Demographic characteristics of the individuals included in this study to compare patients with different K/L grades of OA and control donors using the MRM method developed.

K/L grade	Gender	Age (mean ± SD)
Control = 39	Female (35.9%), male (64.1%)	70.4 ± 7.6
Grade II = 38	Female (63.15%), male (36.8%)	73.1 ± 6.4
Grade IV = 39	Female (87.2%), male (12.8%)	75.6 ± 7

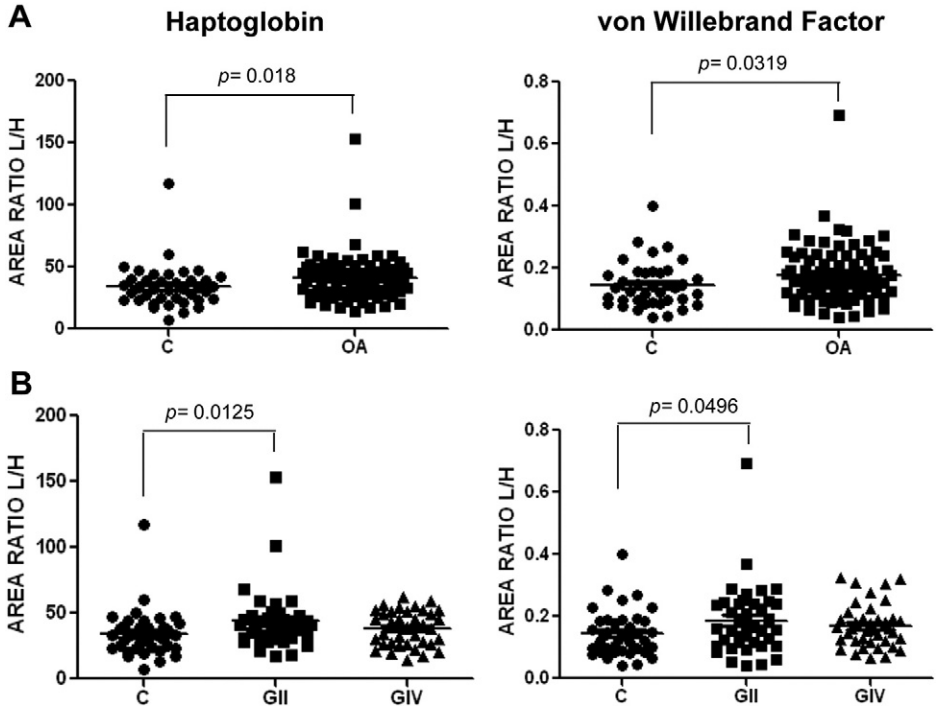

Fig. 4. MRM quantitation data of OA biomarker candidates in serum. A, Verification of the increase of Haptoglobin (HPT) and von Willebrand Factor (VWF) in sera from OA individuals compared to controls. B, HPT and VWF are increased in early stages of radiographic OA (GII) compared to controls. Data were normalized against the internal standard. Scatter plots show the normalized peak area on the y-axes. Horizontal lines depict the mean, and vertical lines the standard deviation.

included in the panel (Supplementary Fig. S2), hence results that were previously reported in shotgun studies failed to be verified [11]. There are several possible explanations for this limited success in the verification step: first, shotgun proteomics analyses are usually performed in sera depleted from their high abundance proteins, thus the sample preparation procedures might have an effect on the proteins targeted in the present analysis. Second, splicing isoforms or post-translational modifications may also have been involved in these variations because iTRAQ ratios are calculated as the average of all contributing peptides from a protein, whereas SRM ratios are obtained by measuring a specific target peptide [39,43]. Third, pooling of samples in the discovery phase of proteomic studies could potentially mask meaningful discrepancies among the different individuals, which were individually analyzed in the present work. Finally, results obtained for ALS, LUM and PEDF are in agreement with previous data reported by MRM analysis of plasma samples from an observational knee OA cohort [44]. In that work, proteotypic peptides of nine proteins (including these three) were evaluated, and authors found that the levels of two peptides representative of clusterin and lubricin in plasma are as predictive of OA progression as age. However, neither ALS nor PDF were associated with joint space narrowing, and LUM showed only a preliminary evidence of association in this study. Although an increased amount of LUM was previously detected by SRM in synovial fluid from osteoarthritic patients compared to healthy [9], this difference is not detected neither in plasma [44] nor in serum, as shown in the present study. Apart from these two studies and the present work, no other analysis using isotope-labeled standards have been carried out for OA analysis by mass spectrometry [45].

3.5. Confirmation of the increase of VWF in an independent analysis

The von Willebrand Factor (VWF) is a protein best known from its critical role in hemostasis, but that is also involved in several pathologic processes including angiogenesis, cell proliferation, inflammation, and tumor cell survival. The 250 kDa-subunit structure of VWF contains four different types of domains, each of them being characterized by its specific type of folding. This diversity provides VWF the potential to interact with a wide spectrum of structures and, indeed, a large number of its protein ligands have been identified [46]. Some of these

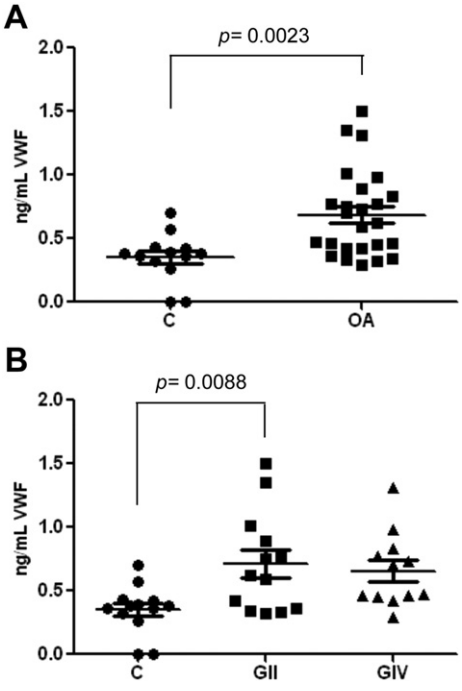

Fig. 5. Absolute quantification of VWF in independent serum samples. 13 samples from OA GII, 12 from OA GIV and 13 healthy individuals were analyzed using Luminex beads. Horizontal bars in each data set indicate the mean serum level (ng/mL) of VWF. The quantitative results and samples used in this analysis are listed in Supplementary Table S6.

proteins are galectin-1,3 [47], thrombospondin 1 [48], and β-glycoprotein, which were found up-regulated together with VWF in our previous study for the discovery of OA biomarkers in serum [11]. Therefore, we decided to confirm the detected increase of VWF in sera from OA patients using an independent set of samples and an orthogonal approach. An assay based on Luminex beads coupled to anti-VWF antibodies was carried out on a group of 38 serum samples (13 OA GII, 12 OA GIV and 13 healthy controls). Demographic data of the individuals included in this analysis and the absolute quantification values obtained for VWF are shown in Supplementary Table S6, and graphically represented in Fig. 5. As illustrated in the Figure, a statistically significant increase of VWF in OA samples was confirmed ($p = 0.0023$), and was already detected in patients with K/L Grade II of the disease (Fig. 4B). A mean concentration of 4201 ng/mL of VWF (range of concentrations 1040–6000 ng/mL) was detected with this assay. This amount is higher than the one determined by SRM (mean concentration of 1115,4 ng/mL) for the peptide AHLLSLVDVMQR (range 214,11–9726,18 ng/mL), which may be explained by the use of single point calibration measurements in our SRM approach and the higher specificity of this method in comparison to antibody-based strategies [49]. Nevertheless, ratios found between patients and controls were comparable (OA GIV/Ctrl = 1,65 by Luminex and 1,23 by SRM, and OA GII/Ctrl = 1,7 by Luminex and 1,29 by SRM).

This is the first time VWF has been verified as increased in the serum from OA patients compared to healthy controls. Interestingly, a large number of proteins that are known to be involved in OA pathogenesis, such as collagens, thrombospondins, a bone morphogenetic protein (BMP) regulator, integrins and matrilins, contain von Willebrand domains. Regarding this issue, a recent work demonstrated that the VWA1 domain of matrilin-3 (a protein expressed by cartilaginous tissues that has been extensively related with OA [50]) is primarily responsible for the induction of IL-6 release in primary human chondrocytes, promoting cartilage catabolism [51]. Furthermore, mutations in the double von Willebrand Factor A domains (DVWA) gene were reported as associated with susceptibility to knee OA [52], a fact that has been recently confirmed in two independent meta-analyses [53,54]. In addition, high levels of VWF have been found in rheumatoid arthritis (RA) as associated with cardiovascular risk prediction [55] and with other chronic synovitis syndromes [56]. Altogether, our finding of increased VWF in OA patients provides impetus for further investigations in larger cohorts and also on the role of this protein in the diverse pathogenic mechanisms that contribute to OA development and progression.

4. Conclusions

A multiplexed method for the relative quantification by single point measurements of a panel of fourteen OA protein biomarker candidates (6 of them encoded by Chromosome 16) has been developed, based on liquid chromatography-multiple reaction monitoring (LC-MRM) mass spectrometry. We demonstrate how this method can be readily applied to any type of joint-derived specimens, such as cells, cartilage, synovial fluid and serum for the evaluation of these biomarker candidates putatively useful for diagnosis or therapeutic targets. The application of this method on a set of 116 crude serum samples from patients suffering different grades of OA and healthy controls led to the verification of von Willebrand Factor, and Haptoglobin as increased in OA, already in early stages, while Serum Amyloid P was found decreased in advanced OA (grade IV). The increase of VWF in OA was confirmed by a Luminex-based assay in an independent set of samples. Further qualification studies will be necessary to establish the usefulness of these proteins for OA diagnosis and progression studies.

Supplementary data to this article can be found online at http://dx.doi.org/10.1016/j.jprot.2016.11.012.

Conflict of interest disclosure

The authors declare no competing financial interest.

Transparency Document

The Transparency Document associated with this article can be found, in online version.

Acknowledgements

This work was funded by grants from Fondo Investigación Sanitaria-Spain (PI12/00329, PI14/01707, CIBER-CB06/01/0040, RETIC-RIER-RD12/0009/0018). C.R.-R. is supported by the Miguel Servet II program from Fondo Investigación Sanitaria-Spain (CPII15/00013). The Proteomics Unit belongs to ProteoRed, PRB2-ISCIII, supported by grant PT13/0001.

References

[1] V. Segura, J.A. Medina-Aunon, M.I. Mora, S. Martinez-Bartolome, J. Abian, K. Aloria, et al., Surfing transcriptomic landscapes. A step beyond the annotation of Chromosome 16 proteome, J. Proteome Res. 13 (2014) 158–172.
[2] C. Ruiz-Romero, V. Calamia, J.P. Albar, J.I. Casal, F.J. Corrales, P. Fernandez-Puente, et al., The Spanish biology/disease initiative within the human proteome project: application to rheumatic diseases, J. Proteome 127 (2015) 406–413.
[3] C. Cooper, J.D. Adachi, T. Bardin, F. Berenbaum, B. Flamion, H. Jonsson, et al., How to define responders in osteoarthritis, Curr. Med. Res. Opin. 29 (2013) 719–729.
[4] D.J. Hunter, M. Nevitt, E. Losina, V. Kraus, Biomarkers for osteoarthritis: current position and steps towards further validation, Best Pract. Res. Clin. Rheumatol. 28 (2014) 61–71.
[5] V.B. Kraus, F.J. Blanco, M. Englund, M.A. Karsdal, L.S. Lohmander, Call for standardized definitions of osteoarthritis and risk stratification for clinical trials and clinical use, Osteoarthr. Cartil. 23 (2015) 1233–1241.
[6] C. Ruiz-Romero, P. Fernandez-Puente, V. Calamia, F.J. Blanco, Lessons from the proteomic study of osteoarthritis, Expert Rev. Proteomics 12 (2015) 433–443.
[7] M. Lotz, J. Martel-Pelletier, C. Christiansen, M.L. Brandi, O. Bruyere, R. Chapurlat, et al., Value of biomarkers in osteoarthritis: current status and perspectives, Ann. Rheum. Dis. 72 (2013) 1756–1763.
[8] R. Aebersold, G.D. Bader, A.M. Edwards, J.E. van Eyk, M. Kussmann, J. Qin, et al., The biology/disease-driven human proteome project (B/D-HPP): enabling protein research for the life sciences community, J. Proteome Res. 12 (2013) 23–27.
[9] S.Y. Ritter, R. Subbaiah, G. Bebek, J. Crish, C.R. Scanzello, B. Krastins, et al., Proteomic analysis of synovial fluid from the osteoarthritic knee: comparison with transcriptome analyses of joint tissues, Arthritis Rheum. 65 (2013) 981–992.
[10] F. Henjes, L. Lourido, C. Ruiz-Romero, J. Fernandez-Tajes, J.M. Schwenk, M. Gonzalez-Gonzalez, et al., Analysis of autoantibody profiles in osteoarthritis using comprehensive protein array concepts, J. Proteome Res. 13 (2014) 5218–5229.
[11] P. Fernandez-Puente, J. Mateos, C. Fernandez-Costa, N. Oreiro, C. Fernandez-Lopez, C. Ruiz-Romero, et al., Identification of a panel of novel serum osteoarthritis biomarkers, J. Proteome Res. 10 (2011) 5095–5101.
[12] F. Finger, C. Schorle, A. Zien, P. Gebhard, M.B. Goldring, T. Aigner, Molecular phenotyping of human chondrocyte cell lines T/C-28a2, T/C-28a4, and C-28/I2, Arthritis Rheum. 48 (2003) 3395–3403.
[13] R. Altman, E. Asch, D. Bloch, G. Bole, D. Borenstein, K. Brandt, et al., Development of criteria for the classification and reporting of osteoarthritis. Classification of osteoarthritis of the knee. Diagnostic and Therapeutic Criteria Committee of the American Rheumatism Association, Arthritis Rheum. 29 (1986) 1039–1049.
[14] S. Kessler, K.P. Guenther, W. Puhl, Scoring prevalence and severity in gonarthritis: the suitability of the Kellgren & Lawrence scale, Clin. Rheumatol. 17 (1998) 205–209.
[15] M.M. Bradford, A rapid and sensitive method for the quantitation of microgram quantities of protein utilizing the principle of protein-dye binding, Anal. Biochem. 72 (1976) 248–254.
[16] P. Desjardins, J.B. Hansen, M. Allen, Microvolume protein concentration determination using the NanoDrop 2000c spectrophotometer, J. Vis. Exp. (2009).
[17] B. MacLean, D.M. Tomazela, N. Shulman, M. Chambers, G.L. Finney, B. Frewen, et al., Skyline: an open source document editor for creating and analyzing targeted proteomics experiments, Bioinformatics 26 (2010) 966–968.
[18] R. Craig, J.P. Cortens, R.C. Beavis, Open source system for analyzing, validating, and storing protein identification data, J. Proteome Res. 3 (2004) 1234–1242.
[19] A.J. Percy, R. Simon, A.G. Chambers, C.H. Borchers, Enhanced sensitivity and multiplexing with 2D LC/MRM-MS and labeled standards for deeper and more comprehensive protein quantitation, J. Proteome 106 (2014) 113–124.
[20] C. Ruiz-Romero, V. Carreira, I. Rego, S. Remeseiro, M.J. Lopez-Armada, F.J. Blanco, Proteomic analysis of human osteoarthritic chondrocytes reveals protein changes in stress and glycolysis, Proteomics 8 (2008) 495–507.
[21] L. Lourido, V. Calamia, J. Mateos, P. Fernandez-Puente, J. Fernandez-Tajes, F.J. Banco, et al., Quantitative proteomic profiling of human articular cartilage degradation in osteoarthritis, J. Proteome Res. 13 (2014) 6096–6106.
[22] J. Mateos, L. Lourido, P. Fernández-Puente, V. Calamia, C. Fernández-López, N. Oreiro, et al., Differential protein profiling of synovial fluid from rheumatoid

arthritis and osteoarthritis patients using LC-MALDI TOF/TOF, J. Proteome 75 (2012) 2869–2878.
[23] C. Fernandez-Costa, V. Calamia, P. Fernandez-Puente, J.-L. Capelo-Martinez, C. Ruiz-Romero, F.J. Blanco, Sequential depletion of human serum for the search of osteoarthritis biomarkers, Proteome Sci. 10 (2012) 55.
[24] V. Calamia, B. Rocha, J. Mateos, P. Fernandez-Puente, C. Ruiz-Romero, F.J. Blanco, Metabolic labeling of chondrocytes for the quantitative analysis of the interleukin-1-beta-mediated modulation of their intracellular and extracellular proteomes, J. Proteome Res. 10 (2011) 3701–3711.
[25] Q. Wang, A.L. Rozelle, C.M. Lepus, C.R. Scanzello, J.J. Song, D.M. Larsen, et al., Identification of a central role for complement in osteoarthritis, Nat. Med. 17 (2011) 1674–1679.
[26] R.T. Blankley, C. Fisher, M. Westwood, R. North, P.N. Baker, M.J. Walker, et al., A label-free selected reaction monitoring workflow identifies a subset of pregnancy specific glycoproteins as potential predictive markers of early-onset pre-eclampsia, Mol. Cell. Proteomics 12 (2013) 3148–3159.
[27] S.A. Carr, S.E. Abbatiello, B.L. Ackermann, C. Borchers, B. Domon, E.W. Deutsch, et al., Targeted peptide measurements in biology and medicine: best practices for mass spectrometry-based assay development using a fit-for-purpose approach, Mol. Cell. Proteomics 13 (2014) 907–917.
[28] A. Aguilar-Mahecha, M.A. Kuzyk, D. Domanski, C.H. Borchers, M. Basik, The effect of pre-analytical variability on the measurement of MRM-MS-based mid- to high-abundance plasma protein biomarkers and a panel of cytokines, PLoS One 7 (2012), e38290.
[29] M.F. Lopez, T. Rezai, D.A. Sarracino, A. Prakash, B. Krastins, M. Athanas, et al., Selected reaction monitoring-mass spectrometric immunoassay responsive to parathyroid hormone and related variants, Clin. Chem. 56 (2010) 281–290.
[30] A.J. Percy, A.G. Chambers, D.S. Smith, C.H. Borchers, Standardized protocols for quality control of MRM-based plasma proteomic workflows, J. Proteome Res. 12 (2013) 222–233.
[31] A.J. Percy, J. Yang, A.G. Chambers, R. Simon, D.B. Hardie, C.H. Borchers, Multiplexed MRM with internal standards for cerebrospinal fluid candidate protein biomarker quantitation, J. Proteome Res. 13 (2014) 3733–3747.
[32] A.G. Chambers, A.J. Percy, J. Yang, C.H. Borchers, Multiple reaction monitoring enables precise quantification of 97 proteins in dried blood spots, Mol. Cell. Proteomics 14 (2015) 3094–3104.
[33] A.Y. Wehr, W.T. Hwang, I.A. Blair, K.H. Yu, Relative quantification of serum proteins from pancreatic ductal adenocarcinoma patients by stable isotope dilution liquid chromatography-mass spectrometry, J. Proteome Res. 11 (2012) 1749–1758.
[34] J. Tsunezumi, S. Higashi, K. Miyazaki, Matrilysin (MMP-7) cleaves C-type lectin domain family 3 member A (CLEC3A) on tumor cell surface and modulates its cell adhesion activity, J. Cell. Biochem. 106 (2009) 693–702.
[35] A.G. Chambers, A.J. Percy, D.B. Hardie, C.H. Borchers, Comparison of proteins in whole blood and dried blood spot samples by LC/MS/MS, J. Am. Soc. Mass Spectrom. 24 (2013) 1338–1345.
[36] J.J. Kennedy, S.E. Abbatiello, K. Kim, P. Yan, J.R. Whiteaker, C. Lin, et al., Demonstrating the feasibility of large-scale development of standardized assays to quantify human proteins, Nat. Methods 11 (2014) 149–155.
[37] P. Brownridge, R.J. Beynon, The importance of the digest: proteolysis and absolute quantification in proteomics, Methods 54 (2011) 351–360.
[38] C.G. Arsene, R. Ohlendorf, W. Burkitt, C. Pritchard, A. Henrion, G. O'Connor, et al., Protein quantification by isotope dilution mass spectrometry of proteolytic fragments: cleavage rate and accuracy, Anal. Chem. 80 (2008) 4154–4160.
[39] J. Kamiie, S. Ohtsuki, R. Iwase, K. Ohmine, Y. Katsukura, K. Yanai, et al., Quantitative atlas of membrane transporter proteins: development and application of a highly sensitive simultaneous LC/MS/MS method combined with novel in-silico peptide selection criteria, Pharm. Res. 25 (2008) 1469–1483.
[40] J.M. Gutteridge, The antioxidant activity of haptoglobin towards haemoglobin-stimulated lipid peroxidation, Biochim. Biophys. Acta 917 (1987) 219–223.
[41] M.J. Nielsen, S.K. Moestrup, Receptor targeting of hemoglobin mediated by the haptoglobins: roles beyond heme scavenging, Blood 114 (2009) 764–771.
[42] M. Arredouani, P. Matthijs, E. Van Hoeyveld, A. Kasran, H. Baumann, J.L. Ceuppens, et al., Haptoglobin directly affects T cells and suppresses T helper cell type 2 cytokine release, Immunology 108 (2003) 144–151.
[43] H. Kume, S. Muraoka, T. Kuga, J. Adachi, R. Narumi, S. Watanabe, et al., Discovery of colorectal cancer biomarker candidates by membrane proteomic analysis and subsequent verification using selected reaction monitoring (SRM) and tissue microarray (TMA) analysis, Mol. Cell. Proteomics 13 (2014) 1471–1484.
[44] S.Y. Ritter, J. Collins, B. Krastins, D. Sarracino, M. Lopez, E. Losina, et al., Mass spectrometry assays of plasma biomarkers to predict radiographic progression of knee osteoarthritis, Arthritis Res. Ther. 16 (2014) 456.
[45] M.F. Hsueh, P. Onnerfjord, V.B. Kraus, Biomarkers and proteomic analysis of osteoarthritis, Matrix Biol. 39c (2014) 56–66.
[46] P.J. Lenting, C. Casari, O.D. Christophe, C.V. Denis, Von Willebrand factor: the old, the new and the unknown, J. Thromb. Haemost. 10 (2012) 2428–2437.
[47] S. Ohshima, S. Kuchen, C.A. Seemayer, D. Kyburz, A. Hirt, S. Klinzing, et al., Galectin 3 and its binding protein in rheumatoid arthritis, Arthritis Rheum. 48 (2003) 2788–2795.
[48] D. Pfander, T. Cramer, D. Deuerling, G. Weseloh, B. Swoboda, Expression of thrombospondin-1 and its receptor CD36 in human osteoarthritic cartilage, Ann. Rheum. Dis. 59 (2000) 448–454.
[49] M.W. Duncan, A.L. Yergey, S.D. Patterson, Quantifying proteins by mass spectrometry: the selectivity of SRM is only part of the problem, Proteomics 9 (2009) 1124–1127.
[50] M.S. Muttigi, I. Han, H.K. Park, H. Park, S.H. Lee, Matrilin-3 role in cartilage development and osteoarthritis, Int. J. Mol. Sci. 17 (2016) 590.
[51] A.R. Klatt, B. Paul-Klausch, G. Klinger, U. Hillebrand, G. Kuhn, B. Kobbe, et al., The matrilin-3 VWA1 domain modulates interleukin-6 release from primary human chondrocytes, Osteoarthr. Cartil. 21 (2013) 869–873.
[52] M. Nakajima, Y. Miyamoto, S. Ikegawa, Cloning and characterization of the osteoarthritis-associated gene DVWA, J. Bone Miner. Metab. 29 (2011) 300–308.
[53] R. Zhang, J. Yao, P. Xu, B. Ji, G. Voegeli, W. Hou, et al., Association between genetic variants of DVWA and osteoarthritis of the knee and hip: a comprehensive meta-analysis, Int. J. Clin. Exp. Med. 8 (2015) 9430–9437.
[54] T. Wang, Y. Liang, H. Li, Q. He, Y. Xue, C. Shen, et al., Single nucleotide polymorphisms and osteoarthritis: an overview and a meta-analysis, Medicine (Baltimore) 95 (2016), e2811.
[55] M. Veselinovic, V. Jakovljevic, A. Jurisic-Skevin, S. Toncev, D.M. Djuric, Carotid enlargement and serum levels of von Willebrand factor in rheumatoid arthritis: a follow-up study, Clin. Rheumatol. 31 (2012) 1727–1732.
[56] A. Ogdie, J. Li, L. Dai, M.E. Paessler, X. Yu, C. Diaz-Torne, et al., Identification of broadly discriminatory tissue biomarkers of synovitis with binary and multicategory receiver operating characteristic analysis, Biomarkers 15 (2010) 183–190.